STABILITY AND NEUTRALISATION CAPACITY OF POTENTIAL MINE BACKFILL MATERIAL FORMED BY NEUTRALISATION OF FLY ASH AND ACID MINE DRAINAGE

by

L. Petrik, C. Burgers, W. Gitari, D. Surender, K. Reynolds, A. Ellendt, O. Etchebers, V.R. Kumar Vadapalli, D. Key, E. Iwuoha

on behalf of

COALTECH 2020

in association with

The University of the Western Cape
Chemistry Department

Report to the Water Research Commission on the project
"Stability and neutralisation capacity of potential mine backfill material formed by neutralisation of fly ash and acid mine drainage"

WRC Report No: 1458/1/06
ISBN No: 1-77005-460-X

DECEMBER 2006

EXECUTIVE SUMMARY

Introduction

Utilisation of fly ash (FA) as ameliorant for the neutralisation of acid mine drainage (AMD) has proved to be feasible and was reported by UWC to the Water Research Commission in 2003 (WRC Final report No 1242/1/05). The free alkalinity imparted by CaO and other ash components and the fact that FA has a very high surface area and small particle size make South African FA a good neutralisation agent and AMD ameliorant. The two waste products (i.e. AMD and FA), usually formed in close proximity to each other, were reacted together and produced much cleaner effluent waters, comparable with lime and limestone treated AMD effluent, and suitable for discharge. The newly developed neutralisation procedure worked best for treating high TDS AMD. Sulphate removal rates achieved were above 90%. Fe, Al and heavy metal removal were often totally depending on the final pH, and EC was seen to drop to a minimum at pH ~10. Post process waters were significantly purified, with only relatively low concentration (parts per billion) of some species of toxic elements remaining in solution (e.g. As, B, W and Mo).

Moreover, the insoluble, pH neutral, bulk solid residues derived from the neutralisation process may be suitable as neutral and stable fill material. By further processing, the bulk solid residues were successfully used to prepare high capacity adsorbents such as zeolites via a high temperature thermal fusion step and via lower temperature routes. Zeolites are high value, micro porous, open structure crystalline aluminosilicates with a void volume of nearly 50%. High quality, high yield, clean phase (as indicated by XRD) zeolites that were formed included zeolite Y (faujasite), zeolite A, and sodalite. These zeolites have widespread potential application as adsorbents in water treatment or as catalysts. Preliminary studies of these high capacity zeolite adsorbents' efficiency for toxic element removal were performed and showed that significant removal of toxic ions such as Hg, Se, B, As, Fe, Mn, Ni is possible, allowing recovery and purification of dilute wastewater.

The initial study funded by both the WRC and Coaltech2020 during 2001-2003 (WRC Final Report No 1242/1/05) provided proof of concept that mixing of coal mine derived AMD and South African fly ash is a suitable method for the low cost treatment of coal derived acid mine drainage, and allows recovery of water as well as the preparation of high quality zeolite adsorbents by post process synthesis of solid waste residues.

Long-term performance and stability criteria were necessary to assess the feasibility of application of fly ash as liming substitute in active acid mine drainage treatment systems, or as an in-situ barrier suitable for ash walling in the passive treatment of acid mine drainage or as backfill material in mines. Larger scale testing was also imperative prior to application of this very promising, low-cost process that addresses remediation of two major wastes (acid mine drainage and fly ash) simultaneously.

In this report covering the period 2003-2005, the larger scale study funded by both the WRC, Coaltech2020 and co-funded by ESKOM is presented in which the larger scale capacity of fly ash for AMD neutralisation was determined. The study included determination of process parameters and the extent of removal of toxic heavy metals from acid mine drainage as well as long-term stability of bulk solid residues. In particular, the focus was on comparing the stability, leaching characteristics and performance of backfill materials useful for underground placement that were prepared from fly ash residues or ash with various

additives. The physical and chemical properties that were ascertained included characteristics such as hardness, strength as well as the chemistry, and long-term phase transition kinetics of solid fill materials that may in future be in contact with acid mine drainage or waters of seepage.

Results and Discussion

Neutralisation of AMD

The study of the neutralisation of AMD requires the analysis of waters prior to neutralisation and after neutralisation has taken place. This characterisation of waters is necessary to quantify the amount of various elements that is no longer soluble.

The concentration of SO_4^{2-} can vary by a large margin and even by magnitudes between different samples of AMD and samples of AMD from the same source, drawn at different times. The pH values of AMD waters are between 2 and 3, some concentration events can cause a pH lower than 2, as with Kromdraai AMD. EC and pH are proportional to each other with a lower pH resulting in a higher EC and dissolved solids. Some AMD's had a low buffering capacity and are quickly neutralised. This is a result of low metal concentrations in the AMD.

In neutralised waters, Fe is reduced to below 0.5 mg/L when the neutralisation reaction is sufficiently aerated or the reaction proceeds for a sufficient length of time to facilitate oxidation (ash walling study). SO_4^{2-} concentration decreases by a greater amount with higher fly ash to AMD ratios. This indicates that the precipitation of SO_4^{2-} is dependant on alkalinity and more specifically the amount of Ca^{2+} in solution. In general, the concentration of SO_4^{2-} in the water is reduced to around 2000 mg/L. The concentration of Al^{3+} is also alkalinity dependant with the greatest Al^{3+} removal occurring at high fly ash to AMD ratios. Lower ratios do, however, show significant Al^{3+} removal to levels below 6 mg/L. Levels of other minor toxic elements are very significantly reduced.

The amount of alkalinity available or the FA to AMD ratio and the amount of time over which the reaction is allowed to proceed, determines the final pH of the solution following the neutralisation of AMD. The dissolution and hydrolysis of CaO and MgO from fly ash contribute to an increase in the pH of AMD. This increase in pH causes the precipitation of acid-contributing metals such as Fe^{3+} and Al^{3+} that consume alkalinity and buffer the reaction.

The importance of precipitation was established by calculating the saturation indices of the elements in solution during the neutralisation of AMD. An increased removal of elements such as B, Mg, Mn, Al, Si, total Fe and Zn was observed at higher FA to AMD ratios. Calculated saturation indices and mineralogical analysis indicated that SO_4, Fe and Al were controlled by mineral solubility. Al concentrations were controlled by secondary phases such as boehmite, basaluminite and gibbsite; Fe by amorphous $Fe(OH)_3$ and goethite and Ca and SO_4^{2-} concentrations were controlled by gypsum solubility. The elements Na, Ca, Ba, Mg, Sr, B, Mo, Se, Si, Mn, and Zn showed development of solubility controls at certain reaction times after the initial dissolution. It is probable that these elements were present as soluble salts and, on dissolution, interacted with components in AMD to form new stable mineral phases that controlled their concentrations.

Mn, Mg, Zn and Cu were removed from solution at a lower pH (5.5 – 7.0) than predicted by thermodynamic calculations, indicating that physical processes such as adsorption and co-precipitation also influence metal removal. The strong association of these elements with the amorphous iron oxide fraction reinforces this hypothesis.

Fe^{2+} is removed through oxidation and subsequent hydrolysis at pH 5.5. A corresponding decrease in SO_4^{2-} concentration is observed indicating the relevance of the iron-oxyhydroxides in SO_4^{2-} removal.

In order to maximise the benefits of neutralising AMD with FA, the optimum process conditions for pilot scale neutralisation of acid mine drainage with fly ash used as ameliorant or as liming substitute, were investigated. Numerous experiments were performed to determine the neutralisation potential of various combinations of different fly ashes and AMD's. These experiments were mostly small scale reactions performed in the laboratory. A large scale mixer with a capacity of 250 L was also applied. The motorised, overhead agitation ensures sufficient aeration for rapid Fe^{2+} oxidation. These small and large scale experiments were performed with different fly ashes and acid mine drainages at different ratios to determine the optimum conditions for reaction. The pH and EC was recorded over time and the waters were analysed.

From the reactions between different fly ashes and AMD sources, it can be concluded that different ratios and reaction times will apply to different combinations. The various fly ashes and AMD's are all very different from each other, and AMD can vary on a day-to-day basis. The various reactions at different ratios give an idea of which waters require a greater amount of alkaline material or a longer process time.

Fly ash from various sources has the capacity to neutralise AMD at low FA to AMD ratios of 1:6. It is clear that Bank and Landau waters require higher amounts of alkaline material to reach high pH values and be decontaminated. Kromdraai and Brugspruit waters were not as highly contaminated and required less fly ash. Matla and Duvha ash have a smaller neutralising capacity than Arnot, which appears to contain the greatest amount of alkalinity. Kendal ash does not provide sufficient alkalinity for adequate neutralisation under the conditions tested. The other important factors that control the neutralising capacity of fly ash are particle size and unburnt carbon content. The smaller the particle size, the more efficient the ash becomes at neutralising AMD. The unburnt carbon in ash may indicate a different mineralogy of the ash due to conditions in the economizer that may reduce the alkalinity available in the fly ash. The variability of the properties of fly ash remains to be investigated.

In a pilot scale plant the pH must be constantly monitored and the fly ash feed must be adjusted according to the pH of the reaction to account for variations in AMD and fly ash, or alternatively the contact time should be adjusted.

Use of FA as mine backfill material

In order to determine the feasibility of using fly ash as mine backfill, it was necessary to monitor the quality of water in contact with ash, either in passive or active treatment systems

over a long-term period. This was assessed in passive column studies using Kendal ash and Middelburg AMD and in active neutralisation with Arnot ash and Landau AMD.

The permeate water (also termed leachates) recovered after passive percolation of AMD through columns of fly ash of various lengths was analysed for chemical composition to understand the changes to water quality over time and to model systems in which long-term contact between ash and raw AMD may occur. Active neutralisation experiments in a pilot scale mixing vessel were conducted for periods longer than those previously used during laboratory scale experiments to ascertain longer term EC and pH trends over the time required for neutralisation.

It was found that fly ash can be utilised to treat AMD in-situ in passive systems and that suitable methods of incorporating fly ash into acid generating pyrite containing mine spoil should be devised to control AMD generation. It was also shown that the AMD water quality significantly improves during permeation through fly ash and that the mineralogy of the fly ash changes as a result of contact with the AMD. Thus passively neutralising Middelburg AMD with coarse Kendal fly ash has the potential to ameliorate the AMD. Long-term column leaching studies suggest that backfilling and ash walling with fly ash has a great potential benefit for AMD remediation. Column leaching shows excellent improvement in terms of toxic element removal within the first few days and over the longer term.

The active neutralisation of Landau AMD at pilot scale with Arnot fly ash proved feasible at the larger scale, replicating results found in small scale experiments. It was found that lower FA to AMD ratios may be used to achieve a similar, post neutralisation water quality as that for higher FA to AMD ratios, if the neutralisation reaction can proceed for a greater period of time. Pilot scale studies exhibit some variations in the reaction when compared to the bench scale studies; this is due to greater aeration.

Hence, whether fly ash is used as a liming agent or as a passive treatment option for AMD, a significant improvement in the quality of water is observed.

Investigation of solids

Solids refer to fly ash or the solid residues composed of fly ash and insoluble solid precipitates recovered after the neutralisation process. It is necessary to characterise the mineralogy and elemental composition of solid material in order to gain a complete understanding of the behaviour of elements and ions. There are, however, difficulties in determining the mineralogy of precipitates from the neutralisation reaction between fly ash and AMD. It is almost impossible to positively identify minerals precipitated during the neutralisation reaction onto the fly ash by XRD because the strong quartz and mullite peaks mask any other less intense peaks.

From the investigation of the various fly ashes used, the following can be concluded:

- There is little significant variation in the mineralogy of different samples of the same ash.
- There is little significant variation in the mineralogy between different fly ash sources.
- Alkalinity and particle size show a good, negative correlation (-67%).
- The correlation between alkalinity and surface area is near to perfect (97%).
- The correlation between particle size and surface area is only 54%.

- The presence of significant amounts of carbon in a fly ash sample would indicate mineralogical changes in ash that may severely retard successful neutralisation.
- Elements that form anionic species (As, Se, B, Mo) at alkaline pH are highly leached from fly ash itself, but stabilized to lower levels as the pH was increased in the neutralisation reaction between fly ash and AMD.

Ash walling

In this deliverable the mineralogical changes in ash after long-term exposure to raw AMD flows were examined, to assess the physical durability of the ash under simulated weathering conditions. XRF results give a clear picture of the movement and mobility of elements in the column. Si and Al appear to be highly mobile. The concentration of Fe in the solids recovered from column studies with Kendal ash, increases greatly after AMD permeation but proportionally there is either not enough of the mineral to be distinguished in XRD, as mullite and quartz peaks tend to mask minerals in lower concentrations, or the Fe precipitates as a mineral with low crystallinity. Although no clear mineralogical changes could be discerned by XRD, the fact that the columns blocked indicated agglomeration or coalescence of ash particles by insoluble precipitates formed upon contact of AMD with the fly ash.

Backfilling

A review of the backfilling literature found that several materials had successfully been used as backfill but that fly ash has not been widely considered for that purpose. In terms of backfilling, fly ash has been tested as an additive only to reduce the amount of cement needed. Some studies looked at desirable mixtures of backfill material, and assessed backfill stability for different materials, determined effects of loading, sheer strength assessment, etc. Few studies assessed long-term chemical changes within backfill or investigated the influence of acid or alkaline waters on the chemical stability of backfill, or weathering by flowing fluids (e.g. influence of AMD entering from another part of the mine). Some studies assessed the physical durability of the backfill materials and strength changes with time. The literature clearly indicates the beneficial potential of using fly ash as mine backfill. There is apparently no literature concerning use of solid residues as a backfill material or of utilising fly ash for ash walling.

Experiments were conducted to determine how the different backfill materials behave when pumped and placed in simulated mine environments. Tests were aimed at determining desirable mixtures of backfill material, and appropriate slurry densities. Difficulty in obtaining laboratory use and consultants time at CSIR resulted in only the strength development, slurry flow and density parameters being evaluated during this study. The strength development of the solid residues from the neutralisation of acid mine drainage with fly ash, by itself or blended with ordinary Portland cement or fly ash was investigated. The moisture content and particle size was determined and a Marsh cone test conducted, prior to curing.

Flow tests were performed using the Marsh cone test. The material from the reaction between Matla fly ash and Navigation AMD had a solids fraction of about 0.7: It was necessary to add water in order to achieve reasonable flow rates in separated solid residues.

The results show the influence of the fly ash properties such as particle size on the flowability of the solid residues from the neutralisation of AMD with fly ash. When

implementing the neutralisation process at large scale, it will be necessary to adjust the operating parameters of the future treatment plant according to the origin and corresponding properties of the fly ash used.

Strength development tests over time were performed. The solid residues were tested by themselves or were blended with a pozzolanic binder (Castle cement) at rates of 1%, 3% and 6% dry weight basis. Strength development in the three different batches was found to be proportional to the proportion of binder used. A more rapid strength development is observed in the first 28 days of curing for the solid residues formulated with process waters than that formulated with tap water. This early accelerated strength development could be due to the formation of gypsum on hydration of the cement binder, with the process waters acting as a rich source of sulphates. Overall the solid residues formulated using the process waters had greater unconfined compressive strength at all levels than the solid residues formulated using tap water.

With the addition of a binder, the strength of the solid residue material is relatively high and it appears suitable for the purpose of confinement of mined-out areas. The stability of the solid residues is demonstrated through its capacity to develop strength over time. Similar results were obtained in a previous study made on unreacted fly ash (Ilgner, 2000). Moreover similar trends were observed in these studies compared to values obtained from the literature (Grice, 1998) for fly ash that indicated addition of a binder increased compressive strength, to between 0.75-4MPa, and values obtained in this study were within this range (1.23-3.03MPa - dependent upon binder content and time). Both compressive strength and elastic modulus were still increasing after one year under the experimental conditions of storage. These experiments tend to confirm that even after being submitted to reaction with AMD, solid residues of fly ash remain suitable as material for backfilling. Hence, the proposed use of fly ash to first ameliorate AMD by use as a substitute liming treatment, and then use the recovered solid residues for backfill material has been shown to be feasible.

The long-term chemical changes within backfill and the influence of acid waters on the chemical stability of backfill (e.g. influence of AMD entering from another part of the mine) was investigated. Simulated AMD was percolated through fly ash and solid residues resulting from the neutralisation of Navigation AMD with Arnot FA in column leaching studies in order to model the chemical and mineralogical changes that could be expected over time when solid residues are placed underground as fill or backfill material in possible contact with AMD flows. Simulated AMD was used in this study because of logistical constraints and to exclude variability. The solid residues from the neutralisation reaction were compared to blends with unreacted fly ash to give mixtures of varying ratio (5, 25 and 40% unreacted fly ash) and one column was prepared with solid residues blended with 6% cement on a dry weight basis and a further column with fly ash only.

The permeate recovered from the column packed with unreacted fly ash showed a gradual decrease in pH with time. The initial pH of the permeate recovered after passage through solid residues were alkaline (pH 8.5). Thereafter pH dropped to 4 for these columns after 124 days. The initial permeates of the 5% fly ash blended solid residues remained neutral for the first 81 days thereafter decreasing to pH 3.5. The initial permeates of the 25% fly ash blended solid residues remained neutral for the first 110 days thereafter decreasing to pH 4. The pH of the 40% fly ash blended solid residues followed the same trend as the column with 25% fly ash. The pH of the permeate of columns containing solid residues blended with 6%

ordinary Portland cement dropped to 4 for these columns after only 24 days, indicating a reduction in neutralisation capacity when using cement as binder.

The solid residues by themselves performed somewhat similarly to the residual solid/fly ash combinations and considerably better than the Portland cement amended blend, once again highlighting their greater suitability as backfill material, than standard ash/cement binder combinations. It is noteworthy that ash as binder replaces cement successfully, and further strength development testing should be performed with these combinations.

GIS mapping of affected area

The objective of this study was to use data available from Coaltech and/or other sources, to compile maps of the affected area. It was envisaged that information on volumes of AMD, quality of AMD, neutralising material available, neutralising potential, coal mine locations suitable for backfill, etc., could be mapped, to give some idea of the practicality of neutralisation followed by backfill and the economic potential for this. However, only some of these objectives could be met due to lack of information sharing by mines, government and industry when approached for information. The amount and quality of the data presented in this report make it clear that further studies need to be conducted with more rigorous and accurate data collection, which will require significantly better collaboration between interested parties.

Observable seasonal variations of water quality could not be seen in any of the three AMD's studied. Variations occurred, though, but were not repeated from one year to another. These results show that the pH and concentrations of dissolved species in AMD are under the combined influence of many uncontrolled factors, such as amount of rainfall, amount of pyrite in the coal, composition of gangue rock, rate of coal extraction and etc.

In future work the monitoring of AMD properties must be set up on a daily or weekly basis, for an extended period of several months or years. This could bring a detailed knowledge of AMD characteristics and variations. It would be highly useful in the evaluation of the remediation capacity of FA.

Zeolite synthesis

Zeolite synthesis from solid residues resulting from the neutralisation of AMD with FA and preliminary testing in simulated wastewater studies was explored. A zeolitic material can be synthesised using the residual solid from the reaction between Arnot fly ash and Navigation AMD. The zeolite adsorbent synthesised with the fusion method has a similar capacity of metal removal compared to a commercial faujasite. The synthesised faujasite removed 100% of Mn in solution and 99.8% of both Co and Pb. In comparison, the commercial ion exchange resin, Lewatit TP207 does not remove metals very efficiently. Manganese removal is only 63%, and over time (24hr) Co removal is 98% and Pb removal is 96%, whereas the zeolite prepared from solid residues removed the maximum amount of all tested contaminant metals after less than an hour of contact with the effluent.

Conclusions and Recommendations

Current AMD treatment plants based on limestone are inefficient and costly and need to be redesigned. A plant using fly ash as the alkaline material is a realistic alternative to more

expensive alkaline material. The potential to employ an integrated waste management scheme, “the Petrik Process” based upon the use of fly ash, is presented:

1. Neutralisation of fly ash and AMD from various sources;
2. Use of solid residues as backfill in real coal mines;
3. Recovery of almost all water;
4. Application of solid residues to prepare zeolites;
5. Use of zeolites for brine stabilisation
6. Use of zeolites for toxic element removal from dilute process streams
7. Use of fly ash for ash walling or lining;
8. Application of solid residues as soil amendment
9. Hydrogen production from AMD
10. Salt recrystallisation from process brines
11. Chlorine production from process brines
12. Use of recovered water for irrigation

The results obtained thus far at UWC show that items 1-7 are very feasible, and plans are being formulated to investigate the feasibility of items 8-12. Site visits and presentations to market the idea to mines has been successful and proposals that have been accepted or are under consideration at present, are appended (see Appendix B). Cost estimates are being prepared for large scale testing of item 1. All costs and volumes quoted are estimates based upon the Anglocoal Navigation treatment plant.

ACKNOWLEDGEMENTS

Funder project mentors

WRC Project leader: Meiring du Plessis
Coaltech 2020 Project leader: Johann Beukes
ESKOM Project mentors: Gerhard Gericke, Siven Naidoo

Research leaders

Task leader (Coaltech 2020 Task 6.1.6): L. Petrik, Dept Chemistry, UWC
Project mentors: R. Meyer, H. Ilgner J. Maree (CSIR); R. Kruger (Ash Resources); G. Gericke (Eskom)
Team Members: Academic supervisors: D. Key, E. Iwuoha, C. Okujeni, and D. Cowan (UWC).

Table of contents **Page**

LIST OF TABLES

LIST OF FIGURES

LIST OF ACRONYMS AND ABBREVIATIONS

AAS	Atomic Adsorption Spectroscopy
AMD	Acid Mine Drainage
BET	Brünauer-Emmett-Teller method
BRAD	Black Researcher Academic Development Programme
CEC	Cation Exchange Capacity
CPP	Coal Processing Plant
CSIR	Council for Scientific and Industrial Research
DMSP	Density Medium Separation Plant
DTA	Differential thermal analysis
DWAF	Department of Water Affairs and Forestry
EC	Electrical Conductivity
EDR	Electrodialysis Reversal
FA	Fly Ash
FAL	Fly Ash Leachate
FTIR	Fourier Transformed Infrared Spectrometry
HDPE	High-Density Polyethylene
IC	Ion Chromatography
ICP-MS	Inductively Coupled Plasma-Atomic Emission Mass Spectroscopy
LFA	Leached Fly Ash
LOI	Loss on Ignition
PLP	Primary Liming Plant
PVC	Poly Vinyl Chloride
RO	Reverse Osmosis
SAMD	Synthetic Acid Mine Drainage
SEM-EDS	Scanning Electron Microscopy - Energy Dispersive X-Ray Spectroscopy
SLP	Secondary Liming Plant
SRP	Sulphate Reduction Plant
TDS	Total Dissolved Solids
TGA	Thermal gravimetric analysis
THRIP	Technology and Human Resources for Industry Programme
TSP	Toe Seep Plant
US	University of Stellenbosch
UWC	University of the Western Cape
WRC	Water Research Commission
XRD	X-Ray Diffraction
XRF	X-Ray Fluorescence Spectroscopy

1. INTRODUCTION

1.1 BACKGROUND

Coal mining in South Africa is estimated to produce 200 Ml of acid mine drainage (AMD) per day in the Pretoria-Witwatersrand-Vereeniging (PWV) area alone (Maree *et al.,* 1996), while electricity production resulted in approximately 27 Mt (Eskom, 2001) of ash in 2001. A large number of collieries in South Africa are tied to power stations where these two waste streams, acid mine drainage and fly ash, have the capacity to neutralise each other and provide an opportunity for co-disposal. Pulverised fuel ash is the material remaining when coal is combusted to power the steam turbines that make electricity. Fly ash is that fraction of waste that enters the flue gas stream and is collected by bag house precipitators or other emission control devices (Adriano *et al*., 1980). This waste is usually disposed of as slurry to a waste dam site. Fly ash is considered to be a ferro-alumino silicate made up of glass spheres (Fisher and Natusch, 1979) of very small particle size (20 – 80 μm) (Carlson and Adriano, 1993; Mattigod *et al.,* 1990) and high surface areas (Summers *et al.,* 1993). The lime that occurs on the surface of the glass spherules originates from the decarbonation of limestone and/or dolomite impurities in the coal and thus causes the fly ash to be alkaline (Warren and Dudas, 1984).

Utilisation of fly ash (FA) as ameliorant for the neutralisation of acid mine drainage (AMD) has proved to be feasible. Alkalinity, in the form of CaO and high surface area and small particle size make South African FA a good neutralisation material and AMD ameliorant. AMD and FA, usually generated in close proximity, were reacted and resulted in cleaner effluent waters, comparable with lime and limestone treated AMD effluent, and suitable for discharge. The newly developed neutralisation procedure worked best for treating high TDS AMD. Sulphate removal rates achieved were high while Fe, Al and heavy metal removal was often total depending on the final pH. EC was seen to drop to a minimum at pH ~10. Post-process waters were significantly ameliorated, with only relatively low concentration (parts per billion) of some species of toxic elements remaining in solution (e.g. As, B, W and Mo).

Moreover, the insoluble, pH neutral, bulk solid residues derived from the neutralisation process may be suitable as neutral and stable fill material. By further processing, the bulk solid residues were successfully used to prepare high capacity adsorbents such as zeolites via a high temperature thermal fusion step and via lower temperature routes. Zeolites are high value, micro porous, open structure crystalline aluminosilicates with a void volume of nearly 50%. High quality, high yield, clean phase (as indicated by XRD) zeolites that were formed included zeolite Y (faujasite), zeolite A, and sodalite. These zeolites have widespread potential application as adsorbents in water treatment or as catalysts. Preliminary studies of these high capacity zeolite adsorbents' efficiency for toxic element removal were performed and showed that significant removal of toxic ions such as Hg, Se, B, As, Fe, Mn, Ni is possible, allowing recovery and purification of dilute wastewater.

The initial study funded by both the WRC and Coaltech2020 during 2001-2003 (WRC Final Report No 1242/1/05) provided proof of concept that mixing of coal mine derived AMD and South African fly ash is a suitable method for the low cost treatment of coal derived acid mine drainage, and allows recovery of water as well as the preparation of high quality zeolite adsorbents by post process synthesis of solid waste residues. This research has received support from industrial partner ESKOM, and is of interest to Sasol and Anglocoal.

The larger scale study funded by the WRC and Coaltech2020 and co-funded by ESKOM during 2004-2005 is presented in this report. This study determined larger scale neutralisation process parameters as well as long-term stability, neutralisation capacity and the extent of potential leaching of toxic heavy metals from such ash or residual solid materials. In particular, the focus was on comparing the stability and performance of backfill materials useful for underground placement that were prepared from fly ash residual solids or ash with various additives. The physical and chemical properties that were ascertained included characteristics such as hardness, strength as well as the chemistry, and long-term phase transition kinetics of solid fill materials that may in future be in contact with acid mine drainage or waters of seepage.

1.2 AIMS

The aims of this project were to:

1. Treat acid mine drainage from coal mines
2. Utilise coal-fired power station fly ash (a waste product with few large scale applications) thus preventing the continued growth of unsightly and environmentally damaging fly ash dumps and ash dams
3. Produce a chemically stable backfill material suitable for extending the life of coalmines and increasing the amount of extractable coal from each mine
4. Control surface acid mine drainage by employment of fly ash as walls within coal mine spoil heaps
5. Produce a bulk material suitable for work-up into high value high quality zeolitic adsorbents
6. Production of backfill material and its application in coal mines will prevent hazardous surface subsidence

These aims were achieved by conducting four site specific studies:

1. Treatment of acid mine drainage waters generated at Bank and Kromdraai colliery by neutralisation with fly ash conducted by Dr. Jalari Rajasekhar (Anglocoal)
2. The potential use of solid residues as neutral and stable backfill material for mines conducted by PhD student Wilson Gitari. This study concentrated both on the chemical and physical durability of the solid residues.
3. The potential use of fly ash as an in-situ barrier for the treatment of acid mine drainage conducted by PhD student Kelley Reynolds (co-funded by Eskom)
4. Zeolites synthesis using the solid residues that were generated during the neutralization experiments explained above was carried out by Ms. N. Hendricks(M.Sc student) and Ms. A. Ellendt(Research Officer).
5. A site specific study of neutralisation with fly ash as measure to treat AMD at Arnot conducted by MSc student Damini Surender (co-funded by Eskom)

1.3 APPROACH

Long-term performance and stability criteria were necessary to assess the feasibility of application of fly ash as liming substitute in active acid mine drainage treatment systems, or as an in-situ barrier suitable for ash walling in the passive treatment of acid mine drainage or as backfill material in mines. Larger scale testing was also imperative prior to application of this very promising, low cost process that addresses remediation of two major wastes (acid mine drainage and fly ash) simultaneously. Since, at laboratory scale it was not possible to adequately assess the bulk neutralisation capacity of the neutralisation process or prepare

sufficient material for stability or long-term neutralisation potential testing. Larger scale testing is also necessary prior to application for DWAF certification of this process.

The application of FA as an AMD ameliorant was ascertained by different neutralization experiments. These experiments included both small and large scale studies using different FA and AMD from a variety of power stations and mines. Full description of these experiments are given in the chapter 2 starting from the section 2.1. Thus it has shown a way to prevent the continuous growth of fly ash dumps. The solid residues that are recovered after the neutralization reactions were tested for their chemical and physical durability to place them underground as a backfill material. The chemical stability was ascertained by columns studies (chapter 2, section: 2.3.5 and in chapter 3). The results of the physical stability of these solids are presented in the chapter 5. Assessment of physical stability is very important as one of the main functions of backfilling is to avoid hazardous surface subsidence. The employment of ash as an in situ barrier was investigated using columns of different length and the results are provided in the chapter 4. Synthesis of zeolites was carried out using the solid residues and the full description of these studies is presented in the chapter 6. Finally, mapping of the area affected by the coalmining activity was achieved using GIS tool which is presented in the chapter 8.

Optimisation of neutralisation process parameters such as slurry densities required, necessary contact time, bulk reaction rates, ash neutralisation potential of different ashes and other issues such as sludge settling time, handling and stability of solid residues, potential for leaching of heavy metals etc., was investigated. Full assessment of neutralisation process variables may now allow implementation of a low cost, bulk ameliorant, namely fly ash, which is readily available in close proximity to sources of acid mine drainage, to replace costly lime or limestone currently used in active systems for acid mine drainage remediation. Moreover, the solid residues derived from the neutralisation process may be suitable as neutral and stable backfill material in mines or as potential ash walling material for passive treatment or channelling of AMD flows.

In order to investigate ash leaching UWC participated in an inter-laboratory leaching study. The aim of the inter-laboratory leaching study was to characterise the heavy metals released from coal utilisation by-products (CUB). This study was also intended to compare the various leaching protocols in terms of efficacy and precision and to produce comparable data. All participants used one ash derived from the combustion of a bituminous coal from the eastern United States. This ash was observed to be very dark in colour, fine grained and containing Fe. The participants of the inter-laboratory leaching study were U.S. Department of Energy National Energy Technology Laboratory (NETL), Virginia Tech, and University of the Western Cape, West Virginia Water Research Institute, University of North Dakota Energy & Environmental Research Center. The University of the Western Cape participated in this study as a basis for changing the standard leaching tests used in South Africa to classify waste. Following participation in this study a further study will be conducted with South African fly ash (FA) and FA and AMD solid residues. The leaching study is presented in Appendix B.

1.4 PROJECT DELIVERABLES

- GIS mapping of affected area
- Optimise pilot scale co-disposal

- Slurry pumping tests
- Zeolite synthesis: process parameter assessment
- Backfill stability assessment
- Backfill: long-term chemical stability assessment
- Backfill: physical durability assessment
- Characterization of bulk solid co-disposal residues
- Characterization of pre & post process waters
- Comparing different backfill materials
- Develop co-disposed AMD/fly ash mine backfill scheme
- Establish long-term monitoring
- Final report

2. NEUTRALISATION OF AMD

2.1 INTRODUCTION

Acid mine drainage (AMD) is produced when meteoric and groundwater comes into contact with sulphide minerals that are undergoing oxidation. This occurs primarily in coal and gold mines and their tailings (Miller and Murray, 1988; Mitchell, 2000) but may also occur in soils that are close to the sea or in drained marshlands. Due to the extremely low pH of AMD many metals such as iron and aluminium are present in toxic concentrations. Sulphate is also present at unacceptably high concentrations. The production of AMD depends on the rate of pyrite oxidation (Singer and Stumm, 1970), the presence of acidophilic bacteria (Chapelle *et al.*, 1993; Colmer and Hinkle, 1947; Nordstrom and Southam, 1997; Waksman and Jåffe, 1921) and the influence of carbonate minerals in the host rock. Active neutralisation with lime (CaO or $Ca(OH)_2$), soda ash (Na_2CO_3) or limestone ($CaCO_3$) is the most common method of remediation (Skousen *et al.*, 1997).

Recent work which exploits the alkaline nature of fly ash has demonstrated the potential to neutralise acid mine drainage by reacting fly ash or aqueous extracts of the fly ash with AMD and subsequently reduce heavy metal concentrations by precipitation (Abanda *et al*., 1999; O'Brien, 2000). It was found in previous studies (WRC Report K5/1242, 2003) that AMD could successfully be neutralised with FA.

In this study further experimentation was conducted to widen the scope of study by neutralising a wide range of acid mine drainages from various locations. These experiments were conducted at small scale beaker tests and in larger scale reactors.

In this section of the report the optimised process conditions for pilot scale neutralisation of acid mine drainage with fly ash used as ameliorant or as liming substitute were investigated. Parameters that were optimised include slurry density, contact time, etc. Numerous experiments were performed to determine the neutralisation potential of fly ash with AMD. These experiments were mostly small scale reactions performed in the laboratory but a range of larger scale experiments have been carried out.

These small and large scale experiments were performed with different fly ashes and acid mine drainages at different ratios to determine the optimum conditions for reaction. The pH and EC was recorded over time and the product waters were analysed for contaminants. This section describes the neutralisation reaction and optimum ratios.

2.2 METHOD

Several discrete groups of neutralisation experiments were conducted each with a slightly different method. The methods described here are divided between small or beaker scale experiments and large or pilot scale experiments.

2.2.1 Small scale neutralisation experiments

2.2.1.1 Small scale and Turbulator neutralisation experiments site specific to Bank and Kromdraai collieries and Arnot, Duvha, Matla, Hendrina and Kendal power stations

For the site specific study of Bank and Kromdraai collieries and Arnot, Duvha, Matla, Hendrina and Kendal power stations open beaker tests were carried out to determine the change in pH and EC with time when different ratios of AMD and FA were mixed. The samples were agitated by means of an overhead stirrer for 3-5 hrs at 240 rpm. Larger scale treatment of AMD with FA for the site specific study of AMD from Bank and Kromdraai collieries and FA from Arnot, Duvha, Matla, Hendrina and Kendal power stations was carried out using a metal container with a capacity of approximately 75 L and an overhead stirrer, called a Turbulator. The pH and EC was recorded and SO_4, Fe, NO_3, acidity and alkalinity were determined. Samples, taken at different time intervals during the neutralisation reaction, were analysed for major, minor and trace elements.

2.2.1.2 Small scale neutralisation experiments site specific to Matla and Arnot power stations and Brugspruit, Navigation, and Bank collieries

In a further site specific study Matla and Arnot fly ashes and Brugspruit, Navigation, and Bank acid mine drainages were combined. An overhead stirrer was used to agitate the solution. Samples were taken at timed intervals during the reaction and divided into three sub-samples varying from 0.5 – 2 mL. These 3 sub-samples were then diluted to 5 mL with distilled water. The first two of these samples were immediately analysed for Fe^{2+} and SO_4^{2-}. The third sub-sample was acidified with two drops of nitric acid in order to preserve it for analysis of Mn, total Fe, Al, Ni, Zn, Co, B and Si.

2.2.1.3 Small scale neutralisation experiments site specific to Arnot power station and Navigation colliery to investigate mineral equilibria

Neutralisation experiments site specific to Navigation colliery and Arnot power station using fresh samples at the ratios 1:3 FA to obtain neutral water and 1:1.5 FA to obtain alkaline water, were conducted. In these studies typically a volume of 500 mL of AMD was mixed with various quantities of fly ash and stirred by overhead stirrer for 3-5 hrs at 240 rpm. The main objective was to understand the $Fe^{2+/}Fe^{3+}$ oxidation/precipitation process, SO_4 removal and major element removal, which helped to establish whether there was a relationship between the mineral phases/precipitates being formed and trace elements removal.

2.2.1.4 Long-term column neutralisation

The solid residues used in the long-term column leaching experiments were obtained from a large scale neutralisation experiment carried out in a Turbulator with a 150 L capacity, which had a stirring rate of approximately 1000 rpm. Arnot fly ash and Navigation AMD was used in the ratio 1:3 (FA:AMD). The aim of this neutralisation reaction was to generate a large volume of solids for packing in the leaching columns. The reaction was carried out for 210 minutes and terminated once the pH was approximately 9, unlike previous small scale tests, which were agitated for 300 minutes to obtain the same pH for the process waters. The mixture was allowed to stand and the liquid phase was drained off. The solids were then air dried. The moisture content was 12.1% after drying for 12 hours at 105 ^{0}C. Large aggregates were broken up and the solids were mixed thoroughly to attain homogeneity and thereafter placed in columns of suitable diameter and length, each column containing 2 kg of solid. Two replicated columns were packed with solid residues only. The solid residues were also blended with unreacted fly ash to give a mixture of varying ratio (0, 5, 25 and 40% unreacted fly ash) on dry weight basis. Comparison columns packed with similar quantities of unreacted Arnot fly ash or with 6% ordinary Portland cement (OPC) blended with residual

solids were also replicated. The solids were packed in the columns manually, in small portions of 500 g. After each addition the material was then gently tamped down until a uniform packing density was obtained. Model solutions simulating AMD were formulated using soluble salts of the major elements found in AMD (Fe, Al, Mn and SO_4). The salts were dissolved in 0.005 M H_2SO_4 solution to prevent immediate precipitation of ferric iron. Metal salts used were anhydrous ferric sulphate, hydrated ferrous sulphate, hydrated aluminium sulphate and manganese (II) nitrate tetrahydrate. Various aliquots of 350 mL of the simulated AMD were percolated through the packed columns at prescribed time intervals over a period of 165 days. The permeate was collected after each aliquot had passed through the respective columns and the pH of the permeate was monitored with a Hanna HI 991301 portable pH/EC/TDS/Temperature meter.

2.2.1.5 Initial small scale neutralisation experiments site specific to Landau colliery and Arnot power station

A small scale study site specific to Landau colliery and Arnot power station was conducted to determine the feasibility of a pilot scale project. The small scale tests were conducted to determine the ratios at which the pilot scale study should be conducted. The following FA:AMD ratios were studied: 1:1, 1:2, 1:3, 1:5, 1:10 and 1:20. Fresh AMD samples were added to the beakers and stirred by overhead stirrers at 250 rpm/min for approximately 30 min to allow the AMD to reach room temperature. The fly ash was weighed and slowly added to AMD with continuous stirring. The pH and conductivity of each mixture was monitored at regular time intervals.

2.2.1.6 Secondary small scale neutralisation experiments site specific to Landau colliery and Arnot power station

The site specific study using with Landau AMD and Arnot FA conducted initial small scale neutralisation experiments to optimise the reaction and determine the neutralisation potential of Arnot fly ash. A volume of 500 mL of AMD was mixed with various quantities of fly ash. This was aimed at obtaining neutrality, heavy metal removal, and optimum conditions for high capacity adsorbent preparation. The FA:AMD ratios 1:3 and 1:5 were tested.

2.2.2 Large scale neutralisation experiments

The site specific study investigating the influence of pilot scale neutralisation sampled fresh AMD (toe seep AMD) from Landau colliery and fly ash from Arnot power station. A volume of 200 L of AMD was added to the tank and stirred to equilibrate. A mass of 33 kg of fly ash was added to the AMD and the mixture was stirred. Electrical conductivity (EC) and pH were monitored at regular time intervals with a portable Hanna pH/EC/TDS/Temperature meter.

2.3 RESULTS

2.3.1 Analyses of AMD's used

It is necessary to determine the quality of an AMD sample prior to use in order to be able to compare it with the quality of the post-process water. By comparing the same AMD sampled at different times (Table 2.1) the variation in quality can be seen (also see Section 10.3 for long-term variation of AMD quality). Sulphate concentration can vary by a large margin and

even by orders of magnitude. The pH values of waters tend to be in the range between 2 and 3, although some concentration events can occasionally cause a pH lower than 2 as with Kromdraai AMD. EC and pH are proportional with a lower pH producing a higher EC and, consequently, dissolved solids. Some AMD waters tested had a low pH but very little buffering capacity due to lower Al and Fe content. The AMD feed water quality will have a significant impact on the operational parameters chosen during neutralisation, as these studies show.

Table 2.1: AMD's used for different batches of experiments.

	Krom	Brug 1	Nav 1	Bank 1	Landau	Brug 2	Nav 2	Bank 2
pH	1.89	2.91	2.35	2.25	2.60			
EC (mS/m)	1 252	991	906	1 085	752			
Acidity (mg/L)	9 500	500	7 000	7 000				
TDS (mg/L)	16 735	8 975	16 765	19 410				
Cl^- (mg/l)					4.10			
SO_4^{2-} (mg/l)	10 200	1 450	5 600	11 750	1 380	7 500	13 500	11 800
Al^{3+} (mg/l)					0.20	59.56	1 021	1 116
Fe^{tot} (mg/l)					5.00	279.2	5 177	6 231
Fe^{2+}	2 206	84	3 211	2 066		153.1	3 725	2 886
Mn^{2+}						32.03	213.6	230.4
NO_3^- (mg/L)	40	7.3	35	5.0				

Note: Krom = Kromdraai; Brug = Brugspruit; Nav. = Navigation

The AMD used for each batch of experiments was analysed by ICP-MS (Table 2.1). Brugspruit 1, Navigation 1, Bank 1 and Kromdraai AMD's were used to investigate their treatment with fly ash (FA) from Arnot, Duvha, Matla, Hendrina and Kendal power stations in the first of the small scale experiments and Turbulator experiments. Brugspruit 2, Navigation 2 and Bank 2 AMD's were used in the second set of small scale neutralisation experiments. The Landau AMD was used in pilot scale experiments where it was neutralised with of AMD fly ash from Arnot.

Table 2.2: Chemical and physical characteristics of Navigation AMD.

Parameter (mg/L)	Navigation AMD	Parameter (mg/L)	Navigation AMD
pH	2.78	SO_4^{2-}	24 880
EC (mS/cm)	13.71	Cl^-	370.0
Acidity (mg/L $CaCO_3$)	14 450	NO_3^-	90.00
TDS	16 765	B	10.30
Al	453.4	Ba	0.108
Ca	146.9	Cu	7.100
Fe^{2+}	4 445	Mn	95.80
Fe^{3+}	2 066	Mo	0.014
K	BDL	Ni	6.160
Mg	399.4	Se	10.39
Na	102.9	Sr	1.950
Si	99.20	Zn	15.71

Table 2.2 details the analysis of Navigation AMD used for the sequential extraction experiments detailed in Section 3.3.6.

There is considerable variation in AMD samples from the same place and even within the same sample. Analysing the same sample twice may not yield similar results as the chemistry of AMD changes with time. Thus general conclusions must be made based on the magnitude of the reduction in dissolved elements and ions.

2.3.2 Small scale and Turbulator neutralisation experiments site specific to Bank and Kromdraai collieries and Arnot, Duvha, Matla, Hendrina and Kendal power stations

The small scale experiments were performed in beakers in the laboratory while the larger-scale experiments were carried out using a metal container with a capacity of approximately 75 L and an overhead stirrer, called a Turbulator. The difference between the pH values of the three fly ashes reacted with Kromdraai AMD (Figure 2.1) is a result in the difference in particle size (discussed in Section 3) with Duvha ash being the smallest and Matla the largest. Arnot and Duvha ashes eventually reach the same pH and EC. The reaction between Kromdraai AMD and Duvha fly ash proceeds at a much faster rate.

The pH is increased and the EC decreased more rapidly than for the reactions with fly ash of greater particle size. This physical difference in ash particle size affects their neutralising capacity and as a result the EC is not reduced to the same level as that for finer ashes.

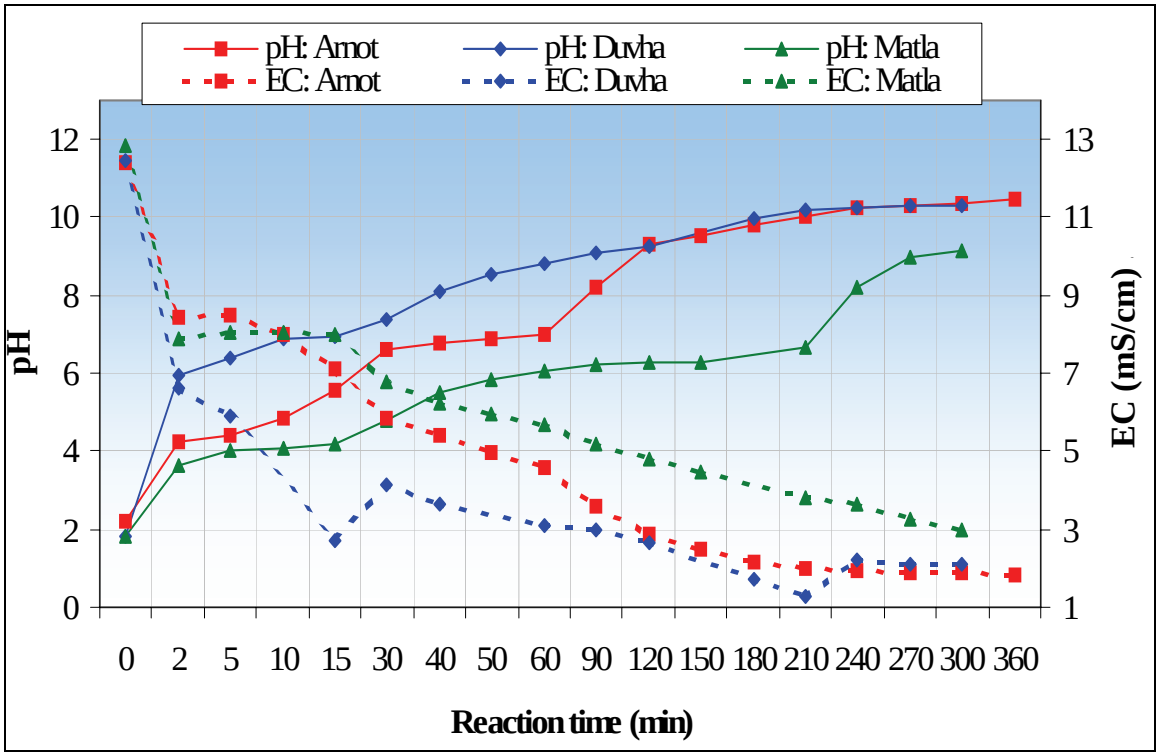

Figure 2.1: pH and EC for the reactions between Kromdraai AMD and Arnot, Duvha and Matla FA in a solid to liquid ratio of 1:3.

Neutralisation reactions between Bank AMD and Hendrina FA and Duvha FA and Kendal FA and Kromdraai AMD, are shown in Figure 2.2. At a 2:1 FA:AMD ratio the reaction between Kendal FA and Kromdraai AMD reaches a maximum pH of 4.33. This indicates that Kendal ash is less suitable for the neutralisation of AMD under these conditions; however the EC was considerably reduced. A 2:1 ratio of Hendrina FA and Bank AMD only reaches a pH of 8.6 after 240 min. The neutralisation reaction between Bank AMD and Duvha FA takes a

long period of time to reach a pH of 10, relative to other reaction with a lower FA:AMD ratio (Figure 2.3). This indicates that Bank AMD has a large amount of acidity and that it contains more contaminants than Kromdraai AMD. The analyses of these waters show that Bank AMD has a high amount of SO_4^{2-} and TDS.

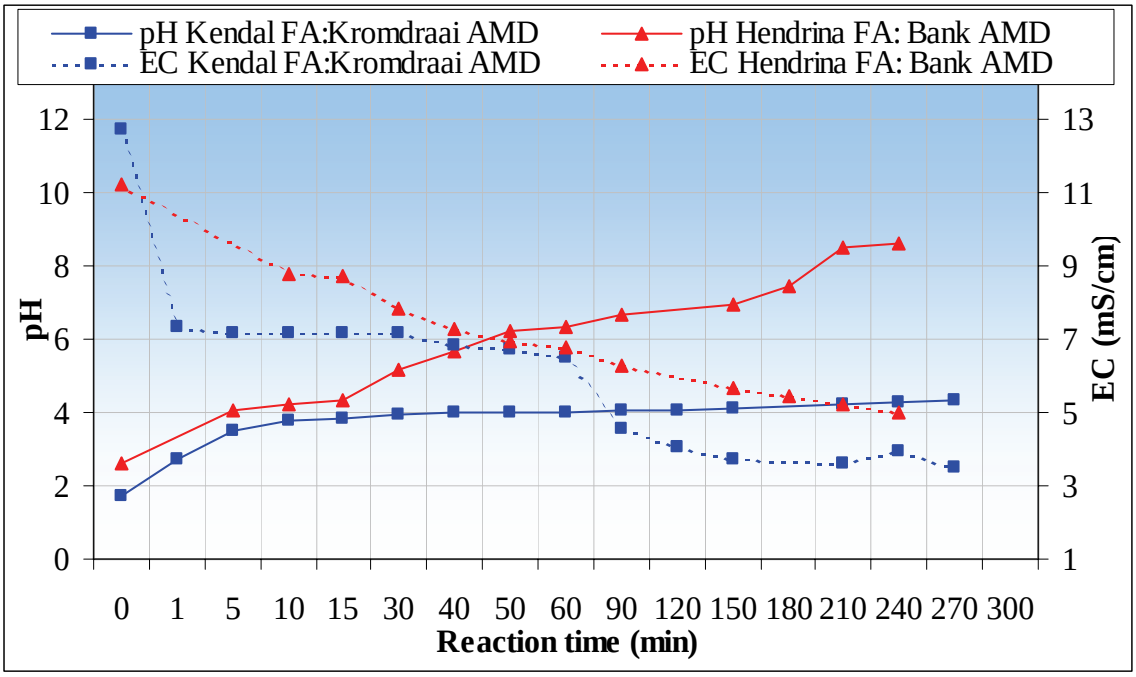

Figure 2.2: pH and EC for the reactions between Kendal FA and Kromdraai AMD and between Hendrina FA and Bank AMD at a ratio of 2:1.

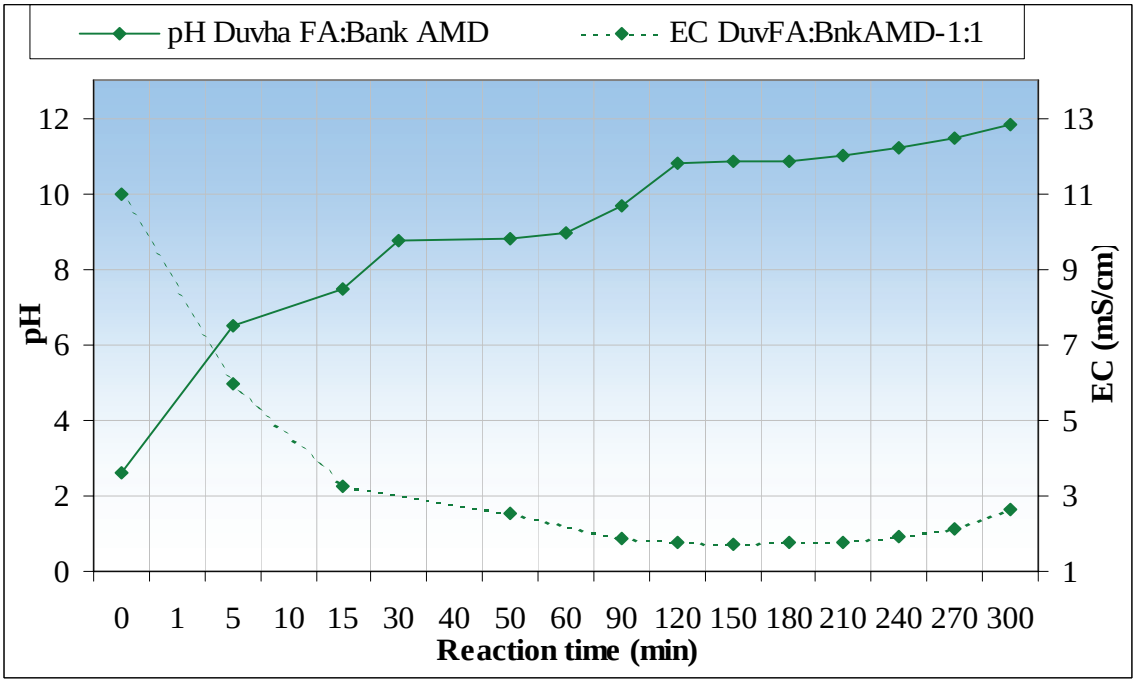

Figure 2.3: pH and EC for the reactions between Duvha FA and Bank AMD at a ratio of 1:1.

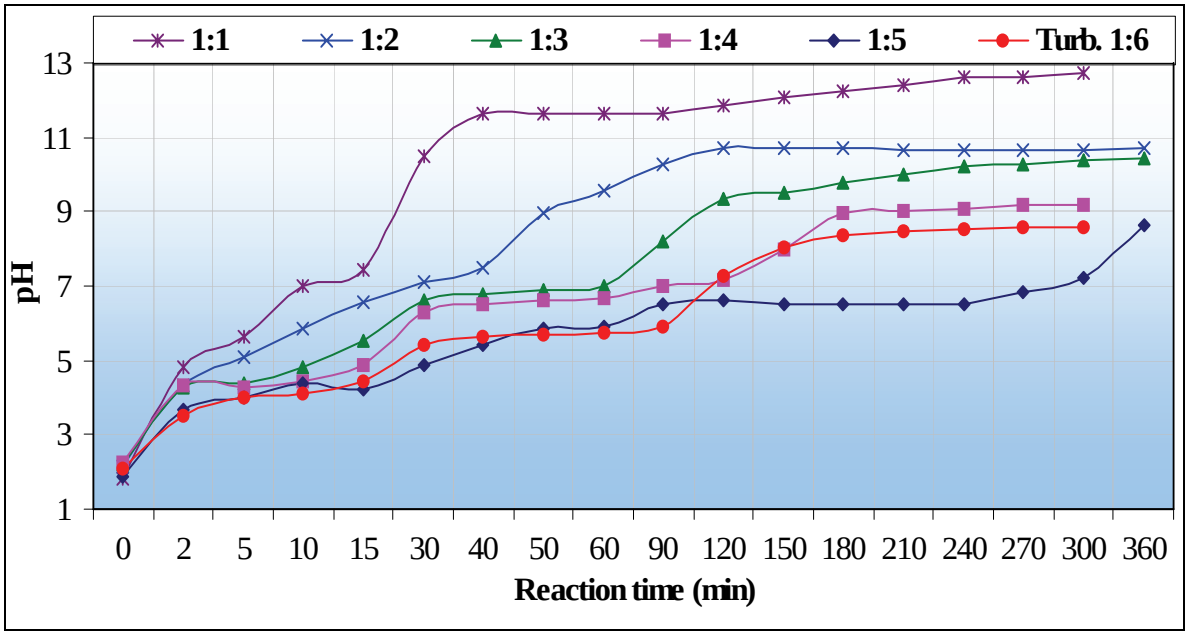

Figure 2.4: pH of Kromdraai AMD reacted with Arnot FA with the ratios representing solid to liquid (FA:AMD) ratios (Turb. 1:6 indicates the reactions performed in the large scale Turbulator rig).

Figure 2.4 gives the pH results of the effluent recovered at different times from the neutralisation reactions of Kromdraai AMD and Arnot FA at different ratios of FA to AMD. The ratios in Figure 2.4 descend in pH according to amount of ash used, as expected, with the highest pH corresponding to the greatest amount of ash (FA:AMD ratio = 1:1) and the lowest pH corresponding to the lowest ratio performed in the open beaker tests (FA:AMD ratio = 1:5). The large scale reaction performed in the Turbulator with a ratio of 1:6 reached a higher pH than the open beaker ratio of 1:5, showing the effect of agitation rate.

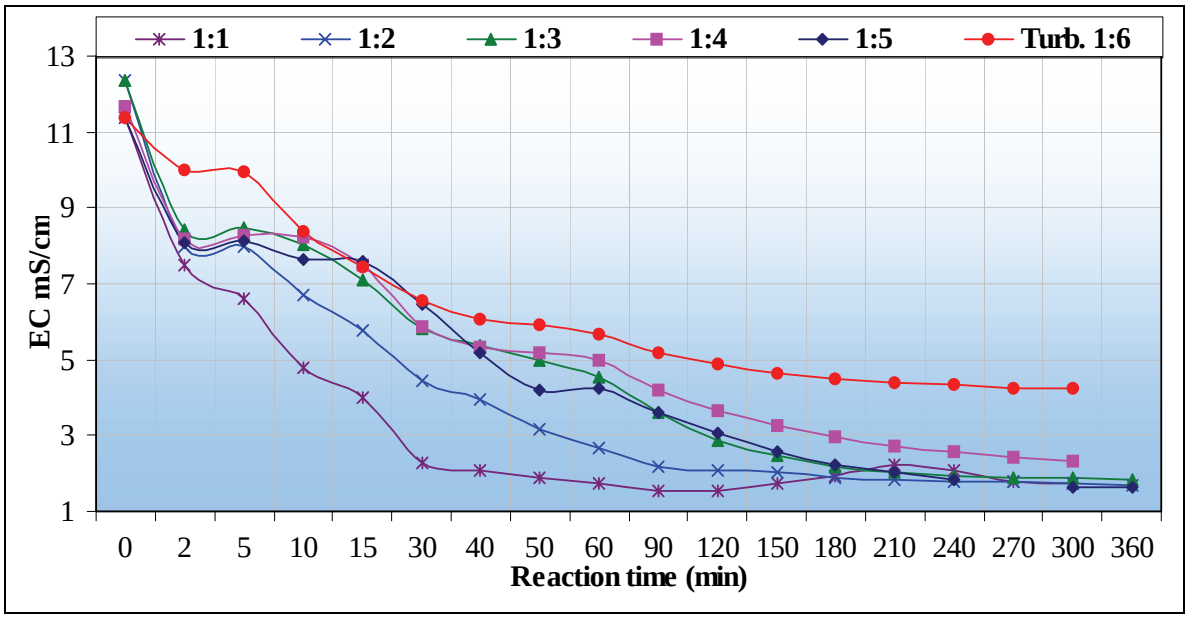

Figure 2.5: EC of Kromdraai AMD reacted with Arnot FA with the ratios representing solid to liquid (FA:AMD) ratios.

Figure 2.5 shows the EC values of the effluent recovered at different times from the neutralisation reactions of Kromdraai AMD and Arnot FA at different ratios of FA to AMD.

The 1:1 FA:AMD ratio has the lowest EC at 300 min, which is below 2 mS/cm, while the reaction performed in the Turbulator at 1:6 FA:AMD has the highest EC at 300 min of approximately 4 mS/cm.

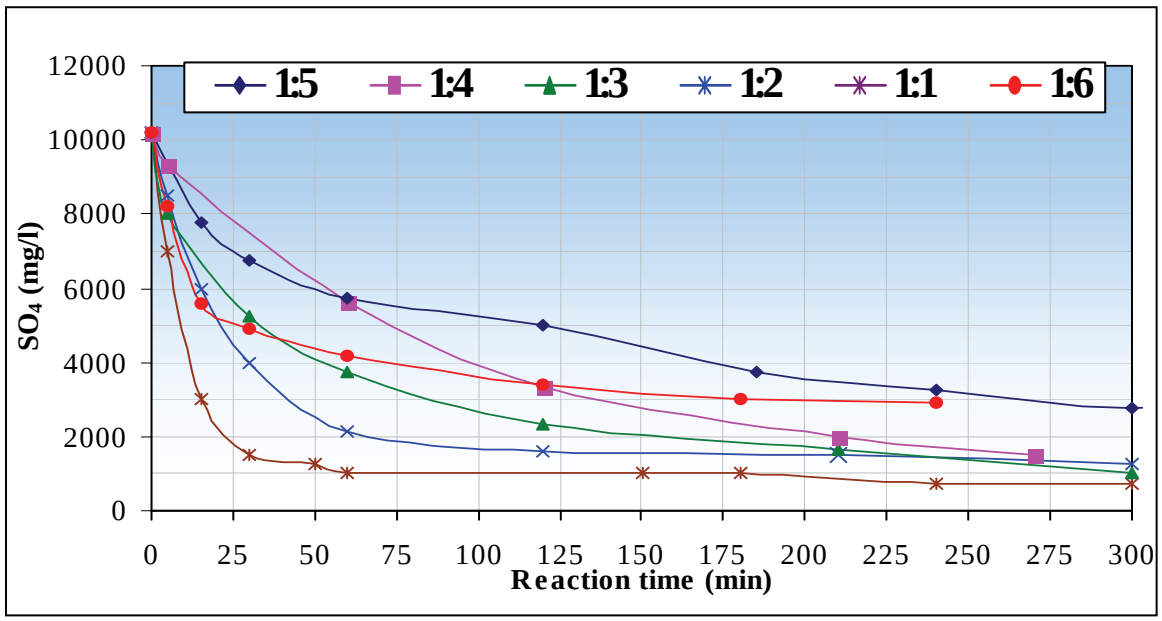

Figure 2.6: SO_4 concentrations of Kromdraai AMD reacted with Arnot FA with the ratios representing solid to liquid (FA/AMD) ratios.

Figure 2.6 shows the SO_4 concentrations of the effluent recovered at different times from the neutralisation reactions of Kromdraai AMD and Arnot FA at different ratios of FA to AMD. At 300 min the SO_4 concentrations drop below 1000 mg/L for the FA/AMD ratio of 1:1. At this time the SO_4 concentrations of the 1:2, 1:3 and 1:4 FA/AMD ratios all reach values of around 1500 mg/L. The lower FA/AMD ratios of 1:5 and 1:6 in the Turbulator have the highest SO_4 concentrations of 3000 mg/L.

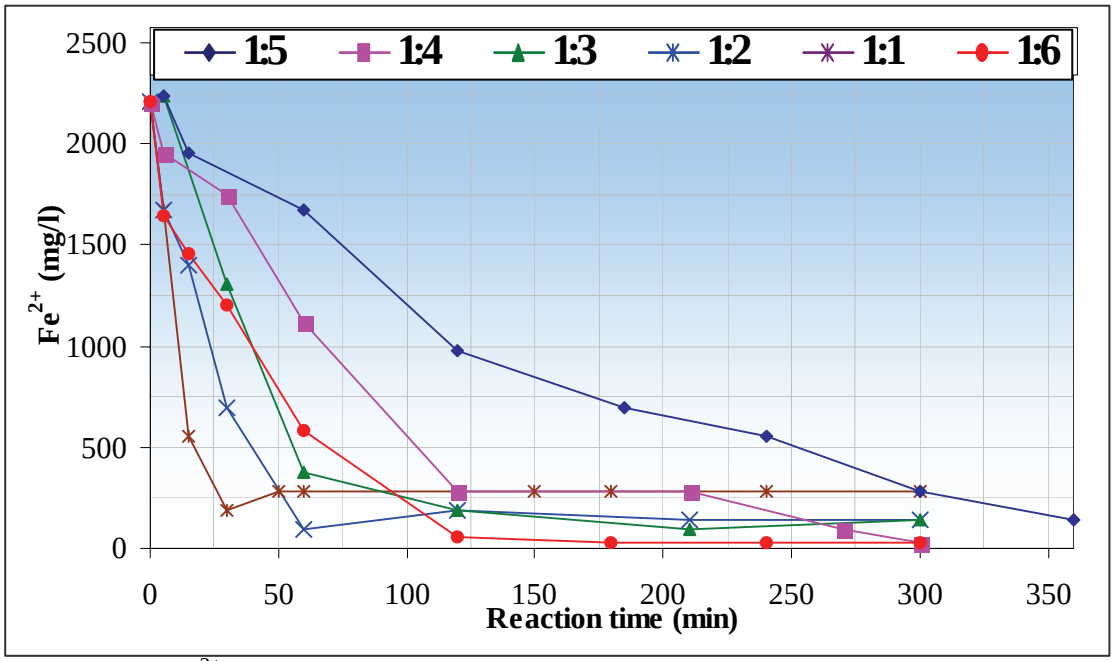

Figure 2.7: Fe^{2+} concentrations of Kromdraai AMD reacted with Arnot FA with the ratios representing solid to liquid (FA/AMD) ratios.

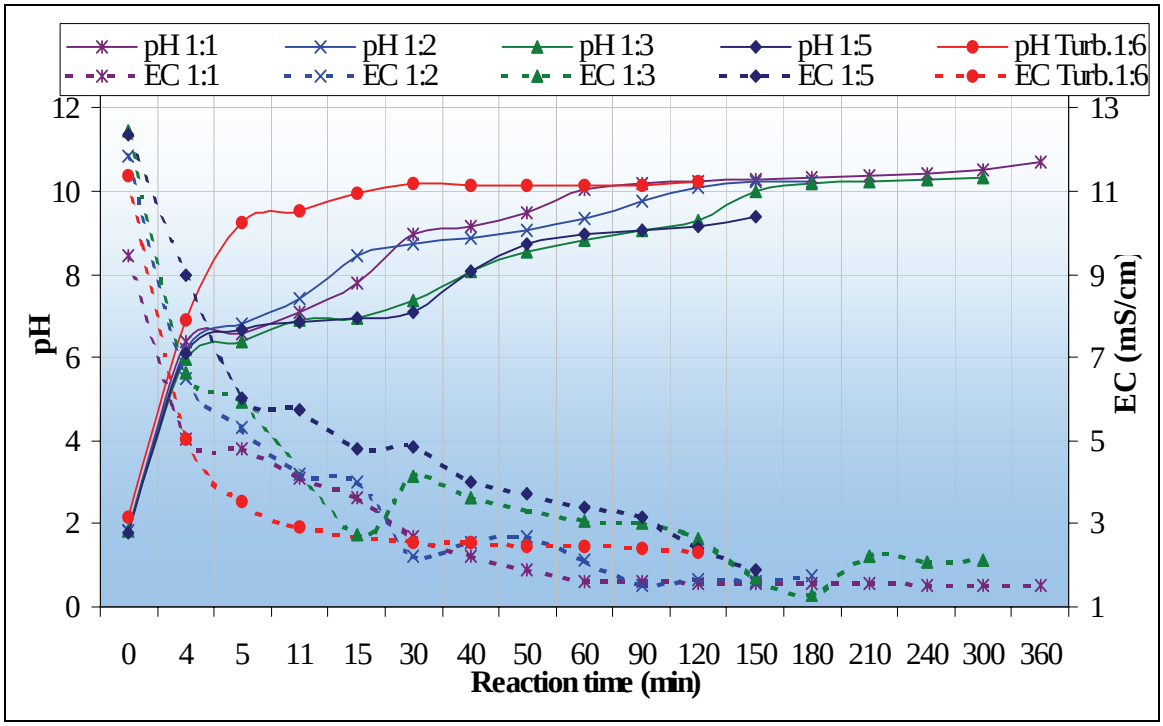

Figure 2.8: Small scale neutralisation of Kromdraai AMD with Duvha fly ash. Ratio 1:6 performed in a Turbulator.

Figure 2.7 shows the Fe^{2+} concentration for the effluent from the reactions between Kromdraai AMD and Arnot FA. The experiment with a FA/AMD ratio of 1:6 that was carried out in the Turbulator has the lowest Fe^{2+} concentrations of approximately 30 mg/L. The Fe^{2+} concentrations decrease at a slower rate with lower FA/AMD ratios. The Fe^{2+} concentration in a solution is largely a factor of the availability of O_2. This can be seen clearly in the difference in Fe^{2+} concentrations between the FA/AMD ratios of 1:5 and 1:6, which was conducted in the Turbulator.

In Figure 2.8 the result of adequate aeration due to effective agitation can be clearly seen. The FA:AMD ratio 1:6 was performed in a Turbulator and can be seen to proceed at almost double the rate of the reactions conducted in a beaker. It takes the 1:6 ratio reaction that was agitated only 15 min to reach a pH of 10 while it takes the 1:1 ratio reaction 60 min and the other ratios between 120 and 150 min to reach the same pH.

2.3.3 Small scale neutralisation experiments site specific to Matla and Arnot power stations and Brugspruit, Navigation and Bank collieries

The pH and EC trends of three of the neutralisation experiments at a solid to liquid ratio of 1:3 are shown in Figure 2.9. Strong buffering can be seen at pH 6, this could be a result of high concentrations of Fe^{2+} in the Navigation AMD. The pH of the sample of Brugspruit AMD obtained in this case, increases very quickly with the addition of Matla FA and the EC does not decrease by a large amount. Buffering is thus the result of high concentrations of Fe^{2+} in the Navigation AMD. In the sample of Brugspruit AMD which had a much lower Fe^{2+} concentration of 153, the pH increased very quickly with the addition of Matla FA while the EC did not decrease significantly and no buffering region was observed. Matla FA does not appear to have a high amount of alkalinity judging by the pH curve of the reaction between Matla FA and Navigation AMD. Furthermore, if the rapid pH increase in the Brugspruit AMD were due to the alkalinity of Matla FA, there would be a greater decrease in

the EC. Thus, the rapid increase in pH and low decrease of EC suggests that Brugspruit AMD is low in acidity and dissolved metals, with concomitant low buffering capacity. These results indicate that the neutralisation capacity of FA is combination specific and that the EC reduction is more significant in cases where the Fe^{2+} content of the AMD is higher.

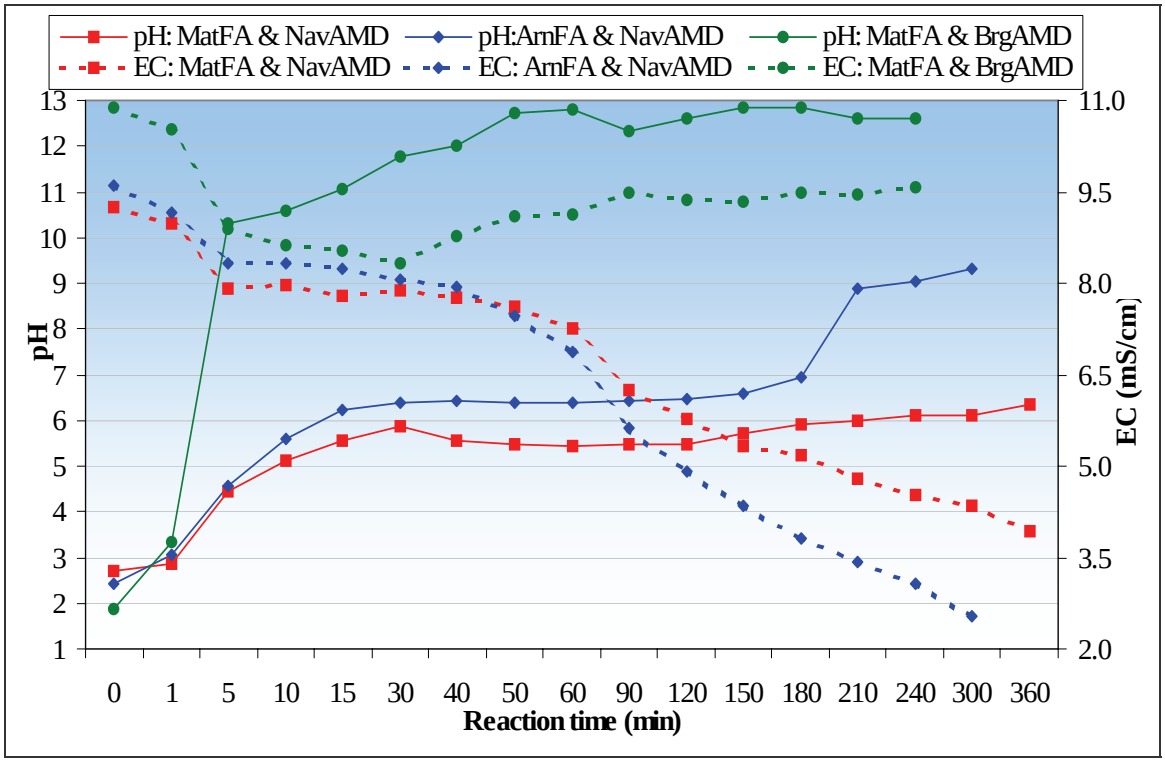

Figure 2.9: pH and EC for the reactions between Matla, Arnot FA and Navigation AMD, and Matla FA and Brugspruit AMD in a solid to liquid ratio of 1:3.

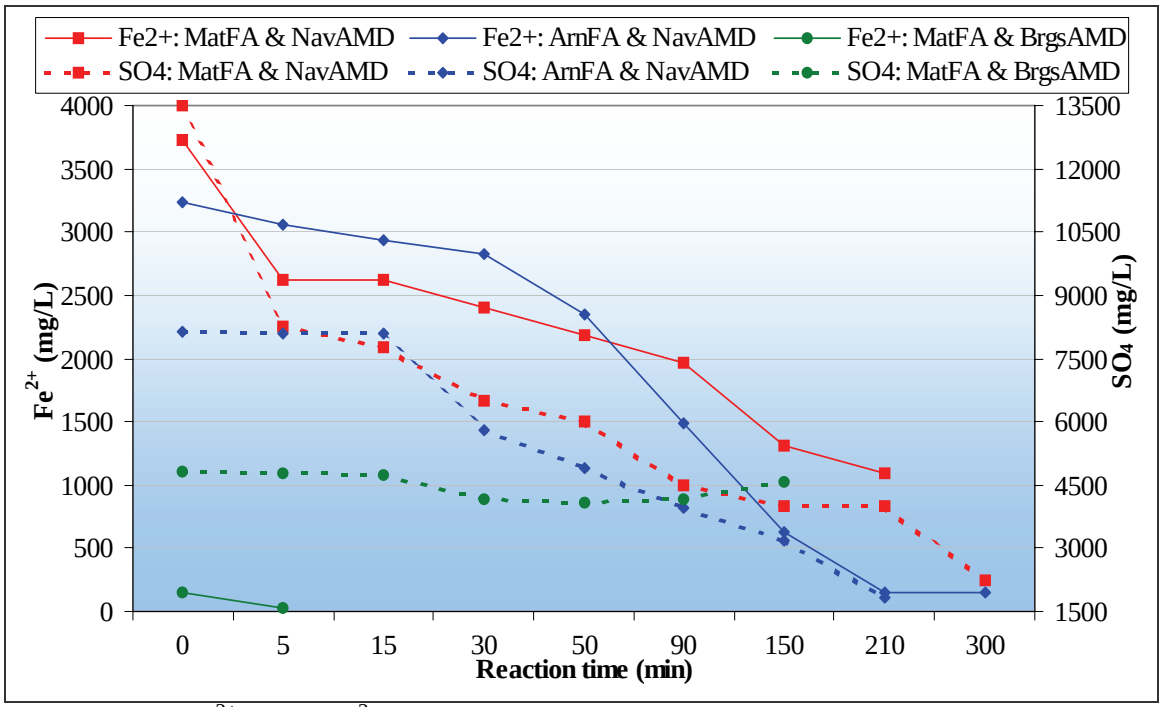

Figure 2.10: Fe^{2+} and SO_4^{2-} concentrations for the reactions between Matla, Arnot FA and Navigation AMD, and Matla FA and Brugspruit AMD in a solid to liquid ratio of 1:3.

The SO_4^{2-} and Fe^{2+} concentrations for the neutralisation reactions conducted are shown in Figure 2.10. The concentration of SO_4^{2-} from AMD follows the same trends found in the other studies and decreases to values around 2000 mg/L. Fe^{2+} removal approaches zero for the reaction between Matla FA and Brugspruit AMD.

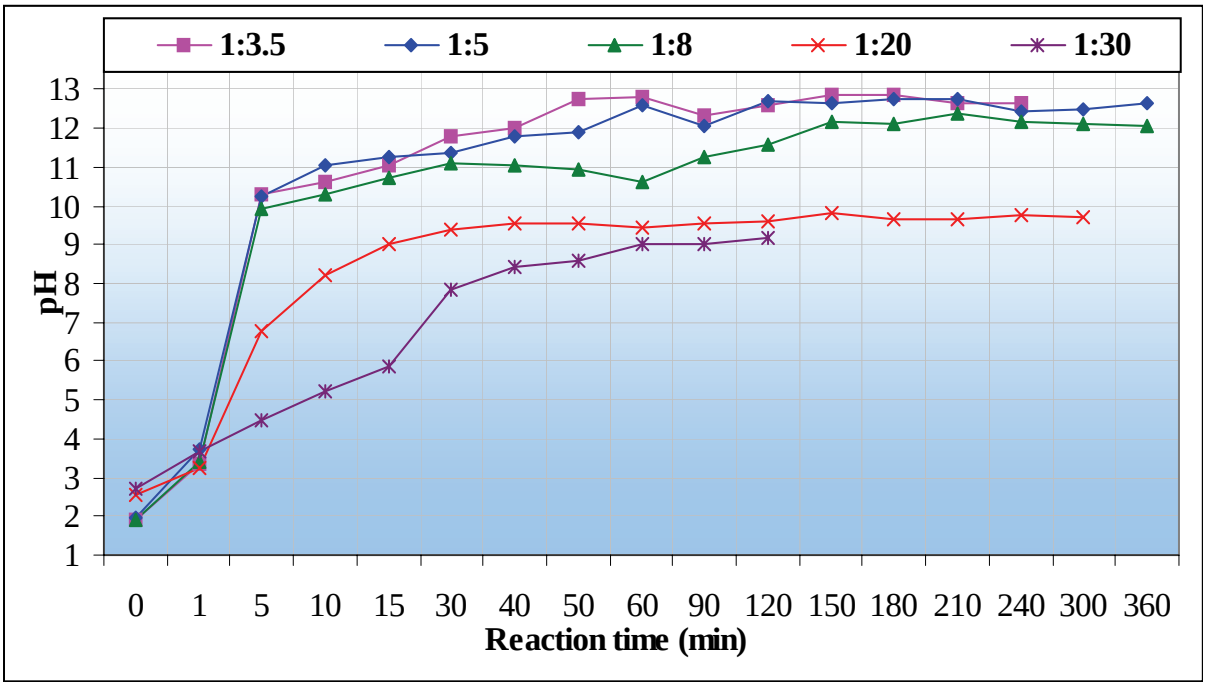

Figure 2.11: pH for different Matla FA: Brugspruit AMD ratios.

The pH reaches above-neutral values at low ratios of 1:30 (Figure 2.11) for different Matla FA: Brugspruit AMD ratios; this means that less fly ash could be used to achieve neutralisation in some cases. The reactions with ratios of FA:AMD between 1:3.5 and 1:8 allowed highly alkaline values of pH (pH >12) to be obtained. The less FA used, the less the EC decreased. This is visible in Figure 2.12, where the EC only reaches minima of 8.5 – 9 mS/cm. After 120 min the further increase in the EC is probably a result of the OH^- ion or the re-dissolution of $Al(OH)_3$. It is expected that a longer reaction time would result in lower EC as was indicated above.

The hydrolysis of AMD constituents such as Fe^{3+}, Al^{3+}, Fe^{2+} and Mn^{2+} offsets the pH increase attributed to the dissolution of the oxide components. The relative quantities of soluble bases (oxides) in FA and hydrolysable constituents in AMD dictate whether the final solution at a given contact time will have a dominant acid or basic character. The two factors that dictate the nature of the final solution in these neutralisation reactions are the FA: AMD ratio and the contact time of the reaction.

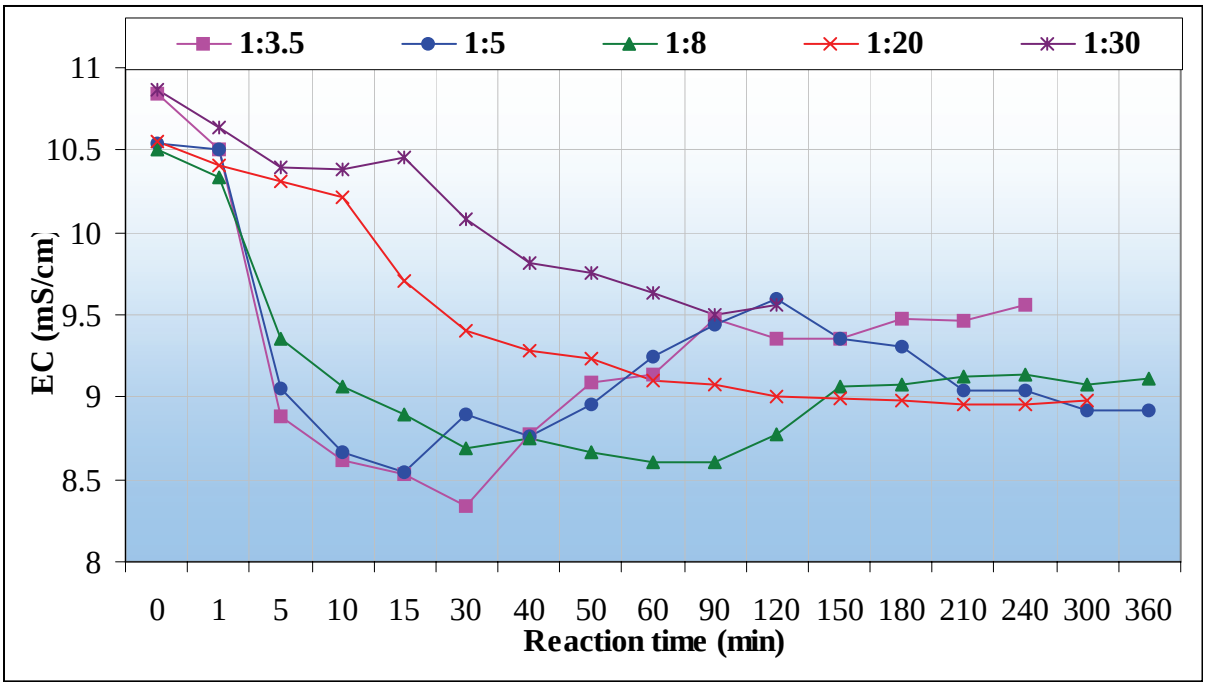

Figure 2.12: EC for different Matla FA: Brugspruit AMD ratios.

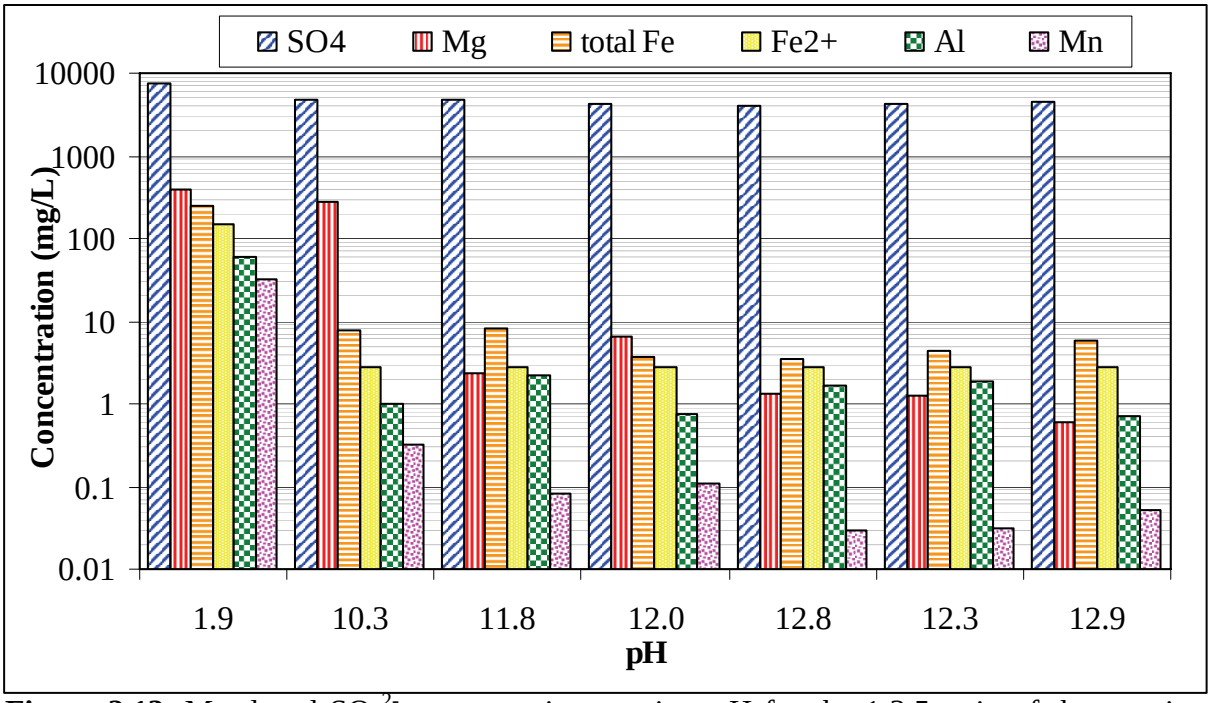

Figure 2.13: Metal and SO_4^{2-} concentrations against pH for the 1:3.5 ratio of the reaction between Matla FA and Brugspruit AMD.

decreases significantly between pH 10.3 and 11.8. Sulphate, however, only decreases from 7500 to 4592 mg/L for this combination.

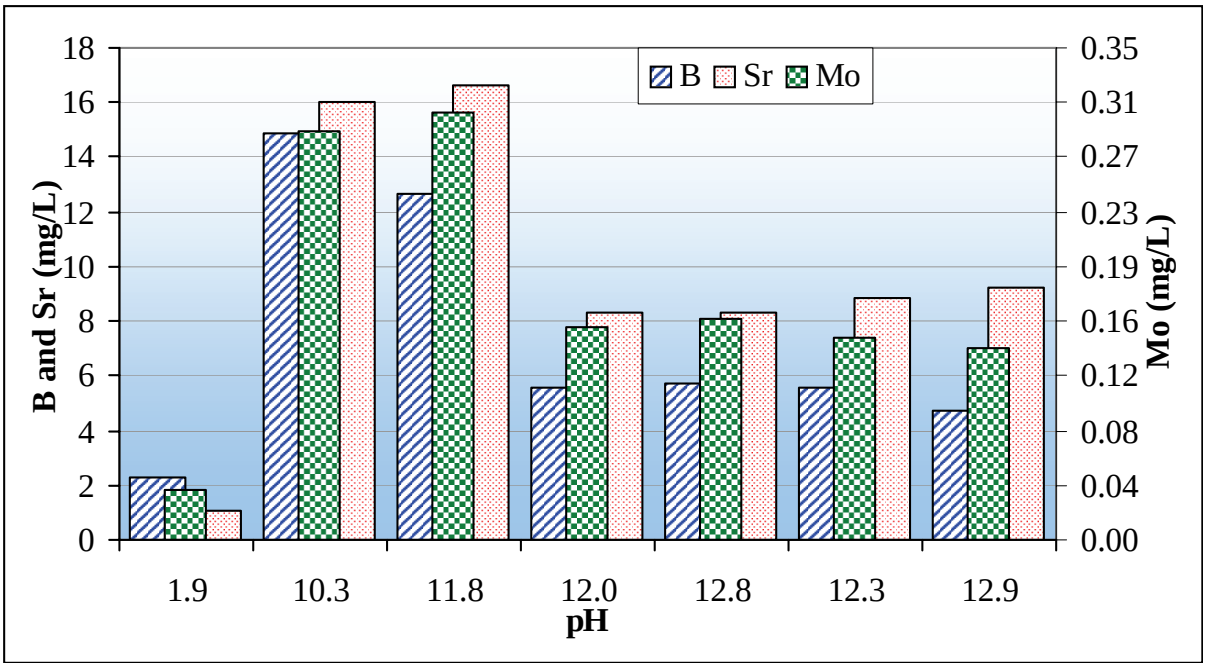

Figure 2.14: Metal concentrations for 1:3.5 ratio against pH of Matla FA reacted with Brugspruit AMD.

Figure 2.14 shows the concentrations of B, Sr and Mo in the initial AMD and in samples taken after neutralisation has occurred at high pH values in the reaction between Matla FA and Brugspruit AMD at a FA:AMD ratio of 1:3.5. The concentration of these elements is high for the samples taken at pH 10.3 and 11.8 and then decreases with pH increase. The concentration of Mo increases from <0.05 mg/L to 0.3 mg/L and then decreases to 0.136 mg/L. The concentration of B increases from ~ 2 mg/L to 15 mg/L and then decreases to 4.7 mg/L. The concentration of Sr increases from ~ 2 mg/L to 17 mg/L and then decreases to 9.3 mg/L. These elements are the main elemental contribution from the ash being used as ameliorant. Since no studies have as yet been performed it is not clear what elemental contribution the use of limestone makes to the process water

2.3.4 Small scale neutralisation experiments site specific to Arnot power station and Navigation colliery to investigate mineral equilibria

The evolution of pH values with time for the 1:3 and 1:1.5 (FA:AMD) ratios is presented in Figure 2.15. The pH values for the 1:3 ratio are characterised by two buffer regions, at pH 4 - 4.5 and pH 6.0. The 1:1.5 ratio shows two buffer regions, at pH 4.5 - 5.0 and at pH 9.0. The buffering exhibited by the AMD at the 1:1.5 ratio is stronger. This is evidenced by the lower gradient of the curves at these buffer regions. The buffering region at pH 9.0 is absent in the 1:3 ratio since the system did not attain pH 9.0 within the contact time investigated. The buffering region at pH 9.0 for 1:1.5 ratio could be attributed to the formation of soluble hydrous complexes by cations such as $Al(OH)_4^-$ at high pH (Ricoh *et al.*, 1999). There are two opposing processes that establish the pH value for the solution in this neutralisation process. The dissolution and hydrolysis of oxide components such as CaO and MgO (equations 1 and 2) from fly ash contributes to an increase in solution pH.

$$CaO + H_2O \rightarrow Ca^{2+} + 2OH^- \quad (1)$$
$$MgO + H_2O \rightarrow Mg^{2+} + 2OH^- \quad (2)$$

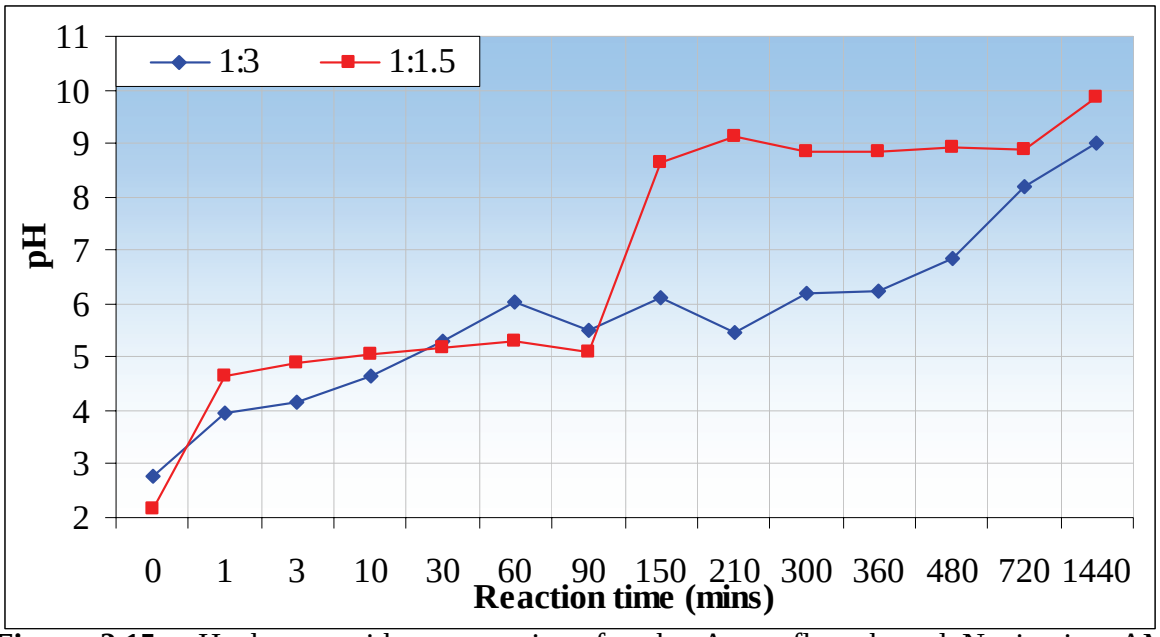

Figure 2.15: pH change with contact time for the Arnot fly ash and Navigation AMD reactions at 1:3 and 1:1.5 ratios (FA:AMD).

The hydrolysis of Fe^{3+}, Al^{3+}, Fe^{2+} and Mn^{2+} buffers the increase in pH when alkaline oxides dissolve in the acid water (Table 2.2). The relative quantities of soluble bases in fly ash and acidic metals in AMD dictate whether the final solution at a given contact time will have a dominant acid or basic character. The two factors that dictate the nature of the final solution in these neutralisation reactions are the FA:AMD ratio and the contact time of the reaction. While the 1:1.5 ratio achieves a breakthrough to alkaline pH (8.0 to 9.0) after only 120 minutes, the 1:3 ratio achieves the same breakthrough after 1440 minutes. This confirms the importance of the amounts of available soluble oxides in controlling the pH of the process waters.

Figure 2.16 shows the SO_4^{2-} trends for the reactions between Arnot fly ash and Navigation AMD for a 24 hour reaction time. Navigation AMD samples were characterised by high SO_4^{2-} levels (24880 mg/L). A decreasing SO_4^{2-} concentration to a minimum was observed with time for both FA:AMD ratios. A sharp decrease was observed when the mixture attained pH 5.5 for ratio 1:1.5. At pH > 6.0 Fe^{2+} oxidation occurs and iron hydroxides that precipitate out are known to adsorb high concentrations of sulphates (Rose and Elliot, 2000). XRD and SEM-EDX detected gypsum in solids collected for all the contact times indicating that it had control on SO_4^{2-} levels.

Doubling the mass of fly ash relative to the volume of AMD did not result in increase of final SO_4^{2-} levels, which further confirms presence of solubility control. At pH 8.00 (AN13) and 9.20 (AN115), SO_4^{2-} levels were observed to increase and then decrease between 720-1440 minutes. Formation of ettringite ($3CaO.Al_2O_3.3CaSO_4.32H_2O$) could account for the decrease at this pH. Ettringite was identified by SEM-EDX in solid residues collected at pH>9.0.

The sulphate concentration decreased gradually and did not vary significantly between the two ratios for the first 60 minutes of contact (Figure 2.16). However, as the mixture attained pH 5.5, the ratio 1:1.5 exhibited a sharp reduction in SO_4^{2-} concentration, stabilising at 3178

mg/L after 150 minutes of contact. A significant reduction was also observed when the ratio 1:3 mixture attained pH 6.0, stabilising at 7000 mg/L. The sharp reduction observed for the two ratios corresponds to the pH for optimum oxidation of Fe^{2+}. Iron oxyhydroxides that precipitate out on oxidation of Fe^{2+} and hydrolysis are known to adsorb or incorporate high concentrations of SO_4^{2-} (Rose and Elliot, 2000). Gypsum was detected by XRD and SEM-EDX for all the solid residues collected at all contact times investigated. The calculation of saturation indices shows saturation with gypsum at contact times of 3 to 210 minutes. Formation of gypsum could probably account for the initial gradual decrease in SO_4^{2-} concentrations.

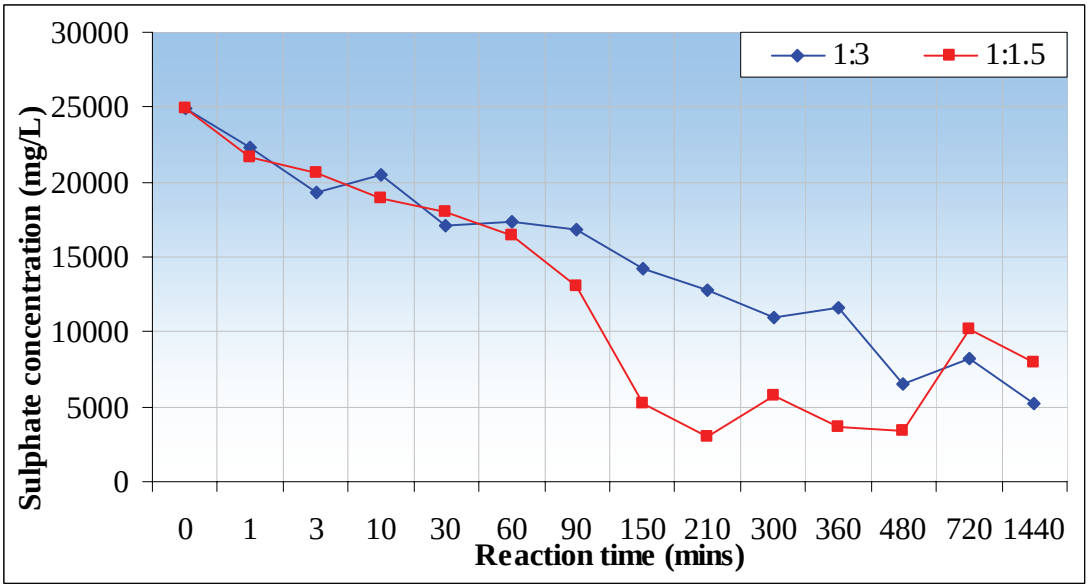

Figure 2.16: Sulphate concentrations in process water for the reactions between Arnot fly ash and Navigation AMD at 1:3 and 1:1.5 ratios (FA:AMD).

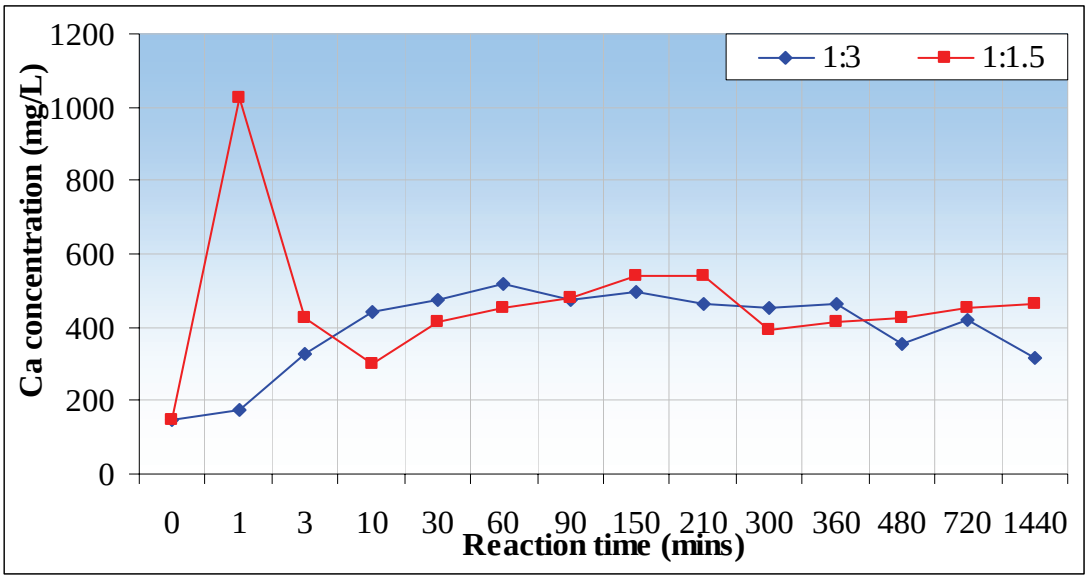

Figure 2.17: Ca concentration in process water for the reactions between Arnot fly ash and Navigation AMD at 1:3 and 1:1.5 ratios (FA:AMD).

Figures 2.17 to 2.21 show the variation of major and minor elements concentrations in the process waters for FA:AMD ratios of 1:3 and 1:1.5. Two groups of elements are evident from the concentration profiles obtained for the two ratios. Ni, Fe, Al, B do not show

doubling of the concentration in solution with doubling of fly ash. This is an equivocal evidence for solubility control on their solution concentration for the entire contact time investigated (Reardon *et al.*, 1995). The second group of elements (Na, Ca, Ba, Mg, Sr, B, Mo, Se, Si, Mn, Zn, and Ni) show doubling of concentration in solution when the fly ash is doubled at certain contact times. This indicates development of solubility controls through dissolution kinetics or equilibrium precipitation that can be predicted by geochemical equilibrium models (Doye and Duchesne, 2003). The main feature prevalent in this group of elements is the doubling of concentration in the first 3 minutes of contact with AMD. This observation indicates that these elements could be present initially as readily soluble mineral phases or salts. New mineral phases formed as a result of the elements leaching from fly ash and interacting with species in AMD could be controlling the concentration of these elements in solution.

The concentration of Ca, Na, Ba and Sr exhibited a similar trend (Figures 2.17, 2.18, 2.19 and 2.20), initially showing an increase (after 3 minutes) for both ratios. The ratio 1:1.5 initially gave higher concentration than the 1:3 ratio which indicates that fly ash is a source of these elements. The concentrations for 1:1.5 ratio, after the initial increase, decreased to values slightly lower than the 1:3 ratio, suggesting a solubility control for these elements.

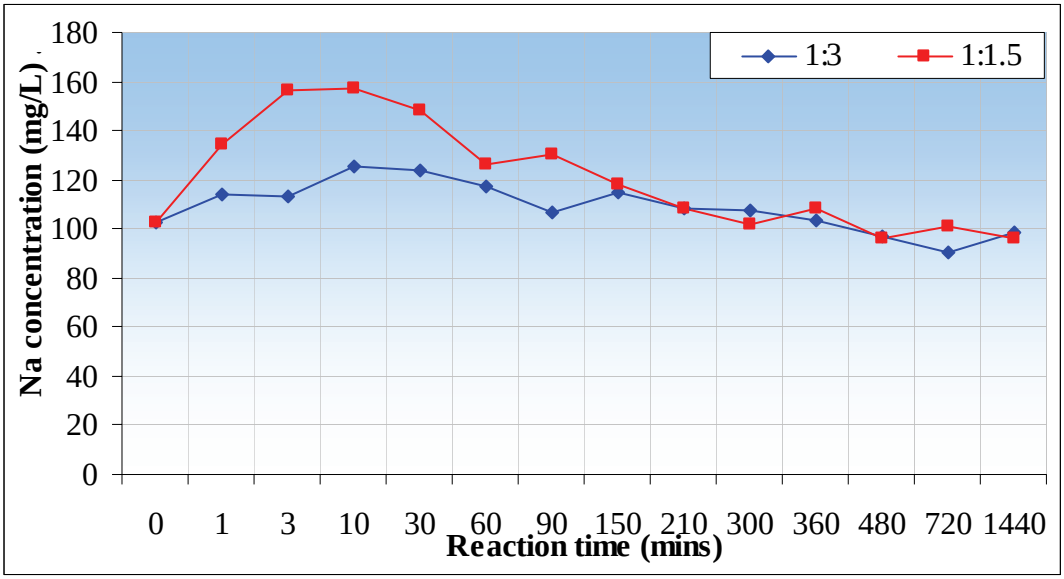

Figure 2.18: Na concentration in process water for the reactions between Arnot fly ash and Navigation AMD at 1:3 and 1:1.5 ratios (FA:AMD).

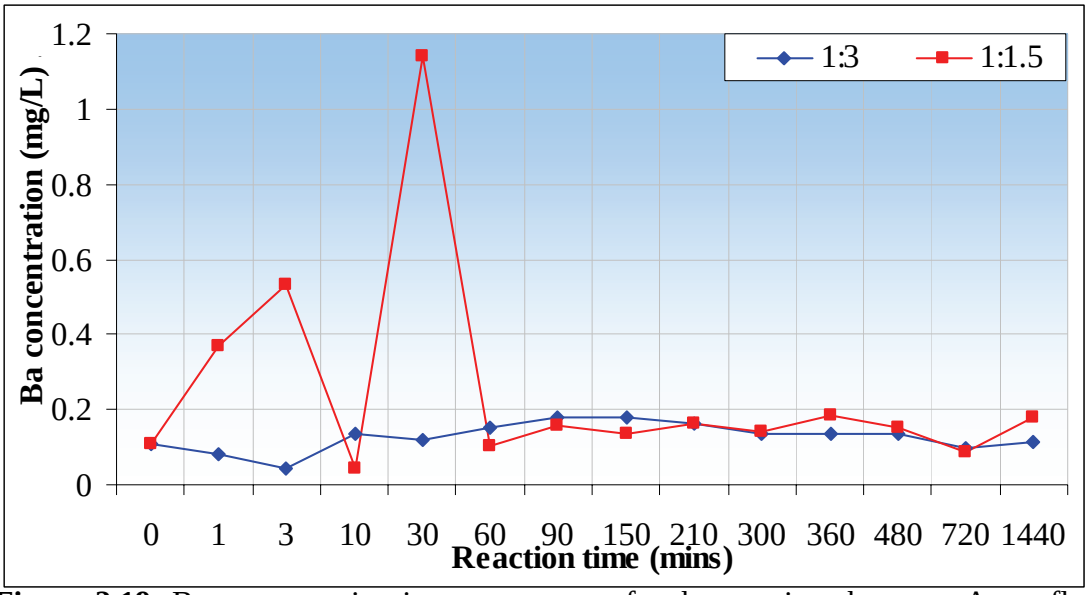

Figure 2.19: Ba concentration in process water for the reactions between Arnot fly ash and Navigation AMD at 1:3 and 1:1.5 ratios (FA:AMD).

B concentrations show pH dependence (Figure 2.21). An initial increase is observed for both ratios. This is followed by a decrease as the pH increases. The initial increase is due to dissolution of soluble surface oxide precipitates (Hullet and Weinbeger, 1980). The higher concentration observed for 1:3 ratio could indicate that B concentration is limited by the dissolution rates of its soluble oxides. Several authors have reported interaction of B with Ca at high pH (Iwashita *et al*., 2005; Kitano *et al*., 1978). Precipitating ettringite is also reported to incorporate oxyanions such as borate in alkaline solutions and could account for the decreasing B concentrations at high pH.

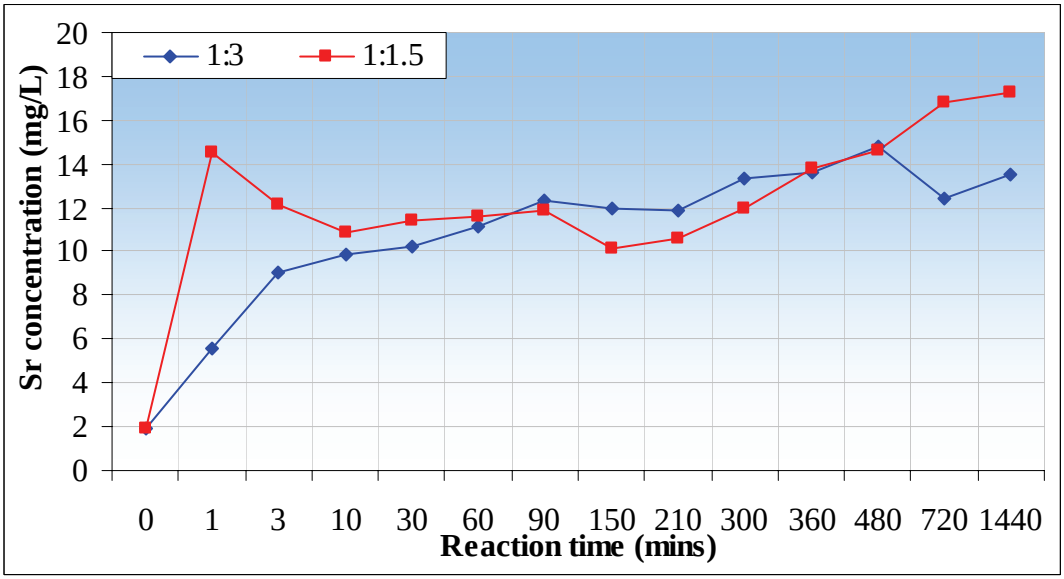

Figure 2.20: Sr concentration in process water for the reactions between Arnot fly ash and Navigation AMD at 1:3 and 1:1.5 ratios (FA:AMD).

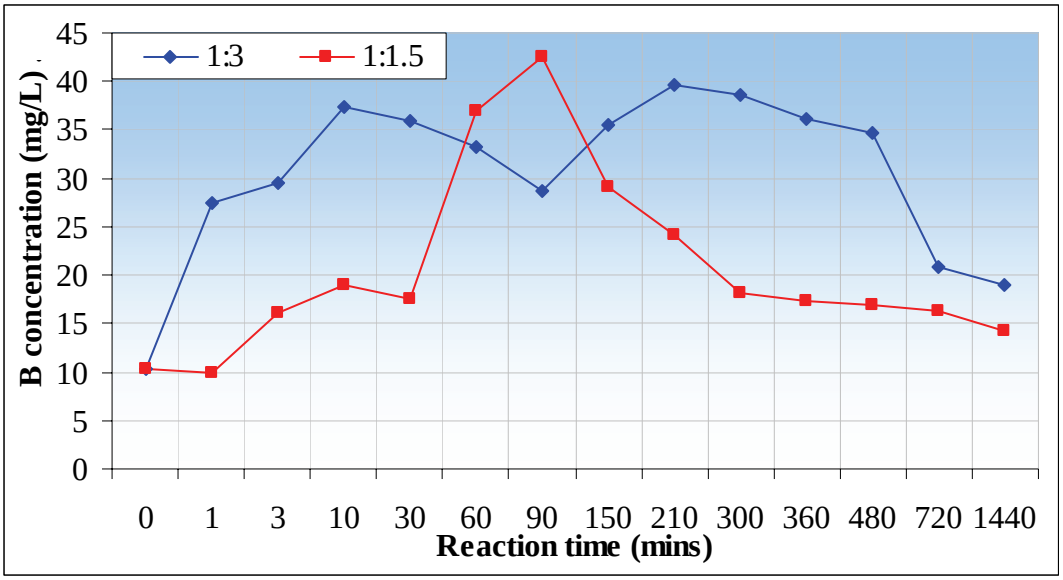

Figure 2.21: B concentration in process water for the reactions between Arnot fly ash and Navigation AMD at 1:3 and 1:1.5 ratios (FA:AMD).

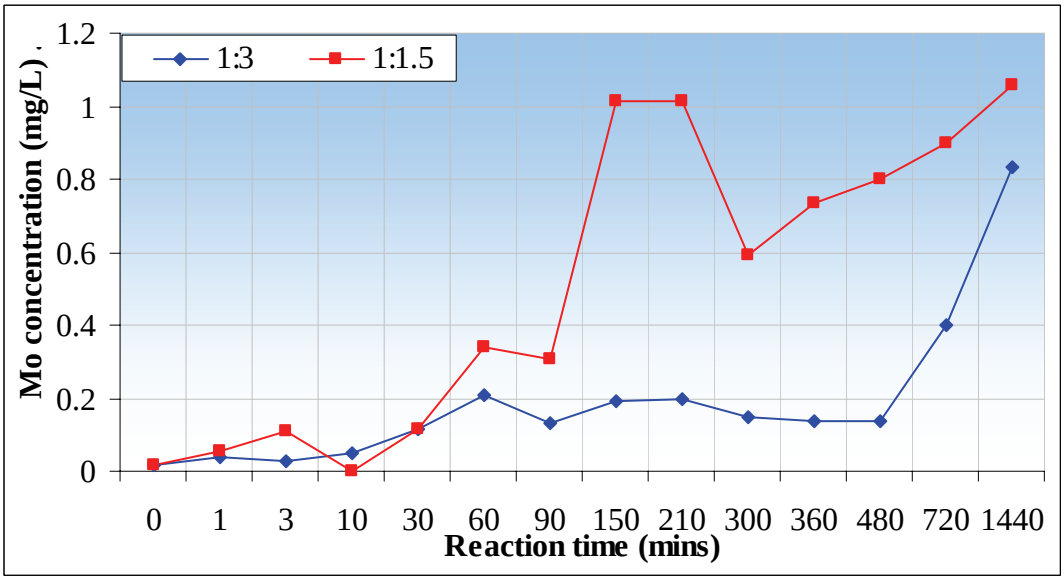

Figure 2.22: Mo concentration in process water for the reactions between Arnot fly ash and Navigation AMD at 1:3 and 1:1.5 ratios (FA:AMD).

Mo exhibited a slight increase in concentration for both ratios until pH = 6-7, when a sharp increase was observed. After 60 minutes of contact, the Mo concentrations doubled with halving of the AMD in the reaction mixture, which is a strong indication of lack of solubility control and that the main source is fly ash (Figure 2.22). Between 1 and 30 minutes of contact, the concentration for both ratios differed slightly, which could indicate presence of solubility control. Eary *et al.* (1990) observed that Mo exists as an oxyanion over most of the pH range and its concentration is likely to be controlled by metal molybdates. Observation of the Mo trends for both ratios indicates that Mo concentration increases significantly when the reaction mixture attains pH > 7 (Figure 2.22). At this pH most of the heavy metals are out of solution. Eary *et al.* (1990) report that Mo concentration could be controlled by metal

molybdates and lack of dissolved metals at high pH explains the increasing concentration of Mo.

Se concentration shows a strong pH dependence with concentration initially high at low pH decreasing to a minimum at near-neutral pH (Figure 2.23) and then showing an increase as the reaction mixture attains pH >7.0 for both ratios. The concentration for the 1:1.5 ratio was higher than the ratio 1:3 by a factor of two for the entire contact time which is a strong indication of lack of solubility control and that fly ash could have been the main source of Se. An observation of the trends for both ratios shows that the concentration starts to increase when the mixture attains pH = 7 for 1:3 ratio and pH = 9 for 1:1.5 ratio. Van der Hoek and Comans (1996) report that aluminium oxide and iron oxide have great adsorption ability for selenite and that adsorption is pH dependent. This is enhanced when mono anionic species are present ($HSeO_3^-$). An observation of the Se trends (Figure 2.23) indicates that minimum Se concentration was attained within a pH range of 4.5 to 7.0 for ratio 1:3 and 5.0 to 9.0 for ratio 1:1.5. The pKa values for selenite are 2.53 and 7.3, which corresponds closely to the pH range observed. The pH ranges correspond to the pH values at which Fe- and Al-oxyhydroxides precipitate from the AMD solution. This indicates that Se is co-precipitating with Fe and Al during the neutralisation reaction.

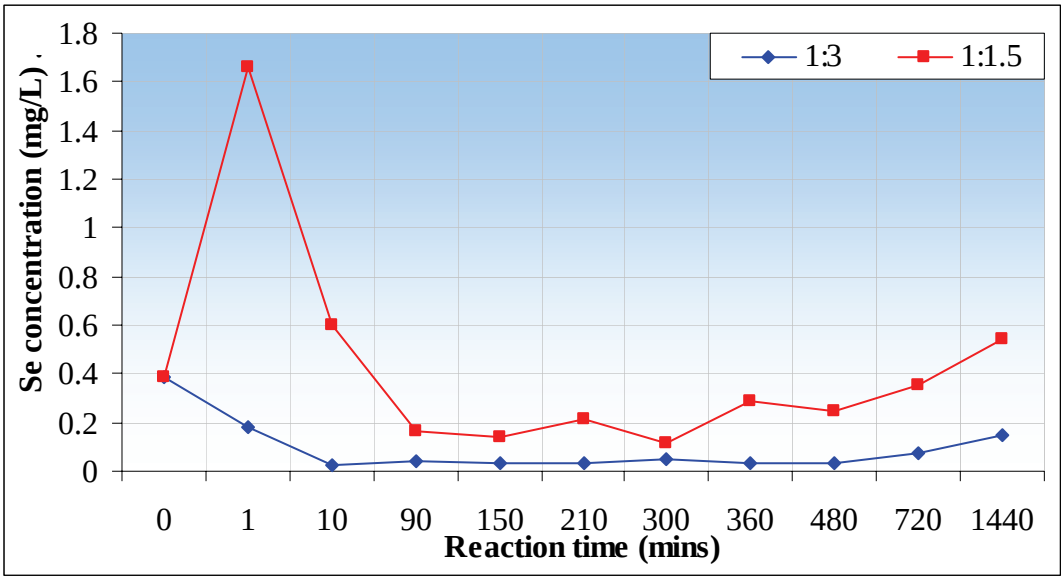

Figure 2.23: Se concentration in process water for the reactions between Arnot fly ash and Navigation AMD at 1:3 and 1:1.5 ratios (FA:AMD).

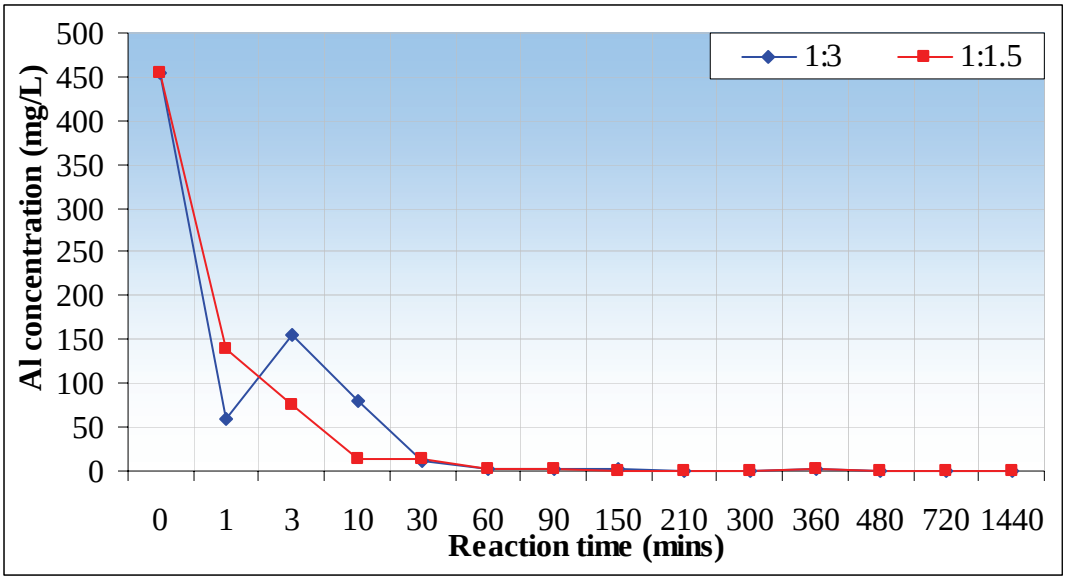

Figure 2.24: Al concentration in process water for the reactions between Arnot fly ash and Navigation AMD at 1:3 and 1:1.5 ratios (FA:AMD).

At both ratios, Al and Si decreased with increasing pH (Figures 2.24 and 2.25). The concentration decreased significantly when the reaction mixture attained pH = 5. At pH = 5.0 - 8.8 the solid $Al(OH)_3$ is most prevalent and controls Al concentration.

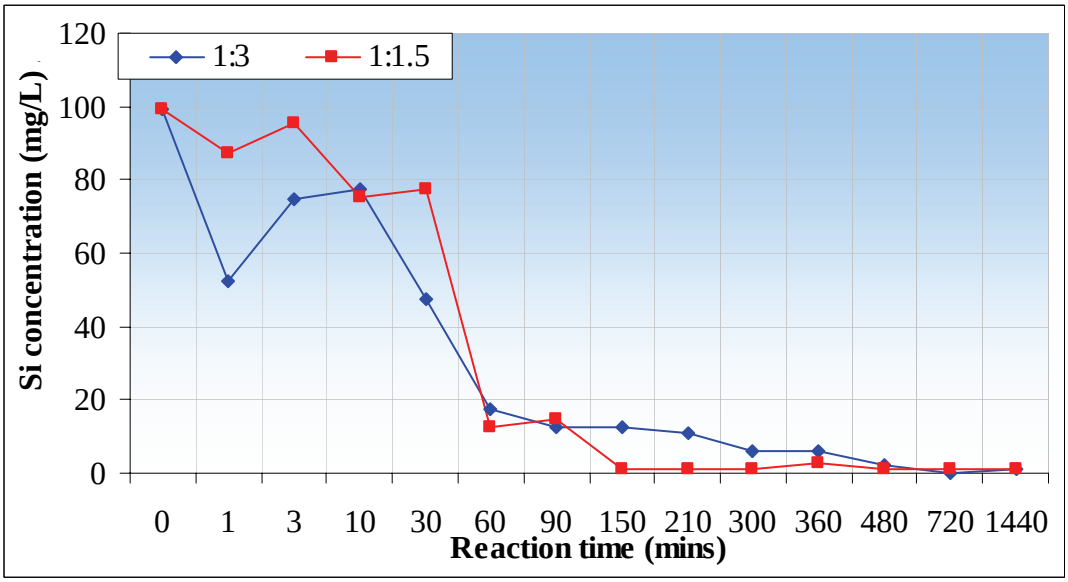

Figure 2.25: Si concentration in process water for the reactions between Arnot fly ash and Navigation AMD at 1:3 and 1:1.5 ratios (FA:AMD).

For both ratios, Mg concentration was observed to increase with contact time, until the mixture attained pH > 5.0. Then a significant drop in concentration was observed (Figure 2.26). The fact that more than 50% of Mg was lost from solution at a lower pH than predicted by thermodynamic calculations (pH = 9.8) of Britton (1956) indicates that other processes such as adsorption could account for its removal. At pH >8.0, saturation index calculations (Table 3.8) indicate super saturation with sepiolite, which could be a control for Mg. Stoessel (1988) observed formation of sepiolite at similar pH conditions. Similarly, a significant proportion of Mn was removed from solution at a lower pH (over 60% at pH = 7, Figure

2.27) than predicted by thermodynamic stability of its hydroxide. However complete removal was achieved when the mixture increased to a pH greater than 8, which is close to the pH when Mn is expected to precipitate out of solution (pH = 9.0). According to Britton (1956), Cu hydroxide precipitates at pH values greater than 5.3, and Zn hydroxide at pH values greater than 7.0.

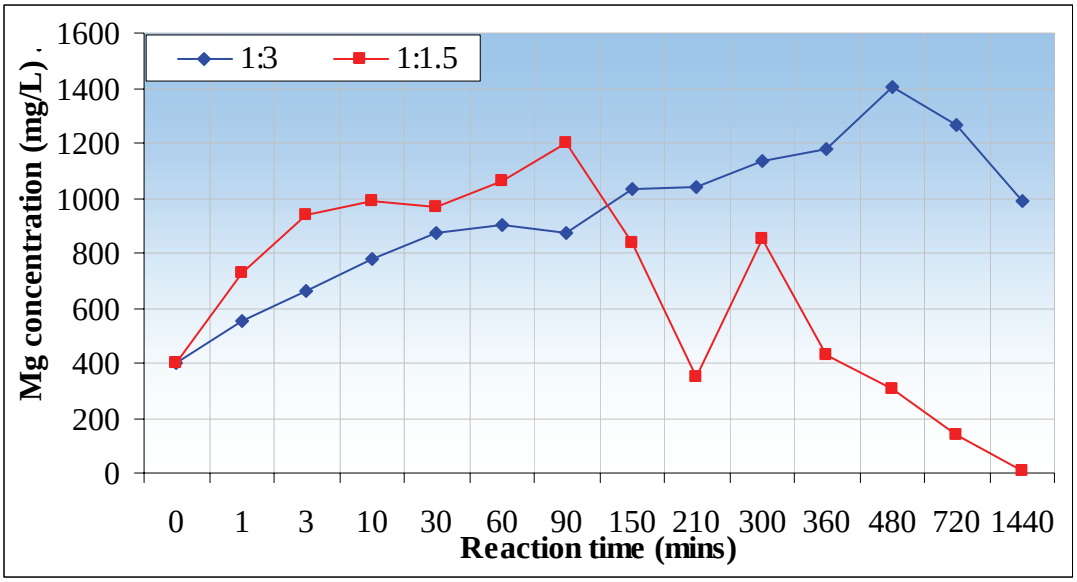

Figure 2.26: Mg concentration in process water for the reactions between Arnot fly ash and Navigation AMD at 1:3 and 1:1.5 ratios (FA:AMD).

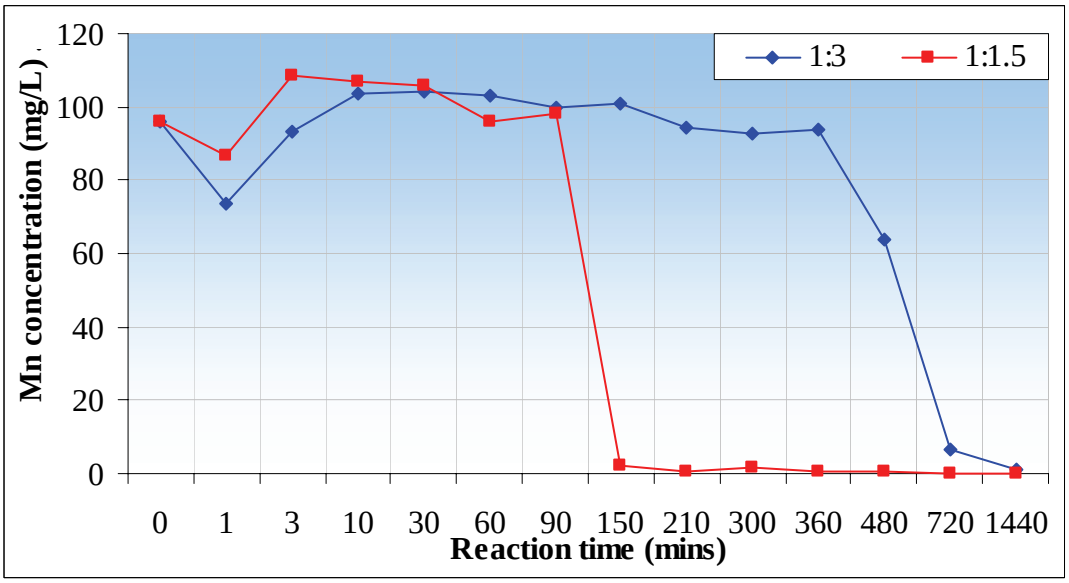

Figure 2.27: Mn concentration in process water for the reactions between Arnot fly ash and Navigation AMD at 1:3 and 1:1.5 ratios (FA:AMD).

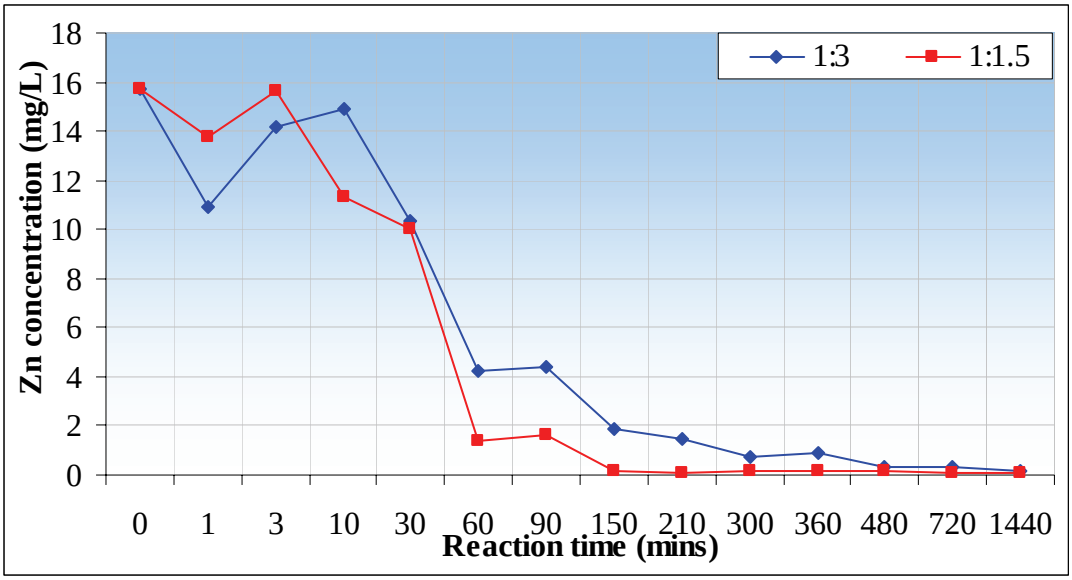

Figure 2.28: Zn concentration in process water for the reactions between Arnot fly ash and Navigation AMD at 1:3 and 1:1.5 ratios (FA:AMD).

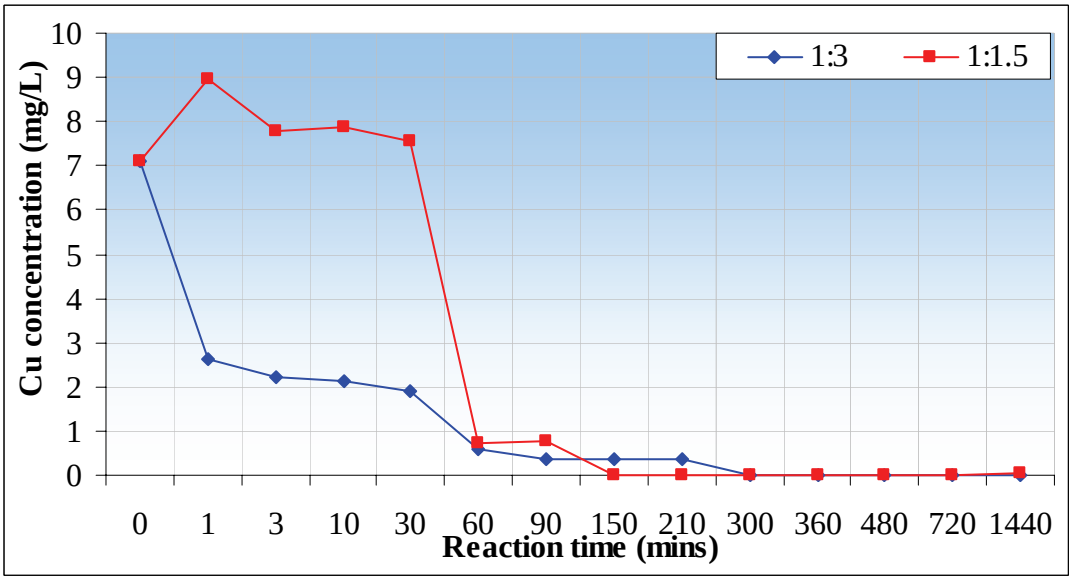

Figure 2.29: Cu concentration in process water for the reactions between Arnot fly ash and Navigation AMD at 1:3 and 1:1.5 ratios (FA:AMD).

Observation of the removal trends for Cu for both ratios indicates that greater than 75% of the total concentration is out of solution when the mixture attained pH > 5.5 (Figure 2.29). At ratio 1:3, a significant drop in concentration was observed at pH < 5.5, which indicates another process apart from hydroxide precipitation was responsible for Cu removal. At pH > 5.0 optimum oxidation of Fe^{2+} was achieved and co-precipitation and adsorption by the iron oxyhydroxides being precipitated could account for earlier removal of Cu (Cravotta III and Trahan, 1999). Similarly it was observed that Zn concentration significantly decreased on the mixture attaining pH > 5.5, which is lower than that predicted by thermodynamic calculations (pH = 6.6) of Britton (1956). Kooner (1993) reported that the relative adsorption of Cu and Zn on iron oxides such as goethite is related to the ability of the metals to be hydrolysed in aqueous solution. Over 50% Cu and Zn was adsorbed at pH > 5.5 and pH >7.0

respectively, which corresponds to the first hydrolysis constants (pK_1) of these metals (7.3 for Cu and 9.5 for Zn).

The removal of total iron follows a similar trend for both ratios, with > 90% being removed on the mixture attaining pH > 7.0 (Figures 2.30 and 2.31). The initial decrease in concentration indicates a removal of Fe^{3+}, probably as $Fe(OH)_3$. According to Britton (1956), Fe^{3+} hydroxide precipitates out at pH 3.0. The increase thereafter could be attributed to leaching from fly ash. Significant quantities of Fe_2O_3 were identified by XRF (Table 3.2) in the fly ash. The H^+ from the AMD reacted with the iron oxide, releasing Fe^{3+} which subsequently hydrolysed. On the mixture attaining pH > 5.5, a significant drop in total Fe concentration was observed for both ratios (Figures 2.30 and 2.31).

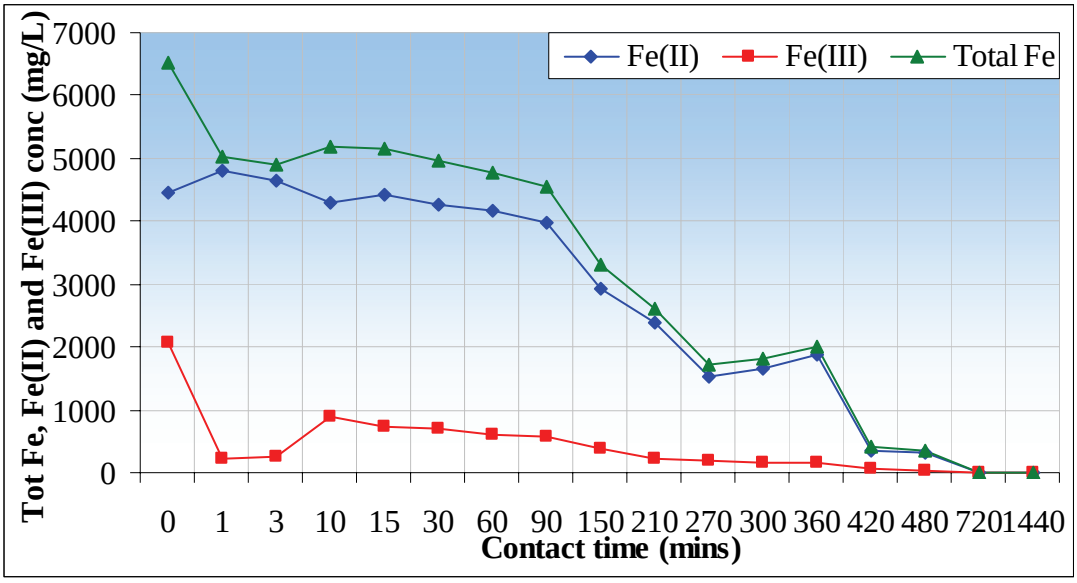

Figure 2.30: Fe concentration as a function of time in process waters for the reactions between Arnot fly ash and Navigation AMD at 1:3 ratio (FA:AMD).

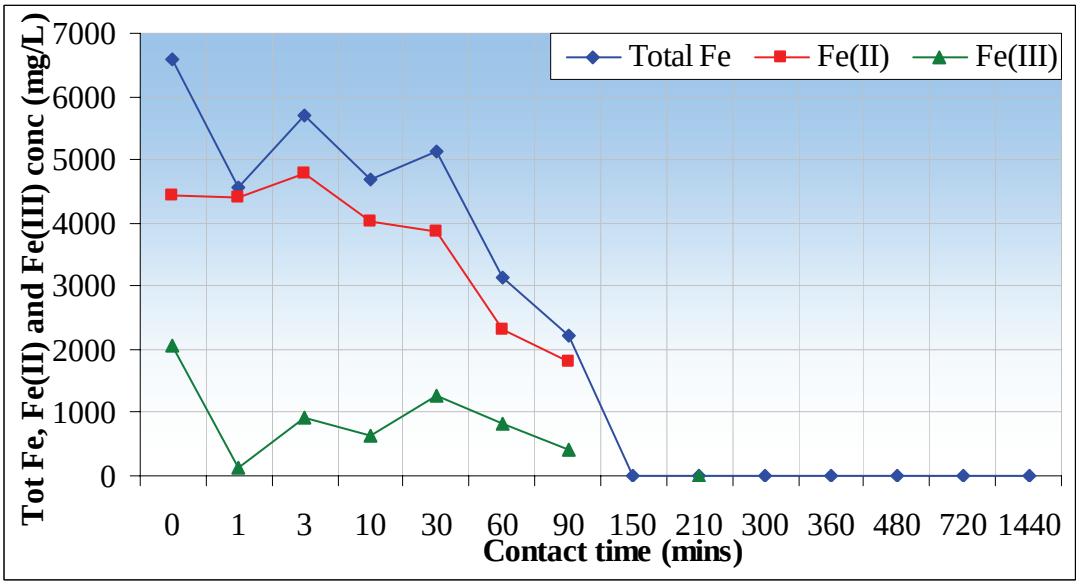

Figure 2.31: Fe concentration as a function of time in process waters for the reactions between Arnot fly ash and Navigation AMD at 1:1.5 ratio (FA:AMD).

The sharp drop on total iron at this pH is accounted for by the optimum oxidation of Fe^{2+} (Stumm and Lee, 1961) followed by hydrolysis. Figure 2.30 indicates that the removal pattern at pH > 6.0 of total Fe follows that of Fe^{2+} for the ratio 1:3. The Fe^{2+} is completely removed from solution at pH 8. The observed pattern indicates that Fe^{2+} is removed from solution by precipitation, probably as $Fe(OH)_3$ after oxidation and subsequent hydrolysis. Calculation of saturation indices shows that amorphous $Fe(OH)_3$ and goethite are at over saturation for the duration of the experiment (Table 3.8). SEM-EDS detected Fe rich mineral phases coating fly ash particles in the solid residues. This indicates that the iron rich mineral phases are too amorphous to be detected by XRD or the concentration is below the detection limits.

2.3.5 Long-term column neutralisation experiments

In this section column leaching studies are presented in order to model the chemical and mineralogical changes that could be expected over time when solid residues are placed underground as fill or backfill material in possible contact with AMD flows (also see sections 4 and 5). Neutralisation experiments were firstly performed and are detailed in subsection 2.3.5.1 and thereafter, in subsection 2.3.5.2 the long-term column neutralisation experiments are detailed.

2.3.5.1 Reaction of simulated AMD

The reaction of simulated AMD treated with Arnot fly ash at FA:AMD ratios of 1:4 and 1:2.5 is shown in Figures 2.32 and 2.33. The buffer regions associated with neutralisation of AMD are observed at pH 2.0-5.0, 5.5-6.0 and 8.5-9.0, as previously reported. Use of simulated AMD resulted in a decrease in pH at longer contact times than expected (based on results from neutralisation tests made with natural AMD). This is probably because of unoxidised ferrous iron, which on oxidation and hydrolysis releases acidity (H^+). Figure 2.33 shows that EC trends are similar for both FA:AMD ratios tested. However, the 1:2.5 ratio shows a faster decrease. A significant decrease is observed once the mixture attains pH 5.5. This has been observed in earlier experiments using raw Navigation and Brugspruit AMD (Gitari *et al.*, 2004).

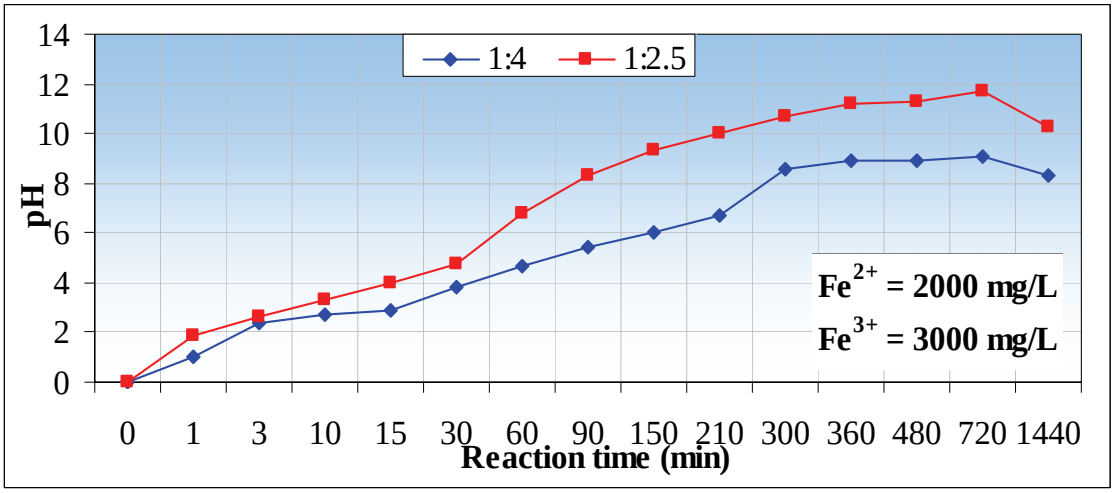

Figure 2.32: Evolution of pH with time for simulated AMD at different FA:AMD ratios.

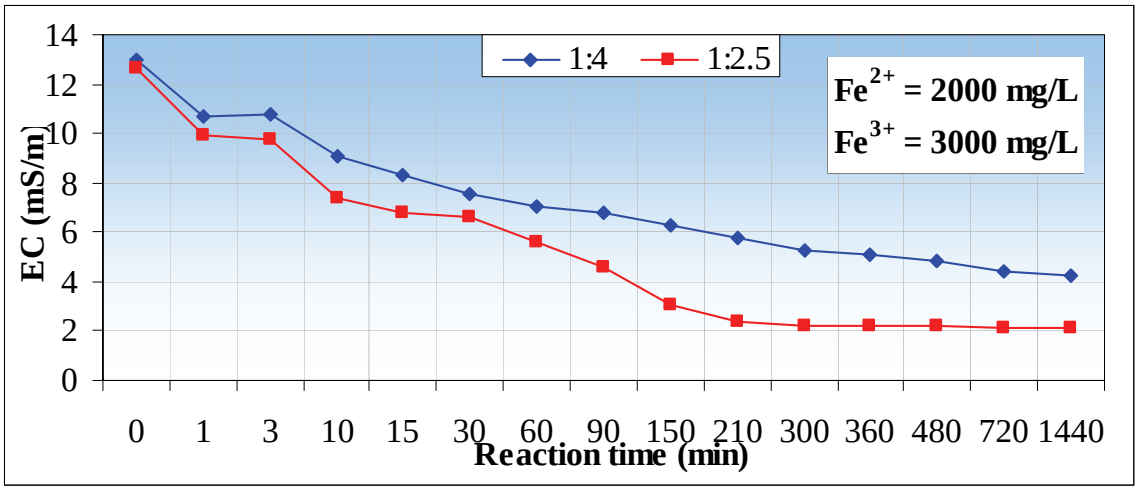

Figure 2.33: Evolution of EC with time for simulated AMD at different FA:AMD ratios.

2.3.5.2 Evolution of pH in column permeates

Simulated AMD was treated by percolation through columns packed with Arnot fly ash or solid residues in column leaching studies in order to model the chemical and mineralogical changes that could be expected over time when solid residues are placed underground as fill or backfill material in possible contact with AMD flows. Simulated AMD was used in this study because of logistical constraints and to exclude variability. Ash can be applied as passive treatment system for AMD, and a high amount of Fe, Al and SO_4 was removed. It would however, be useful to first apply the FA to actively neutralise the AMD so that the full benefit of the FA alkalinity is exploited. A comparison was thus necessary between the behaviour of ash by itself and that of solid residues and various combinations of the two.

Table 2.3: Composition of simulated acid mine drainage (SAMD) used for column leaching.

Compound	Mass g/L	mmol/L	Ion	mmol/L
$FeSO_4.7H_2O$	14.934	55.13	Fe^{2+}	55.13
$Fe_2(SO_4)_3.7H_2O$	7.160	13.80	Fe^{3+}	27.60
$Al_2(SO_4)_3.18H_2O$	11.34	17.50	Al^{3+}	34.99
$Mn(NO_3)_2.4H_2O$	0.9138	3.701	Mn^{2+}	3.701
H_2SO_4 (0.005 M)	0.272 mL	0.00136	SO_4^{2-}	149.0

A synthetic solution simulating acid mine drainage (SAMD) was made using soluble salts of the major components in AMD (Fe, Al, Mn and SO_4) (Table 2.3). The salts were dissolved in 1L of water to which 0.272 mL of 0.005 M H_2SO_4 had been added to prevent immediate precipitation of ferric iron. The metal salts used were ferric sulphate, ferrous sulphate, aluminium sulphate and manganese(II) nitrate tetrahydrate.

The column assembly used for the drainage experiments is shown in Figure 2.34. The solid residues from the large scale reaction between Navigation AMD and Arnot FA were packed into columns in small portions of 500 g. After each addition the material was then gently pressed with a 1 L PVC bottle in order to pack sediments. Each column was duplicated for each different composition of solid material.

Figure 2.34: Column assembly used for the leaching experiments.

Table 2.4: The various SAMD drainages through the columns and the corresponding time and cumulative volume of SAMD.

Drainage number	Time (days)	Volume of synthetic AMD added (L)		
		Columns 1, 2, 3 and 8	Column 5	Column 6
1	1	0.35	0.45	0.555
2	7	0.70	0.90	1.11
3	15	1.05	1.35	1.67
4	22	1.40	1.80	2.22
5	29	1.75	2.25	2.78
6	36	2.10	2.70	3.33
7	44	2.45	3.15	3.89
8	53	2.80	3.60	4.44
9	67	3.15	4.05	5.00
10	81	3.50	4.50	5.55
11	97	3.85	4.95	6.11
12	110	4.20	5.40	6.66
13	124	4.55	5.85	7.22
14	138	4.90	6.30	7.77
15	153	5.25	6.75	8.33
16	165	5.60	7.20	8.88

Columns 1, 2, 3 and 8 were leached with batches of 350 mL of SAMD, approximately once a week for the first 53 days and thereafter once every two weeks for the remainder of the experiment. As columns 5 and 6 contained different masses of solid material, they were

leached with 450 and 555 mL, respectively, in order to maintain a consistent liquid to solid ratio between all the columns. Table 4.4 shows the number of drainages, the corresponding day form the start of the experiment and the cumulative volume of SAMD for each point. The volume of SAMD added varies according to the dry mass of the solids in the columns. Table 2.5 shows the composition along with the mass of solids for each column.

Table 2.5: Column compositions, masses , drainage volumes and liquid to solid ratios for each column.

Column number	Column composition	Mass solids (kg)	SAMD added per drainage (L)	Total SAMD added after 16 drainages (L)	Liquid:Solid ratio per drainage (L/kg)	Total Liquid:Solid ratio (L/kg)
1	Fly ash (FA)	1.000	0.350	5.60	0.350	5.600
2	Solid residue (SR)	0.897	0.350	5.60	0.390	6.243
3	SR + 5% FA	0.925	0.350	5.60	0.378	6.054
5	SR + 25% FA	1.172	0.450	7.20	0.384	6.143
6	SR + 40% FA	1.465	0.555	8.88	0.379	6.061
8	SR + 6% cement	0.935	0.350	5.60	0.374	5.989

Figures 2.35 to 2.40 show the evolution of pH in permeate collected after passage of simulated AMD through various combinations of ash and binder over time. The investigated materials packed into columns were unreacted fly ash; solid residues; solid residues blended with 5, 25 and 40% fly ash; solid residues blended with 6 % ordinary Portland cement (see experimental details in Section 3.4.4). The pH values of all column leachates were initially alkaline (pH>7). Buffering was observed for all columns but the number of buffering regions and the pH at which the buffering occurred differed.

The permeate recovered from the column packed with unreacted fly ash shows a gradual decrease in pH with time (Figure 2.35). The decrease in pH occurred stepwise through three buffer stages. The buffering regions were observed as the pH decreased, at pH 12-10, 8-7, 5-5.5 and 4. The second column replicate exhibited a buffer zone at pH 12.0-10.0 after 1.40 L of SAMD was added, on day 22. The first replicate exhibited a drop in pH from 12 to less than 8 after 1.05 L of SAMD was added, on day 15. It was followed by an increase, back to pH 8-9, which constituted the second buffer zone. This buffer zone was sustained after 3.15 L/kg of SAMD were added, on day 67 when the pH started to decrease again. The second replicate exhibited a pH drop to pH<6 after 2.10 L of SAMD were added, on day 36 after the first buffer zone. The pH 5-5.5 was sustained after 3.85 L of SAMD were added, when it started dropping further. This comprised the second buffer zone for the second replicate. The second buffer zone for the first replicate was sustained for a long time and at a higher pH than for the second replicate. After 3.85 L of SAMD were added, on day 97 both columns showed a decrease in pH to below 5. A buffer zone was observed at pH 4 and was sustained from 4.20 L to 5.60 L of SAMD being added, from days 110 to 165, respectively.

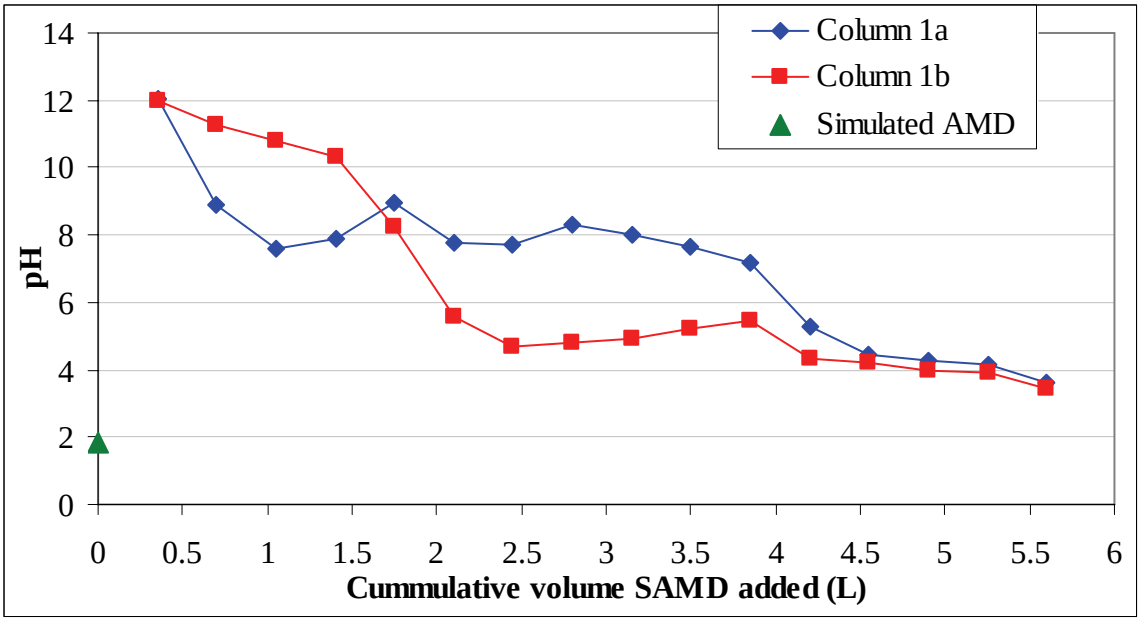

Figure 2.35: Evolution of pH in the leachate of unreacted fly ash (Column 1).

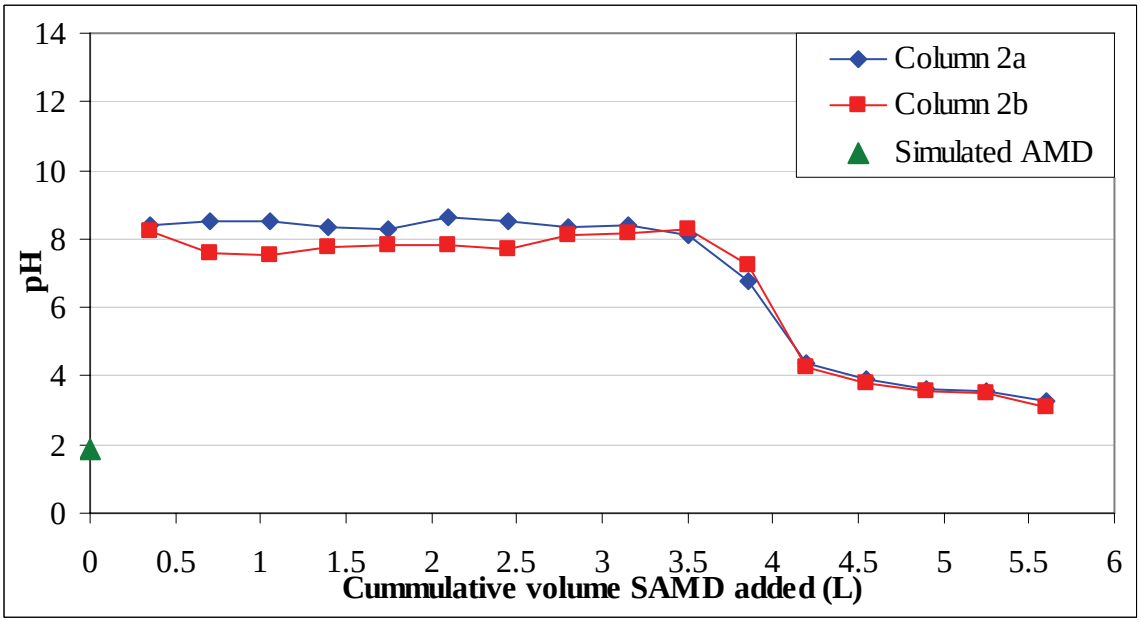

Figure 2.36: Evolution of pH in the leachate of solid residues (Column 2).

The initial pH of the permeates recovered after passage through solid residues were alkaline (pH 8.5) for both columns (Figure 2.36). In the first replicate, pH 8.5 was reached after 3.50 L of SAMD were added, on day 81 when pH dropped to below 7. This comprised the first buffer zone for the first replicate. In the second replicate, the pH of the leachate dropped slightly to ≈ 7.5. This was followed by a gradual increase to pH 8 after 3.50 L of SAMD were added, on day 81. This comprised the first buffer zone for the second replicate. Thereafter pH dropped to 4 for both columns after 3.85 L and 4.20 L SAMD were added, on days 97 and 110, respectively. A gradual drop in pH was subsequently observed (pH 4.0 - 3.5) after 5.60 L of SAMD were added, on day 165. This comprised the second buffer zone for both columns. In the first replicate, the first buffer zone was observed at a slightly higher pH than for the second replicate. It is interesting that the solid residues appear to have a greater buffering capacity for a longer time than the ash by itself.

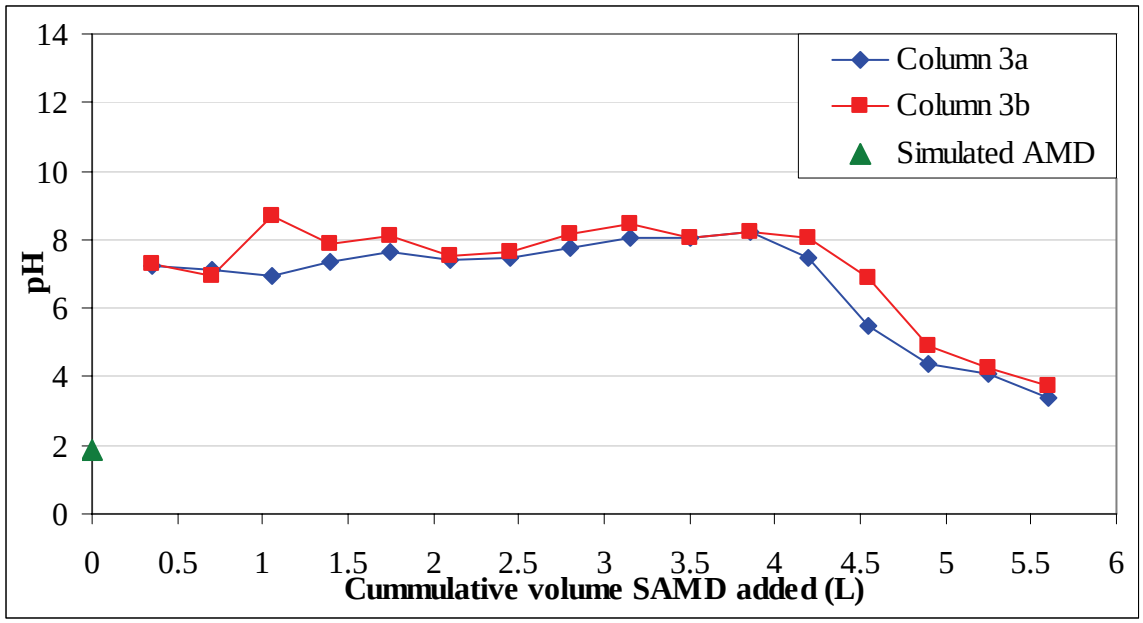

Figure 2.37: Evolution of pH in the leachate of solid residues blended with 5% fly ash (Column 3).

The initial permeates of the 5% fly ash blended solid residues remained neutral after 3.50 L of SAMD was added, on day 2 (Figure 2.37). The second replicate exhibited an increase to pH 8.5, followed by a decrease to pH 8.0. This pH was stable till 4.20 L of SAMD were added, on day 110, when a drop was observed. This comprised the first buffer zone for the second replicate. The first replicate remained stable at pH 7-8 from a SAMD volume of 1.05 L to 3.85 L added, between days 15 to 97, when a decrease was observed. After 4.20 L of SAMD were added, both columns exhibited a decrease in pH to below 4. A slight buffering was observed for both columns after 4.90 and 5.25 L of SAMD were added, on days 138 and 153, respectively. The second replicate exhibited a slightly higher pH values than the first one for the entire duration of the experiment.

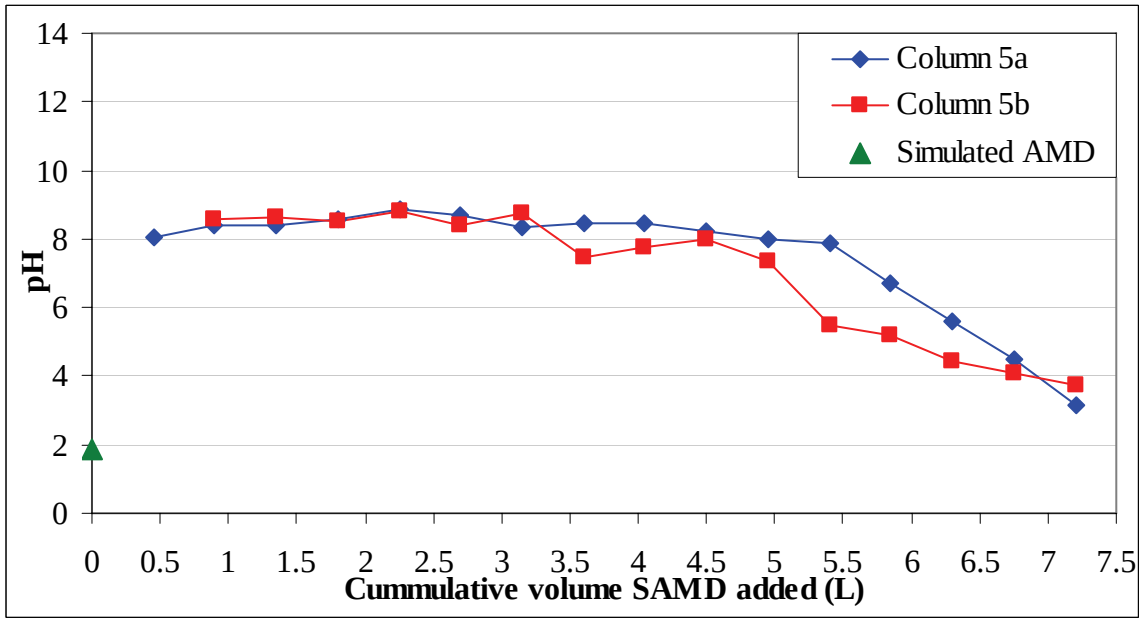

Figure 2.38: Evolution of pH in the leachate of solid residues blended with 25% fly ash (Column 5).

The 25% fly ash blended solid residues were characterized by an increase in the pH of the permeate to an initial value of 8.5 (Figure 2.38). The first replicate remained stable at this pH from 0.90 L till 4.05 of SAMD added, from day 2 to day 67, respectively, when a drop to pH 8 was observed. This was maintained until 5.40 L of SAMD were added, on day 110. This comprised the first buffer zone for the first replicate. After 5.40 L of SAMD were added, on day 110, a steady decrease was observed, finally taking the pH below 4 after 7.20 L of SAMD were added, on day 165. The second replicate maintained a pH of 8.5 until 3.15 L of SAMD were added, on day 44, when a slight decrease to the pH of 8 was observed. This was maintained until 4.50 L of SAMD were added, on day 81. This comprised the first buffer zone for the second replicate. A steady decrease in pH after 4.50 L of SAMD were added, on day 81 was observed. A slight buffering was observed after 6.30 and 6.75 L of SAMD were added, on days 138 and 153, respectively. After 3.60 L of SAMD were added, on day 53 until the end of the experiment on day 165, the first replicate exhibited a higher pH in leachate than the second one. No leachate breakthrough occurred with the addition of 0.45 L of SAMD on day 1.

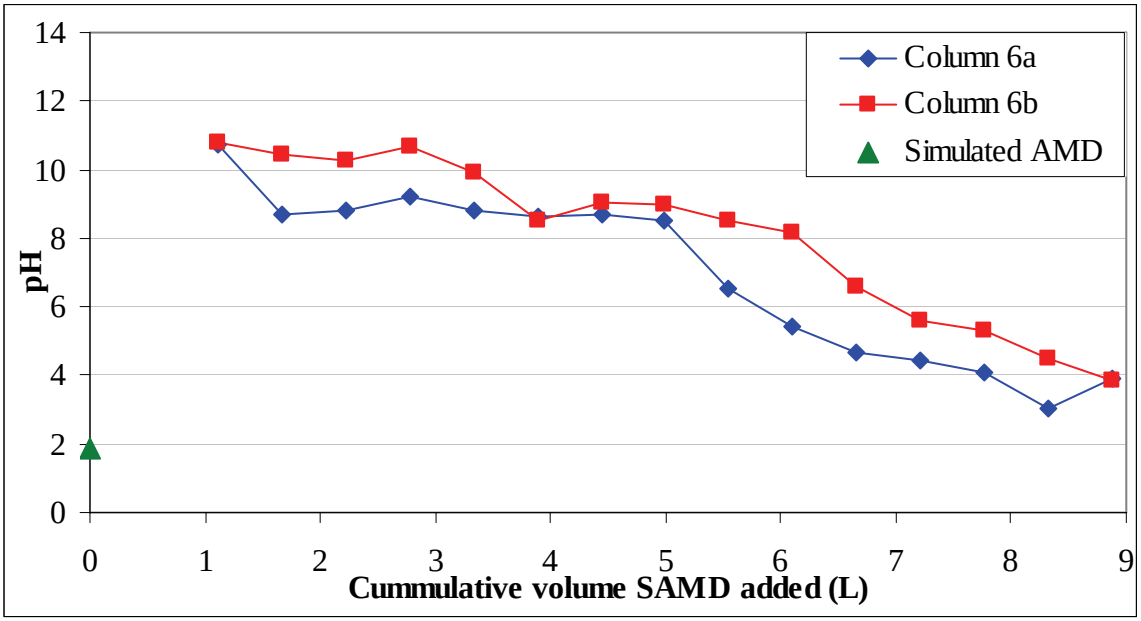

Figure 2.39: Evolution of pH in the leachate of solid residues blended with 40% fly ash (Column 6).

The permeate of the 40% fly ash blend showed an initial increase of pH to a value of 11 (Figure 2.39). The pH decrease for the two columns occurred stepwise with two buffer zones being exhibited. The first replicate exhibited a decrease to pH 9 after 1.665 L of SAMD was added, on day 15. This pH was maintained until the addition of 4.995 L of SAMD, on day 67, when a decrease in pH was observed. This constitutes the first buffer zone for the first replicate. After 5.550 L of SAMD were added, on day 81, a steady decrease in pH was observed until pH 5. A slight buffering was observed after 7.770 and 8.325 L of SAMD were added, on days 124 to 138, respectively before a decrease in pH to 3, followed by an increase to pH 4 after 8.880 L of SAMD were added, on day 165. The second replicate maintained pH 11 until 2.775 L of SAMD were added, on day 29, when a pH decrease to pH 9 was observed. This constituted the first buffer zone for column the second replicate. This pH was stable between the additions of 3.885 and 6.105 L of SAMD, between days 44 to 97,

respectively. A gradual drop to pH 8 occurred after 6.105 L of SAMD were added, on day 97. A pH decrease was thereafter observed between the additions 8.325 and 8.880 L of SAMD, on days 153 to 165, respectively, to pH 4. The second replicate exhibited a higher pH in the permeate than the first one, for the whole duration of the experiment.

The 6% ordinary Portland cement (OPC) blended solid residues initially showed an increase in the pH of the permeate to 11.5 (Figure 2.40). Two buffer zones were exhibited as the pH decreased: the first one at pH 12 and the second one at pH 4. The first replicate maintained the initial pH 11.5 until 1.05 L of SAMD was added, on day 15, when a sharp reduction to pH 5.0-5.5 was observed. Thereafter a gradual decrease to pH 4 occurred after 2.10 L of SAMD were added. This was maintained for the first replicate until the 5.25 L of SAMD were added, on day 153, when a decrease to pH 3.5 was observed. A similar pH profile was observed for the second replicate, but the initial pH was maintained until 1.40 L of SAMD were added, on day 22. A slight increase in pH was observed after 3.85 L of SAMD were added, on day 97, and thereafter the pH decreased to 4. This was maintained until 5.25 L of SAMD were added, on day 153, when a decrease to pH 3.5 occurred.

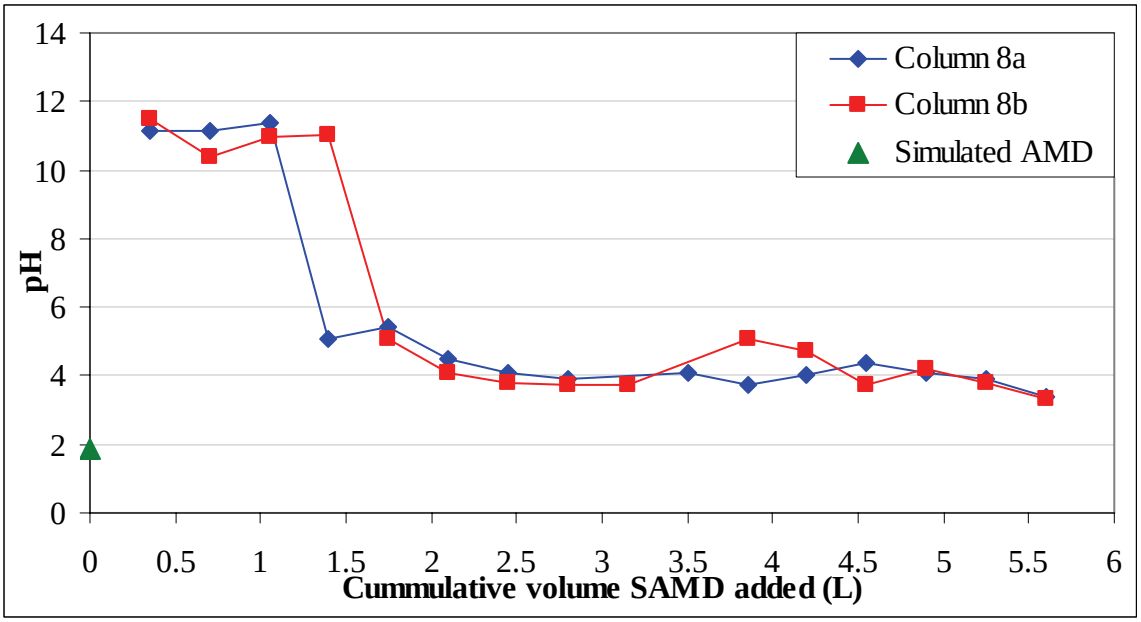

Figure 2.40: Evolution of pH in the leachate of solid residues blended with 6% ordinary Portland cement (Column 8).

The 40% fly ash blend closely mirrored the unreacted fly ash, showing gradual decrease in pH with three buffer regions being observed, at pH 11 – 10, 9 – 8 and 5.5 – 4 (Figures 2.35 and 2.39). Warren and Dudas (1984) observed a stepwise decrease in pH in a column leaching experiment of an alkaline fly ash using a 0.005 mol/L solution of H_2SO_4 as the leachant. The initial leachates were alkaline and three buffer zones were observed, at pH 12 – 11, 10-8.5 and 3.6, as the leaching progressed.

The solid residues blended with 5% and 25 % fly ash exhibited a buffer zone at pH 7.0-8.5 for a long duration (81-124 days) (Figures 2.36, 2.37 and 2.38). Seoane and Leiros (2001) amended sulphide rich lignite mine spoil with fly ash (10 to 20%) and subjected them to alternate cycles of wetting and drying. They observed that neutralisation in the lower fly ash dosage blends was slow, but more sustainable than in the higher dosage. They attributed this to the neutralisation process by dissolution of sillimanite. The observed similarity in pH

trends of the 40 % fly ash blend with the unreacted fly ash could indicates that at this ratio the higher % of unreacted fly ash will mask the effect of the solid residue and dissolution kinetics of the fly ash will dominate.

Most interestingly the columns filled with solid residues by themselves performed somewhat better over the period tested than the fly ash columns and significantly better than the Portland cement amended blend. The solid residues appeared to have a significant buffering capacity, maintaining neutral to alkaline pH for an extended period of time (97 days). If placed in a mining area generating AMD, these solids could provide a passive method of treatment of polluted water. The alkaline properties of the original FA or of the solid residues would thus give a possibility to passively treat AMD, with a neutralisation reaction taking place in situ over an extended period of time. The use of Portland cement as binder reduces this neutralisation capacity to 22 days. Results obtained in the case of addition of the cement binder may indicate possible excessive aggregation of particles with the Portland cement amendment that may have reduced the active surface area of particles available for neutralisation. This indicates that caution is necessary in the choice of binder.

2.3.5.3 Major and trace element concentration in the leachate

Figures 4.41 – 4.48 represent the experimental results of the removal efficiency of major elements, SO_4 and mobilization of toxic elements for unreacted fly ash and solid residues columns

2.3.5.3.1 Columns containing only fly ash

The pH values of the unreacted fly ash columns were initially alkaline (pH > 12.0). Acidification of the ash occurred in a step-wise fashion with the columns exhibiting three buffer regions. However, the pH of the buffer regions differed for the duplicate columns which could have occurred due to channelling effects. This stepwise acidification of fly ash has been observed by other researchers (Warren and Dudas, 1984; Komnitsas *et al*., 2004; Hodgson *et al*., 1982)

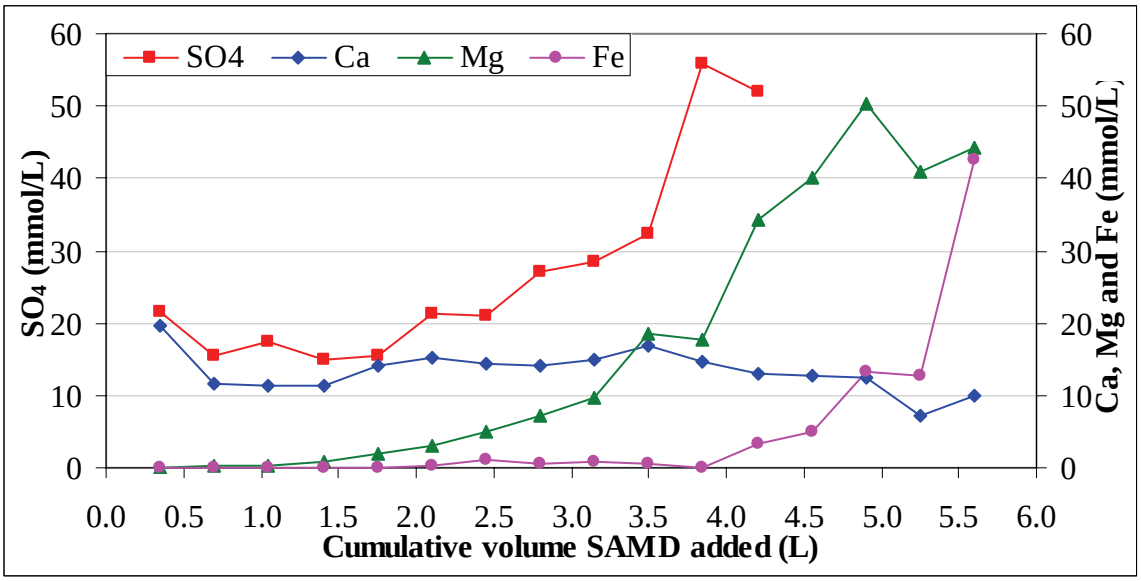

Figure 2.41: Concentration of SO_4, Ca, Mg and Fe (mmol/L) against cumulative volume (L) for fly ash columns.

The simulated AMD contained 150 mmol/L of SO_4, in addition to release of SO_4 from the fly ash. At the onset of the drainage experiments, the pH of the leachate was highly alkaline due to dissolution of Ca and Mg oxides in the fly ash. The removal of SO_4 from the AMD was quite efficient initially, with SO_4 in the leachate dropping to ≈ 20 mmol/L (Figure 2.41). Dissolution of soluble Ca salts and subsequent precipitation of gypsum accounts for the low levels of SO_4 in the leachates. The parallel trends displayed by the concentrations of Ca and SO_4 in the leachate thereafter probably indicate that gypsum could be controlling their concentration in solution. As the SO_4 concentration increased after an addition of 2 L of SAMD, the corresponding Ca started to decrease, indicating that the Ca concentration had dropped below the level at which gypsum super saturation was attained. The highest concentration of SO_4 (Figure 2.41) observed after the addition of 3.39 L of SAMD was 30% of the original concentration. indicating that SO_4 attenuation mechanisms were still operational even though the pH entered the acidic buffer region. Magnesium followed the same trend as SO_4 (Figure 2.41), increasing in concentration in the leachate with increasing volume of SAMD added. This indicates that Mg was retained in the column until approximately 1 L of SAMD was added, whereupon it rapidly increased in concentration, reaching a maximum after 4.75 L of SAMD were added, and decreased thereafter. The initial SAMD contained 82.72 mmol/L of total iron. The concentration of Fe (Figure 2.41) was low to undetectable until 3.8 L of SAMD had been added, where after the concentration in the leachate increased rapidly. It is clear that the pH of the column was greater than 5 and that after the addition of 4 L of SAMD there was increasingly less alkalinity in the column to precipitate the Fe from the SAMD solution.

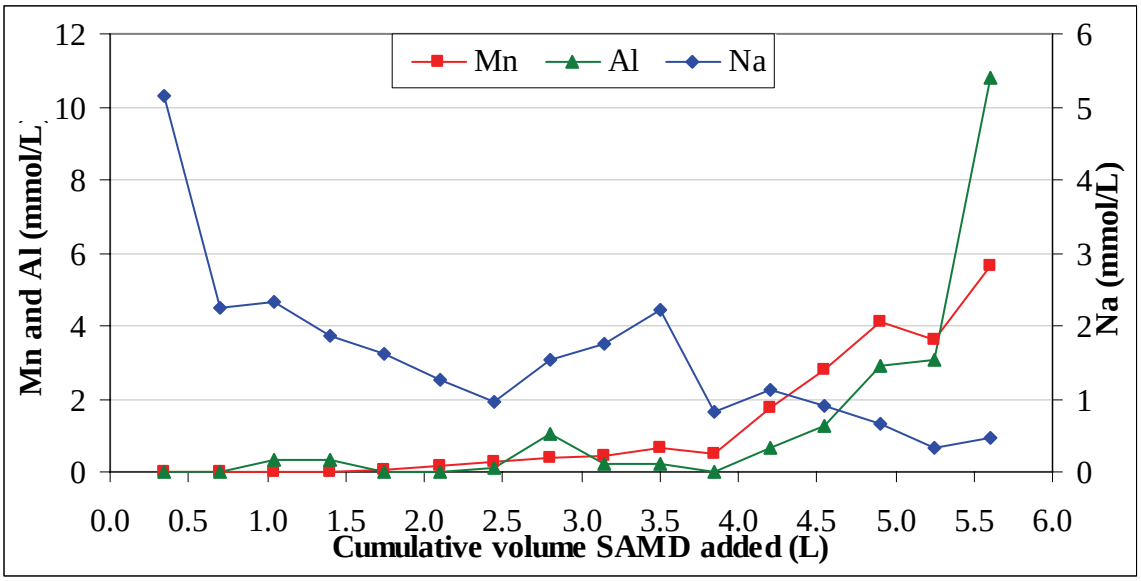

Figure 2.42: Concentration of Mn, Al and Na (mmol/L) against cumulative volume (L) for fly ash columns.

The initial simulated AMD contained 35.0 mmol/L of Al^{3+} and 3.7 mmol/L of Mn^{2+}. The concentrations of Mn and Al (Figure 2.42) in the leachates were similar and followed the same trend as that of Fe (Figure 2.41). The concentrations were low while there was still excess alkalinity in the column to precipitate these metals. After the addition of 3.8 L of SAMD, there was no longer enough alkalinity to precipitate all of the Mn and Al and the concentrations of these metals increased in the leachate with each SAMD addition. Despite this, a large amount of SAMD would still have to be added for the leachate concentration of Al to resemble the SAMD concentrations. The concentration of Mn, however, in the last

three drainages, was close to or above the concentration of Mn in the SAMD. This indicates that the Mn which had previously precipitated out of the SAMD solution was now becoming soluble and was being leached out. The initial concentration of Na was approximately 5 mmol/L. The Na concentration in the leachate decreased with each leaching of the solid. The concentration increased slightly when the pH was between 8 and 4. This could be a consequence of the insolubility of other elements at this pH range, resulting in an under saturated solution matrix, which in turn allows a greater amount of Na to enter the solution. As the pH decreased and other elements dissolved the Na concentration in the leachate returned to the rate of decrease seen previously.

The concentration of K varied considerably (Figure 2.43). A highly soluble salt K was leached from the column with little interaction with the SAMD solution, other than as a medium for dissolution. The concentrations for K were relatively low (0.9 – 0.2 mmol/L) and showed a decrease with increasing SAMD added. This decrease is unlikely to be a result of increased acidity and is more likely to be a result of increased leaching. The concentrations of Sr (Figure 2.43) were also low (0.5 – 0.2 mmol/L) and showed a slight decrease with increasing volumes of SAMD. As with K, this is likely to be a case of the Sr being washed out of the column. The concentration of B showed a decrease between the first and second leachings. This indicates the oxyanionic nature of B: high concentrations at high pH, low concentrations when the pH fell between 8 and 5 and high concentrations again when acidic pH values were reached. According to available thermodynamic data, secondary B solids are not likely to form in waste disposal environments (Eary *et al*., 1990).

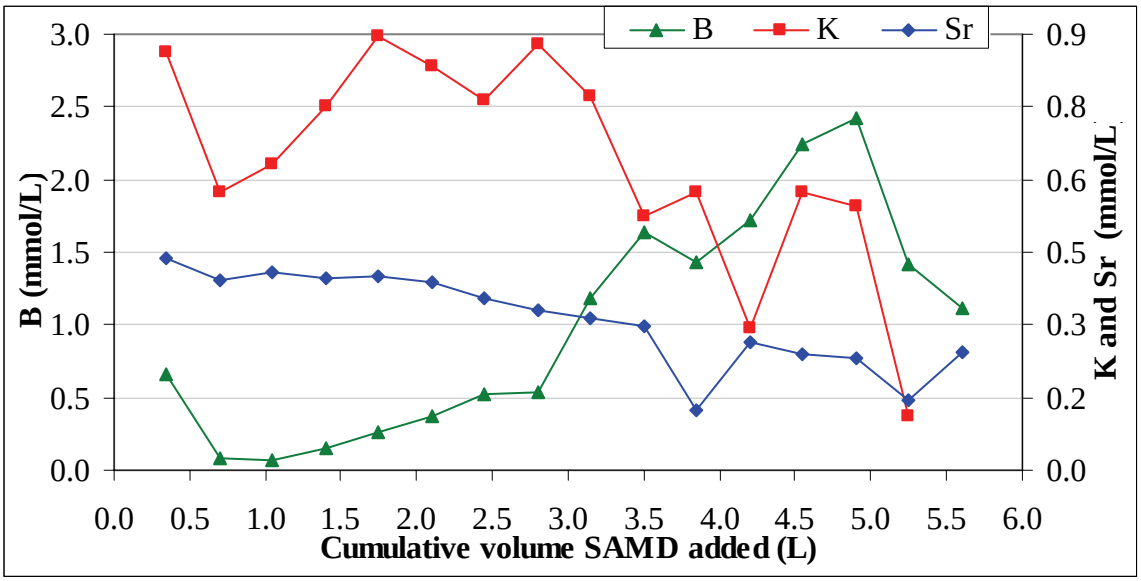

Figure 2.43: Concentration of B, K and Sr (mmol/L) against cumulative volume (L) for fly ash columns.

The concentrations of Ni, Cu, Zn and Co showed similar trends with differences in magnitude (Figure 2.44). The concentrations of Ni, Cu and Zn were stable and low (< 5 µmol/L) until a volume of 2.8 L of SAMD had been added, whereupon the concentrations of Cu and Zn spiked to 24 and 17 µmol/L, respectively. They dropped immediately afterward. The concentration of Ni spiked to an amount of 35 µmol/L after 3.1 L of SAMD had been added. Following this spike in concentration, after 3.8 L SAMD had been added to each column, the concentrations of Ni, Cu, Zn and Co increased with each addition of SAMD. These metals are clearly leaching out of the FA with increasing acidity. The concentrations

of Mo and Cr followed the trend of oxyanionic species: high at high pH values and decreasing to low when the pH decreased to ~ 8. Studies indicate that Cr is present in fly ash mainly as Cr^{3+} (Rai and Szelmecka, 1990). The initial increase in concentration at the alkaline pH could be due to the formation of $Cr(OH)^{4-}$. As the leaching progressed and pH dropped, $Cr(OH)^{4-}$ was converted to $Cr(OH)_3$ which precipitated out. The decrease in concentration to non-detectable limits with reduction in pH could indicate the stability of the formed precipitates, or that Cr in the fly ash matrix was completely dissolved.

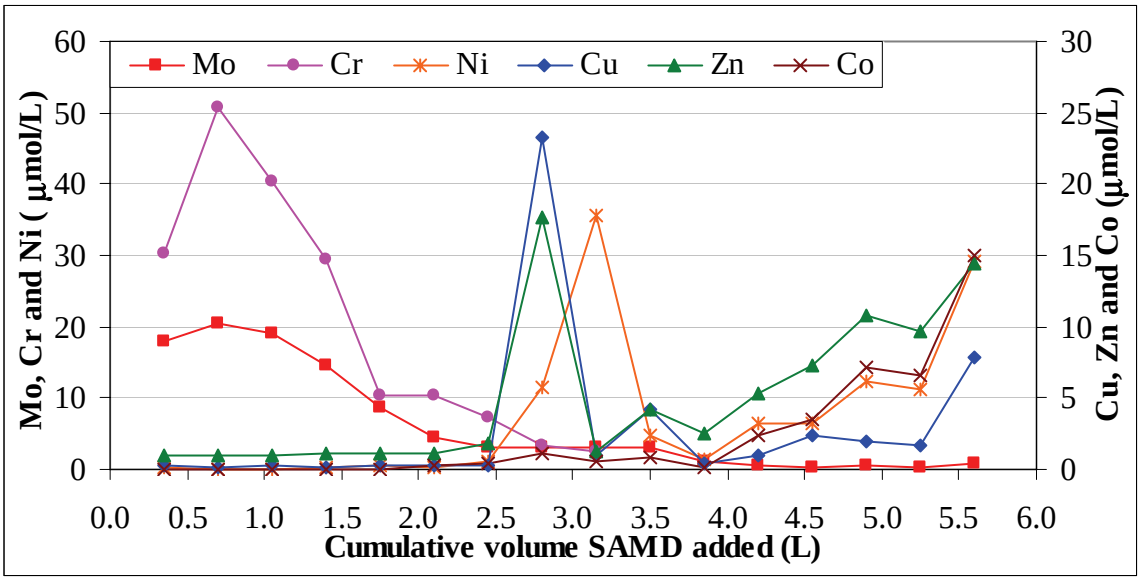

Figure 2.44: Concentration of Mo, Cr, Ni, Cu, Zn and Co (µmol/L) against cumulative volume (L) for fly ash columns.

2.3.5.3.2 Columns containing only solid residue

The following results detail the elements leached out of the column consisting solely of solid residue from the reaction between Arnot fly ash and Navigation AMD at a ratio of 1:3.

The Ca concentrations in the solid residue columns followed a similar trend to the FA columns: a stable concentration tending to decrease with each successive leaching. The solid residue columns leached 36.4 mmol/L less Ca than the FA columns (Table 2.6). The Fe and SO_4 concentrations on the leachate followed trends similar to those for the fly ash leachate. The concentrations of SO_4 were stable till 2.5 L of SAMD had been added Then they increased sharply, at a much faster rate than the leachate from the FA columns, reaching a concentration close to 100 mmol/L after 4.3 L of SAMD were added. It is clear that under alkaline conditions FA and solid residue have the same capacity to adsorb SO_4, but from neutral to acid conditions the solid residue has a diminished capacity to adsorb the SO_4. The solid residue columns leached 120.1 mmol/L more SO_4 than the FA columns. The concentration of Fe followed a similar trend of low concentrations till 3.8 L of SAMD had been added. Afterwards the concentrations increased sharply, reaching a concentration of approximately 50 mmol/L after the addition of 5.6 L of SAMD. The solid residue columns leached 71.5 mmol/L more Fe than the FA columns (Table 2.6). The concentration of Mg also increased at a greater rate in the leachates for the solid residue column, reaching a concentration of 70 mmol/L after 4.1 L of SAMD had been added. But thereafter it decreased to approximately 40 mmol/L after 5.6 L of SAMD had been added, roughly the same concentration in the FA leachate at the same amount of SAMD added. The total amount of

Mg leached from the solid residue column was much higher than from the fly ash column, by 123.1 mmol/L (Table 2.6).

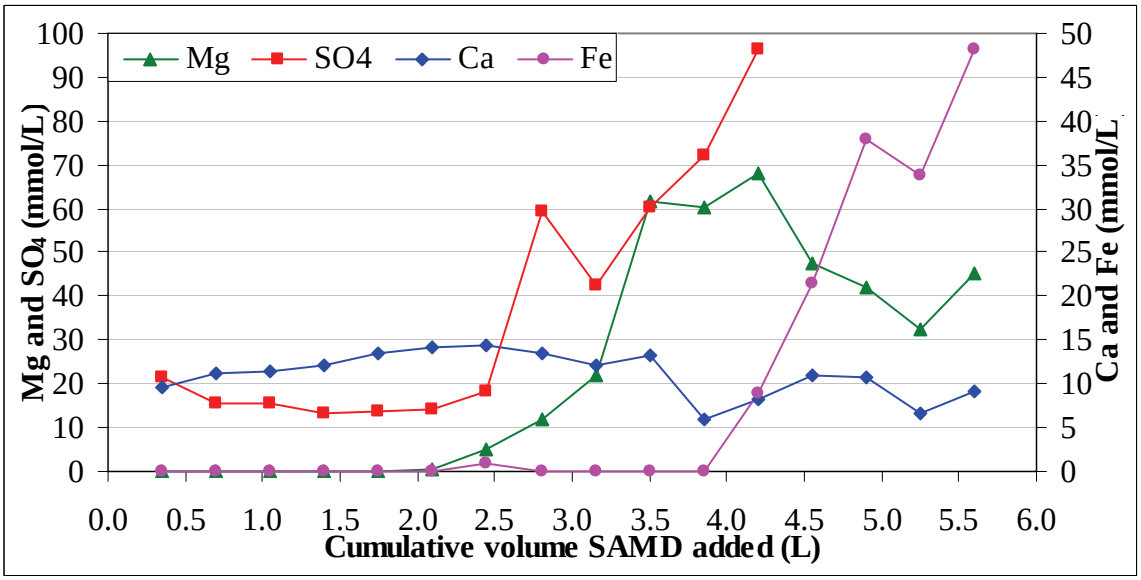

Figure 2.45: Concentration of Mg, SO_4, Ca and Fe (mmol/L) against cumulative volume (L) for solid residue columns.

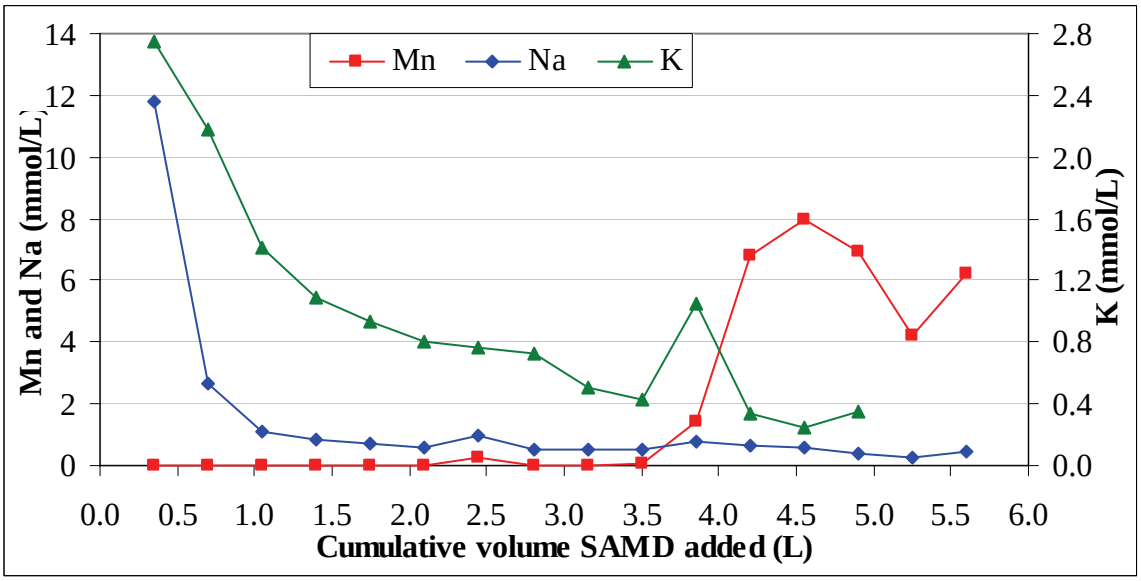

Figure 2.46: Concentration of Mn, Na and Al (mmol/L) against cumulative volume (L) for solid residue columns.

The concentration trend for K in the leachate from the solid residue columns (Figure 2.46) was different from that for the fly ash columns. In the fly ash columns the concentration of K were low (0.9 mmol/L) and did not show a consistent trend before decreasing slightly to 0.2 mmol/L when the leachate became acidic. In the solid residue columns the K was higher (2.8 mmol/L) and decreased gradually to 0.4 mmol/L with decreasing pH. Since K is a highly soluble element the concentration trend from the solid residue leachates indicate that the K is being washed out of the columns with an increasing volume of SAMD. The difference in concentrations for K in the FA columns may not be significant as the variability may be due to analytical errors. The Na concentration (Figure 2.46) in the solid residue column leachates

was initially higher (12 mmol/L) than the Na concentration in the FA leachates (5 mmol/L) but decreased to 0.5 mmol/L after the addition of only 1 L of SAMD. Sodium is thus much more mobile in the solid residue column, with the largest amount being leached in the first two washings. Overall the total amount of Na leached out of the FA column was only 1.87 mmol/L greater than the total amount of Na leached out of the solid residue column (Table 2.6). The Mn concentrations (Figure 2.46) reached a slightly higher value of 8 mmol/L in the solid residue column leachate after 4.5 L of SAMD had been added, as opposed to the FA column leachate where the highest concentration of 6 mmol/L was reached after 5.6 L of SAMD had been added. The total Mn leached from the solid residue columns was 13.6 mmol/L greater than the total Mn leached from the FA columns (Table 2.6).

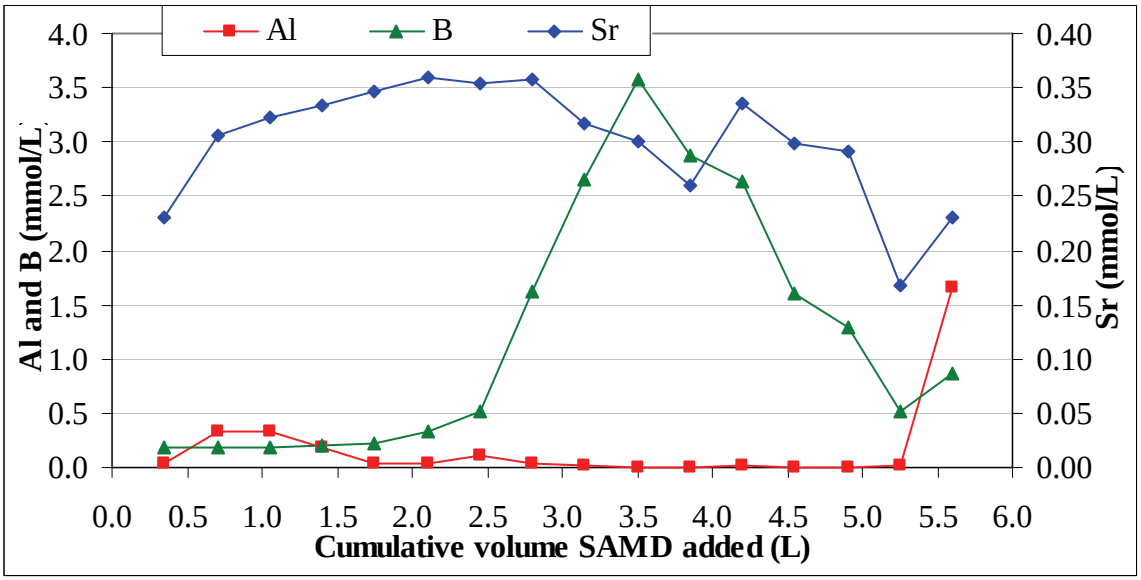

Figure 2.47: Concentration of B, K and Sr (mmol/L) against cumulative volume (L) for solid residue columns.

The Al concentrations for the solid residue columns (Figure 2.47) were very low and reached a maximum of 1.5 mmol/L only under highly acidic conditions. This indicates that a great deal of Al is adsorbed onto the surface and that the solid residue has a high capacity to adsorb Al. The concentration trend for B (Figure 2.47) was the same for both the FA and solid residue columns, with very similar maximum concentrations in the leachate, 2.5 and 3.5 mmol/L, respectively. The only difference being that the FA column had a greater amount of alkalinity and therefore it took a greater amount of SAMD (4.90 L) to reach maximum concentrations in the leachate while it took only 3.0 L of SAMD to reach the same B concentration in the solid residue leachate. The Sr concentrations (Figure 2.47) in the solid residue followed no discernable trend and decreased only marginally with increasing acidity. The Sr concentrations in the leachates of the FA columns displayed the same lack of trend and the differences in concentration between each column were negligible.

The concentration of Mo (Figure 2.48) in the leachates for the solid residue column decreased swiftly from 15 µmol/L and remained stable, at approximately 2.5 µmol/L, before decreasing to below detectable limits when the solution turned acidic. The Cr concentrations (Figure 2.48) decreased to zero from approximately 15 µmol/L and spiked up to 7 µmol/L after 2.5 L of SAMD had been added. This spike is due merely to one point and may be the artefact of an anomalous analysis. The concentration of Ni was low to undetectable until 2.6 L of SMAD had been added, whereupon the concentration spiked up to 15 µmol/L,

decreased again and then increased swiftly to 30 µmol/L, when the leachate became acidic. The concentrations of Cu and Zn (Figure 2.48) remained low (< 2 µmol/L) until the leachate solution became acidic, whereupon Zn increased to 10µmol/L and Cu increased slightly up to 10 µmol/L. Neither of these elements showed the spike at circumneutral pH values as they did for the fly ash column leachates, possibly as a result of the differences in pH of each column leachates. The concentration trend of Co (Figure 2.48) in the solid residue leachates was identical to that of the fly ash column leachates with a small difference in the magnitude of the concentration. The concentrations of Mo, Cu, Zn, Cr, Ni and Co in the solid residue column leachates were all much lower than in the fly ash column leachates (Table 2.6).

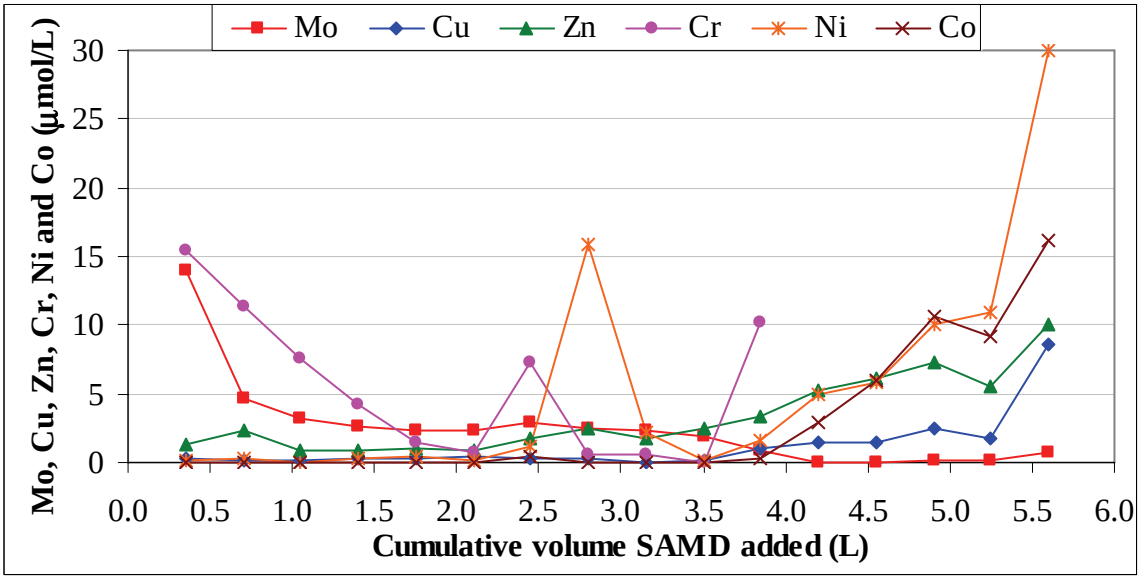

Figure 2.48: Concentration of Mo, Cr, Ni, Cu, Zn and Co (µmol/L) against cumulative volume (L) for solid residue columns.

2.3.5.3.3 Discussion

The removal of elements from solution can be seen in Table 2.6 where the total amount (mmol) of each constituent drained through the columns with a total of 5.6 L of SAMD and the total amount (mmol) of each constituent in the leachates for each column may be seen. The fly ash and solid residue column have a high capacity to remove SO_4, Fe and Al. This is a result of alkalinity in each column raising the pH of the SAMD solution which results in the precipitation of those elements from solution. The precipitated compounds are, however stable and do not re-enter the leachate solution. The concentration of these elements only starts to increase in the leachate once the alkalinity in each column has been exhausted and the pH drops to 4.

Table 2.6: Total amount of elements/ions in mmol drained through each column based on the total SAMD volume of 5.60 L and the % removed by each column.

	Total input (mmol)	Fly ash leachate (mmol)	% Removed	Solid residue leachate (mmol)	% Removed
SO_4	834	99.9	88.0	140	83.2
Al	196	6.42	96.7	0.90	99.5
Fe	463	24.4	94.7	48.5	89.5
Mn	20.7	6.22	70.0	10.9	47.5

Table 2.7: Average concentration (mg/L) for each element and at two different pH values (8 and 4) for fly ash and solid residue column leachates, compared to DWAF water quality limits. Values less than irrigation or domestic quality limits in bold.

Element/ Ion	Irrigation	Domestic use	Fly ash leachate			Solid residue leachate		
pH		6 - 9	(Average)	8	4 (avg 3)	(Average)	8 (avg 10)	4
B	0.5	0 – 0.5	10.62	2.753	21.92	13.33	10.46	28.59
Ca	-	32	528.5	560.3	432.0	444.8	501.8	326.9
Co	0.05	0 – 0.05	139.4	**0.00224**	0.3374	170.4	**0.003543**	0.1692
Cu	0.2	1	188.2	**0.01348**	**0.1299**	76.71	**0.01510**	**0.087922**
K	-	50	**23.38**	**35.01**	**16.03**	**31.35**	**45.32**	**12.93**
Mg	-	30	417.6	45.45	1063	612.6	247.3	1655
Mo	0.01	0 – 0.05	576.0	0.8460	**0.039094**	214.7	0.3710	**0.001284**
Na	70	100	459.6	**36.89**	**14.47**	311.8	**46.50**	**15.18**
Ni	0.2	0 – 0.02	29.75	**0.03182**	**0.588297**	23.71	**0.1227**	0.2866
Sr	-	-	27.01	34.94	17.92	26.54	28.28	29.36
Zn	1	3	337.2	**0.07113**	**0.6044**	219.6	**0.1033**	**0.3413**

Since the SAMD only contained SO_4, Al, Fe and Mn all other elements seen in Table 2.6 originate from the solid material and are leached out with each successive drainage. These elements in average concentrations for all drainages compared to the DWAF quality guidelines are seen in Table 2.7. Included in Table 2.7 are the concentrations for each element at pH 8 and 4 (these values are averaged where there is more than one drainage with that pH). The concentrations below water quality guidelines are given in bold. It is clear that the fly ash and the solid residue leach a great deal of Ca, Mg and Sr, although these elements do not have quality limits for irrigation water as they are not harmful to plants, and in fact Ca and Mg are beneficial. At a pH of 8 the passive neutralisation does not leach Co, Cu, K, Na, Ni and Zn to levels above the irrigation quality limits for both fly ash and solid residue. At a pH of 4 Co concentrations rise above water quality limits but Mo concentrations decrease to below water quality limits. Concentrations of B are at both pH values higher than water quality limits for irrigation.

2.3.5.3.4 Conclusions

- Fly ash has a greater capacity to neutralise and remove Fe, Al, Mn and SO_4 than solid residue.
- Solid residue removes a large quantity of Fe, Al, Mn and SO_4 from water with a low concentration of acidity.
- The total concentration of each element leached when fly ash comes in to contact with a weak acid at a ratio of 5.6 L/kg is much higher than irrigation water quality limits, except for K.
- The total concentration of each element leached when solid residue comes in to contact with a weak acid at a ratio of 6.243 L/kg is much higher than irrigation water quality limits, except for K.
- The concentrations of Co, Cu, K, Na, Ni and Zn are below irrigation water quality limits in the fly ash and solid residue leachates for liquid to solid ratios of ~0.35 (L/kg).

- Fly ash and neutralisation solid residues can remove Fe, Al, Mn and SO_4 from a weak acid and will not leach harmful amounts of other metals if in contact with small volumes.

2.3.6 Small scale neutralisation experiments site specific to Landau colliery and Arnot power station

2.3.6.1 Initial small scale experiments

Small scale experiments were conducted to demonstrate the neutralisation potential of Arnot fly ash with Landau AMD. These experiments were conducted in order to determine the ratio at which to conduct pilot scale experiments with the same AMD and ash.

Rapid increase in pH from 2.67 to 12.97 was noted within the first 30 minutes of the reaction for the 1:1, FA:AMD ratio (Figure 2.49). The pH increased steadily for all ratios with a corresponding decrease in electrical conductivity. However, an increase in EC was noted at approximately 300 min, where after the EC decreased again to relatively low levels. The chemistry behind this reaction requires further investigation to ensure that metals are not being leached from the fly ash.

The 1:1 ratio resulted in a thick slurry, which was difficult to stir and filter. Due to the large amount of ash used, the consistency of this mixture, the extremely rapid and high pH increase and the mixing difficulties encountered, the 1:1 ratio is not a viable ratio for a neutralisation process. The 1:3 ratio steadily increased to neutrality in an hour and eventually stabilised at a pH of 11.67.

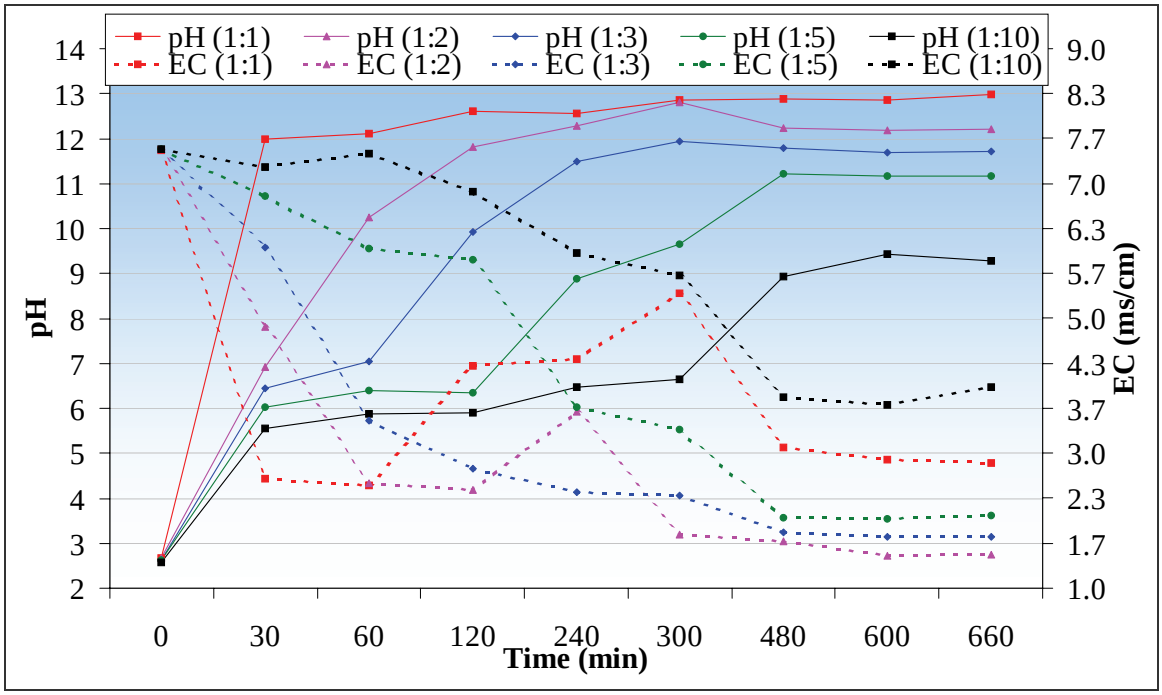

Figure 2.49: Neutralisation of Landau AMD with Arnot fly ash.

A significant reduction for Fe, SO_4 and Al concentration was noted at all FA:AMD ratios (Figure 2.50). However the post neutralisation samples analysed were recovered by filtration between pH 9-12. Samples need to be obtained at neutral pH for IC and ICP analysis. Almost

complete removal (99%) of iron and aluminium was achieved by reacting the AMD with fly ash. A 96 % reduction in sulphate was achieved.

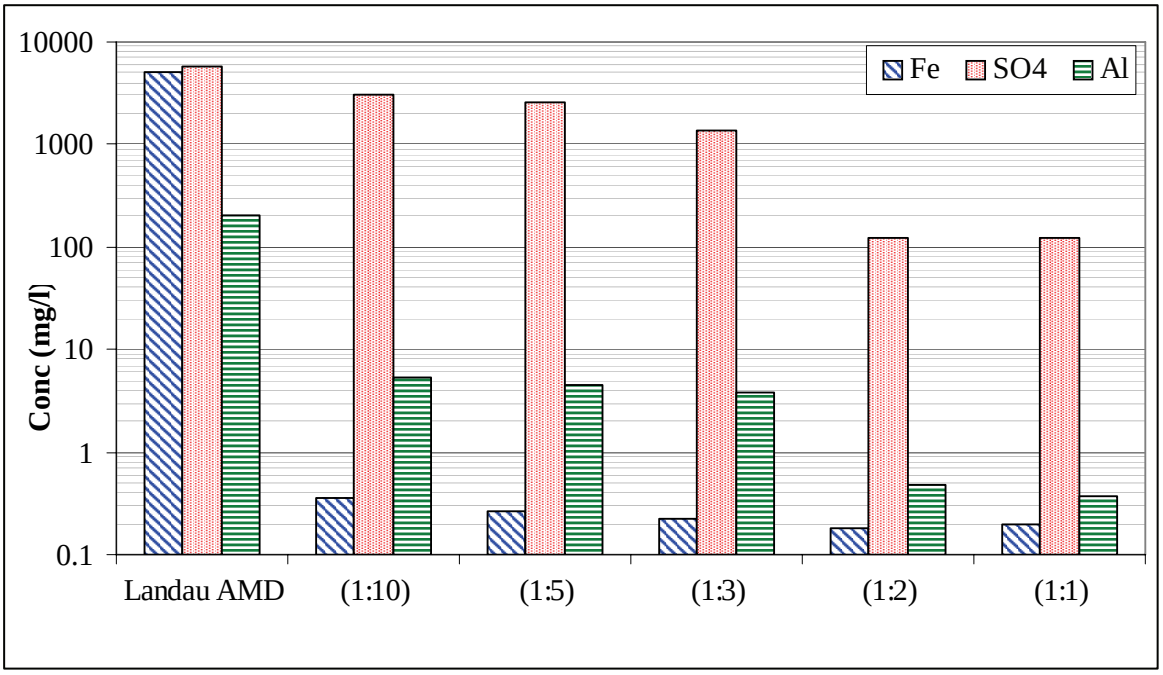

Figure 2.50: Fe, SO_4 and Al concentrations in process waters compared to original AMD.

A similar rapid initial increase in pH was seen (Figure 2.51) for the 1:1 ratio with a gradual decrease in conductivity for all ratios. A short lived rise in conductivity at 300 minutes was observed for both the 1:1 and 1:2 ratios, where after the EC decreased again to relatively low levels. The 1:3 ratio exhibited a continuous decrease in conductivity, which stabilised at 1.7 ms/cm. The experiments were repeated and monitored for higher ratios to determine the final stable pH and conductivity.

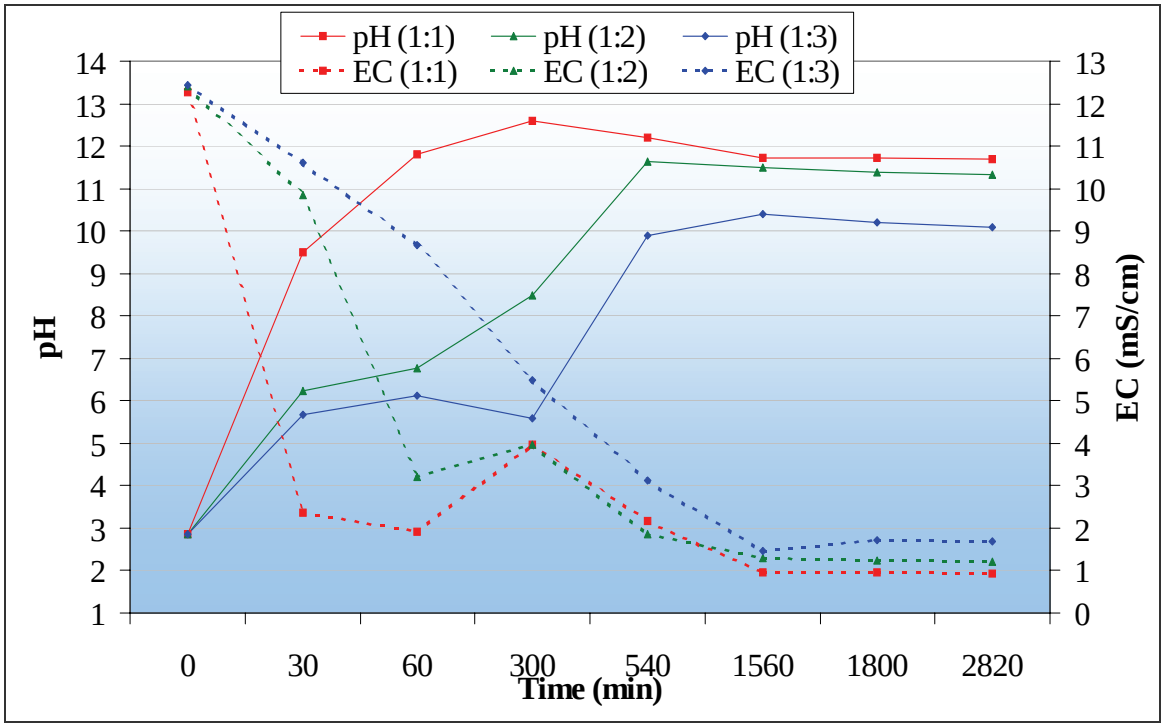

Figure 2.51: pH and EC of the long-term reaction between Arnot fly ash and Landau AMD at ratios of 1:1, 1:2 and 1:3.

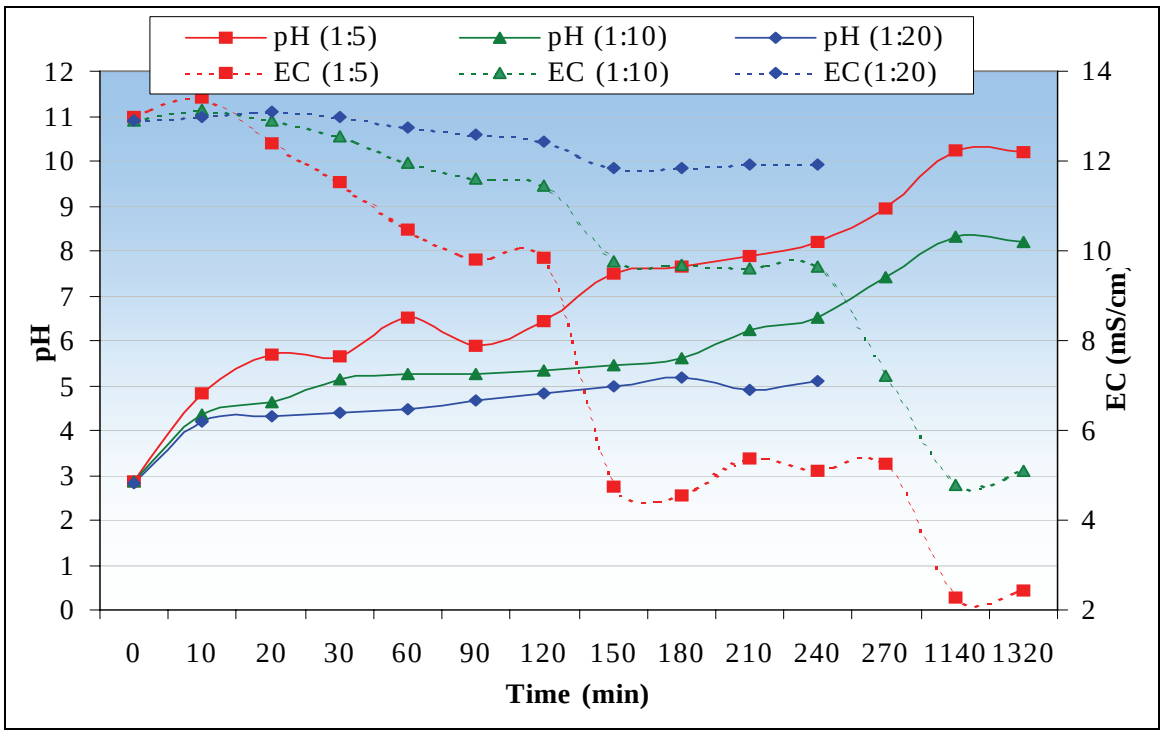

Figure 2.52: pH and EC of the long-term reaction between Arnot fly ash and Landau AMD at ratios of 1:5, 1:10 and 1:20.

An additional ratio 1:20 was added to this batch of experiments (Figure 2.52). The 1:20 FA:AMD neutralisation study was stopped after 4 hours as there was no significant change in pH and conductivity during this time. The 1:5 and 1:10 demonstrated a gradual increase to a neutral pH with a corresponding decrease in conductivity.

2.3.6.2 Secondary small scale experiments

The initial small scale experiments were conducted some time before commencement of pilot scale testing and a considerable amount of time had lapsed. As a result further, secondary, small scale tests were conducted immediately prior to the initiation of pilot scale experiments to confirm that the materials would give results consistent with the initial small scale experiments.

At a FA:AMD ratio of 1:3 a pH of 6 was obtained within 15 min of mixing (Figure 2.53). This neutralisation ratio, although having achieved the desired pH, requires a large mass of fly ash. If one were to apply this ratio in pilot or full-scale trials, large amounts of fly ash would have to be transported to the neutralisation site resulting in higher transportation costs. Therefore, while effective neutralisation must be achieved, the time taken to reach a near neutral pH and mass of ash applied must be considered.

A pH of approximately 6 was achieved in less than 30 min with the 1:5 and 1:4 ratios (Figure 2.53). These reactions are more controllable as the pH increases steadily and the solid residues component is of a more acceptable volume for handling and disposal. The mixing time was extended to 30 hours, after which pH values of 8.2 and 5.5 were obtained for the 1:4 and 1:5 ratios, respectively. The pilot scale mixer is equipped with a variable speed drive mixer with aeration, which was expected to provide more efficient mixing as compared to beaker trials. From the above data, a decision was taken to conduct the pilot scale trials with a 1:6 FA:AMD ratio. This would allow for a smaller amount of fly ash to be used.

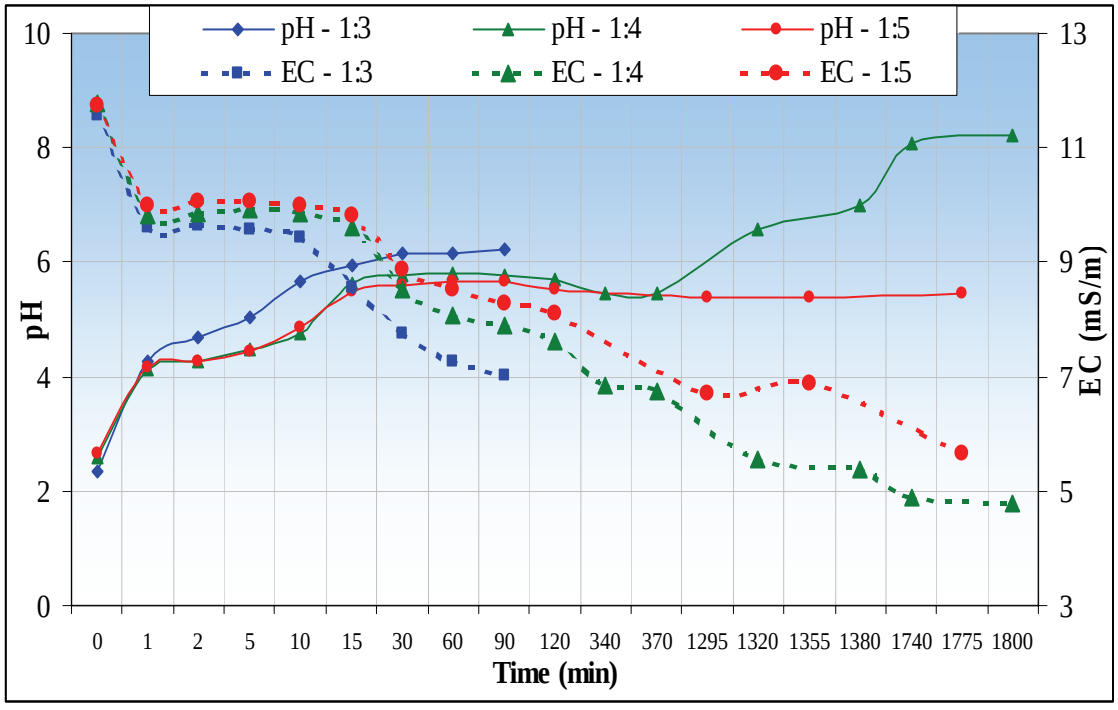

Figure 2.53: Neutralisation of Landau AMD with Arnot fly ash at solid to liquid ratios of 1:3, 1:4 and 1:5 ratios.

The results of these secondary small scale experiments differ slightly from the initial beaker experiments with similar ratios not reaching the same pH values. This is ascribed to the drought conditions experienced in the area and a subsequent concentration effect in the AMD

resulting in more polluted water. The pH of the Landau AMD used in these experiments is lower than Landau AMD used in the initial small scale experiments.

2.3.7 Large or pilot scale neutralisation experiments site specific to Landau colliery and Arnot power station

This pilot scale study was aimed at the development of a site specific protocol for the neutralisation of Arnot AMD with Arnot fly ash. The long-term reaction between Arnot fly ash and Landau AMD was studied in this site specific investigation.

Initial small scale neutralisation experiments were conducted to optimise the neutralisation reaction and determine the neutralisation potential of Arnot fly ash (section 2.3.5). This was aimed at obtaining neutrality, heavy metal removal, and optimum conditions for high capacity adsorbent preparation.

Figure 2.54: Pilot scale mixer with 250 L tank capacity and Turbulator/aeration unit.

Pilot scale neutralisation was performed and waters in contact with fly ash were equilibrated for longer periods to ascertain longer term EC and pH trends, and necessary reaction times for various slurry compositions (FA:AMD ratios). A longer time interval for equilibration of 2820 min was tested in the case of the pilot neutralisation study. The following variables were taken into consideration when designing the pilot scale mixer.

- Efficiency of agitation
- Slurry density and flocculation
- Bulk solids separation and handling
- Water recovery.

Upon consultation with the CSIR, it was decided to design the pilot scale mixer using a Turbulator/aerator unit for mixing with a 250 L tank capacity (Figure 2.54). This ensured

adequate agitation of the AMD/fly ash mixture with aeration to enhance iron oxidation. The slight conical base of the tank allowed for separation of the sludge from the liquid. Turbulator CC was contracted to construct and install the pilot scale mixer. The mixer has been installed at Eskom premises and co-funded by Eskom. The top view in Figure 2.55 shows the extra baffle plates that were added to enhance mixing.

Figure 2.55: Agitation achieved with pilot rig.

From Figure 4.56, it can be seen that in the pilot scale reaction, the pH increased to 6.7, with a corresponding decrease of EC (from 14 to 7.5 mS/cm), in less than 2 hours. The optimised FA:AMD ratio of 1:6 allowed to attain circumneutral pH during the neutralisation reaction at pilot scale. Furthermore, the pilot scale vessel designed for this study proved to be an effective mixer.

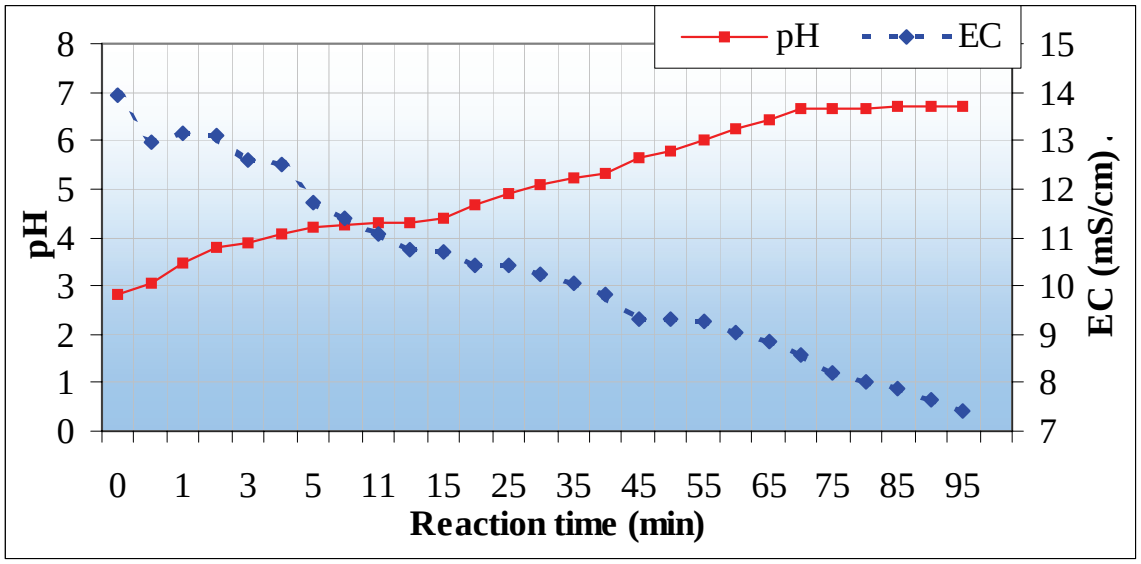

Figure 2.56: Pilot scale neutralisation with an FA:AMD ratio of 1:6.

Some results for Al, Fe and Mn have been rejected and not reported due to analytical error (Table 2.9). More than 90% of Al and Fe were removed from the AMD. There was no Mn removal, but this result was expected as Mn precipitates at pH values greater than 8. Although the quality of water has improved, it should be noted that this data cannot be

compared to that being obtained by the Primary Liming Plant at Landau, which treats the less contaminated Schoongezicht AMD using limestone, as the toe seep AMD used here has a lower pH and much higher metal concentration (see also Section 10).

Table 2.8: Data obtained from neutralisation experiments.

Alkalinity of fly ash (mg/L)	10000
Acidity of AMD (mg $CaCO_3$/L)	15060
Concentration of solids after neutralisation (%)	17
Solids/water ratio (after neutralisation)	1:4.7
Settling rate for 1:6 ratio (min)	4-5

Below a pH of 4 there is very little Al removal, but the majority of Al has precipitated out of solution by the time the pH reaches 4.5. Below a pH of 5 approximately half of Fe is still in solution. This is likely to be unoxidised Fe^{2+} as Fe^{3+} precipitates from solution at a pH around 3.5. The time till complete iron removal is dependant on the amount of unoxidised Fe^{2+} as the oxidation step takes the greatest amount of time; hydrolysis is relatively quick. The concentration of SO_4^{2-} can be seen to be relatively high at the conclusion of the reaction with a removal of only 32%. From previous experiments it has been seen that SO_4^{2-} removal may only be reduced to a concentration of around 2000 mg/L and then only if the pH is increased to >7. The SO_4^{2-} concentrations shown in Table 2.9 display a good, negative correlation with pH (75%) and a good, positive correlation with Fe (79%) and only a 50% correlation with Al. The greatest amount of SO_4^{2-} removal occurs in the first 2 min at pH 3.63 when Fe^{3+} is precipitating. There is no difference in SO_4^{2-} concentrations when the remainder of the Fe precipitates at pH ~5. This suggests that SO_4^{2-} readily co-precipitates with oxidised Fe but that OH^- is preferable to Fe in the process of oxidation and hydrolysis. In a previous study (Burgers, 2003) it was found that high concentrations of Al facilitate greater SO_4^{2-} removal. In this case the concentration of Al is very relative to the concentration of Fe in solution and thus has no positive effect on SO_4^{2-} removal.

Table 2.9: Analysis of water during pilot-scale neutralisation of Landau AMD at 1:6 ratio (FA:AMD).

Reaction time (min)	pH	Al (mg/L)	Fe (mg/L)	SO_4^{2-} (mg/L)
0 (Landau AMD)	2.55	267	4800	4812
2	3.63	232	3002	3546
4	3.81	230	2870	3486
6	3.93	195	2821	3430
10	4.03	155	2736	3900
20	4.24	79	2709	3795
30	4.45	33	2658	3620
45	4.76	-	2194	3659
60	4.98	1.98	-	3600
100	5.49	1.47	-	3364
120	5.66	0.14	182	3264
% Removal		99.9	96.2	32.2

The FA:AMD ratio of 1:6 was effective in neutralising the AMD and removing the major contaminants. The quality of post neutralisation water is such that it could be applied in other process applications while the residual solids could be pumped into underground mines to further treat AMD or prevent AMD formation.

During further pilot scale investigations, a problem was experienced whereby the pH did not increase to the desired level (Figure 2.49). Upon further investigation and analysis of the fly ash, it was noted that the fly ash contained a large percentage of unburned carbon. This was attributed to problems with the parent coal and combustion conditions in the combustion chamber at Arnot power station. The percentage of carbon in this fly ash sample was 6.6%, which is in large excess of the usual 3.2%. The excess carbon is indicative that the mineralogy of the fly ash is probably different as it would not have been exposed to the usual high temperatures in the combustion chamber or economizer. This demonstrates that variations in the mineralogy and composition of fly ash can occur randomly and affect neutralisation reactions. The maximum percentage of unburned carbon in fly ash for effective neutralisation will have to be determined and the effect upon the mineralogy of fly ash should be studied.

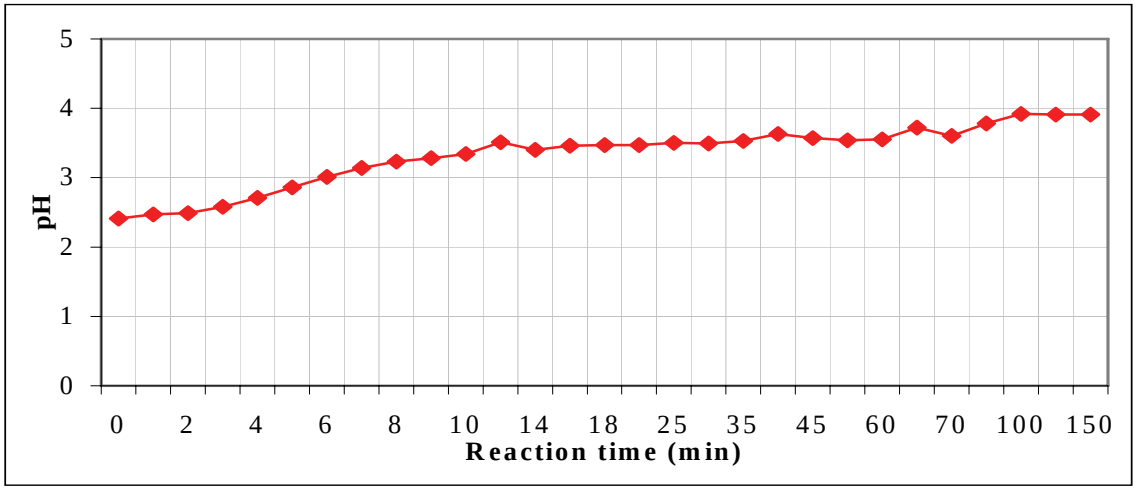

Figure 2.57: pH of water during pilot-scale test run with high carbon content fly ash.

Variations in the quality of AMD with respect to pH and metal content have also been experienced. This will also affect the neutralisation reactions. As such, the optimised neutralisation process may change with varying AMD quality and fly ash composition. It would thus be recommended that a flexible protocol be applied in which the pH and EC of AMD being treated is monitored and the outcome used for adjusting residence times in the treatment plant until the optimum water quality is achieved.

2.4 COMPARISON OF NEUTRALISATION REACTIONS

2.4.1 Introduction

The following three tables compare the removal of toxic metals from AMD with various ratios of FA:AMD and removal of some metals from AMD after neutralisation with limestone. The tables include the DWAF water quality guidelines for irrigation and domestic consumption. Where the parameter exceeds the water quality limit as defined by DWAF, for irrigation water (or domestic if no limit for irrigation is given), the cell in the table is shaded in grey. Where the parameter has been reduced from the original AMD the value is in bold.

2.4.2 Tabulated data

Table 2.10 shows the neutralisation of Navigation AMD in the primary liming plant between August 2004 and June 2005. One kg of impure limestone treated 725 L of AMD.

Table 2.10: Process water composition (mg/L) after reaction between Navigation acid mine drainage and limestone at the Navigation liming plant. (Bold values are reduced from AMD)

Element/ Ion	DWAF water quality standard		Acid mine drainage[+]	Process water
	Irrigation	Domestic use		
pH	-	6 – 9	3.94	5.74
SO_4^{2-}	-	200	2477	**2373**
Al	5	0.15	15.36	**0.1796**
Ca	-	32	472.1	556.1
Fe	-	0.1	49.77	**11.21**
Mg	-	30	188.0	189.6
Mn	0.02	0.05	19.23	20.97

[+]Shaded blocks are values >irrigation limit or domestic where no limit is given for irrigation.

Table 2.11: Process water composition (mg/L) after reaction between Navigation acid mine drainage and Arnot fly ash. BDL=below detection limit. (Bold values reduced from AMD)

Element/ Ion	DWAF water quality standard		Acid mine drainage[+]	Process waters with different fly ash : acid mine drainage ratios[*]		
	Irrigation	Domestic use		1 : 1	1 : 3	1 : 4
pH	-	6 - 9	2.79	11.48	9.48	5.92
SO_4^{2-}	-	200	18 890	**1 705**	**2 627**	**6 793**
Al	5	0.15	13.84	**BDL**	**1.59**	**7.38**
As	0.1	0.01	0.0088	0.0120	0.0194	0.0114
B	0.5	0 – 0.5	1.130	4.593	4.570	4.939
Be	0.1	-	0.2990	0.0015	0.0017	0.0035
Ca	-	32	497.2	462.5	731.0	545.7
Cd	0.01	0.005				
Cl	100	100	95.00	**24.99**	**12.14**	**24.88**
Co	0.05	0 – 0.05	0.6400	**0.0089**	**0.0037**	0.5430
Cu	0.2	1	0.3200	**0.0390**	**0.0370**	**0.1220**
F	2	1	BDL	2.320	1.300	BDL
Fe	-	0.1	3523	**BDL**	**BDL**	**444.4**
I	-	-	0.0500	0.5125	0.2829	0.0679
K	-	50	20.52	**17.43**	23.04	22.05
Li	2.5	0 – 2.5	0.2240	0.7490	0.5410	0.5200
Mg	-	30	293.5	**20.37**	**121.4**	404.6
Mn	0.02	0.05	BDL	0.2480	0.0632	BDL
Mo	0.01	0 – 0.05	BDL	0.3720	0.0920	0.0590
Na	70	100	76.80	**64.84**	73.34	76.73
Ni	0.2	0 – 0.02	0.9220	**0.0626**	**0.0279**	**0.8070**
Pb	0.2	0.01	0.0336	**0.0040**	**0.0052**	**0.0110**
Se	0.02	0.02	0.0267	0.0620	0.0920	0.0590
Sr	-	-	1.331	**0.0115**	3.171	4.113
Ti	-	-	2.774	3.289	**2.509**	**2.442**
Zn	1	3	4.911	**0.0203**	**0.0370**	**1.021**

[+]Shaded blocks are values >irrigation limit or domestic where no limit is given for irrigation.

Table 2.11 shows the reactions performed with different ratios of Arnot fly ash to Navigation acid mine drainage. One kg of fly ash was used to treat 1, 3 and 4 L of AMD.

Table 2.12 shows the reactions performed with different ratios of Arnot fly ash to Kromdraai acid mine drainage. One kg of fly ash was used to treat 1, 3 and 4 L of AMD.

Table 2.12: Process water composition (mg/L) after reaction between Kromdraai acid mine drainage and Arnot fly ash. BDL = Below Detection Limit

Element/ Ion	DWAF water quality standard		Acid mine drainage[+]	Process waters with different fly ash : acid mine drainage ratios[*]		
	Irrigation	Domestic use		1 : 1	1 : 3	1 : 4
pH	-	6 - 9	1.80	12.72	10.38	9.16
SO_4^{2-}	-	200	10 200	**1 200**	**1 350**	**1 750**
Al	5	0.15	1 689	**BDL**	**0.5063**	**0.0513**
As	0.1	0.01	0.3918	**0.0001**	**0.0009**	**BDL**
B	0.5	0 – 0.5	0.5586	**BDL**	**0.2765**	**0.3473**
Ca	-	32	209.7	**8.574**	**23.16**	**BDL**
Cd	0.01	0.005	0.1316	**0.00005**	**BDL**	**BDL**
Co	0.05	0 – 0.05	10.46	**0.0002**	**0.0014**	**BDL**
Cu	0.2	1	3.467	**BDL**	**0.0029**	**0.0036**
Fe	-	0.1	6 202	**43.28**	**21.64**	**14.14**
Hg	-	1	0.028	**BDL**	**0.025**	**0.0006**
K	-	50	4.705	**BDL**	**BDL**	**BDL**
Li	2.5	0 – 2.5	2.519	**0.0038**	**0.0071**	**0.0082**
Mg	-	30	117.0	**0.0142**	**0.0790**	**2.314**
Mn	0.02	0.05	19.51	**0.0008**	**0.00005**	**0.0002**
Mo	0.01	0 – 0.05	0.022	**0.0105**	**0.0178**	**0.0131**
Na	70	100	11.04	**0.7662**	**0.8155**	**0.9735**
Ni	0.2	0 – 0.02	20.85	**0.0070**	**0.0075**	**0.0046**
Pb	0.2	0.01	0.6250	**BDL**	**0.0009**	**BDL**
Se	0.02	0.02	0.1026	**0.0046**	**0.0119**	**0.0089**
Sr	-	-	3.109	**0.4241**	**0.1724**	**0.1641**
Zn	1	3	75.23	**BDL**	**0.0229**	**0.0037**

[+]Shaded blocks are values >irrigation limit or domestic where no limit is given for irrigation.
[*]Bold values are reduced from AMD

Table 2.13 shows the reactions performed with different ratios of Duvha fly ash to Kromdraai acid mine drainage. One kg of fly ash was used to treat 1, 3 and 4 L of AMD.

Table 2.13: Process water composition (mg/L) after reaction between Kromdraai acid mine drainage and Duvha fly ash. BDL = Below Detection Limit

Element/ Ion	DWAF water quality standard		Acid mine drainage[+]	Process waters with different fly ash : acid mine drainage ratios[*]		
	Irrigation	Domestic use		1 : 1	1 : 3	1 : 4
pH	-	6 - 9	1.80	10.41	10.23	9.80
SO_4^{2-}	-	200	10 200	**1750**	**1450**	**1550**
Al	5	0.15	1 689	**0.1069**	**0.3739**	**0.2310**
As	0.1	0.01	0.3918	**BDL**	**BDL**	**0.0005**
B	0.5	0 – 0.5	0.5586	**0.0883**	**0.0316**	**0.0646**
Ca	-	32	209.7	**BDL**	**BDL**	**7.228**
Cd	0.01	0.005	0.1316	**BDL**	**0.00002**	**0.00004**
Co	0.05	0 – 0.05	10.46	**BDL**	**BDL**	**0.0002**
Cu	0.2	1	3.467	**BDL**	**0.0030**	**0.0016**
Fe	-	0.1	6 202	**BDL**	**BDL**	**BDL**
Hg	-	1	0.028	**BDL**	**BDL**	**BDL**
K	-	50	4.705	**BDL**	**BDL**	**BDL**
Li	2.5	0 – 2.5	2.519	**BDL**	**0.0022**	**0.0024**
Mg	-	30	117.0	**0.0458**	**0.0725**	**0.1104**
Mn	0.02	0.05	19.51	**0.0248**	**0.0005**	**0.0020**
Mo	0.01	0 – 0.05	0.022	**0.0026**	**0.0029**	**0.0026**
Na	70	100	11.04	**0.7780**	**0.8299**	**0.7533**
Ni	0.2	0 – 0.02	20.85	**0.0110**	**0.0067**	**0.0053**
Pb	0.2	0.01	0.6250	**BDL**	**0.0047**	**0.00004**
Se	0.02	0.02	0.1026	**BDL**	**BDL**	**0.0034**
Sr	-	-	3.109	**0.0186**	**0.0235**	**0.0217**
Zn	1	3	75.23	**0.6556**	**0.0263**	**0.0163**

[+]Shaded blocks are values >irrigation limit or domestic where no limit is given for irrigation.
[*]Bold values are reduced from AMD

2.4.3 Discussion

The two AMD's analysed, Navigation and Kromdraai, in Tables 2.11 – 2.14 are different and have neutralised effluent with different concentrations of elements. In general it can be stated that Kromdraai AMD has a high concentration of harmful metals than Navigation. In Kromdraai water the Al, As, Co, Cu, Fe, Li, Mn, Mo, Ni, Pb, Se, Sr and Zn are higher while the pH is lower than Navigation AMD. Navigation water contains more SO_4, B, Ca, K, Mg, and Na, while the pH is slightly higher than Kromdraai AMD. In Table 2.10 it can be seen that only half of the parameters are above irrigation or domestic water quality limits, while Tables 2.13 and 2.14 show 84% of Kromdraai water being above quality limits. Only half of the element/ion concentrations given for Navigation water were reduced from the original concentration upon neutralisation while all the element/ion concentrations were reduced for Kromdraai water upon neutralisation with Arnot and Duvha ash.

Higher ratios of AMD to FA produce the greatest number of element concentrations below water quality limits. This may be a result of increasing the pH to very alkaline levels and thus removing a greater concentration of toxic elements. It can be seen from the 1:4 FA:AMD ratio for Navigation and Arnot neutralisation at pH~6 that there are fewer toxic metals

removed than the other two ratios. For the Kromdraai and Arnot and Duvha neutralisations it appears to make little difference as the reaction reaches pH values greater than 9.

To effect the greatest contaminant removal from AMD the pH should be raised to a value >8. Thereafter the pH of the unbuffered water may be lowered artificially to conform to water quality limits. Based on leaching studies, as yet uncompleted, lowering the pH of neutralised solid residue requires less than 0.5 mmol of acid per g of solid.

2.5 DISCUSSION

A minimum concentration of Fe^{2+} and probably other elements in solution could be required for the effective performance of the neutralisation reaction. Burgers (2002) observed high SO_4 removal in presence of high Al^{3+} concentration but Fe^{3+} had little effect on SO_4. Research workers employing synthetic solutions (Tamaura *et al.*, 1991) have been able to optimise the removal of non-ferrous elements using optimum concentrations of Fe^{2+}/Fe^{3+}. Loewenthal *et al.* (2004) used magnetite seed to induce co-precipitation of non-ferrous toxic elements in SAMD using NaOH for pH control, 99.9% removal was observed for the heavy metals investigated

In the small scale and Turbulator reactions fly ash from various sources has the capacity to neutralise AMD at low FA/AMD ratios of 1:6. The neutralisation reaction can be seen to be considerably faster with greater amounts of ash and with the added aeration in the large scale experiments conducted in a Turbulator. Sulphate values still remain quite high but are reduced by a factor of ten from approximately 10 000 mg/L to under 2000 mg/L which is a considerable improvement. Higher FA/AMD ratios were more successful at removing Fe^{2+} from solution but the results suggest that the Fe^{2+} concentration is dependent on aeration rather than amount of ash. This is proven by the fact that the least Fe^{2+} occurs in effluent recovered from the Turbulator reactions. This is an indication of oxidation occurring more rapidly and efficiently in a turbulent system.

The pilot scale Arnot fly ash and Landau AMD neutralisation process has been successfully implemented at a ratio of 1:6 FA:AMD. Effective neutralisation was achieved in a short time period with improved water quality. However, due to the possible variations in fly ash and AMD quality, this ratio or the contact time will have to be adjusted to accommodate for these variations. Further, the fly ash must be analysed at each stage to determine the percentage unburned carbon, as this may indicate changes in the mineralogy that will affect the neutralisation reaction.

2.6 CONCLUSIONS

In acid mine drainages:

- The concentration of SO_4^{2-} can vary by a large margin and even by magnitudes between different samples and samples from the same source.
- The pH values of waters are between 2 and 3, some concentration events can cause a pH lower than 2, as with Kromdraai AMD.
- EC and pH are proportional with a lower pH resulting in a higher EC and dissolved solids.
- Lack of buffering capacity was observed in some waters, leading to very rapid neutralisation.

- To effect the greatest contaminant removal from AMD the pH should be raised to a value >8.

In neutralised water:

- Fe was reduced to below 0.5 mg/L in samples with sufficient aeration (Pilot study and 1:6 Turbulator reaction) or with sufficient time to oxidise.
- SO_4^{2-} concentration decreases by a greater amount with higher fly ash to AMD ratios. This indicates that the precipitation of SO_4^{2-} is dependant on alkalinity and more specifically the amount of Ca^{2+} in solution.
- The concentration of Al^{3+} is also alkalinity dependant with the greatest Al^{3+} removal occurring at high fly ash to AMD ratios. Lower ratios do, however, show significant Al^{3+} removal to levels below 6mg/L.

3. INVESTIGATION OF SOLIDS

3.1 INTRODUCTION

In this section the fly ashes used in each experiment were analysed in order to determine the effect of soluble components and the physical effect of the solid on the neutralisation reaction. The physical, chemical and mineralogical properties of fly ashes depend on the composition of the parent coal, the conditions within the combustion chamber and the type of emission control devices used and their efficiency. Fly ash is that fraction of combustion waste that enters the flue gas stream. The ash is then collected by emission control devices or allowed to escape into the atmosphere (Adriano *et al*., 1980). The physical characteristics of combustion wastes affect the reactivity of these wastes. Factors such as the particle size and morphology, bulk density, specific gravity, permeability and etc. are all important factors when considering the geochemistry of weathering reactions and element mobilization.

Fly ash is a complex heterogeneous substance composed of amorphous and crystalline phases. Particles are small, glass-like spherules ranging from 0.01 to 100 µm in size. These spherical particles are a result of the melting of silicate minerals in the combustion chamber (Carlson and Adriano, 1993). Two classes of particles are defined: cenospheres, which are hollow and plerospheres, which are filled with smaller amorphous particles and crystals. Between 70 and 90 % of fly ash consists of glassy spheres (Fisher and Natusch, 1979).

The predominant elements in FA are Al, Si, Fe, Ca, K, and Na in higher concentrations relative to those found in the parent coal. Elements such as Al, Ca and Fe occur in concentrations typical of soils. Sodium is present in concentrations generally exceeding those found in soil. Fossil fuel wastes are also enriched with S when compared with soil (Mattigod *et al*., 1990).

The pH of fly ash tends to vary between 4.5 and 12 depending on the sulphur content of the parent coal. South African ashes tend be highly alkaline. Fresh ash contains a high concentration of soluble salts. These high concentrations can be reduced if the ash is leached or weathered. Another characteristic of ashes is that they are frequently pozzolanic. Reaction with water in the presence of lime creates a cement that leads to pore clogging, reduced infiltration and impedes root penetration in ash deposits (Carlson and Adriano, 1993; Chermak and Runnels, 1997). Campbell (1999) found that South African ashes have a tendency to display pozzolanic activity.

The most common minerals in fly ash are quartz (SiO_2) and mullite ($3Al_2O_3 \cdot 2SiO_2$). The Fe-containing compounds include hematite (Fe_2O_3) and magnetite (Fe_3O_4); the Ca-compounds include anhydrite ($CaSO_4$) and lime (CaO). Periclase (MgO) represents the Mg fraction and some unburned carbon makes up approximately 1 to 2% of the ash (Mattigod *et al*., 1990).

3.2 METHOD

A sample of fly ash was retained and milled and standard analytical methods including XRD, XRF, FTIR, etc. were employed in order to characterise it. Subsequent to the neutralisation of AMD with FA a sample of the solid residue, consisting chiefly of FA with some Fe-oxyhydroxide minerals precipitated onto the surface of the glass spheres, was collected and analysed. As a results of this solid consisting mainly of glass spheres it is very difficult to

identify any changes in the mineralogy and composition of the material after neutralisation with XRD and IR as quartz and mullite dominate and interfere with the detection of any other minerals present at low concentrations. Consequently, further analytical techniques such as SEM must be employed to detect any alteration in the FA matrix.

Fly ash was obtained directly from the Arnot power station in South Africa and kept in tightly locked PVC buckets to prevent ingress of CO_2, which leads to loss of alkalinity (Dold, 2003). AMD samples were obtained at Navigation colliery in Witbank, South Africa.

Neutralisation experiments site specific to Navigation colliery and Arnot power station using fresh samples at the ratios 1:3 FA to obtain neutral water and 1:1.5 FA to obtain alkaline water, were conducted. In these studies typically a volume of 500 mL of AMD was mixed with various quantities of fly ash and stirred by overhead stirrer for 3-5 hrs at 240 rpm. The main objective was to understand the $Fe^{2+/}Fe^{3+}$ oxidation/precipitation process, SO_4 removal and major element removal, which helped to establish whether there was a relationship between the mineral phases/precipitates being formed and trace elements removal. The solid residues resulting form the neutralisation reaction were further investigated.

These solid residues prepared during the small scale neutralisation experiments site specific to Arnot power station and Navigation colliery to investigate mineral equilibria (Section 2.3.4) were dried for 12 hours at 105^oC and ground to a fine powder. The dried samples were then suspended in ultra-pure water at a water to solid ratio of 20:1 and agitated in an ultrasonic bath for 4 hours. The suspension was allowed to stand for 10 minutes and then filtered through 0.45 µm nucleopore membrane to collect the very fine and light fraction. The remaining fraction was allowed to settle completely. From the settled material two fractions were distinct hereby referred to as coarse and fine and were separated manually by using a spatula. The 3 size fractions (coarse, fine and very fine) were oven dried for 3 hours at 60^0C before and after solvent extractions. The dissolution of the 3 size fractions was done by reaction with 0.2 M ammonium oxalate at pH 3.0 in the dark using the method of Jackson *et al*. (1986) but the extraction time was increased to 4 hours. Differential x-ray diffraction (DXRD) was done following the method of Schulze (1981) after NH_4-oxalate extraction of the three size fractionated samples.

X-ray diffraction spectra of the untreated and oxalate treated size fractions were obtained by step-scanning at intervals of 0.02^0 2θ from 5^0 to 85^0 and counted for 0.5 seconds per step. A Phillips PANalytical instrument was used with a PW3830 x-ray generator operated at 40 kV and 25 mA. The X'pert Graphics and identify program was used to identify the mineral phases using the JCPDF database.

Samples for scanning electron microscope (SEM) investigation were disaggregated in ethanol in an ultra-sonic bath. Drops were dispersed on a carbon tape using a Pasteur pipette and then air dried. A scanning electron microscope (Hitachi X-650 Micron analyser) was used to characterize the change in the morphology and chemical characteristics of the fractionated and extracted samples. Analysis by scanning electron microscope coupled to energy dispersive analysis of X-rays spectrometer (SEM-EDX) of the solid residues and unreacted fly ash was done to identify mineral phases that were in concentrations too low to be detected by XRD.

The activities of aqueous species and mineral saturation indices of selected mineral phases were calculated using PHREEQC software (Parkhurst, 1995) and the WATEQ4F database.

Saturation index (SI) is used when large deviations from equilibrium are observed. For SI=0, there is equilibrium between the mineral and the ions in solution; SI<0 reflects under saturation, and SI>0 super saturation. For a state of under saturation dissolution of the solid phase is expected and super saturation suggests that precipitation will occur.

The solid residues from the neutralisation reaction between Navigation AMD and Arnot fly at a ratio of FA:AMD ratio 1:3 were subjected to a sequential extraction procedure to investigate trace metal partitioning in mineral phases. The methods described by Jackson *et al*. (1986), Muller and Seiler (1999) and Shuman (1982) were adopted.

The following fractions were identified:

- soluble in water (milliQ water, 2 hours)
- specific surface complexes (NH_4OAc 1M, pH 6.4, 24 hours)
- Mn-oxides (NH_2OH-HCl in 0.01M HNO_3, pH 2.0, 0.5 hour)
- crypto-crystalline Fe-oxides amorphous (NH_4Oac 0.2 M + oxalic acid 0.2 M, pH 3.0, 4 hours)
- crystalline Fe oxides (NH_4Oac 0.2 M + oxalic acid 0.2 M + ascorbic acid 0.1 M, pH 3.25, 0.3 hour at 96^oC in dark)
- residual (aqua regia digestion, 7.5 mL 37 % HCl + 2.5 mL 65 % HNO_3).

3.3 RESULTS

3.3.1 Fly ash used in small scale neutralisation experiments

Table 3.1: Comparison of the composition and surface area for the fly ashes used in the study specific to Bank and Kromdraai collieries and Arnot, Duvha, Matla, Kendal and Hendrina power stations.

FA	SO_4^{2-} (mg/L)	NO_3^- (mg/L)	Fe^{2+} (mg/L)	Alkalinity (mg/L)	Particle size (μm)	Surface Area (m^2/g)
Arnot	50	1.6	55.9	699.6	26.38	3.630
Duvha	800	6.2	111.7	582.2	17.75	2.325
Matla	50	1.5	55.9	428.4	30.95	1.000
Kendal	50	1.6	55.9	150.0	114.5	0.315
Hendrina	50	1.0	55.9	304.8	13.30	1.065

Duvha FA contains the highest amounts of SO_4 and Fe^{2+} (Table 3.1), while Arnot FA has the highest alkalinity. Arnot and Duvha ash have the smallest particle size with close to 100% of particles being under 45 μm, while Hendrina, Matla and Kendal ash have 75%, 62% and 21% respectively, of particles below 45μm in size, and Kendal ash thus has the lowest surface area.

The alkalinity of an ash, determined from a leachate, shows good correlation with particle size. This correlation is further seen in the neutralisation capacity of each ash with AMD as discussed in Section 4. From the fact that Duvha FA has such a high capacity to neutralise AMD it can be concluded that not necessarily all of the available alkalinity of a FA may be determined from a leachate. The neutralising capacity also depends on the physical structure of the ash as evidenced by the very close correlation between alkalinity and surface area. The influence of particle size and morphology and surface area need to be further investigated as they could have a major influence on fly ash neutralisation. Fly ash that due to its coarseness may be suitable for backfilling may not be as suitable for neutralisation as fine ash is.

The difference between Arnot and Matla ash in terms of the major oxides is small (Table 3.2). There is a difference in the amounts of Fe and Al present in the ash as a result of the composition of the gangue rock, where the sediments that Matla coal resides in containing more clay minerals than the rock which Arnot coal resides in which contain more pyrites. The calcium content of both ashes is very similar (Table 3.2) but the alkalinity of each ash is markedly different (Table 3.1). This difference may be attributed to the higher reactivity of Arnot ash in terms of its greater surface area. In general Matla ash has lower concentrations of trace metals than Arnot ash except for Sr and Ba of which it has relatively high quantities.

Table 3.2: Chemical characteristics of fly ash used in the study specific to Brugspruit, Navigation and Bank collieries and Arnot and Matla power stations and long-term column leaching.

Oxides %	Arnot FA	Matla FA
SiO_2	53.4	53.8
Al_2O_3	23.4	26.2
CaO	8.43	8.50
Fe_2O_3	4.72	3.40
MgO	2.70	2.48
TiO_2	1.34	1.44
K_2O	0.49	0.86
Na_2O	0.35	0.49
MnO	0.06	0.05

3.3.2 Fly ash used in large or pilot scale neutralisation experiments

It was found in the Pilot study that as a result of a malfunction in the combustion process there was a batch of fly ash used for these studies that had a high percentage of unburnt coal indicating a changed mineralogy. Use of this fly ash caused the neutralisation reaction to fail and the process waters only reached a pH of 4. The cause of this inability to achieve neutralisation may partially have to do with the amphiprotic nature of coal and the fact that in an acid environment it is positive and may be scavenging OH^- out of solution. This assumption however, requires further investigation, as does the influence of particle size and the changes in mineralogy associated with changes in the combustion chamber.

Table 3.3: Chemical and mineralogical composition of Arnot fly ash.

Oxides	%	Oxides	%	Minerals	%
SiO_2	50.9	K_2O	0.40	Mullite – $Al_2Si_2O_{13}$	14.2
Al_2O_3	26.5	P_2O_5	0.33	Alpha Quartz – SiO_2	8.35
CaO	6.90	SO_3	0.06	Lime – CaO	4.90
Fe_2O_3	5.20	MnO	0.05	Maghemite – Fe_2O_3	9.96
MgO	2.70	Na_2O	0.01	Amorphous or glassy phase	52.6
TiO_2	1.40				

When comparing the different analyses of Arnot fly ash the variation between different samples can be seen (Tables 3.2 and 3.3). This variation is confined to a small range and is likely to be negligible in terms of its performance as a liming agent although a 1% variation in Ca concentration and hence alkalinity may have a large effect in terms of the equivalent volumes of fly ash needed for AMD neutralisation.

3.3.3 Identification by FTIR of fly ash and neutralisation solids site specific to Bank and Kromdraai collieries and Arnot, Duvha, Matla, Kendal and Hendrina power stations

In order to gain a better understanding of the fly ash composition and compare variation in neutralisation reactions, various fly ash sources and solid residues from site specific combinations of AMD from Bank and Kromdraai collieries and FA from Arnot, Duvha, Matla, Kendal and Hendrina power stations was analysed with infrared spectroscopy. From the literature (Styszko-Grochowiak *et al*., 2004) fly ash has the following characteristics when viewed with FTIR spectroscopy; as summarized in Table 3.4.

Table 3.4: Assignments of infrared active bands that are detected for fly ash.

*Wave number (cm^{-1})	Assignment	
1080 (sh)	Asymmetric stretching	Si-O-Si and Al-O-Si
1074 (s)	Asymmetric stretching	Si-O-Si and Al-O-Si
1165 (sh)	Asymmetric stretching	Si-O-Si
1138 (sh)	Asymmetric stretching	Si-O-Si and Al-O-Si
950-1200 (s)	Asymmetric stretching	Si-O-Si and Al-O-Si
882 (s)	Si-O stretching, OH bending	Si-OH
798 (m)	Symmetric stretching	Si-O-Si
727 (sh)	Symmetric stretching	Si-O-Si and Al-O-Si
620 (sh)	Symmetric stretching	Si-O-Si and Al-O-Si
561 (s)	Symmetric stretching	Al-O-Si
466 (s)	Bending	Si-O-Si and O-Si-O

*s = strong, m = medium, sh = shoulder

- The strong bands at 1165 and 1080 cm^{-1} and the medium band at 798 cm^{-1} are attributable to α-Quartz.
- The strong band at 561 cm^{-1} and the shoulders at 1138 and 620 cm^{-1} are indicative of mullite.
- An amorphous aluminosilicate phase is likely to cause vibration at around 1070-1080 cm^{-1} since similar vibrations can be observed for natural and glassy aluminosilicate materials.
- The broad band located at 500-650 cm^{-1} is also indicative of silicate and aluminosilicate glasses, which possess long range structural order in the form of rings of tetrahedron or octahedron.
- The very broad band between 950 and 1200cm^{-1} at the T-O-Si (T=Al and Si) stretching vibration region is due to the multi phase nature of the fly ash.

Table 3.5: The major infrared peaks for each fly ash and their assignments.

Fly ash	OH	H_2O	CO_3	Al/Si-O-Si	CO_3	CO_3	Al-O-Si	Si-O-Si
	ν_1	ν_2	ν_3	ν_3	ν_2	ν_2	ν_1	ν_4
Arnot				1097			559	470
Duvha	3454	1628	1428	1097	874	710	559	470
Matla	3454	1628		1097			559	470
Hendrina	3454	1628		1095			559	470
Kendal	3454	1628		1092			559	470

Figure 3.1 shows transmittance spectra for Arnot, Duvha, Matla, Hendrina and Kendal fly ashes. The transmittance (%) is plotted along the primary y-axis and the wave number (cm^1)

is plotted on x-axis. The major peaks are labelled on the spectra and subsequently listed in Table 5.5 with their assigned vibrational modes.

The major absorption peaks correspond to asymmetric stretching (Si-O-Si and Al-O-Si) at 1097 cm^{-1} and symmetric stretching of mullite (Al-O-Si) at 559 cm^{-1} and bending vibrations (Si-O-Si and O-Si-O) at 470 cm^{-1} (Styszko-Grochowiak *et al.*, 2004). Duvha ash also contains carbonate as CO_3, which could be as a result of the ash being exposed to the atmosphere and absorbing CO_2.

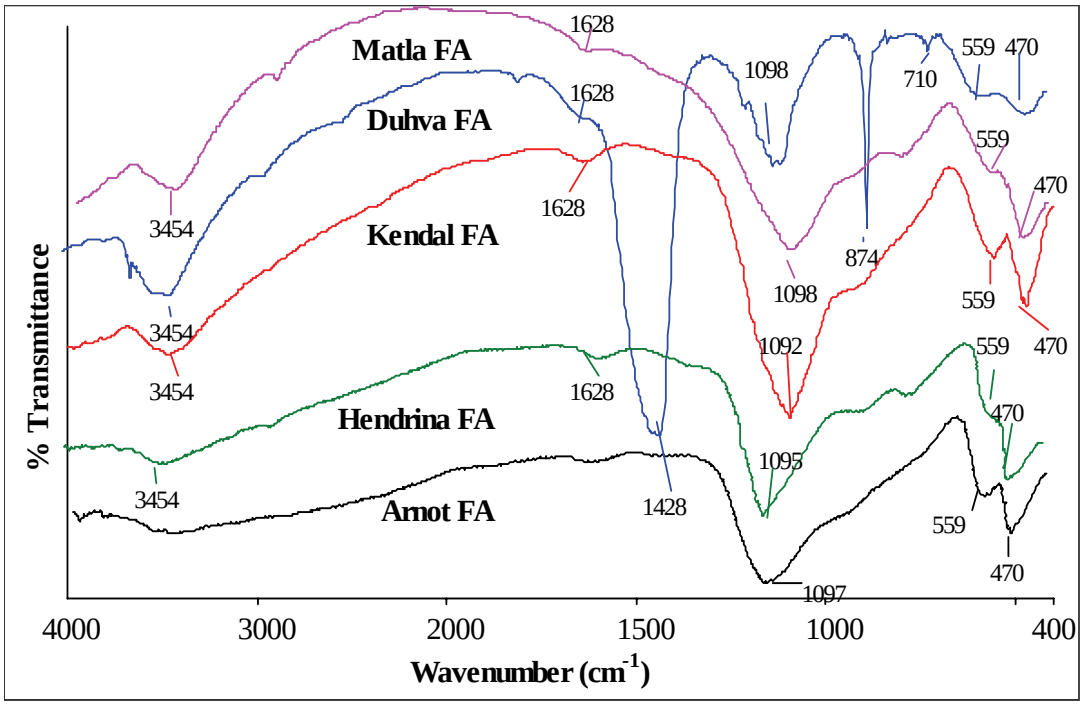

Figure 3.1: FTIR spectra for fly ash from Arnot, Duvha, Matla, Hendrina and Kendal power stations.

Figure 3.2 shows the infrared spectra of 5 different solid residues obtained from fly ashes used to neutralise Kromdraai AMD. When comparing these spectra to the parent ash there are several differences that can be noted. Firstly, the Al/Si-O-Si asymmetric stretching band at ~1097 cm^{-1}, visible in the raw FA's has been reduced in intensity. Two new peaks are visible at 1150 cm^{-1} and 452 cm^{-1} with a small broad shoulder at 603 cm^{-1}. It is possible that these peaks are a result of $CaSO_4$ precipitation. Carbonate is still present in the Duvha ash, although the peak intensity is reduced, which suggests that some of the CO_3 has taken part in the neutralisation reaction. Aside from the CO_3 signature in the Duvha ash, there is not much difference in the product material. Thus, the type of ash has little effect on the composition of the solid residue recovered as a waste product.

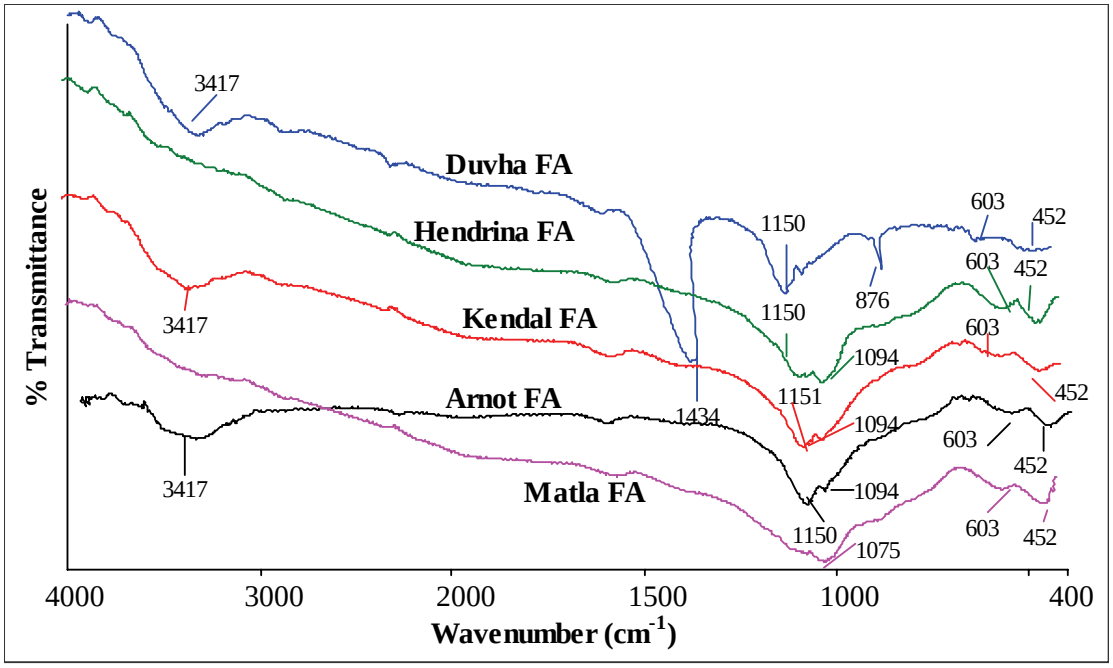

Figure 3.2: FTIR spectra for solid residues at neutral pH for all fly ashes treated with Kromdraai AMD.

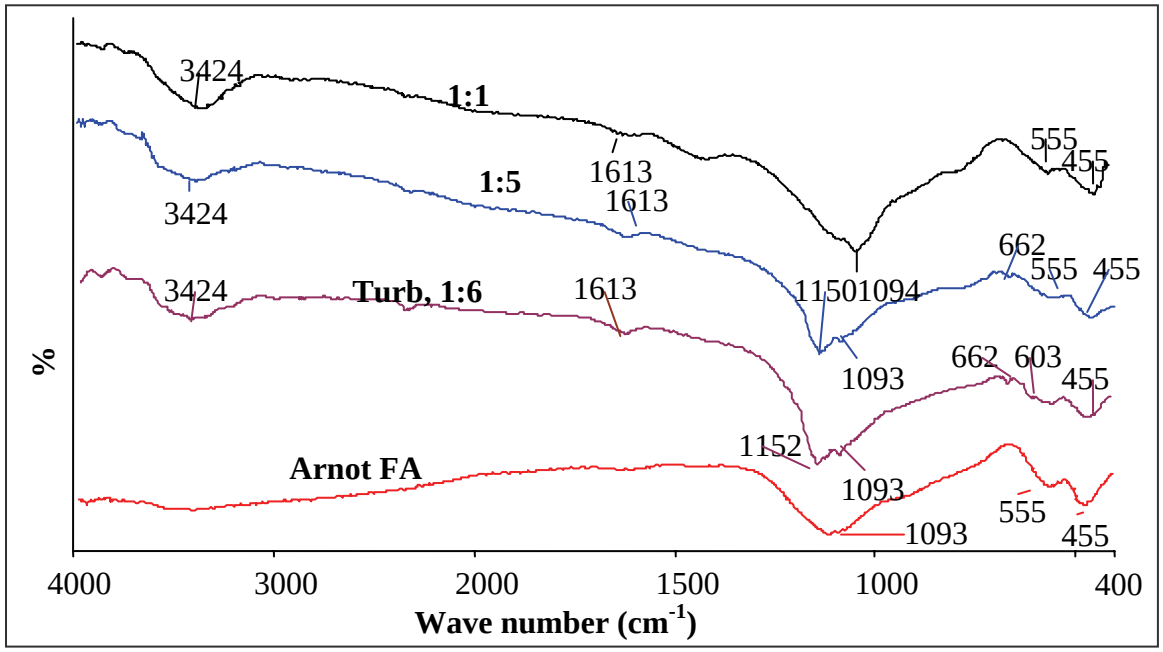

Figure 3.3: FTIR spectra for Arnot Fly Ash and residual solids at the ratios 1:1, 1:5 and at Turbulator ratio 1:6 treated with Kromdraai acid mine drainage.

Figure 3.3 compares FTIR spectra for solid residues recovered at neutral pH at different solid to liquid (S/L) ratios of the neutralisation of Arnot ash with Kromdraai AMD. There is virtually no difference between the different ratios, thus it can be said that the ratio of S/L does not significantly affect the composition of the product material. When the infrared spectra of different S/L ratios are compared with the infrared spectra of different ashes there is no significant difference.

3.3.4 Identification of fly ash and neutralisation solids site specific to Bank and Kromdraai collieries and Arnot, Duvha, Matla, Kendal and Hendrina power stations

Identification of fly ash and neutralisation solids was performed by scanning electron microscopy (SEM) looking at solid residues from site specific combinations of AMD from Bank and Kromdraai collieries and FA from Arnot, Duvha, Matla, Kendal and Hendrina power stations The morphology of the (Arnot, Hendrina) fly ash is characterised by well-rounded glass spheres. The higher proportion of glass spheres in the fly ash indicates a higher degree of melting of the mineralogical content of the parent coal. This can be attributed to a higher operating temperature in the combustion chamber furnace or to the higher CaO content of the mineral fraction.

During burning, CaO acts as a flux, lowering the melting temperature of the mineral phases in the parent coal. A high CaO content in the parent coal results in a higher degree of melting, and thus causes an increase in concentration of smooth glass spheres. On the other hand (Kendal, Matla) fly ash is characterized by an apparently larger grain size and more angular particles (O'Brien, 2000).

Observations based upon SEM images of the various FA:

1. The unburned carbon particles are larger and form irregular grains. (Kendal FA)
2. The size of grains in the fly ash is related to the amount of unburned carbon.
3. The amount of unburned carbon is less in ashes that are finer. (Arnot FA)
4. The application of low NOx combustion systems causes high residual carbon levels in ash. (Duvha).
5. The carbon content is closely related to particle size distribution in fly ash. Kendal FA, which has a larger particle size, thus, also has more unburned carbon.
6. The unburned carbon was characterized in terms of size distribution, surface area, crystal structure and density.
7. The inorganic portion of the fly ash samples consists predominantly of glassy spheres.

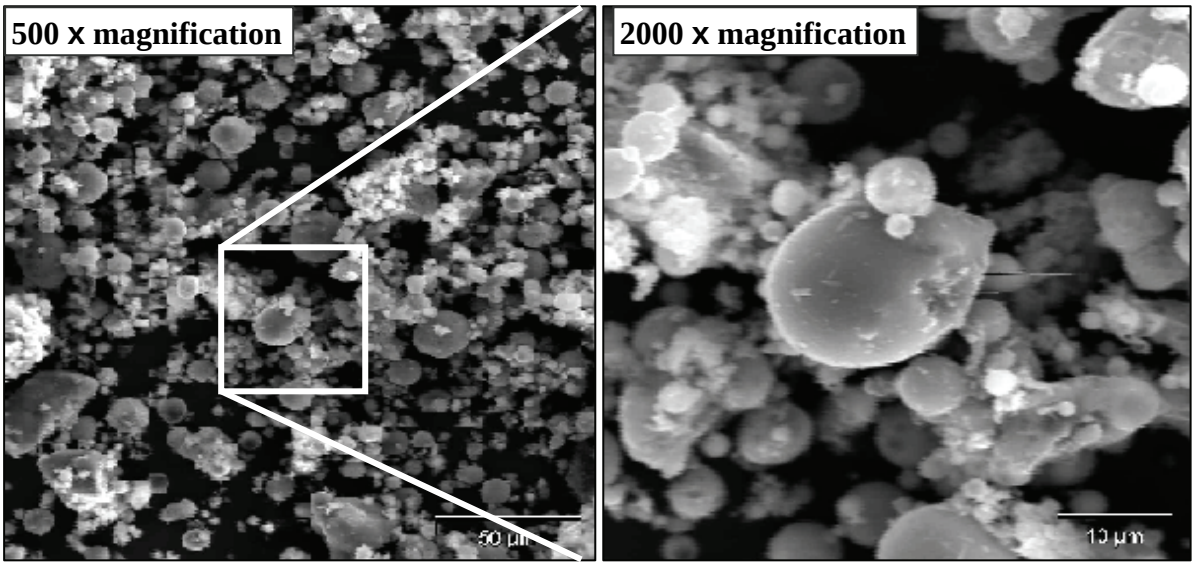

Figure 3.4: SEM images of solid product from the neutralisation of Kromdraai AMD and Arnot FA at the S/L ratio 1:1 at pH 11-12.

In Figures 3.4 -6 various SEM micrographs are presented that show the typical morphology of solid residues recovered from the neutralisation reaction between Kromdraai AMD and

Arnot FA at different S/L ratio at pH 11-12. The typical FA morphology is altered and the precipitated phases are visible between and upon the spherical ash particles

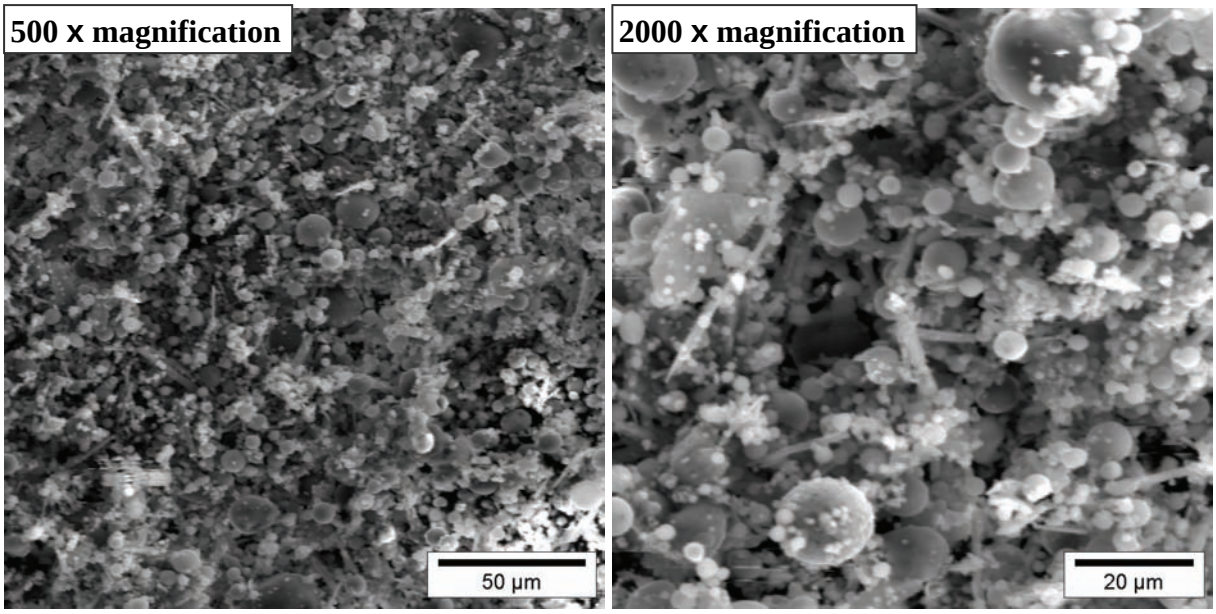

Figure 3.5: SEM images of solid product from the neutralisation of Kromdraai AMD and Arnot FA at the S/L ratio 1:6 conducted in the Turbulator at pH 11-12.

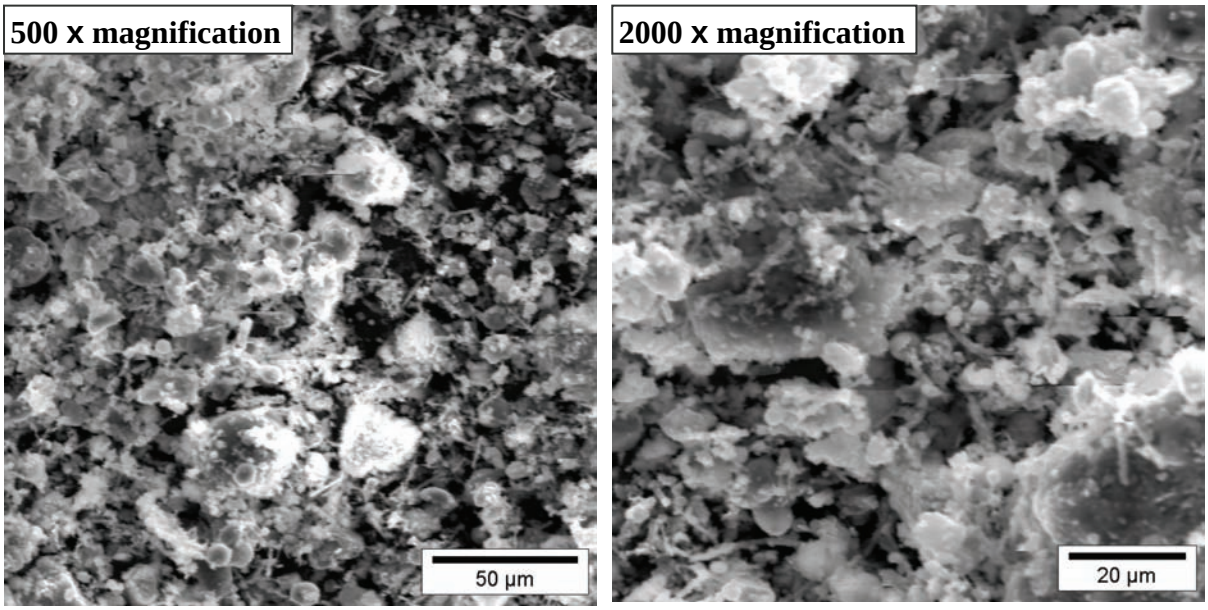

Figure 3.6: SEM images of solid product from the neutralisation of Kromdraai AMD and Arnot FA at the S/L ratio 1:6 conducted in the Turbulator at pH 10-11.

3.3.5 Identification of fly ash and neutralisation solids site specific to Matla and Arnot power stations and Brugspruit, Navigation and Bank collieries

Identification was performed by scanning electron microscopy (SEM) of fly ash and neutralisation solids site specific to Matla and Arnot power stations and Brugspruit, Navigation and Bank collieries. The solids collected at pH 9.33 from the reaction between Arnot FA and Navigation AMD at a ratio of 1:3 clearly show gypsum crystals, identified by SEM-EDS (Figure 3.7). The solids collected at pH 12.5 from the reaction between Arnot FA

and Navigation AMD at a ratio of 1:5 show needle-like crystals identified by SEM-EDS to be ettringite. Analysis of the solid residues collected at neutral pH by SEM-EDS (not shown here) showed increasing concentration of Fe in most of the areas analysed.

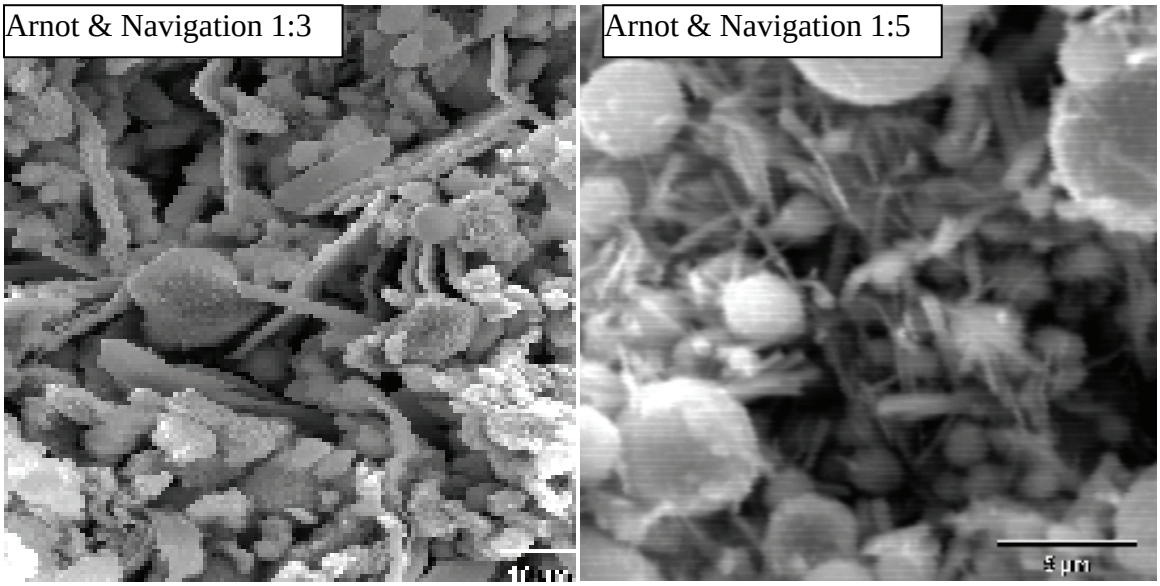

Figure 3.7: SEM pictures of residual solids from the reaction between Arnot FA and Navigation AMD.

3.3.6 Mineralogy and trace element partitioning in solid residues site specific to Matla and Arnot power stations and Brugspruit, Navigation, and Bank collieries

Mineralogy and trace element partitioning in solid residues recovered from site specific combinations of FA from Matla and Arnot power stations and AMD from Brugspruit, Navigation, and Bank collieries was studied. Understanding the behaviour and ultimate fate of the SO_4^{2-}, major and trace elements in AMD and fly ash during the treatment process is a major determinant in use of fly ash as a liming agent. It was deemed necessary to establish the mineralogy and trace element partitioning in solid residues. The objective of this section of the study was thus to evaluate the chemistry of the resulting process water as the sulphate and metal rich AMD interact with fly ash, to relate the solution chemistry and formation of solid phases upon the ash. This section furthermore evaluates the development of solubility controls through dissolution kinetics or the role of equilibrium precipitation that can be predicted by geochemical equilibrium models. The importance of precipitation reactions should be established. Calculated saturation indices and mineralogical analysis were used to establish whether solubility controls relating to mineral solubility of major and minor elements or on the other hand, adsorption and co-precipitation were responsible for increased metal removal.

In this section, the solid residues from the reaction between Arnot fly ash and Navigation AMD at 1:3 ratio (FA:AMD) will be referred to as AN13. The solid residues from the reaction between Arnot fly ash and Navigation AMD at 1:1.5 ratio (FA:AMD) will be referred to as AN115. The mineralogy of these solid residues was investigated using XRF and sequential extraction was applied.

The XRF results (Table 3.2) show that the fly ash consists of three major phases: Al_2O_3, Fe_2O_3 and SiO_2. The American Society for Testing and Materials (1988) uses these three

major phases to classify fly ashes based on coal source. From the analysis (SiO_2 $+Al_2O_3+Fe_2O_3 \geq 70\%$) Arnot fly ash can be categorized as class F, which is either derived from anthracitic or bituminous coals (Mattigod *et al.*, 1990). Among the minor elements, Arnot fly ash shows high concentrations of Sr, Ba, Cr, Zr and Ni. Traces of Mo are also present. These concentrations are within the concentration ranges reported by Eary *et al.* (1990) and are higher than values generally found in coals and soils indicating that the combustion process tends to enrich the fly ash with minor elements.

Navigation AMD is strongly acidic (pH = 2.39) (See Table 2.1). Low pH values of the AMD imply a deficiency of calcareous minerals and absence of carbonate buffering in mine tailings or boulders through which the groundwater flows. Major elements include Na, Ca, Mg, Al, Mn and Fe. Dissolution of silicate minerals such as feldspar, kaolinite and chlorite accounts for most or all of the dissolved K, Na, Mg, Al and Ca (Crouse and Rose, 1976). Navigation AMD has high SO_4^{2-} content typical of leachate from sulphide rich coal mine tailings and underground mine lakes (Uhlmann *et al.*, 2004).

3.3.7 XRD and SEM-EDS analysis of the solid residues from the neutralisation reaction between Navigation AMD and Arnot FA.

The SEM-EDX spot analysis of AN13 solid residues collected at pH 8.0 - 9.2 is shown in Figures 3.8 and 3.9.

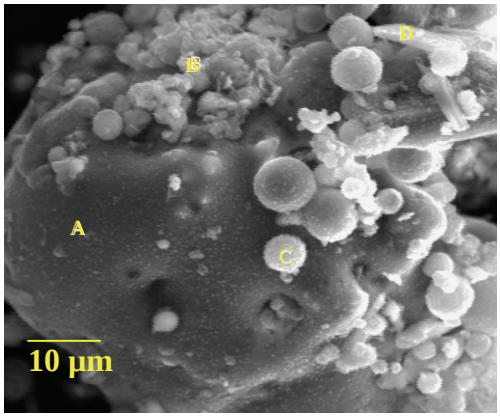

Figure 3.8: SEM micrograph of AN13 solid residues showing the areas (A, B, C, D) where spot analysis was done.

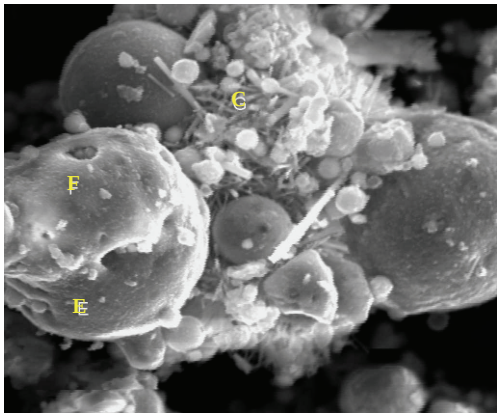

Figure 3.9: SEM micrograph of AN13 solid residues showing the areas (E, F, and G) where spot analysis was done.

Analysis of the aggregating fly ash spheres by EDS (Table 3.6) indicates an increase in Fe, suggesting that an iron-rich phase is being formed (AN13 area B). Analyses of the small fly ash spheres with fine coatings also reveal increased Fe content (AN13 area C). Analysis of area C of this sphere showed increased Ca, Mg, Fe, P, and S (Table 3.6). The presence of P, S and Ca suggests a type of jarosite mineral being precipitated where Ca and/or Mg are replacing K or Na in the jarosite. Jarosite is a hydroxysulphate of Fe and K or Na, Fe can be replaced by Al and by smaller amounts of Zn and Cu. Ca, Pb, Ba, Sr, or Ce can replace K. Sulphate may also be replaced by PO_4, AsO_4, CO_3, SbO_3, CrO_4 or SiO_4 (Scott, 1987).

It can be deduced from SEM-EDS analysis (Table 3.6) that the mechanism of the reaction is the dissolution of the soluble surface salts upon FA particles. The dissolved salts react with the acidic metals and ions in the AMD and the minerals either precipitate on the surface of the large spheres or fill in gaps between the small spheres leading to aggregation.

Table 3.6: SEM-EDS spot analysis (given as % of major elements) of the AN13 solid residues collected at pH 9.20. BDL: Below detectable limits

Element	Arnot fly ash	AN13 area A	AN13 area B	AN13 area C	AN13 area D	AN13 area E	AN13 area F	AN13 area G
O	32.7	15.2	33.3	30.4	36.0	19.5	27.5	34.1
Al	20.8	19.6	15.6	14.6	11.2	28.7	32.8	10.2
Si	33.6	39.2	20.1	24.1	23.9	27.7	36.3	6.45
P	BDL	BDL	1.70	2.82	0.72	BDL	BDL	BDL
S	BDL	BDL	1.95	1.00	8.8	0.98	BDL	11.2
Mg	BDL	3.14	5.07	3.13	1.26	2.05	BDL	0.96
Ca	6.76	13.8	10.9	14.3	16.0	6.57	0.76	34.6
K	1.46	BDL	0.43	0.61	0.45	1.60	0.78	BDL
Ti	3.08	5.56	1.01	2.69	0.30	2.84	0.21	0.45
V	BDL	0.34	BDL	0.2	BDL	1.08	BDL	BDL
Fe	1.60	3.23	10.0	6.24	1.38	8.97	1.64	2.08
Total	100	100	100	100	100	100	100	100

The SEM-EDS elemental profiles indicated a general increase in content of Ca, Mg and Si in most of the spots analysed. These spots do not show any crystallinity. Analysis of the crystals observed, especially AN13, area D and AN13 area G, suggests gypsum and ettringite are precipitating out, respectively.

Ettringite could not be detected by XRD though. The only new mineral phase formed that can be detected, in the solid residues from the neutralisation of Navigation AMD with Arnot FA, by XRD is gypsum (Figure 3.10).

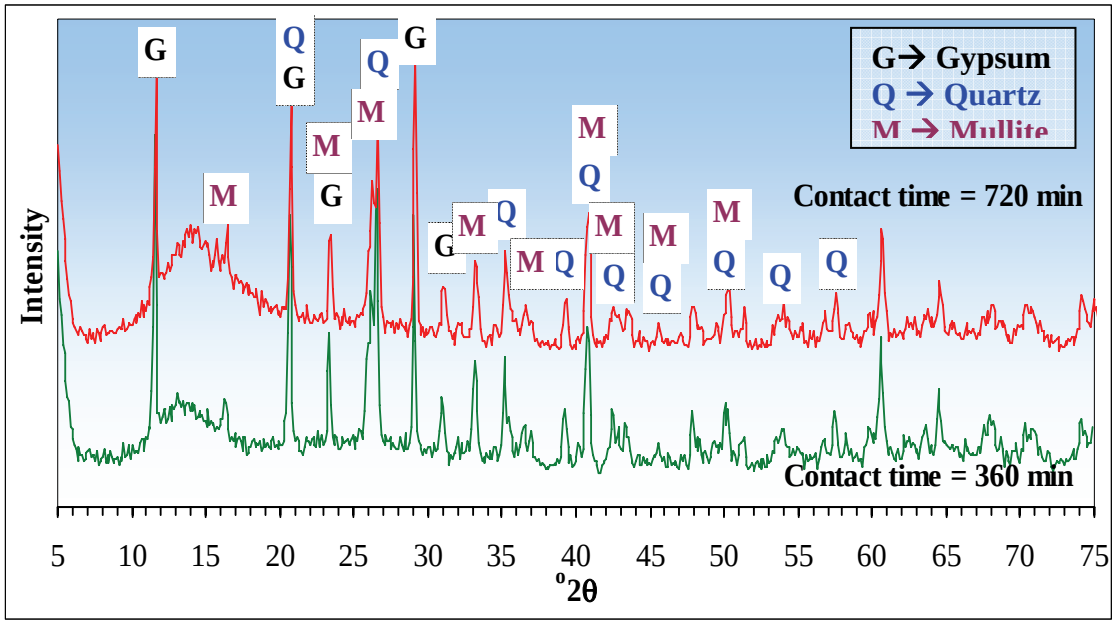

Figure 3.10: XRD spectra of solid residues collected at 360 and 720 minutes of contact (G-gypsum, Q-quartz, M-mullite)

3.3.8 DXRD analysis of size fractionated solid residues

In DXRD analysis of size fractionated solid residues no significant difference was observed in the total Fe extracted with oxalate between the three size fractions of solid residues (Table 3.7). The concentration of extractable Fe varied from 0.692% to 0.726%. The fine and the very fine fraction had slightly higher concentration than the coarse fraction. The DXRD pattern did not show the presence of ferrihydrite (Figure 3.11). The XRD patterns of the NH_4-oxalate extracted and non-extracted sample fraction were similar except that the intensity of the main crystalline peak quartz increases in relative intensity. The baseline was observed to straighten with a disappearance of some of the smaller peaks which could indicate that some mineral phases were dissolved but could not be detected probably due to their low concentration.

The size fractionated solid residues samples had a ratio of oxalate extractable Fe below 2.9% (Table 3.7).

Table 3.7: Total Fe extracted with oxalate from three size fractions of solid residues.

Sample	Fe concentration (mg/kg)
AN13 coarse fraction	6919
AN13 fine fraction	7256
AN13 very fine fraction	7200

Figure 3.11 shows the DXRD pattern of the fine fraction. Schwertmann *et al.* (1982) observed ferrihydrite in soil samples with 13.3% oxalate extractable Fe but not in samples with 2.9%. They concluded that the lower limit of detection of ferrihydrite lies somewhere between these two values.

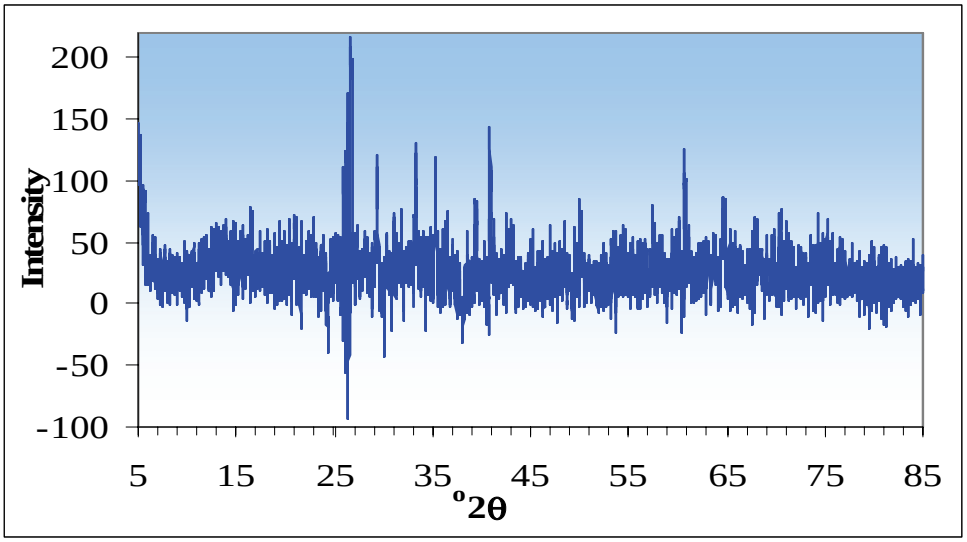

Figure 3.11: DXRD pattern of fine fraction of solid residues AN13 after 4 hours of treatment with NH_4-oxalate.

Gypsum was detected by XRD in all the solid residues collected at different contact times (Figure 3.10). Saturation indices (Table 3.8) show that the solution was slightly oversaturated with gypsum from 3 to 210 minutes of contact: gypsum controlled Ca concentration in process waters.

Table 3.8: Calculated saturation indices for selected mineral phases at different contact times.

	Samples taken at various times (min)						
Mineral phases	1	3	30	90	210	480	1440
Al $(OH)_3$ (a)	-4.11	-3.19	-0.86	-0.86	-1.16	0.02	-2.44
Barite ($BaSO_4$)	1.03	0.79	7.99	1.36	1.29	1.11	1.03
Basaluminite ($Al_4(OH)10SO_4$)	-4.41	-1.34	1.36	4.99	3.58	5.27	-8.96
Boehmite (AlOOH)	-1.91	-0.98	4.99	1.35	1.05	2.23	-0.22
Celestite ($SrSO_4$)	-0.07	0.2	0.23	0.3	0.27	0.22	0.20
Fe $(OH)_3$ (a)	1.53	-6.79	1.82	4.16	3.73	4.23	2.68
Gibbsite ($Al(OH)_3$)	-1.39	-0.48	-2.2	1.85	1.54	2.72	0.26
Goethite (FeOOH)	4.88	5.32	5.16	7.59	7.18	7.68	6.14
Gypsum ($CaSO_4$:2H2O)	-0.29	0.04	0.18	0.17	0.14	-0.12	-0.15
Jarosite-Na ($NaFe_3(SO_4)_2(OH)_6$)	6.58	7.54	7.62	10.1	8.85	5.62	-5.54
Jurbanite ($AlOHSO_4$)	0.64	1.21	-0.09	0.72	0.37	-1.49	-8.32
Kaolinite ($Al_2Si_2O_5(OH)_4$)	0.09	2.21	-1.6	5.26	4.49	5.46	-0.48
Quartz (SiO_2)	1.03	1.18	1.0	0.37	0.30	-0.4	-0.92
Sepiolite ($Mg_2Si_3O_7.5OH:3H_2O$)	-14.1	-12.8	-13.9	-9.46	-9.53	-5.57	1.38
SiO_2 (a)	-0.27	-0.11	-0.3	-0.91	-0.98	-1.68	-2.19

The solution was highly oversaturated with Na-jarosite (Table 3.8), which could account for the decreasing levels of Na. Although Sr and Ba show evidence of solubility control after the initial release from fly ash, Sr was observed to increase steadily for the rest of the experiment for both ratios (Section 2.3.6). The solution was at saturation with celestite but oversaturated with barite for the entire contact time (Table 3.8).

No crystalline Al phases were detected by XRD. Calculation of saturation indices indicates that basaluminite, boehmite, gibbsite were oversaturated between 30 and 480 minutes of contact (Table 3.8). At low pH, jurbanite is slightly oversaturated, indicating control on Al concentration. For Si, the concentration for the 1:3 ratio remained slightly higher than the 1:1.5 ratio for the rest of the experiment. A sharp decline in Si concentration was observed when the mixture attained pH > 5.0 for both ratios. An observation of the saturation indices for kaolinite (Table 3.8) indicates super saturation at 90 minutes of contact when the solution attained pH >5.0. Amorphous SiO_2 is near equilibrium with the solution for the first 210 minutes of contact (pH < 5.5) but quartz appears to be oversaturated over the same period of contact. Arnot fly ash consists of quartz as a major constituent (Table 3.2). It is probable that the solubility of the aqueous H_4SiO_4 is controlled largely by quartz rather than amorphous silica.

3.3.9 Sequential extraction

The sequential extraction results of the AN13 solid residues are presented in Figure 3.12. It is very important to note that this extraction process is indicative of the potential fate of the insoluble components of the solid residues recovered after the neutralisation reaction. A significant finding is that the species precipitated out of solution upon the FA particulates are mainly poorly soluble or insoluble. Only Ca , B and Sr remained soluble in water in low percentages.

The extraction established that a very significant percentage of trace elements (except B) is associated with amorphous (cryptocrystalline) Fe-oxides (Figure 3.12). This indicates that Fe-oxides are an important sink for trace metals in this process. B was significantly associated with the specific surface complex fraction. Eary *et al*. (1990) argued that B concentration in leachates may only be limited by the dissolution rates of surface precipitates in fly ash and the glassy particles and subsequent adsorption on precipitates formed. Cravotta and Trahan (1999) reported a removal of dissolved Mn, Zn, Ni and Co from solution, and the corresponding enrichment relative to Fe in particles and coatings on limestone. They attributed the enrichment to sorption and co-precipitation reactions with hydrous oxides of Fe^{3+}, Mn^{2+} and Mn^{4+}. Several authors (Rose and Ghazi, 1997; Webster *et al.*, 1998) reported that sorption of trace elements could be enhanced by the incorporation of SO_4^{2-} with hydrous Fe^{3+} oxides, where SO_4^{2-} could be part of the crystal lattice as in schwertmannite.

A sharp reduction in SO_4^{2-} concentration was observed when the reaction mixture attained pH 5.5 for both ratios (Figure 2.16), suggesting either adsorption or incorporation into the iron (III) oxyhydroxides being formed. At this pH, a corresponding sharp reduction in both total Fe and Fe^{2+} was observed (Figure 4.31). An observation of the trends (Figures 2.28, 2.29 and 2.27) for trace elements Zn, Cu and Mn indicates a significant removal at pH 5.5.

A significant proportion of Al and Si is associated with the amorphous Fe-oxide phase (Figure 3.12). Although the reagent NH_4-oxalate solution (pH 3.0) has been used extensively to identify amorphous Fe-oxides (Schwertmann *et al*, 1982; Schulze, 1981; Dold, 2003), it extracts non crystalline aluminosilicates and this could account for the large proportion of Al and Si associated with this fraction. Ca and Sr were observed to be associated to some degree with the soluble fraction and with the residue. Gypsum was identified by XRD and SEM-EDX and celestite was predicted to be precipitating out (Table 3.8). This could indicate the presence of these elements as soluble salts such as gypsum or celestite on the surface of the solids and also locked in the unaltered aluminosilicate matrix of the fly ash. A significant

proportion of Ca, B and Sr was also associated with the Mn-oxide fraction, probably through adsorption.

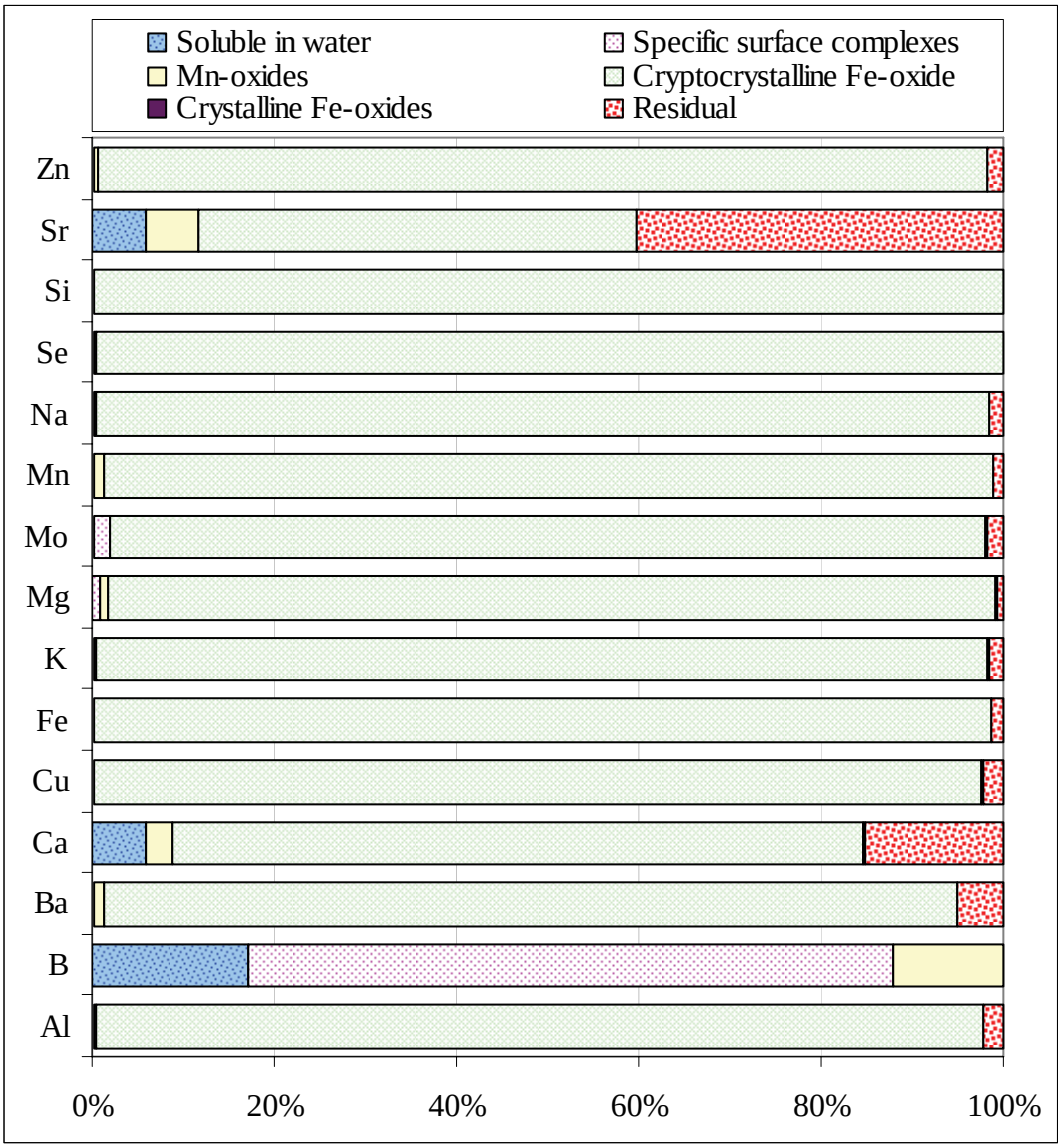

Figure 3.12: Sequential extraction results for AN13 solid residues collected at pH 9.20.

3.4 DISCUSSION

The objective of this section of the study was to evaluate the chemistry of the resulting process water as the sulphate and metal rich AMD interact with fly ash, to relate the solution chemistry and formation of solid phases. Understanding the behaviour and ultimate fate of SO_4^{2-}, major and trace elements in AMD and fly ash during the treatment process is a major determinant in usage of fly ash as a liming agent.

The dissolution and hydrolysis of oxide components such as CaO and MgO from fly ash on contact with AMD contributed to an increase in solution pH. In turn an increase in dissolved concentration of Ca and Mg was observed as the reaction progresses. There are two factors that finally dictate the final pH of the process waters: AMD: FA ratio and contact time.

An increased removal of elements such as B, Mg, Mn, Al, Si, total Fe, Zn and was observed at the lower FA:AMD ratio indicating the importance of precipitation reactions in this process. Calculated saturation indices and mineralogical analysis indicated that SO_4, Fe and Al were controlled by mineral solubility. Al concentrations were controlled by secondary phases such as boehmite, basaluminite and gibbsite; Fe by amorphous $Fe(OH)_3$ and goethite; Ca and SO_4^{2-} by gypsum. The elements Na, Ca, Ba, Mg, Sr, B, Mo, Se, Si, Mn, and Zn showed development of solubility controls at certain contact times after the initial dissolution. It is probable that they were present as soluble salts and, on dissolution, interacted with components in AMD to form new and stable mineral phases that controlled their concentrations.

Mn, Mg, Zn and Cu were removed from solution at a lower pH (5.5 – 7.0) than predicted by thermodynamic calculations, indicating that other processes such as adsorption and co-precipitation were responsible for increased metal removal. The strong association of these elements with the amorphous iron oxide fraction reinforces this hypothesis. The pH at which Mn is least soluble is between 9.0 and 9.5. Iron minerals may play a very significant role in the removal of Mn, through co-precipitation processes if the iron concentration in the water is approximately four times that of the Mn content. Mn may also be removed by the formation of Rhodochrosite ($MnCO_3$) or Pyrocroite [$Mn(OH)_2$] (Jenke and Pagenkopf, 1983).

Fe^{2+} was removed through oxidation and subsequent hydrolysis and this was evident when the mixture attained pH 5.5. A corresponding decrease in SO_4^{2-} concentration was observed indicating the relevance of the iron-oxyhydroxides in SO_4^{2-} removal in this process. This was clearly evident at 1:1.5 (FA:AMD) ratio with levels dropping to a minimum on the mixture attaining pH > 5.5 as compared to 1:3 ratio.

The neutralising potential of fly ashes with small amounts of Ca (Class F) can be attributed to the existence of charged OH—silanol groups. Hydrolysis of these surfaces –SiOH contributes a significant amount of alkalinity to a fly ash solution [1]. This amphoteric reaction results in an excess of charge, negative or positive depending on the pH, on the fly ash particles making them potential adsorbents (Polat *et al.*, 2004).

$$—SOH_2 + OH^- \Leftarrow —SOH + H_2O \Rightarrow —SO^- + H_3O^+ \qquad [1]$$

The mechanism of adsorption for cations onto silica normally involves surface complex formation between “free” metal ions and deprotonated surface functional groups and can be illustrated by the following equation (Panday *et al.*, 1985) :

$$\rightarrow SiOH + M^{Z+} \rightleftharpoons (\rightarrow SiOM^{(Z-1)} + H^+ \qquad [2]$$

Where

- M represents the metal ion
- z indicates the oxidation state of the metal ion
- SiOH represents the surface groups of the silica compound

3.5 CONCLUSIONS

- There is little significant variation in the mineralogy of different samples of the same ash.
- There is little significant variation in the mineralogy between different fly ashes.
- Alkalinity and particle size show a good, negative correlation (-67%).

- The correlation between alkalinity and surface area is near to perfect (97%).
- The correlation between particle size and surface area is only 54%.
- The presence of carbon in a fly ash sample severely retards successful neutralisation.
- Elements that form anionic species (As, Se, B, and Mo) at alkaline pH were highly leached from fly ash but stabilized to lower levels as pH increased in the neutralisation reaction.
- A significant finding is that the species precipitated out of solution during the neutralisation reaction and forming part of the solid residues recovered after the reaction are mainly poorly soluble or insoluble species. Only Ca , B and Sr remained soluble in water in low percentages.

The relationship between alkalinity and particle size needs to be investigated more closely to determine to what extent this affects the neutralisation capacity of fly ash. The chemistry behind the retardation effect that unburnt coal has on the neutralisation reaction must also be further investigated.

4. ASHWALLING STUDY

4.1 INTRODUCTION

Acid mine drainage (AMD) is one of the most serious environmental problems facing the mining industry. It is formed by the oxidation of pyritic compounds in the surrounding strata of the mineral being mined. This oxidation is often catalysed by bacteria.

When water (rain or ground) comes into contact with this oxidation product a highly acidic effluent is formed. As this effluent flows through the surrounding environment it leaches heavy metals forming a more complex solution. The equation is simplified as follows:

$$2FeS + 7.5O_2 + 7H_2O \text{ -----> } 2Fe(OH)_3 + 4H_2SO_4$$

Although it is known that bacteria catalyse this reaction, the exact mechanism is unknown. Twenty two different species of bacteria have been proven to associate with mine waters, *Thiobacillus ferroxidans* being the most common (O'Brien, 2000). *Thiobacillus* metabolises inorganic compounds including sulphates to obtain energy (White, 2000).

The concentration of heavy metals within the effluent is dependant on the surrounding strata. In some cases the high buffering capacity of the rock may cause the effluent to be circumneutral (O'Brien, 2000). Normally, however, the leachate has a low pH, dissolved solids of 4000-5000mg/L and sulphate concentrations in the thousands of mg/L (Gericke *et al.*, 2001).

Coal mining in South Africa is estimated to produce 200 Ml of acid mine drainage (AMD) per day in the Pretoria-Witwatersrand-Vereeniging (PWV) area alone (Maree *et al.*, 1996). Several treatment technologies are available for the treatment and control of AMD. These range from lime neutralisation (Gericke, *et al*, 2001) and electrochemical protection (Pulles *et al*, 1996) for treatment to capping and neutralisation with alkaline materials for control and minimisation. AMD treatment is costly and requires constant management (Anon, 2000). In the case of lime draining the drains foul quickly with iron precipitates and the failed, heavy metal containing residues have to be disposed of and stored in hazardous waste sites in the long-term.

Eskom burns approximately 100 Mt of coal annually and in so doing produces 22 Mt of inorganic, aluminosilicate fly ash (Willis, 1999). Approximately 1% of this is used in various commercial applications while the remainder is stored on ash dumps (Reynolds, 1999). Eskom power stations are mostly situated in the Mpumalanga coalfields and thus the fly ash and AMD are in close proximity.

Fly ash has been used to reduce AMD as a backfill and capping media internationally (pers. comm.. Dr D Hassett). The high pH, small grain size, high availability, low water content, low permeability and pozzolanic activity of fly ash make it an effective means of combating AMD.

In this section results are reported of column studies performed to simulate conditions in which FA is in contact with AMD over long periods (280 days) to model the placement of ash in acidic environments for establishing suitable monitoring criteria and to understand the

mineralogical characteristics and the chemical interactions taking place in ash in contact with AMD over the longer term. Various FA and AMD combinations were studied.

4.2 METHOD

Kendal, Matla and Duvha FA were tested in this study. AMD samples were obtained from Middelburg mine at a natural decant point into a small tributary to the Olifants river. At present a clay bund wall dams the AMD, which is then pumped to the existing lime treatment plant. The Middelburg AMD source was tested using Kendal FA. For the Matla and Duvha columns Landau and Navigation AMD's were used respectively. Fly ash from the Kendal power station was obtained from the Ash Resources classification plant. Due to the coarse texture of this ash it was believed that the AMD would percolate easily through the ash and be easily treated. The ash was analysed for size distribution and chemistry. A sample of each AMD was sent for chemical analysis. It was decided to terminate the Kendal column tests after 280 days in order to initiate new experiments with Matla fly ash at ESKOM.

Figure 4.1: Gravity fed AMD through Ash columns

The ash was packed into 100mm diameter, perspex columns, 1.5; 1.0; 0.5 and 0.25m long. Each column was duplicated and given the annotation A or B. The weight of the column before and after filling was noted to ensure that duplicate columns contained the same amount of fly ash.

The AMD was gravity fed through all 8 columns set up for each FA simultaneously (Figure 4.1) As the treated AMD passed out of the column, the permeate was collected and analysed for pH, electrical conductivity (EC), sulphate concentration (SO_4^{2-}) and heavy metal concentration.

The columns were run until the alkaline permeate from the columns returned to pH 8.5, indicating a slow loss of neutralisation capacity over time. Once this end point was achieved

the flow was stopped and the ash removed from the Perspex as a solid column. The column was sectioned into top, middle and bottom and samples of each section were submitted for XRF, XRD and SEM analysis.

Once the AMD was passed into the columns the columns had to be sealed to withstand the water pressure of the head of water, as the AMD did not pass directly through the ash. The AMD permeate broke through the Kendal 0.5m ash column on day 2, while the 1.0 m and 1.5m columns broke through on days 3 and 5 respectively. The AMD passed through the 0.25m and 0.5m Matla columns on day 1 and 4 respectively while the 1.0 and 1.5m columns only passed through on day 15. This may be due to the particle size of the Matla ash. All the Duvha columns allowed AMD passage after day 2. This is attributed to the larger particle size of the Duvha ash and lower CaO concentrations. From the onset of the AMD addition iron deposition was noted on the surface of the ash (Figure 4.2).

Although it was attempted to run Kendal columns till the effluent was at pH 8.5, the 1.5 m columns tests were terminated at pH 8.0 because of the length of time (280 days) it took to reach this pH. However column 1.5A blocked before this pH could be achieved and 1.5B column remained above 8.2. It was decided to terminate the tests after 280 days in order to initiate new experiments with Matla fly ash.

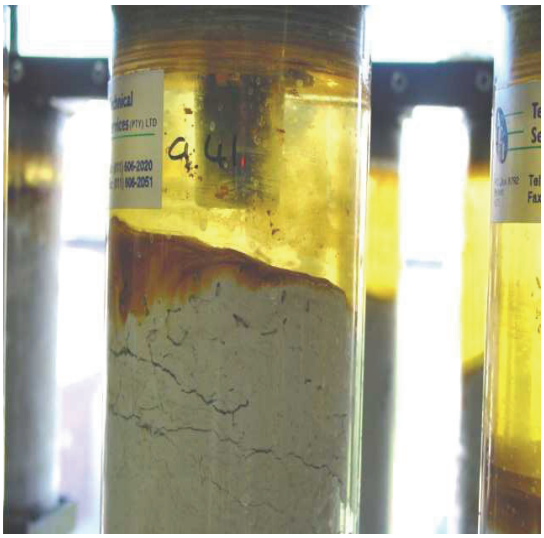

Figure 4.2: Iron deposition on the surface of the ash during column tests.

4.3 RESULTS

Table 4.1 shows the metal analyses for the three samples of AMD used in each column experiment. For the Matla and Duvha columns Landau and Navigation AMD's were used as a consequence of a lack of Middelburg AMD.

Table 4.1: Parameters of the raw Middelburg, Landau and Navigation AMD and Kendal, Matla and Duvha fly ash.

	Kendal columns	Matla columns	Duvha columns
AMD	Middelburg	Landau	Navigation
pH	2.88	2.88	2.70
EC (mS/cm)	0.47	9.70	38.1
Sulphate (mg/L)	3 654	4 015	17 926
Al (mg/L)	33.5	272	470
B (mg/L)	0.06	0.701	BDL
Ba (mg/L)	0.01	0.172	BDL
Be (mg/L)	BDL	BDL	0.07
Cd (mg/L)	0.04	BDL	2.00
Co (mg/L)	0.54	BDL	0.90
Cr (mg/L)	BDL	1.28	1.00
Cu (mg/L)	0.05	0.532	BDL
Fe (mg/L)	122	3 900	8 169
Mn (mg/L)	43.0	35.0	106
Ni (mg/L)	0.68	0.50	2.0
Pb (mg/L)	0.03	0.04	0.2
Sr (mg/L)	0.71	BDL	BDL
Zn (mg/L)	2.80	6.34	16.0
Fly ash	Kendal	Matla	Duvha
pH	11.34	11.50	11.20
EC (mS/cm)	676	0.68	3.88

XRF analysis of each fly ash is given with the XRD results and the XRF results for all the columns.

The time =0 data in the figures in this chapter represents the raw AMD.

4.3.1 Kendal ash column results

Column studies were performed as detailed in section 4.2 with Kendal FA being used to treat Middelburg AMD, by percolation through the column. The pH of the permeate recovered from Middelburg AMD after passing through the Kendal columns was initially raised to greater than 12 (Figure 6.3). This indicates the alkaline nature of the fly ash.

It was found (Figure 4.3) that the shorter the column the less the pH was buffered and the sooner the pH of the permeate effluent started to decrease, as expected. AMD was passed through the ash columns until a plateau pH of 8.5 was obtained over time. However, the levelling out stage of the pH was not as evident in the short columns as it was in the long columns from day 74 until the end of the tests. In the case of the 1.5m columns the pH

remained above 8 from day 74. Any future column studies should be run to a pH of 7 to ensure that this plateau is evident in all samples.

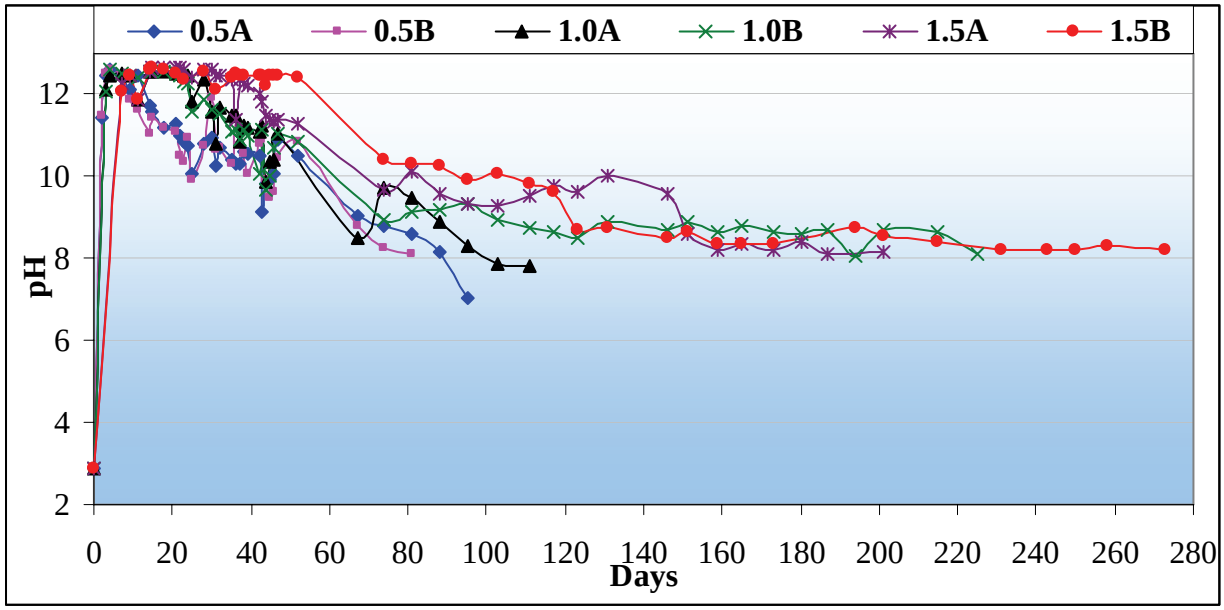

Figure 4.3: pH of Middelburg AMD before and after passage through Kendal columns. Sample numbers indicate length of column in metres and replicate number (A or B).

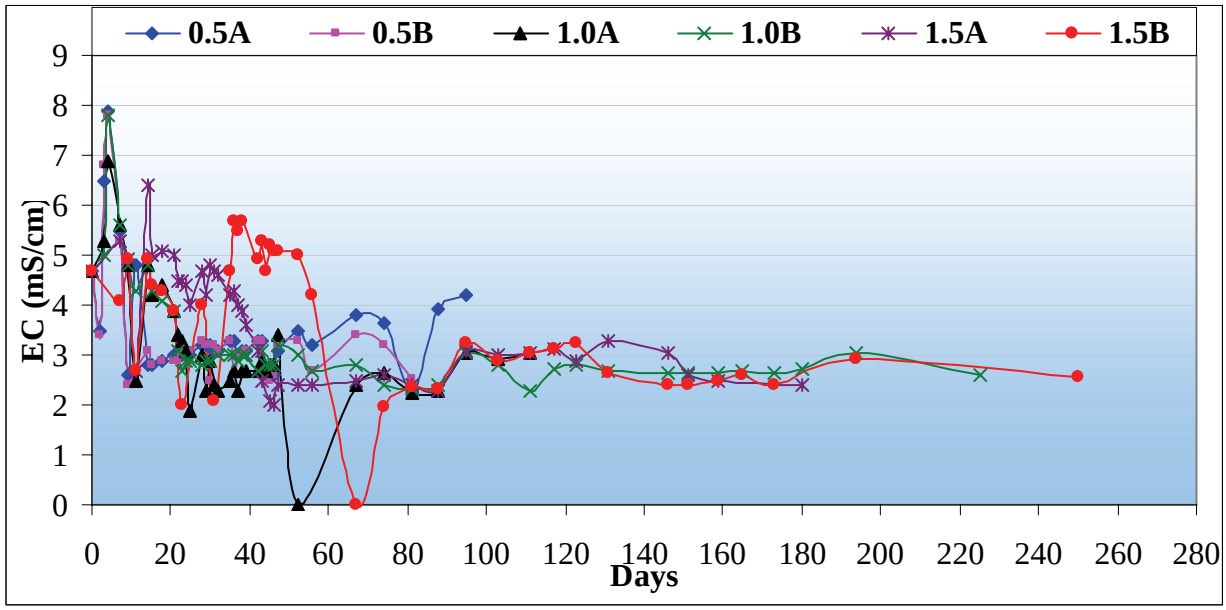

Figure 4.4: EC (mS/cm) of Middelburg AMD before and after passage through Kendal columns. Sample numbers indicate length of column in metres and replicate number (A or B).

The conductivity (EC) remained relatively constant after an initial high peak experienced in all columns (Figure 4.4). This may be due to the solubilisation of elements in the ash as the AMD first comes into contact with FA. There is a decreasing trend in the EC of the permeate before stabilising between 2 and 4 mS/cm. The EC of 1.5A seemed to take longer to stabilise and only dropped into the 2 - 4 mS/cm range after day 80. Column 1.5B followed the general trend until day 32 where an inexplicable increase occurred until day 81. This may be due to

the dissolution of the glass phase in this column, but why the phenomenon was not seen in all the columns is unknown.

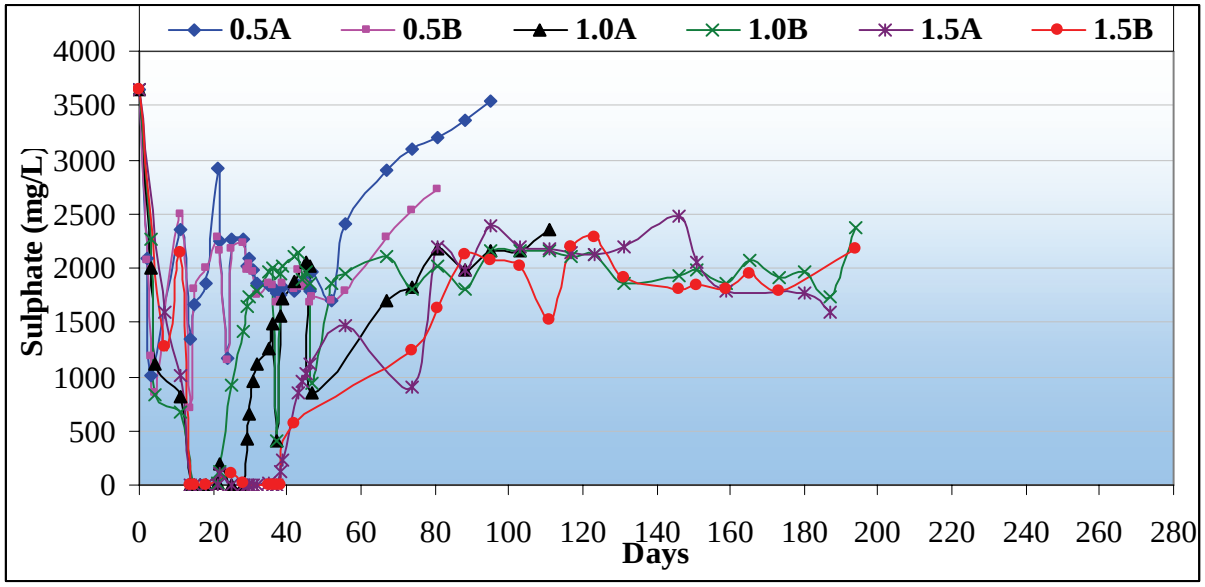

Figure 4.5: Concentration of SO_4 in Middelburg AMD before and after passage through Kendal columns. Sample numbers indicate length of column in metres and replicate number (A or B).

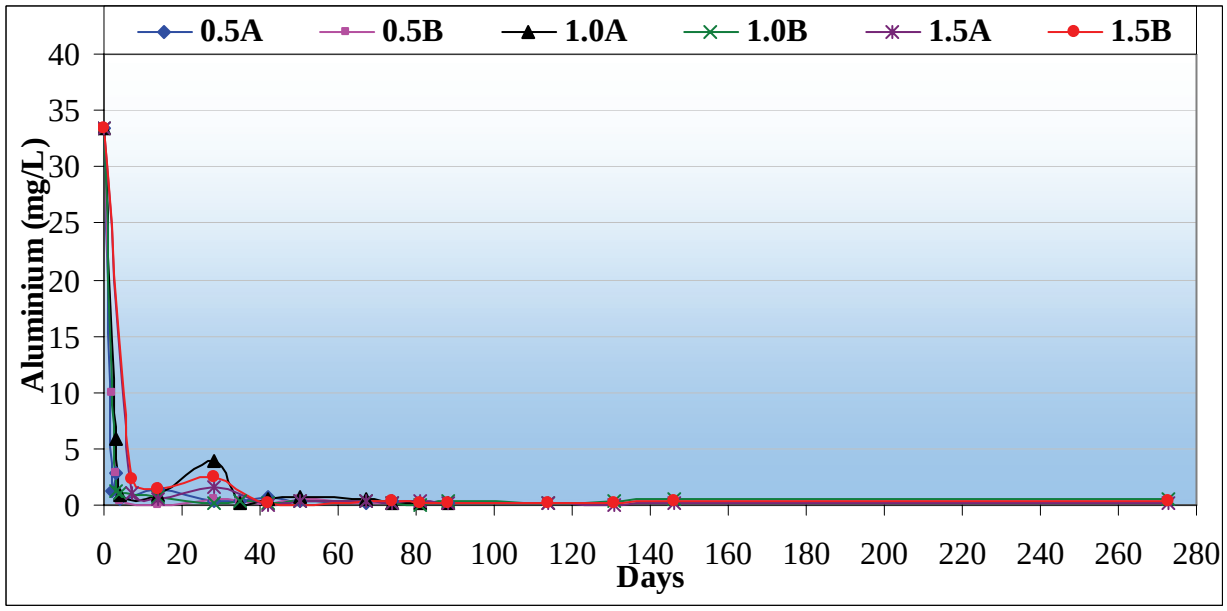

Figure 4.6: Concentration of Al in Middelburg AMD before and after passage through Kendal columns. Sample numbers indicate length of column in metres and replicate number (A or B).

All the column permeates showed an initial decrease in the sulphate concentrations (Figure 4.5). This may due to the formation of $CaSO_4$ on reaction with the fly ash. After the initial decrease the 0.5m columns started an immediate erratic increase to stabilise at approximately 2000mg/L until day 67, where after sulphate levels increased towards the initial concentration. The 1.0 and 1.5m columns reduced the sulphate concentration to below 200mg/L. The concentrations began increasing on days 24, 30, 40 and 42 for 1.0A, 1.0B,

1.5A and 1.5B respectively. The concentration of sulphate in the permeate drawn from these columns remained between 1500 and 2500mg/L from day 40 for the 1.0m columns and from day 103 for the 1.5m columns. These results are indicative of what the relative thickness of a future ash wall may need to be in order to act as passive barrier over time and achieve the necessary durability or neutralisation capacity.

In general the heavy metals concentrations in permeate waters collected after passage through the column decreased. Beryllium, Cd, Co, Pb and Ni concentrations were all low and decreased to below detectable levels. The concentration of Al decreased from 33.5 mg/L to 1mg/L (Figure 4.6). The concentration of aluminium did not increase over 273 days.

Barium concentrations showed a slight initial increase but remained at a very low concentration (Figure 4.7). The Ba concentrations increase at 14 days. This is most likely a result of the pH dropping to slightly lower values at which Ba becomes soluble. When the pH drops further Ba precipitates again. Once again, overall, no increase in concentration was detected over 273 days.

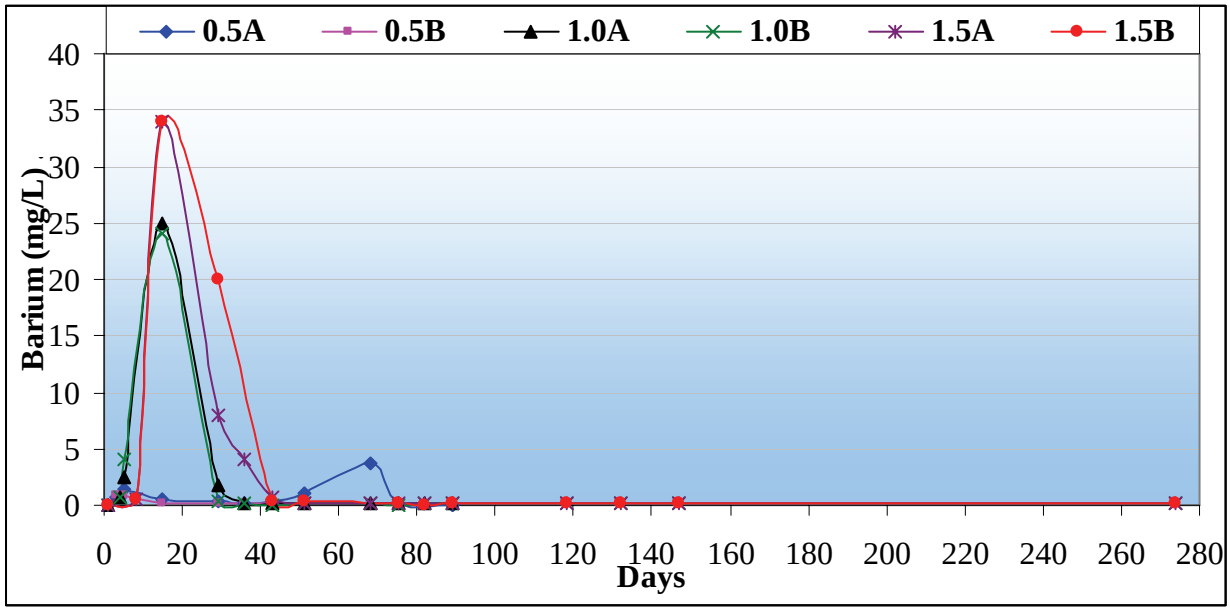

Figure 4.7: Concentration of Ba in Middelburg AMD before and after passage through Kendal columns. Sample numbers indicate length of column in metres and replicate number (A or B).

Boron concentrations in the permeate from the columns increased initially (Figure 4.8). Boron is fused to the fly ash particle during combustion to form borates, which are not detected as boron. The borates are solubilised in the AMD and boron is released. The 1.5m columns took 14 days to reach the maximum of 17 and 26mg/L. All the effluents stabilised below 5mg/L after day 14 except the 0.5m columns, which spiked and did not restabilise. After day 77 all the permeate concentrations of boron exceeded 5mg/L but remained relatively stable below 7mg/L for 273 days.

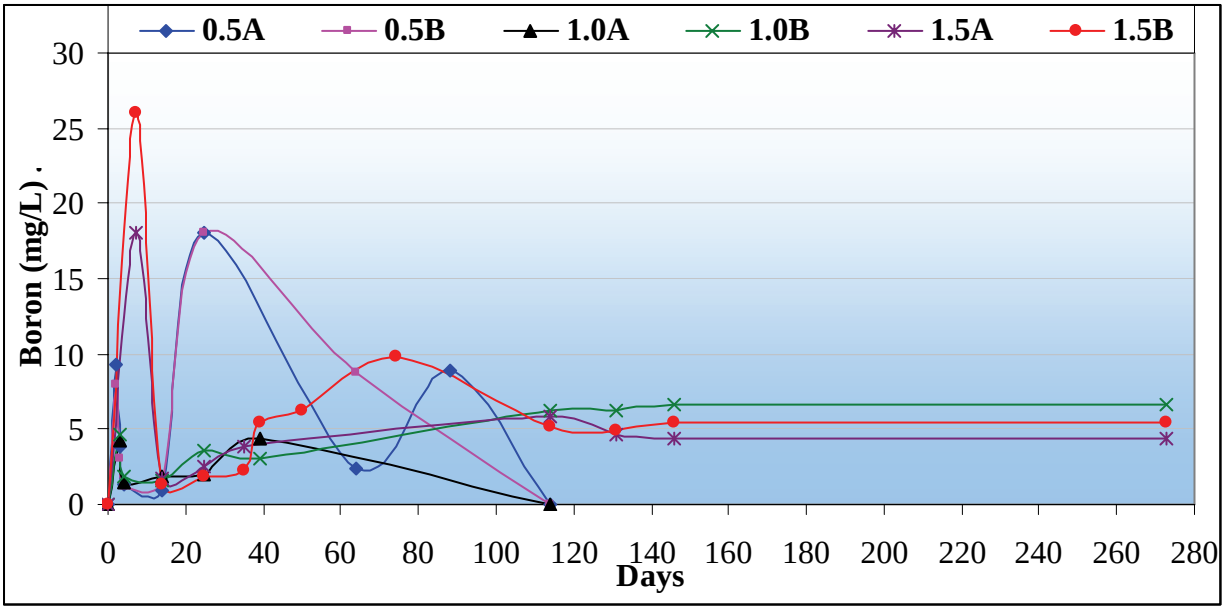

Figure 4.8: Concentration of B in Middelburg AMD before and after passage through Kendal columns. Sample numbers indicate length of column in metres and replicate number (A or B).

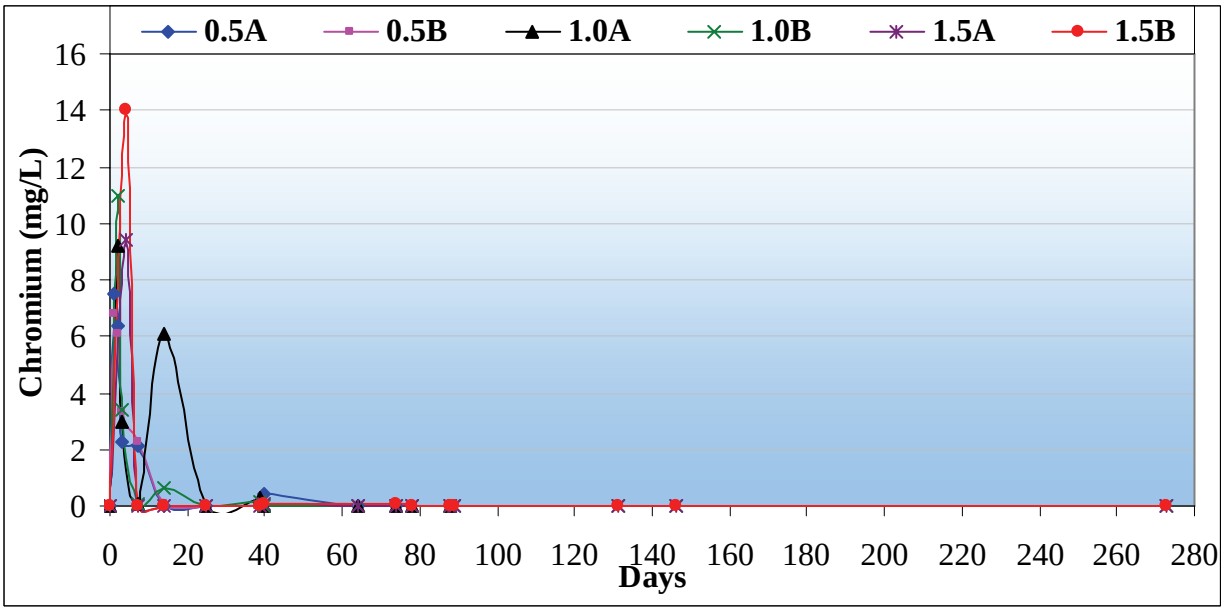

Figure 4.9: Concentration of Cr in Middelburg AMD before and after passage through Kendal columns. Sample numbers indicate length of column in metres and replicate number (A or B).

The Cr concentrations show an initial slow increase in the permeates, followed by a quick reduction to below detection limits (Figure 4.9) over time (273 days). The peak concentration is reached after a longer duration in the longer columns. It is noted that the longer the column the higher the peak concentration of chromium. This can be attributed to the fact that the AMD would have been in contact with more fly ash and thus been able to collect any possible chromium from the ash. The spiked concentration in 1.0A on day 28 cannot be explained except that these concentrations are at low levels and the variability may be within analytical error. The concentration of chromium did not increase over the duration of the test.

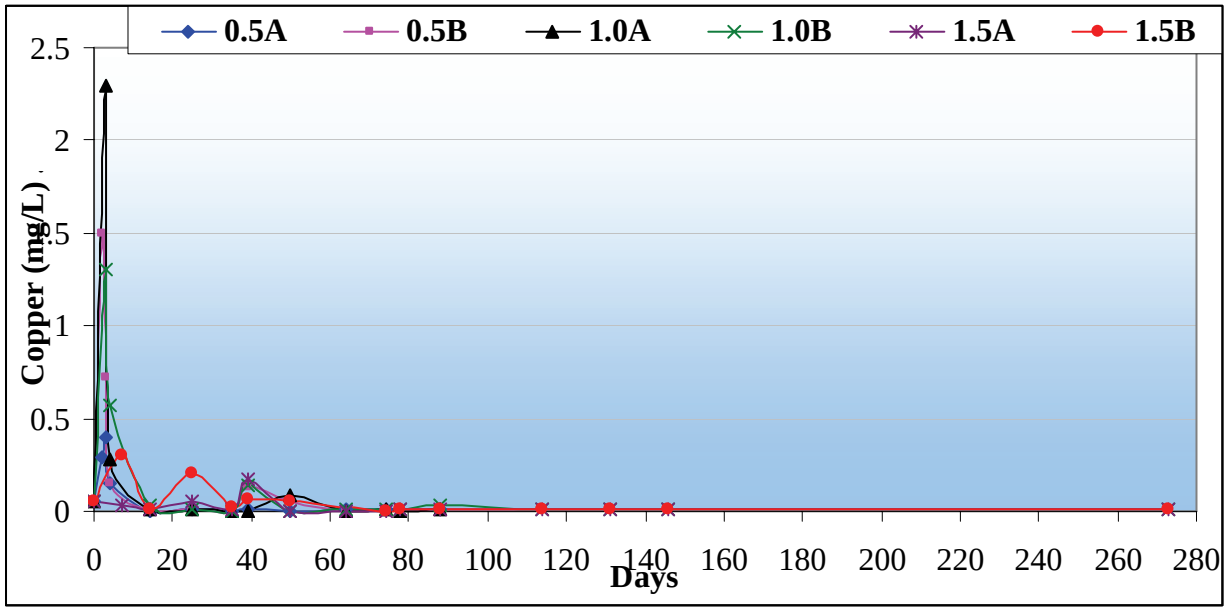

Figure 4.10: Concentration of Cu in Middelburg AMD before and after passage through Kendal columns. Sample numbers indicate length of column in metres and replicate number (A or B).

The Cu concentrations indicate an initial and brief excursion as soluble copper is extracted by AMD passing through the column, followed by an equally quick reduction to stabilised levels below 0.25mg/L (Figure 4.10). The concentration of copper in the permeate from the column does not increase again through the duration of the test.

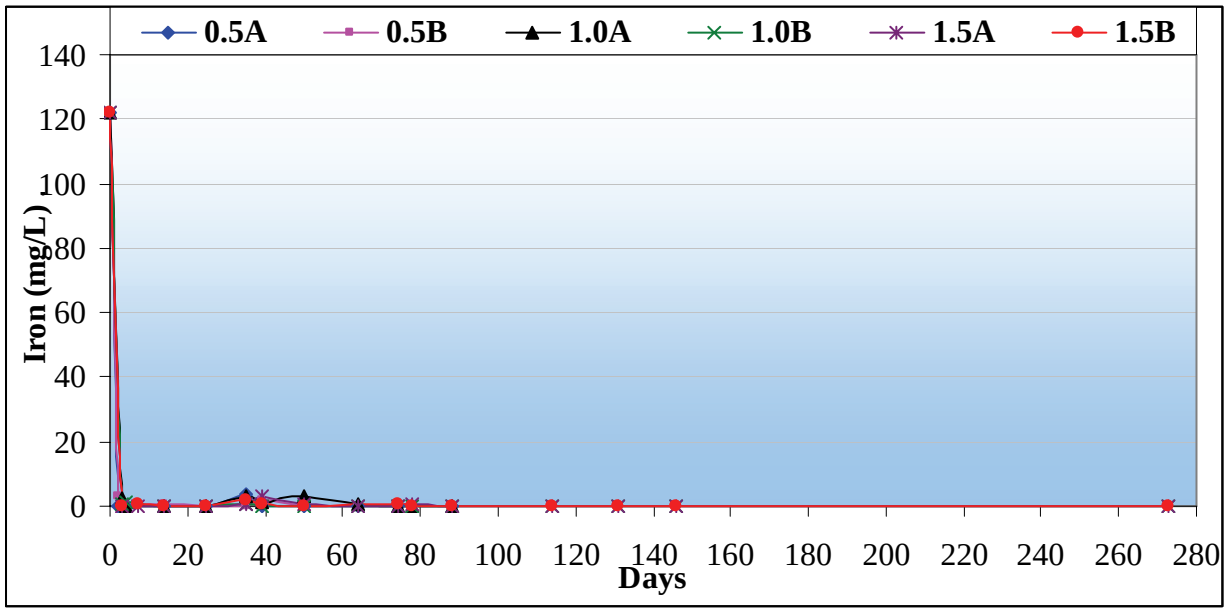

Figure 4.11: Concentration of Fe in water Middelburg AMD before and passage through Kendal columns. Sample numbers indicate length of column in metres and replicate number (A or B).

Iron concentrations (Figure 4.11) decrease immediately and significantly from 122 mg/L to 0.01 mg/L over time. This is due to the formation of hematite and precipitation of other Fe-

oxide minerals on the top of the columns as seen in Figure 4.11. The iron concentration in the permeate from the columns does not increase throughout the 273 day test.

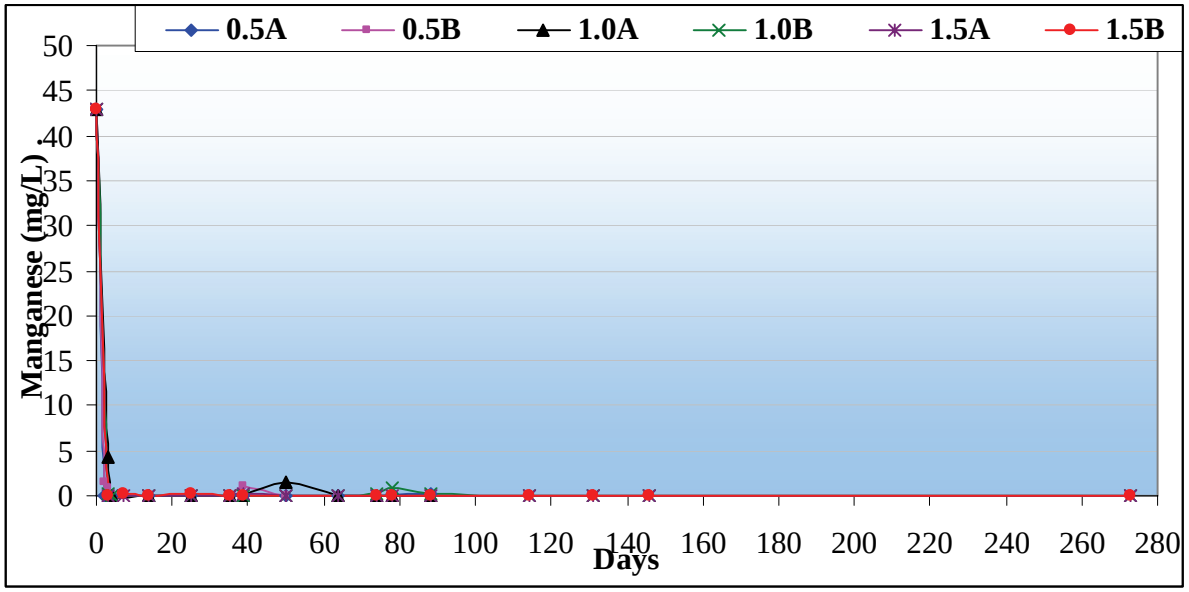

Figure 4.12: Concentration of Mn in Middelburg AMD before and after passage through Kendal columns. Sample numbers indicate length of column in metres and replicate number (A or B).

The Mn results show an immediate decrease in the concentrations from 43 mg/L to near the detection limit of 0.005mg/L (Figure 4.12). The concentration in the permeate from the columns did not increase for the duration of the test.

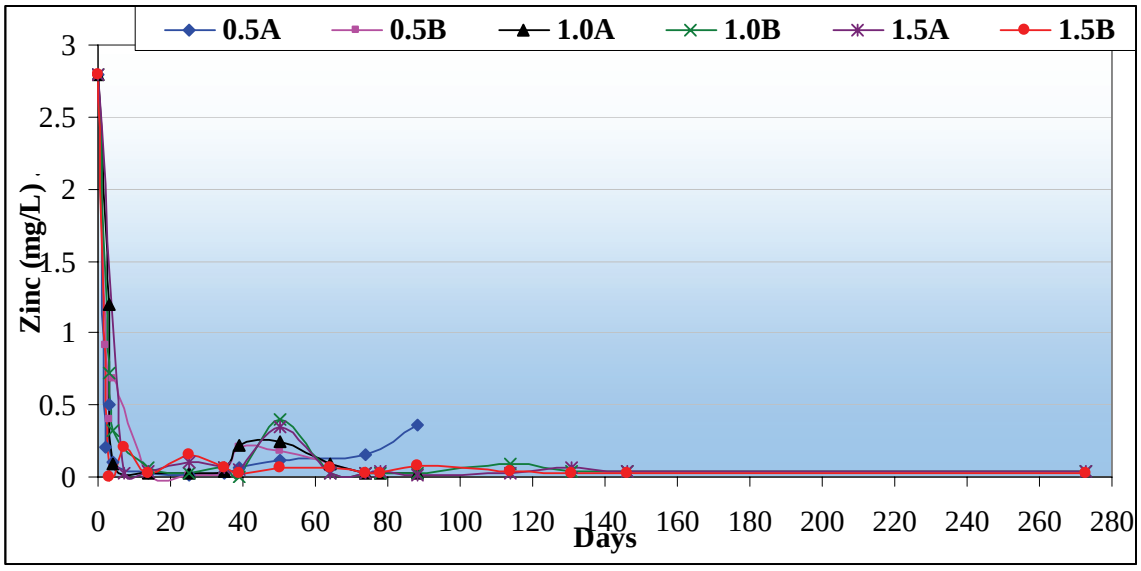

Figure 4.13: Concentration of Zn in Middelburg AMD before and after passage through Kendal columns. Sample numbers indicate length of column in metres and replicate number (A or B).

The concentrations of Zn also decreased after passing through the column. The concentrations dropped from 2.8 mg/L to 0.1 mg/L over time. The concentration of the 0.5A m column increased slightly from day 67, the reason for this cannot be explained. The

concentrations of Zn of the remaining column permeate remained below 0.1mg/L (Figure 4.13) over time.

4.3.2 Matla ash column results

Landau AMD was percolated through columns of Matla ash as described in section 4.2 for a period of 45 days.

Figure 4.14 shows the pH of the Matla ash column permeates. The pH of the permeate in all the columns increased immediately from 2.88 to above 12. The pH remained above 11.5 for the period of the test with the exception of 0.5B where the pH dropped below 11 after 36 days. Column 1.0B showed a lower pH between day 7 and day 20 before returning to above 12 for the duration of the test.

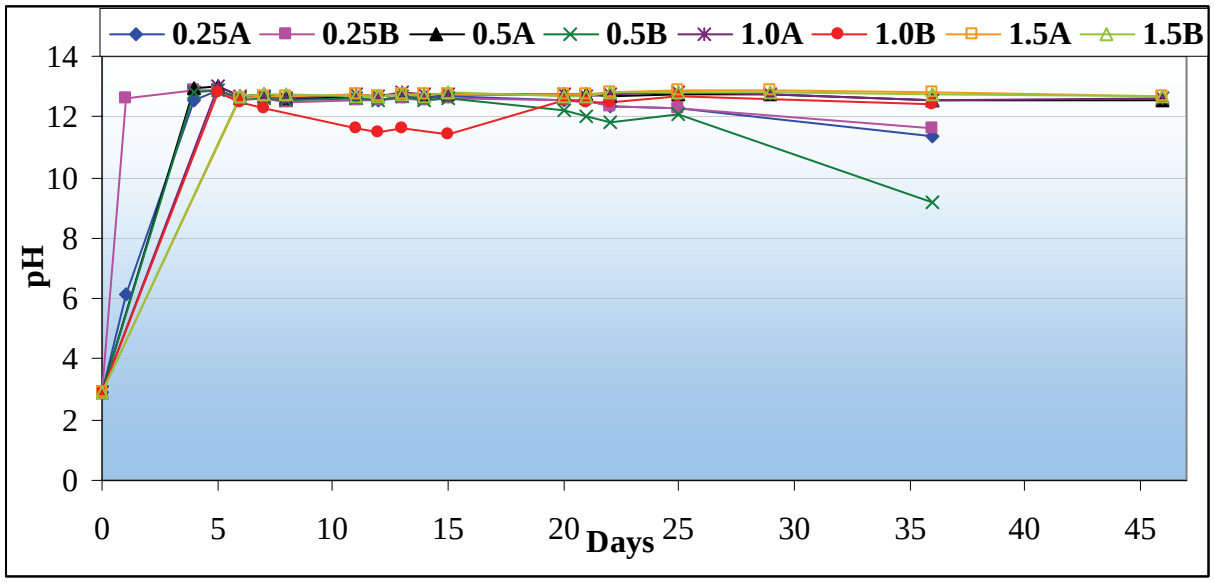

Figure 4.14: pH of Landau AMD before and after passage through Matla columns. Sample numbers indicate length of column in metres and replicate number (A or B).

The EC of the effluents is depicted in Figure 4.15. The EC in the columns shows a slight increase followed by a downward trend. No increasing trend was noted at the end of the test after 45 days. This may be attributed to the blocking of the column. It is interesting to note that the decreased pH levels in column 1.0B and the decrease in 0.5B correlate to decreases in the EC.

Sulphate concentrations of the various column effluents are shown in Figure 4.16. The concentration decreases from 4000mg/L to below 100 mg/L. This was followed by a slight increase, remaining under 500mg/L, before decreasing below 50 mg/L.

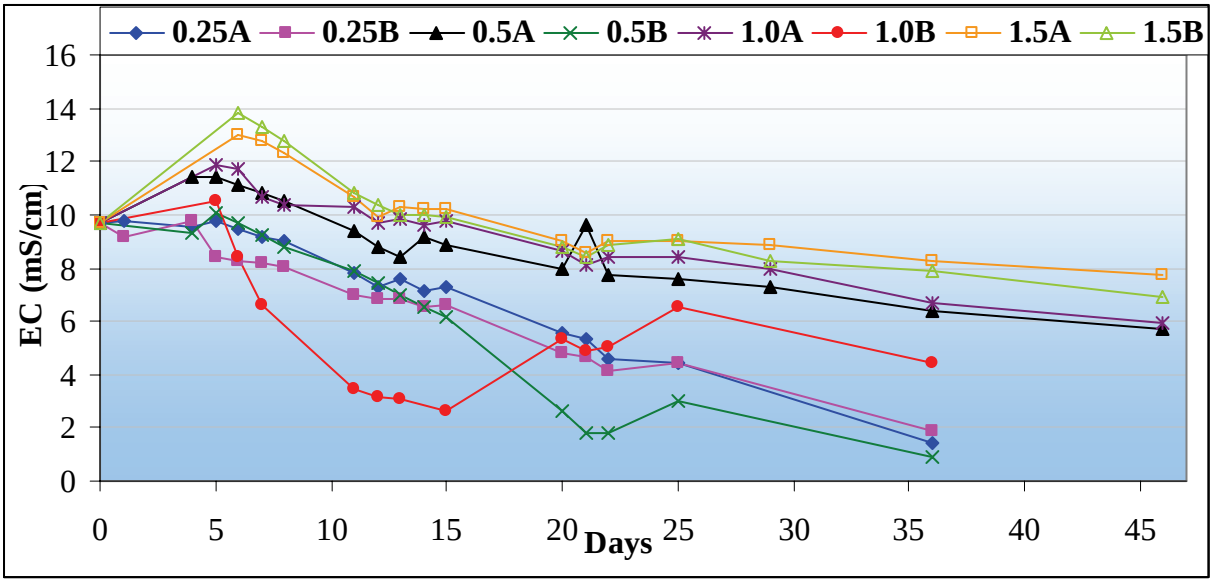

Figure 4.15: EC (mS/cm) of Landau AMD before and after passage through Matla columns. Sample numbers indicate length of column in metres and replicate number (A or B).

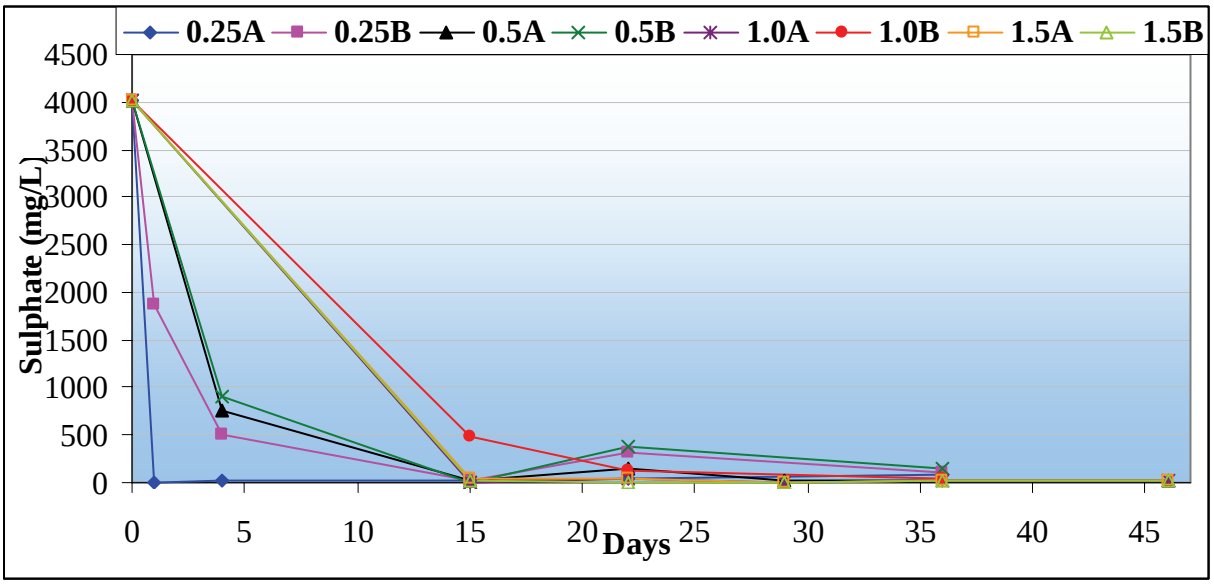

Figure 4.16: Sulphate (mg/L) concentration of Landau AMD before and after passage through Matla columns. Sample numbers indicate length of column in metres and replicate number (A or B).

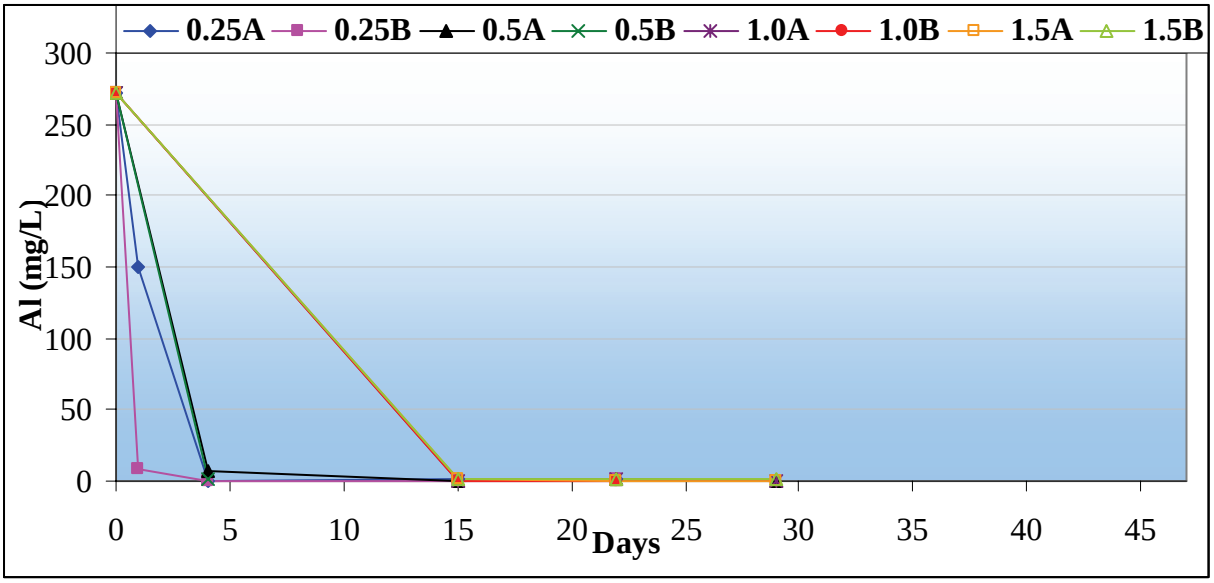

Figure 4.17: Al (mg/L) concentration of Landau AMD before and after passage through Matla columns. Sample numbers indicate length of column in metres and replicate number (A or B).

Figure 4.17 shows the Al concentration in the column permeates. There is an immediate reduction in concentration from 272mg/L to below 5mg/L and generally below 1mg/L. Levels remained in this range for the duration of the test. The Barium and Boron concentrations of the effluents are shown in Figures 4.18 and 64.19 respectively. The concentrations are extremely erratic and no trends were evident during the period evaluated. This may be due to the solubility of Barium and Boron at high pH values.

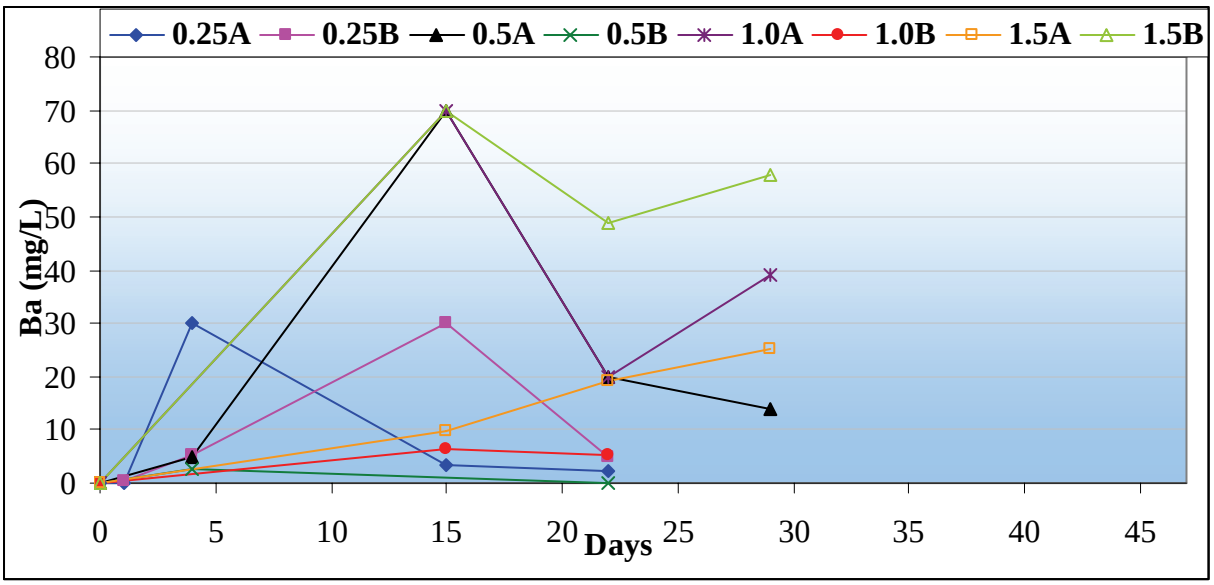

Figure 4.18: Ba (mg/L) concentration of Landau AMD before and after passage through Matla columns. Sample numbers indicate length of column in metres and replicate number (A or B).

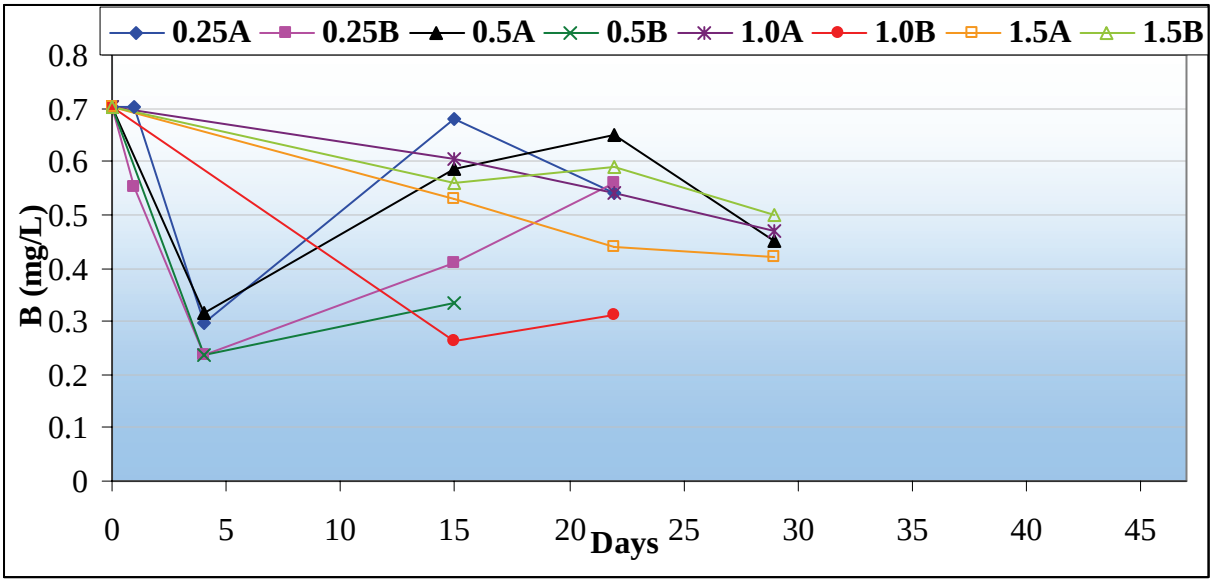

Figure 4.19: B (mg/L) concentration of Landau AMD before and after passage through Matla columns. Sample numbers indicate length of column in metres and replicate number (A or B).

Figure 4.20 shows the concentrations of Chromium in the permeate. After an initial spike in concentration of approximately 3.7mg/L the concentrations dropped to below 0.01mg/L and remained there for the duration of the test.

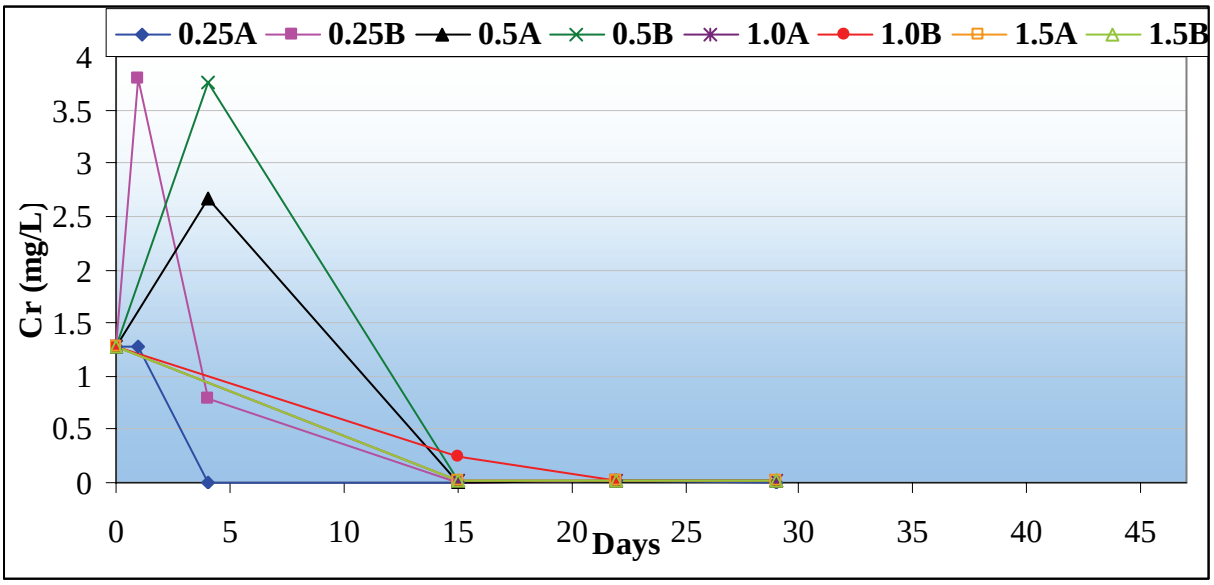

Figure 4.20: Cr (mg/L) concentration of Landau AMD before and after passage through Matla columns. Sample numbers indicate length of column in metres and replicate number (A or B).

Copper concentrations are shown in Figure 4.21. The concentrations indicate an initial decrease in concentration followed by slight increases. Column 1.5A however showed minimal reduction followed by a marked increase. Column 1.0B followed the same trend but at a smaller magnitude.

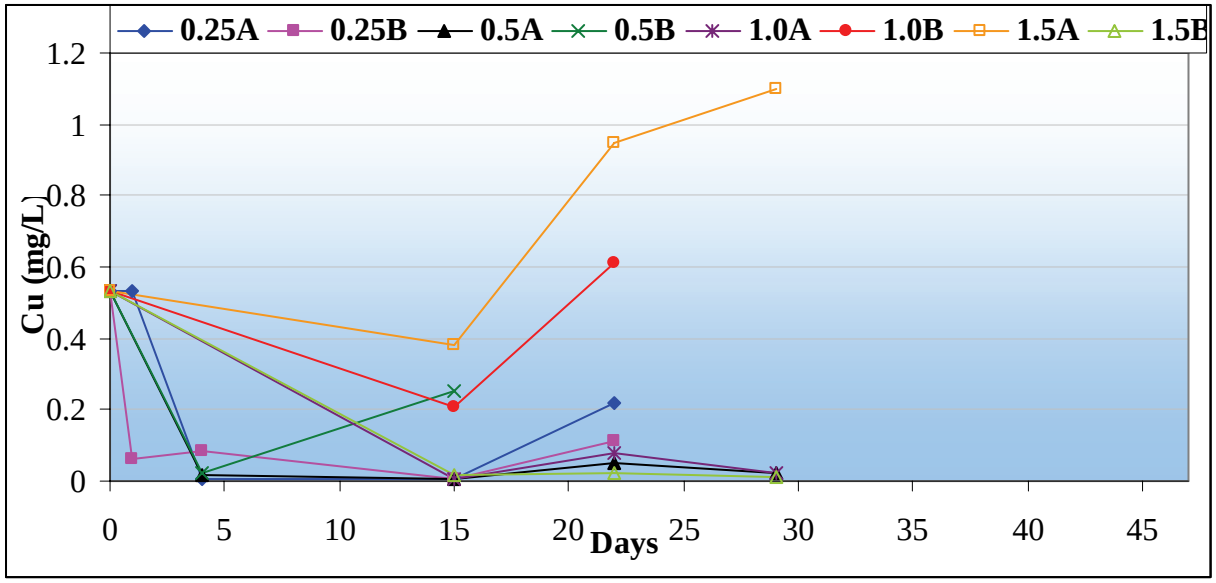

Figure 4.21: Cu (mg/L) concentration of Landau AMD before and after passage through Matla columns. Sample numbers indicate length of column in metres and replicate number (A or B).

Iron concentrations are depicted in Figure 4.22. There is a significant decrease in concentration from 3900mg/L to less than 3mg/L.

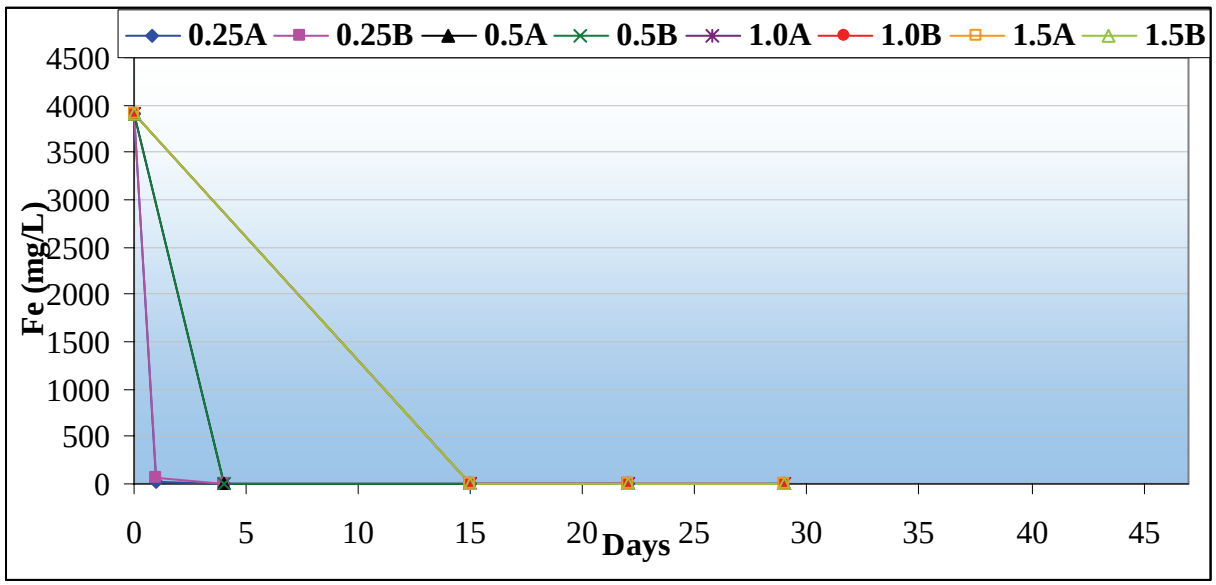

Figure 4.22: Fe (mg/L) concentration of Landau AMD before and after passage through Matla columns. Sample numbers indicate length of column in metres and replicate number (A or B).

Manganese concentrations (Figure 4.23) follow the same trend as Iron but the decrease was from 34.95mg/L to <0.005mg/L.

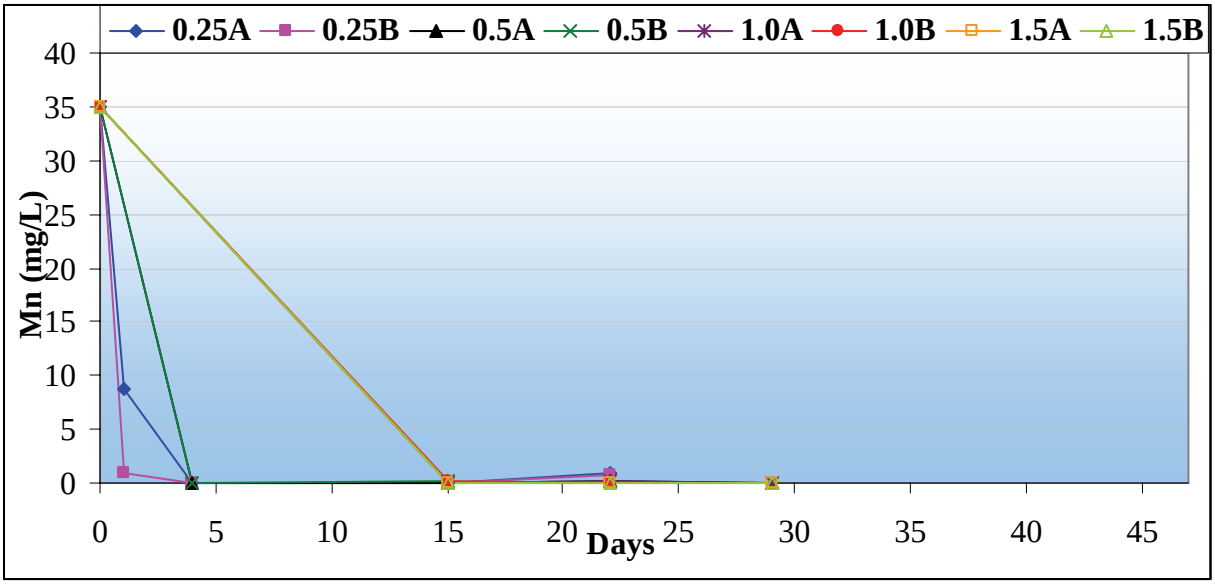

Figure 4.23: Mn (mg/L) concentration of Landau AMD before and after passage through Matla columns. Sample numbers indicate length of column in metres and replicate number (A or B).

Figure 4.24 shows the Zinc concentrations of the permeates, which all decreased. The permeates from the 1.0 and 1.5m columns took a longer time to decrease. After 15 days, all the columns except 1.0B and 1.5A were below 1mg/L. After day 15, 0.25A increased slightly to 1.3mg/L.

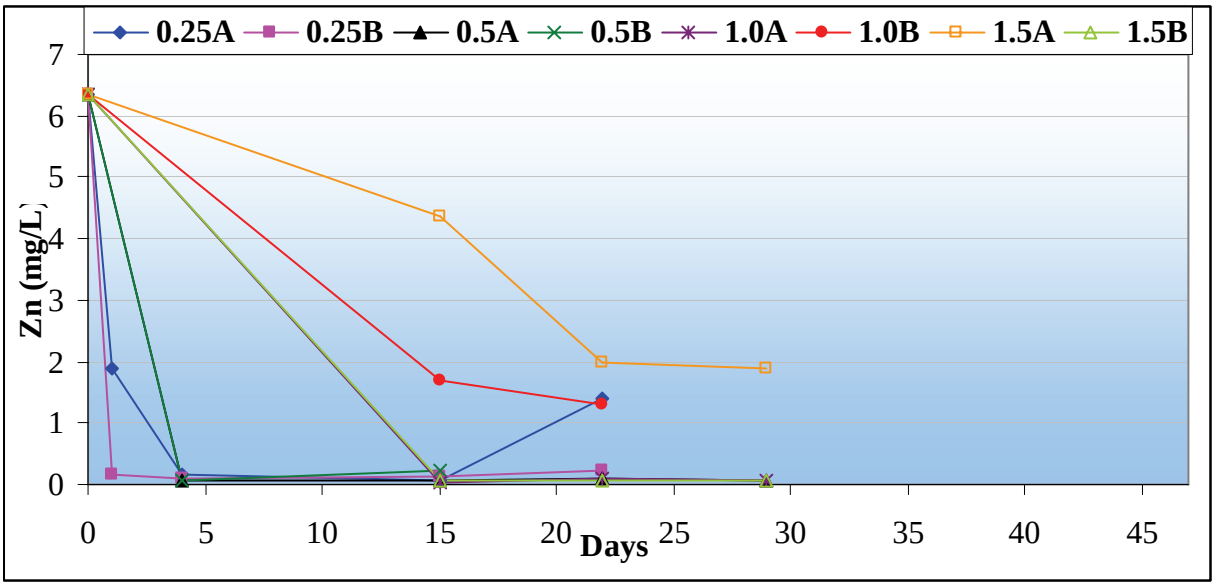

Figure 4.24: Zn (mg/L) concentration of Landau AMD before and after passage through Matla columns. Sample numbers indicate length of column in metres and replicate number (A or B).

4.3.3 Duvha ash column results

Navigation AMD was treated by percolation through columns of Duvha FA as described in section 4.2 for a period of 160 days.

Figure 4.25 shows the pH of the permeates from the various columns. The results obtained show a good correlation between the duplicate columns. The pH of the 0.25m columns started to decrease after day 20. The pH reached below 6 after day 51. The pH of the 0.5m columns was not as complementary and 0.5B had a sharp decrease in pH after day 74. The 1.0 and 1.5m columns maintained their pH above 12 until day 136 where after they dropped rapidly to below 8.

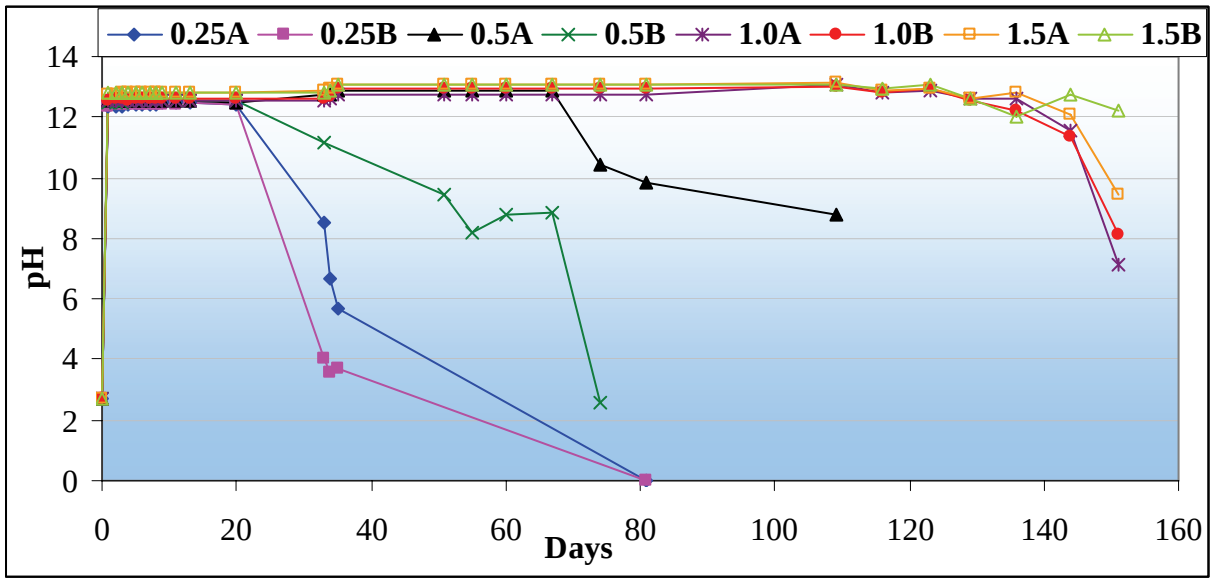

Figure 4.25: pH of Navigation AMD before and after passage through Duvha columns. Sample numbers indicate length of column in metres and replicate number (A or B).

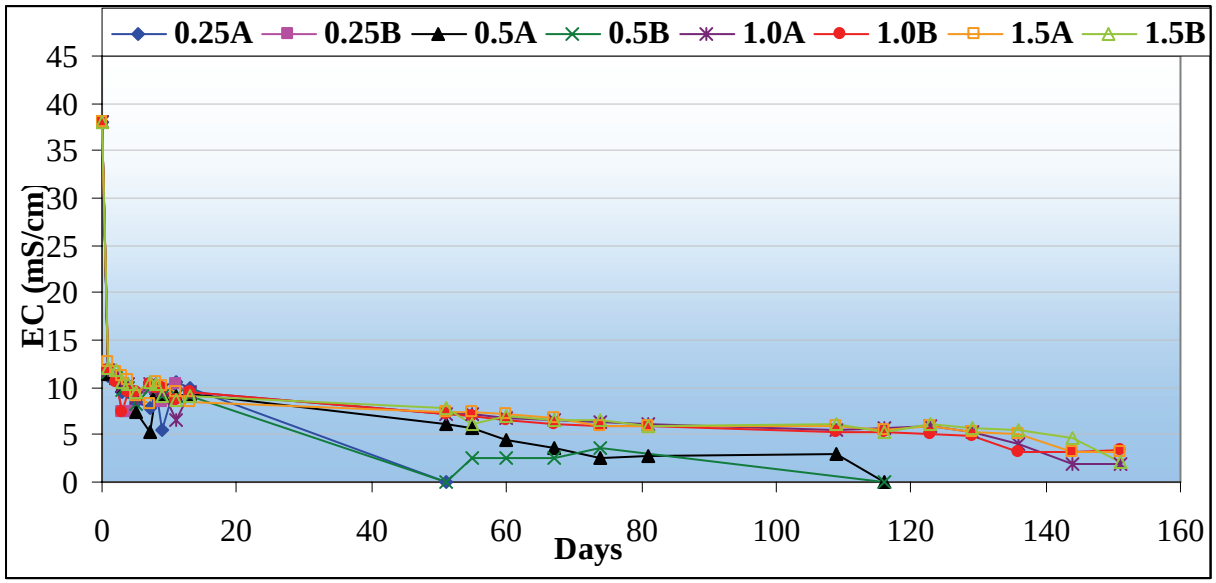

Figure 4.26: EC (mS/cm) of Navigation AMD before and after passage through Duvha columns. Sample numbers indicate length of column in metres and replicate number (A or B).

The EC trends are shown in Figure 4.26 and indicate a sharp and immediate decrease from 38100µS/cm to 11000 µS/cm. This decreasing trend continued for the duration of the test and all the column effluents were below 5000 µS/cm at completion after 160 days

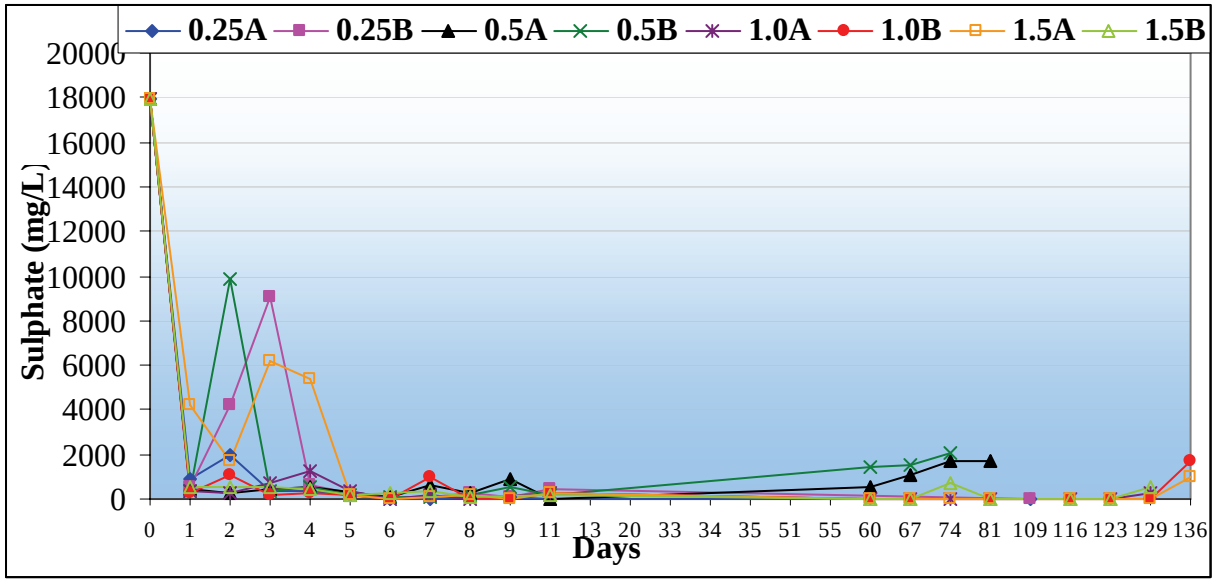

Figure 4.27: Sulphate concentration (mg/L) of Navigation AMD before and after passage through Duvha columns. Sample numbers indicate length of column in metres and replicate number (A or B).

Sulphate concentrations are shown in Figure 4.27. The concentration decreases quickly from 17926mg/L to less than 500mg/L before a quick spike to 10000mg/L followed by a sustained decrease below 500mg/L. The concentrations remained below 2000mg/L until the completion of the test after 136 days.

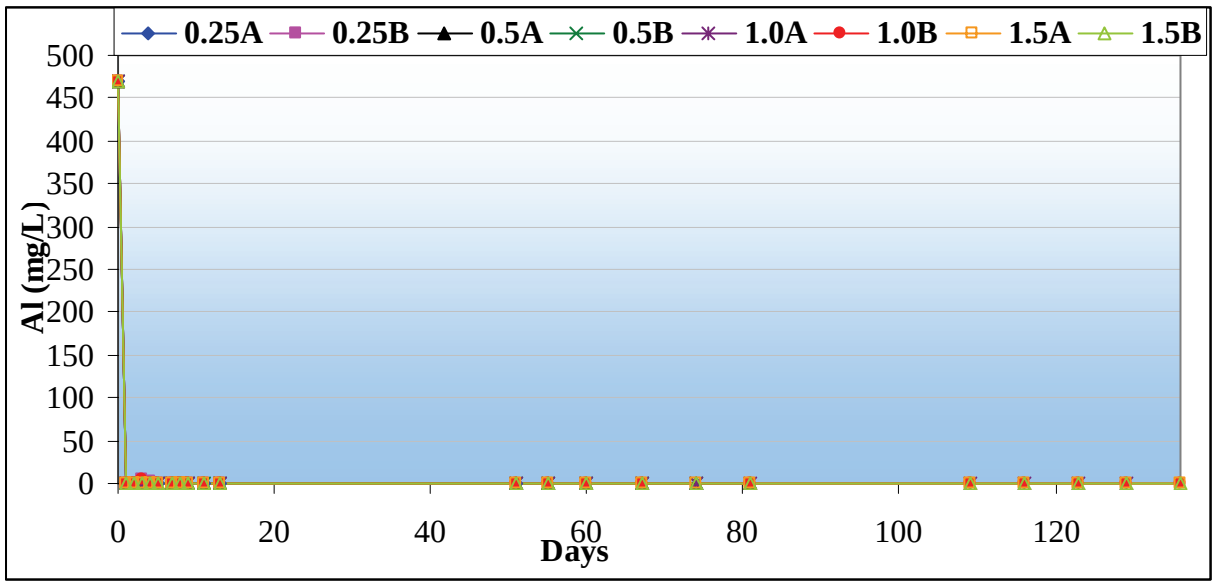

Figure 4.28: Al concentration (mg/L) of Navigation AMD before and after passage through Duvha columns. Sample numbers indicate length of column in metres and replicate number (A or B).

Aluminium concentrations are indicated in Figure 4.28 and show an immediate decrease from 470mg/L to <0.06mg/L for the duration of the test.

Figures 4.29 and 4.30 show the concentration of Barium and Boron respectively in the permeates. Both these elements are extremely soluble at high pH. The concentrations

increased from 0.03mg/L in both cases to above 90mg/L and 0.65mg/L then decreasing and stabilising below 20mg/L and 0.3mg/L for Barium and Boron respectively.

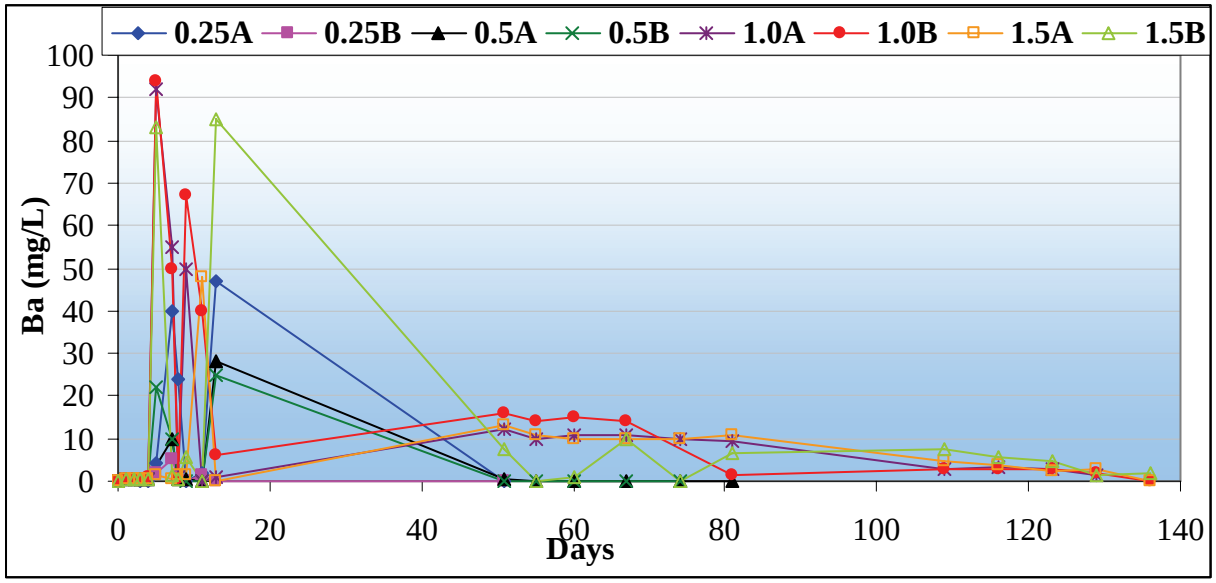

Figure 4.29: Ba concentration (mg/L) of Navigation AMD before and after passage through Duvha columns. Sample numbers indicate length of column in metres and replicate number (A or B).

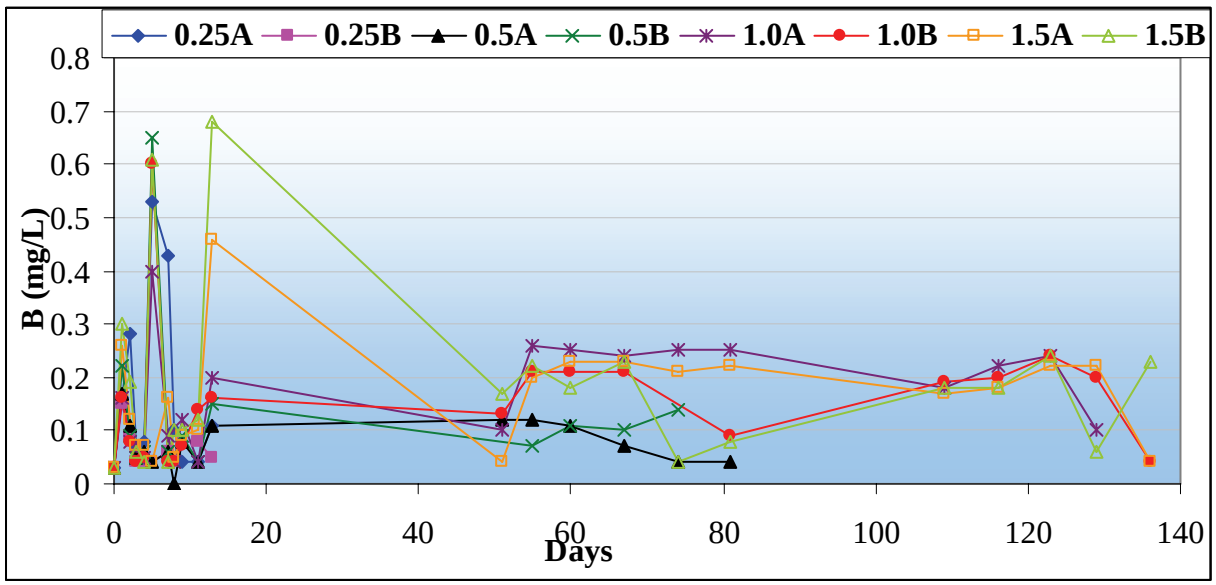

Figure 4.30: B concentration (mg/L) of Navigation AMD before and after passage through Duvha columns. Sample numbers indicate length of column in metres and replicate number (A or B).

Figure 4.31 shows the chromium concentrations of the permeate from the columns. The concentration drops from 1mg/L to below the detection limit of 0.005mg/L.

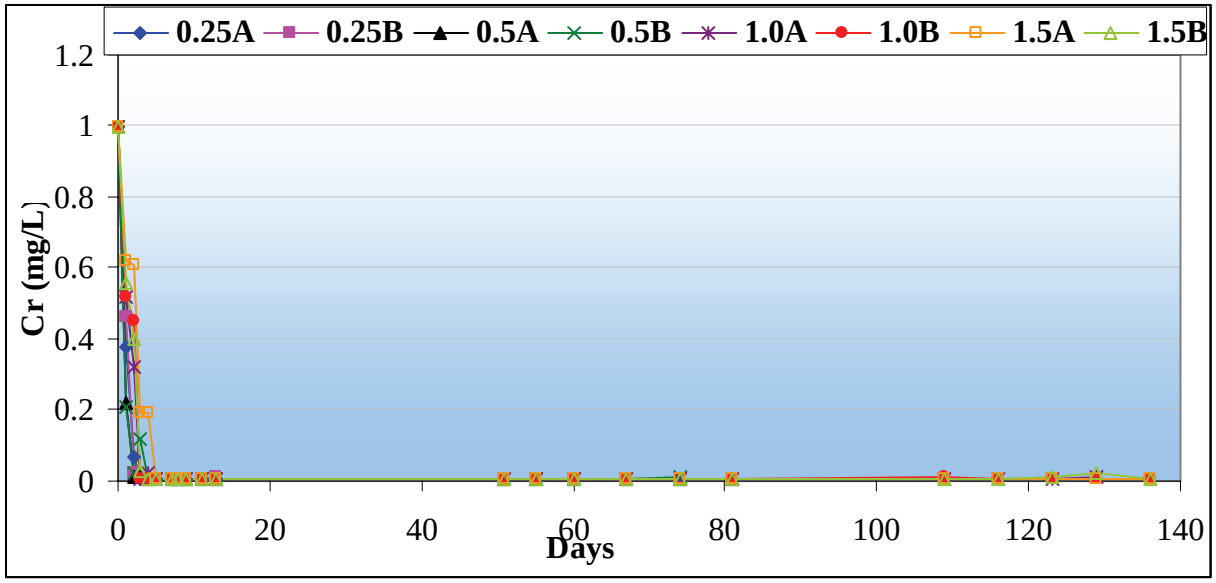

Figure 4.31: Cr concentration (mg/L) of Navigation AMD before and after passage through Duvha columns. Sample numbers indicate length of column in metres and replicate number (A or B).

The Copper concentrations in Figure 4.32 increase erratically from 0.03mg/L to a maximum of 0.69mg/L. Thereafter they stabilise to about 0.07mg/L for the rest of the duration of the experiment.

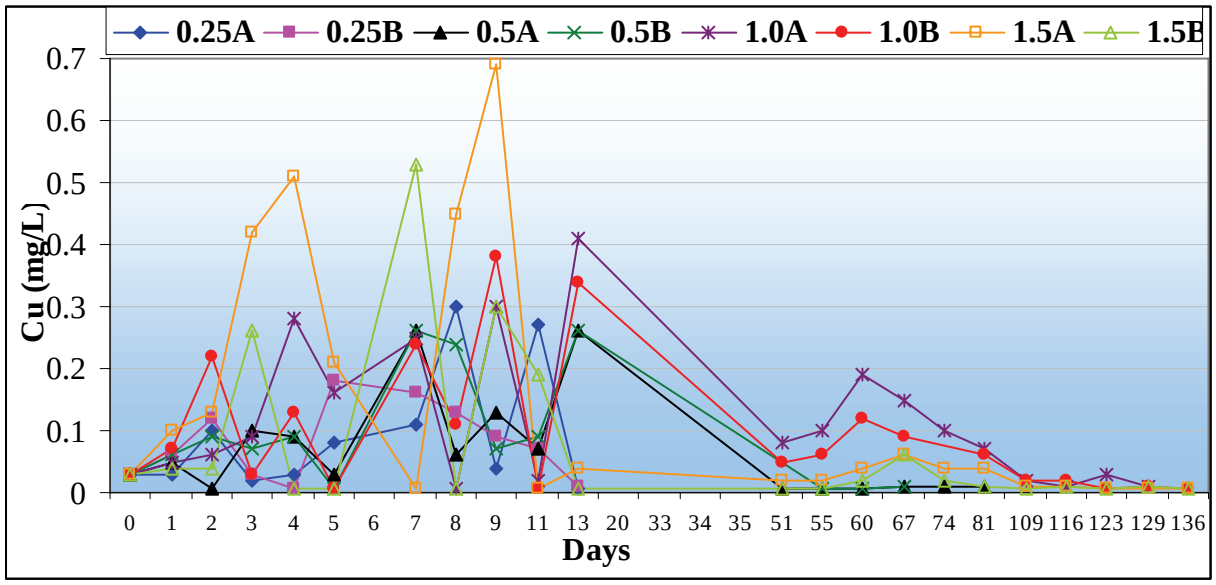

Figure 4.32: Cu concentration (mg/L) of Navigation AMD before and after passage through Duvha columns. Sample numbers indicate length of column in metres and replicate number (A or B).

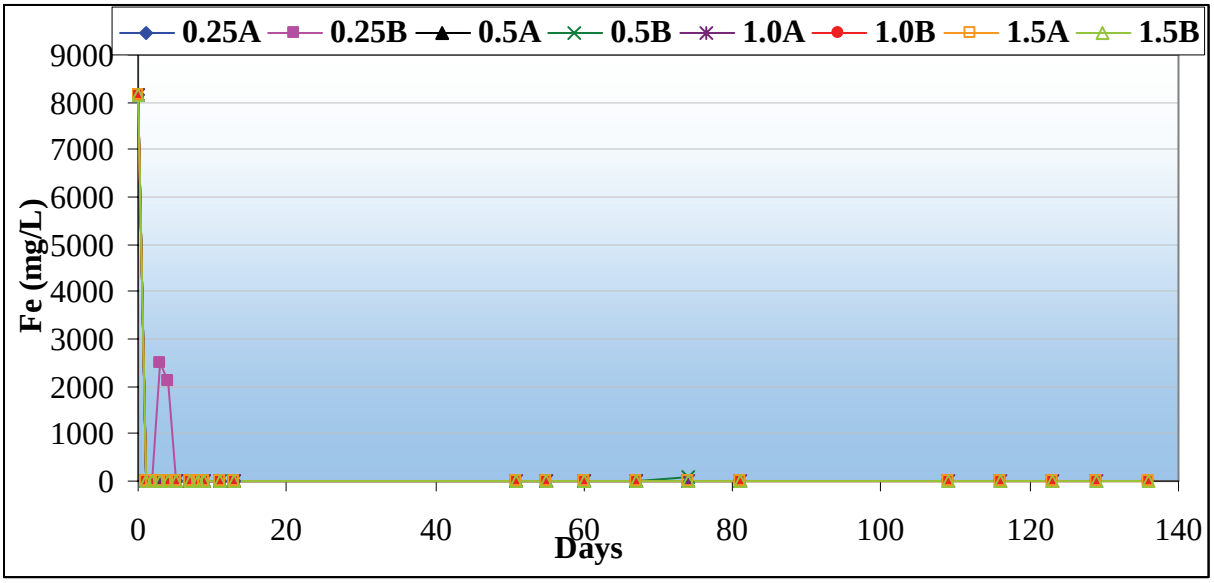

Figure 4.33: Fe concentration (mg/L) of Navigation AMD before and after passage through Duvha columns. Sample numbers indicate length of column in metres and replicate number (A or B).

The Fe concentrations (Figure 4.33) decreased immediately from 8169mg/L to below the 0.005mg/L detection limit. A slight concentration spike was noted in the 0.25B column but this is believed to be analytical error, as the trend was not followed by the duplicate test.

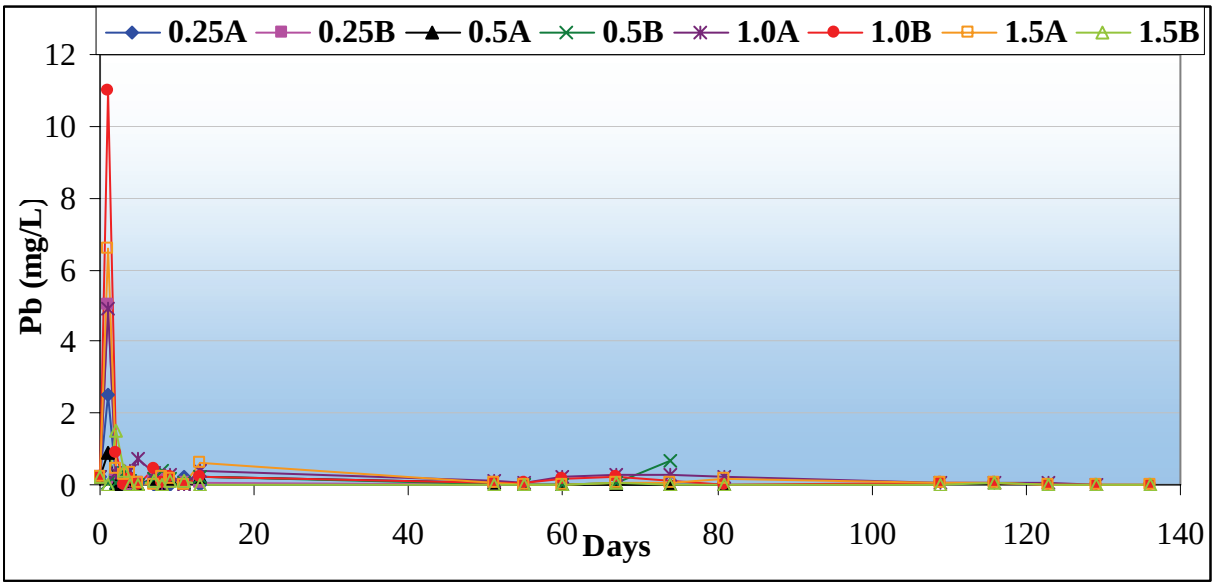

Figure 4.34: Pb concentration (mg/L) of Navigation AMD before and after passage through Duvha columns. Sample numbers indicate length of column in metres and replicate number (A or B).

Lead concentrations (Figure 4.34) spiked from 0.2 mg/L to 11 mg/L on day 1 followed by a return to below 1.0 mg/L, where the concentration remained relatively stable for the duration of the test.

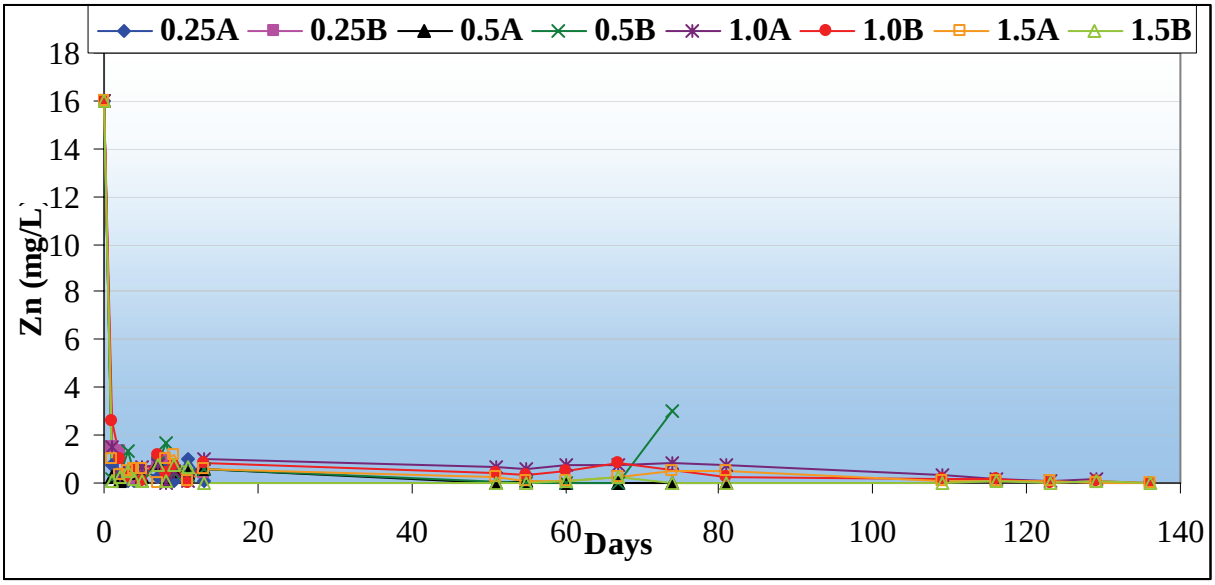

Figure 4.35: Zn concentration (mg/L) of Navigation AMD before and after passage through Duvha columns. Sample numbers indicate length of column in metres and replicate number (A or B).

The concentrations of Zinc are shown in Figure 4.35. The concentration is immediately reduced from 16 mg/L to less than 1.0 mg/L. The concentrations remained low for the duration of the test with the exception of the 0.5B column, where the concentration rose to 3 mg/L on day 74.

The column studies performed with combinations of different sources of FA used to passively treat different sources of AMD, generally show similar trends. In all cases the AMD is significantly purified, with the significant reduction in major, minor and trace elements, with the exception of B, Ba and in some cases Cu. Sulphate was not so effectively treated in the shorter columns applied in the case of Kendal FA to treat Middelburg AMD. These results are indicative of what the relative thickness of a future ash wall may need to be in order to act as passive barrier over time and achieve the necessary durability or neutralisation capacity. The fact that columns blocked also indicates the potential to use ash as a passive barrier to direct AMD flows.

This study shows that various FA sources are suitable as materials for the passive treatment of AMD flows. Thus significant potential exists to reduce the AMD pollution arising in spoil heaps and underground by application of ash walls to prevent AMD generation, or as passive AMD treatment systems or as barriers to direct AMD flows.

4.3.4. Analysis of fly ash from columns

After these column studies were completed, the solids within the columns, that comprised both FA and the precipitates that formed during percolation of AMD through the column, were characterized by XRF and XRD. The characterization was performed in order to understand the longer term changes in the passive FA barrier in contact with AMD and to determine whether significant changes in the elemental composition (XRF) and mineralogy (XRD) had occurred. The characterization results are presented in this section.

4.3.4.1 X-ray diffraction

Major and minor phases that were present in the various columns were determined by XRD. Major and minor phases of the various duplicate and different length Kendal ash columns are presented in Table 6.2; major and minor phases of the various duplicate and different length Matla ash columns are presented in Table 6.3; Major and minor phases of Duvha ash columns are presented in Table 6.4 in °2θ so that the peaks representing the different phases can be assigned and the XRD spectra for the Duvha columns are presented in Figures 6.36-6.38.

Table 4.2: XRD of Kendal ash columns (mullite - $Al_6Si_2O_{13}$, quartz – SiO_2, gypsum – $CaSO_4$, hematite – Fe_2O_3).

Sample	Major Phase	Minor Phase
Fly ash	Mullite, Quartz	Not detected
A0.5 Top	Gypsum, Hematite	Mullite, Quartz
B0.5 Top	Gypsum, Hematite	Mullite, Quartz
A0.5 Middle	Gypsum, Hematite	Mullite, Quartz
B0.5 Middle	Gypsum, Hematite	Mullite, Quartz
A0.5 Bottom	Gypsum, Hematite	Mullite, Quartz
B0.5 Bottom	Gypsum, Hematite	Mullite, Quartz
A1.0 Top	Gypsum, Hematite	Mullite, Quartz
B1.0 Top	Gypsum, Hematite	Mullite, Quartz
A1.0 Middle	Gypsum, Hematite	Mullite, Quartz
B1.0 Middle	Gypsum, Hematite	Mullite, Quartz
A1.0 Bottom	Gypsum, Hematite	Mullite, Quartz
B1.0 Bottom	Gypsum, Hematite	Mullite, Quartz
A1.5 Top	Gypsum, Hematite	Mullite, Quartz
B1.5 Top	Gypsum, Hematite	Mullite, Quartz
A1.5 Middle	Gypsum, Hematite	Mullite, Quartz
B1.5 Middle	Gypsum, Hematite	Mullite, Quartz
A1.5 Bottom	Gypsum, Hematite	Mullite, Quartz
B1.5 Bottom	Gypsum, Hematite	Mullite Quartz

Table 4.3: XRD of Matla ash columns (mullite - $Al_6Si_2O_{13}$, quartz – SiO_2, gypsum – $CaSO_4$, calcite – $CaCO_3$)

Sample	Major Phase
Fly ash	Mullite, Quartz
A0.25 Top	Quartz, Mullite, Gypsum
B0.25 Top	Quartz, Mullite, Gypsum
A0.25 Middle	Quartz, Mullite, Gypsum
B0.25 Middle	Quartz, Mullite, Gypsum
A0.25 Bottom	Quartz, Mullite, Gypsum
B0.25 Bottom	Quartz, Mullite, Gypsum
A0.5 Top	Quartz, Mullite, Gypsum
B0.5 Top	Quartz, Mullite, Calcite
A0.5 Middle	Quartz, Mullite, Gypsum, Calcite
B0.5 Middle	Quartz, Mullite, Calcite
A0.5 Bottom	Quartz, Mullite, Calcite
B0.5 Bottom	Quartz, Mullite, Calcite
A1.0 Top	Quartz, Mullite, Gypsum
B1.0 Top	Quartz, Mullite, Calcite
A1.0 Middle	Quartz, Mullite, Calcite
B1.0 Middle	Quartz, Mullite, Gypsum, Calcite
A1.0 Bottom	Quartz, Mullite, Calcite
B1.0 Bottom	Quartz, Mullite, Gypsum, Calcite
A1.5 Top	Quartz, Mullite, Gypsum
B1.5 Top	Quartz, Mullite, Gypsum
A1.5 Middle	Quartz, Mullite, Calcite
B1.5 Middle	Quartz, Mullite, Calcite
A1.5 Bottom	Quartz, Mullite, Gypsum, Calcite
B1.5 Bottom	Quartz, Mullite , Gypsum, Calcite

Table 4.4: XRD of Duvha ash columns in °2θ (mullite - $Al_6Si_2O_{13}$, quartz – SiO_2, gypsum – $CaSO_4$).

Quartz	**Gypsum**	**Mullite**	**Mullite**
20.7	11.6	16.5	47.0
26.5	20.7	23.5	48.0
36.5	23.4	25.9	48.5
39.4	29.1	26.1	49.6
40.2	31.1	30.8	49.6
42.4	32.1	33.1	50.6
45.8	33.3	35.1	53.1
50.0	36.0	36.9	53.5
50.6	40.6	37.2	53.8
54.8	43.3	39.0	57.1
55.2	43.6	39.1	58.0
57.1	47.8	40.8	58.7
60.0	48.4	42.5	59.8
	50.3	42.9	
	51.3	46.0	

The visible differences in the XRD spectra of the various column samples are not significant in terms of changes in the overall mineralogy of the samples. Spectra are different when new, strong peaks appear despite the fact that peak strength may vary it is always relative. Peak absence is not necessarily significant in minor peaks but extremely significant in major peaks. The major peak of any mineral is defined as having 100% intensity and all other visible peaks of that mineral have a percentage intensity relative to it. If the major peaks, i.e. those with greatest % intensity are absent the mineral is likewise absent.

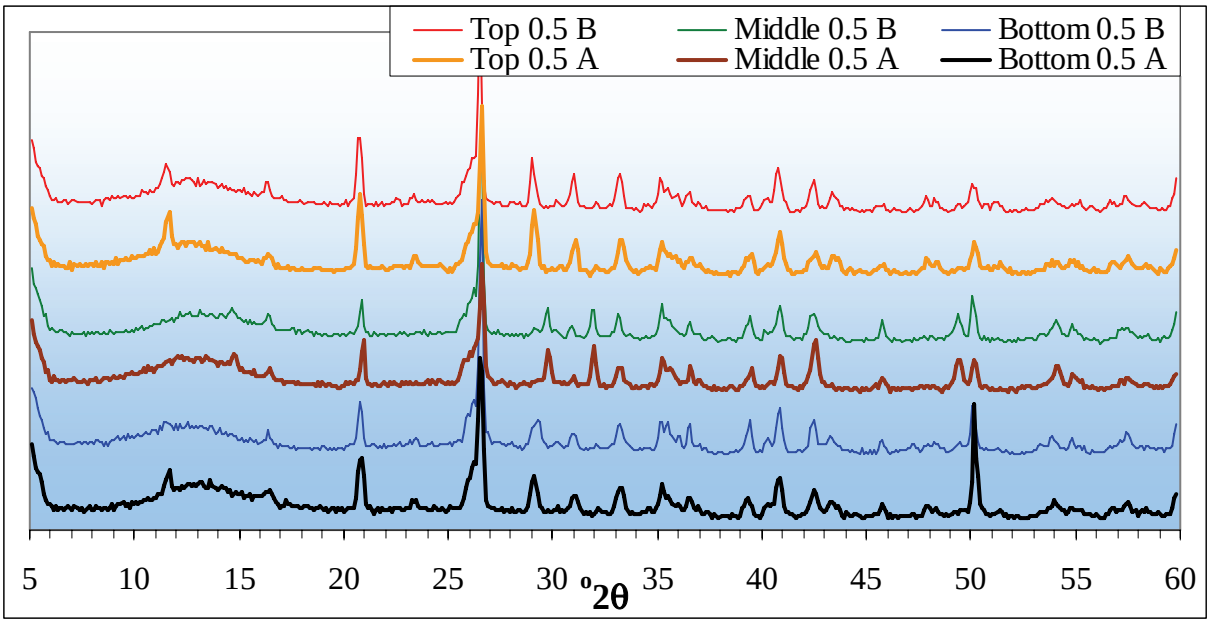

Figure 4.36: XRD spectra for the Duvha 0.5 m column

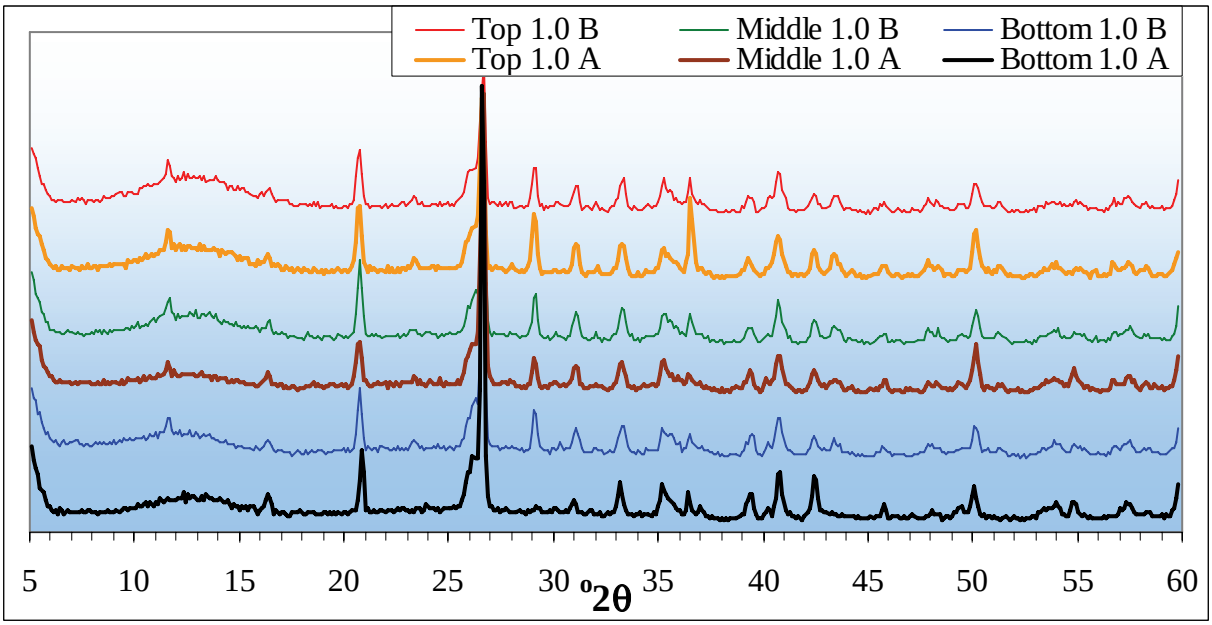

Figure 4.37: XRD spectra for the Duvha 1.0 m column

In the Duvha column 0.5 m in length (Figure 4.36) all samples from the bottom middle and top sections contain quartz and mullite. In the Duvha column 1.0 m in length (Figure 4.37) all samples contain quartz and mullite. In the Duvha column 1.5

m in length (Figure 4.38) all samples contain quartz and mullite. Most Duvha column samples analysed contain gypsum except for middle 0.5 A& B and bottom 1.0A, 1.5 B. Since gypsum is soluble (Burgers 2003) it is possible that under certain conditions such as a pH decrease precipitated gypsum resolubilises, which corresponds to the decrease in pH and increase in sulphate levels observed after time in these columns (section 1.3).

In the Duvha samples called middle 0.5 A and B and middle 1.5 B, another mineral is present. The peaks at 14.5 and 49 °2 θ do not match any of the peaks for quartz, mullite or gypsum. There is a possibility that this mineral is boehmite, since these two peaks match a low intensity peak and the highest intensity peak, respectively. It is also possible that small amounts of hematite may be present but the highest peak at 33.1 °2 θ is masked by mullite and gypsum, the next intense peak at 35.5 °2 θ may be seen as a shoulder on the mullite peak at 35 °2 θ.

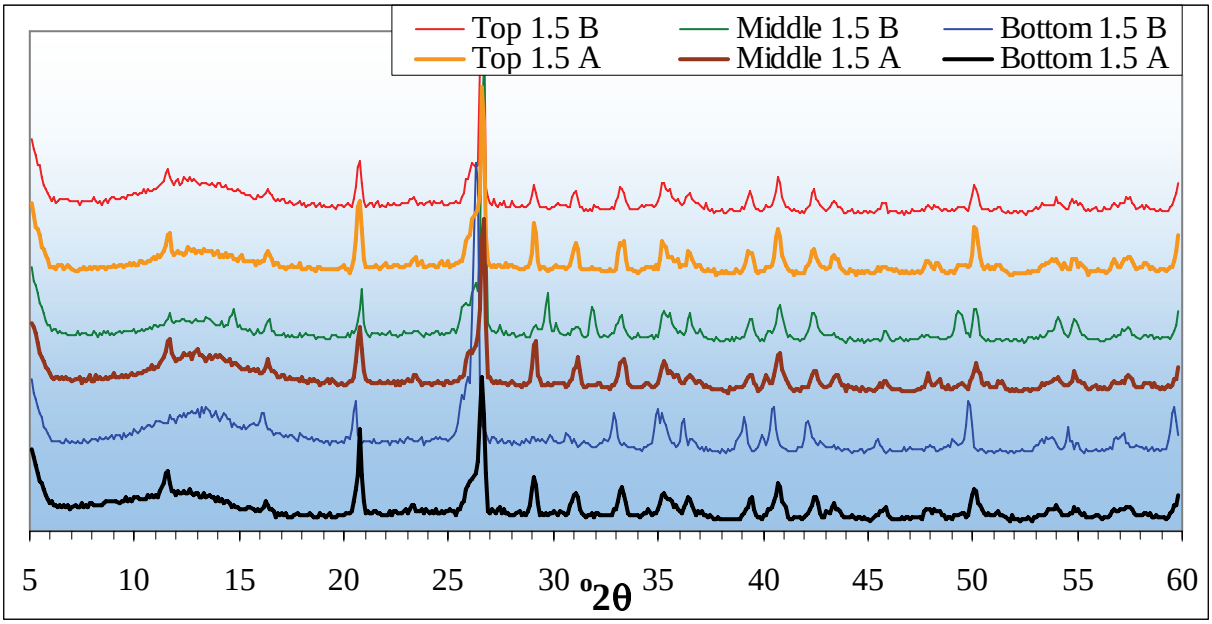

Figure 4.38: XRD spectra for the Duvha 1.5 m column

The XRD results presented in this section thus show that in general Mullite and Quartz were the major phases in the fresh FA whereas in the solids recovered from the columns Quartz and Mullite originating from the parent FA remained and new mineral phases, namely Gypsum, Calcite and in some cases Hematite or Boehmite were formed after passage of AMD through the FA columns. The formation of the mineral phase Gypsum which may cement particles together is most likely the cause of the observed column blockage.

4.3.4.2 X-ray fluorescence

The XRF analyses giving the elemental composition for the different columns of various lengths are shown in Tables 4.5, 4.6 and 4.7. In general there are higher amounts of Si and Al towards the bottom of each column. This suggests that while the pH of the solution is high enough for Si and Al to be mobile, these elements are leached out of the column. The initial pH must be greater than 12 for Si and Al to be

mobile and a slight decrease will ensure precipitation. In a real world scenario, the pH probably would not stay at such alkaline levels for long.

Table 4.5: XRF for Kendal ash columns.

Mass %	SiO_2	Al_2O_3	CaO	Fe_2O_3	TiO_2	MgO	SO_3	K_2O	P_2O_5	MnO	Na_2O	LOI	Total
Fly Ash	55.3	33.1	4.70	3.50	1.70	1.50	0.50	0.50	0.43	0.04	0.01	0.50	102
0.5 A Top	47.5	33.5	3.30	3.10	1.40	1.70	1.60	0.50	0.44	0.09	0.01	3.20	96.3
0.5 B Top	46.3	31.4	3.30	2.90	1.40	1.90	1.50	0.40	0.42	0.12	0.01	6.60	96.3
0.5 A Middle	49.4	32.4	3.60	3.10	1.50	2.20	1.50	0.50	0.44	0.08	0.01	3.40	98.1
0.5 B Middle	48.3	31.9	3.70	3.00	1.50	2.00	1.50	0.50	0.43	0.06	0.01	5.10	98.0
0.5 A Bottom	48.6	32.1	3.50	3.10	1.50	2.10	1.30	0.40	0.41	0.09	0.01	3.70	96.8
0.5 B Bottom	47.0	32.0	3.50	3.00	1.40	2.20	1.30	0.50	0.42	0.08	0.01	5.80	97.2
1.0 A Top	48.3	32.8	3.40	3.20	1.50	2.00	1.50	0.40	0.44	0.08	0.01	3.30	96.9
1.0 B Top	49.0	32.4	3.80	3.10	1.50	2.10	1.90	0.50	0.45	0.09	0.01	3.60	98.5
1.0 A Middle	47.8	32.0	4.10	3.00	1.40	1.80	1.30	0.50	0.43	0.04	0.01	4.80	97.2
1.0 B Middle	48.3	33.2	3.50	3.10	1.50	2.30	1.30	0.50	0.43	0.09	0.01	3.00	97.2
1.0 A Bottom	48.9	33.2	4.30	3.20	1.50	1.50	0.80	0.50	0.42	0.04	0.01	2.60	97.0
1.0 B Bottom	49.4	34.1	4.40	3.10	1.50	1.80	1.40	0.30	0.45	0.04	0.01	3.50	100
1.5 A Top	49.9	32.5	3.60	3.10	1.50	1.90	1.50	0.50	0.44	0.10	0.01	2.90	98.0
1.5 B Top	49.8	32.6	3.50	3.10	1.50	1.90	1.60	0.50	0.44	0.11	0.01	2.60	97.7
1.5 A Middle	49.0	31.8	3.70	3.10	1.50	1.90	1.00	0.50	0.41	0.07	0.01	3.60	96.6
1.5 B Middle	48.7	31.9	4.20	3.00	1.50	1.70	1.20	0.50	0.42	0.04	0.01	4.40	97.6
1.5 A Bottom	48.6	31.4	4.00	3.00	1.50	1.70	1.10	0.40	0.42	0.05	0.01	4.80	97.0
1.5 B Bottom	50.9	31.6	4.20	3.10	1.60	1.60	1.10	0.60	0.42	0.05	0.01	5.30	100

The Kendal columns (Table 4.5) show no increase in Fe precipitation as a result of there being very little Fe in the Middelburg AMD to start with. The concentration of Fe is increased in the other columns (Matla and Duvha) as would be expected as soluble Fe salts precipitate out of the AMD solution as hydroxide minerals. More precipitation seems to occur midway down the Duvha columns (Table 4.7) as evidenced by the increase in Fe concentration between the top and the middle samples, while the greatest concentration of Fe in the Matla columns (Table 4.6) is at the top. This may be as a result of oxygen diffusion through the column, the lower half of the Duvha column being better oxygenated than the top due to experimental set-up.

The concentrations of Mg and Ca, as well as Na to a lesser degree increase towards the bottom of the columns. The most likely reason for this is the matrix effect of the solution. The AMD has a high EC and as a consequence a large amount of dissolved constituents, which, combined with dissolved alkalinity, create a saturated solution. The precipitation of minerals allows other salts to be dissolved, to saturate the solution and precipitate further down the column.

The concentration of S and hence, SO_4, concentration is much higher at the top of the columns. This is likely a result of the fact that an ettringite mineral was forming and then dissolving and causing gypsum to become supersaturated enough to promote precipitation.

Table 4.6: XRF for Matla ash columns.

Mass %	SiO_2	Al_2O_3	SO_3	CaO	Fe_2O_3	TiO_2	P_2O_5	MgO	Na_2O	K_2O	LOI	Total
Fly Ash												
0.25 A Top	36.9	29.8	14.6	9.98	3.69	1.32	1.28	0.67	0.89	0.84	10.4	110
0.25 B Top	36.1	29.6	15.4	9.97	4.01	1.38	1.34	0.73	0.82	0.64	10.6	111
0.25 A Middle	38.2	26.0	9.83	8.88	10.1	1.27	1.69	2.04	1.14	0.89	5.20	105
0.25 B Middle	38.3	26.2	9.80	8.85	9.52	1.32	1.46	2.65	1.15	0.79	6.00	106
0.25 A Bottom	42.0	28.5	5.80	12.3	3.10	1.84	1.37	3.20	0.91	1.05	4.80	105
0.25 B Bottom	41.8	28.1	7.08	9.59	6.53	1.50	1.30	2.24	1.02	0.83	6.00	106
0.5 A Top	36.8	26.0	11.0	9.25	9.82	1.45	1.29	2.58	1.09	0.77	6.40	106
0.5 B Top	36.3	25.6	10.4	9.30	11.4	1.49	1.18	2.47	1.03	0.81	6.50	106
0.5 A Middle	44.7	30.4	3.37	11.3	2.38	1.83	1.57	2.57	1.09	0.90	3.60	104
0.5 B Middle	40.9	27.7	8.16	10.9	3.66	1.44	1.41	4.00	1.12	0.78	5.40	105
0.5 A Bottom	47.3	31.6	1.20	9.74	2.31	1.51	1.86	2.33	1.17	0.96	3.40	103
0.5 B Bottom	47.3	31.6	1.23	9.98	2.42	1.77	1.38	2.23	1.02	1.07	3.50	103
1.0 A Top	36.8	25.9	10.7	10.1	9.14	1.51	1.41	2.66	0.94	0.79	6.00	106
1.0 B Top	37.8	26.4	10.5	9.72	7.49	1.49	1.57	3.33	0.86	0.78	6.00	106
1.0 A Middle	47.2	31.5	1.25	10.2	2.25	1.53	1.72	2.22	1.16	0.99	3.80	104
1.0 B Middle	47.1	31.5	1.20	10.1	2.34	1.66	1.96	2.22	1.07	0.90	3.60	104
1.0 A Bottom	45.4	31.0	1.40	11.4	2.71	1.79	1.84	2.43	1.03	0.95	3.60	104
1.0 B Bottom	47.3	31.2	1.15	10.2	2.57	1.69	1.72	2.16	1.17	0.93	3.60	104
1.5 A Top	38.7	26.9	9.06	10.7	6.73	1.48	1.33	3.25	0.98	0.86	6.20	106
1.5 B Top	37.8	26.3	10.3	9.20	8.16	1.32	1.78	3.22	1.09	0.79	6.40	106
1.5 A Middle	46.2	31.6	1.46	10.4	2.46	1.74	1.72	2.35	1.08	0.98	3.60	104
1.5 B Middle	46.8	31.1	1.75	10.2	2.66	1.68	1.48	2.21	1.17	0.99	3.70	104
1.5 A Bottom	45.5	31.2	1.30	11.4	2.99	1.89	1.60	2.03	1.07	1.03	4.40	104
1.5 B Bottom	47.2	31.5	1.05	10.3	2.31	1.91	1.64	1.99	1.05	1.01	4.30	104

Table 4.7: XRF for Duvha ash columns.

Mass %	SiO_2	Al_2O_3	CaO	Fe_2O_3	SO_3	TiO_2	MgO	K_2O	P_2O_5	MnO	Na_2O	H_2O-	LOI	Total
Fly Ash														
0.5 A Top	44.4	21.5	5.35	9.22	4.88	1.04	0.93	0.46	0.42	0.07	BDL	3.77	7.12	99.3
0.5 B Top	44.8	21.5	5.29	10.4	4.29	1.06	1.03	0.48	0.43	0.08	0.05	3.24	6.9	99.5
0.5 A Middle	42.5	19.5	6.14	11.9	5.47	1.07	2.10	0.44	0.41	0.2	0.13	3.70	6.27	99.9
0.5 B Middle	45.9	20.7	5.42	12.0	3.78	1.09	1.29	0.48	0.44	0.12	0.12	2.79	5.62	99.8
0.5 A Bottom	45.0	20.4	6.2	10.0	3.93	1.11	2.18	0.48	0.44	0.19	0.17	3.29	5.96	99.4
0.5 B Bottom	47.5	21.2	6.57	9.59	2.71	1.13	1.83	0.5	0.45	0.13	0.11	1.87	6.41	100
1.0 A Top	43.8	21.8	5.34	8.92	5.10	1.03	0.89	0.45	0.42	0.07	0.05	3.86	7.31	99.1
1.0 B Top	43.4	21.8	5.01	9.88	4.67	1.06	0.96	0.47	0.42	0.08	0.04	3.98	7.65	99.5
1.0 A Middle	45.6	20.6	5.10	12.2	3.57	1.09	1.51	0.48	0.43	0.14	0.19	2.57	6.11	99.6
1.0 B Middle	42.8	19.8	5.83	11.8	5.07	1.04	1.95	0.45	0.42	0.17	0.16	3.66	6.35	99.6
1.0 A Bottom	48.6	22.2	6.88	9.27	1.21	1.18	1.74	0.53	0.47	0.08	0.20	1.58	5.97	99.9
1.0 B Bottom	44.4	19.6	5.97	11.00	4.78	1.05	2.02	0.46	0.42	0.18	0.11	3.34	6.45	99.9
1.5 A Top	44.4	21.8	4.85	9.66	4.27	1.04	1.06	0.46	0.42	0.09	BDL	3.73	7.28	99.1
1.5 B Top	43.7	19.5	3.39	14.1	2.8	1.06	0.8	0.46	0.41	0.07	0.11	3.73	9.2	99.5
1.5 A Middle	43.2	19.4	5.83	12.0	4.94	1.03	1.85	0.44	0.41	0.14	0.13	3.87	6.39	99.7
1.5 B Middle	43.8	19.9	5.73	11.0	4.91	1.06	2.12	0.45	0.42	0.22	0.10	3.57	6.39	99.7
1.5 A Bottom	43.7	19.5	6.06	10.9	5.15	1.04	2.00	0.46	0.42	0.2	0.09	3.31	6.37	99.2
1.5 B Bottom	48.7	21.9	6.65	9.11	1.11	1.17	1.71	0.53	0.46	0.08	0.16	1.53	6.23	99.3

Table 4.8 shows the trace metal concentrations. The concentrations of Cr, Ni, V and Zn are higher at the top of the columns suggesting that precipitation occurs as soon as the pH is increased. The concentrations of Cu and Mn are high towards the middle of the column, which suggests that they are slightly more mobile at high pH values. The concentrations of the other trace elements do not change appreciably from the top of the column to the bottom. It cannot be said what concentration of these elements are from the AMD as there is no trace element analysis for the raw fly ash as yet.

4.4 CONCLUSIONS

These column leaching experiments show that fly ash has the long-term capacity to neutralise AMD and remove metals from the water and that eventually the fly ash barrier will clog, preventing AMD percolation and neutralisation. Thus, diminishing the production of AMD and acting as an aquiclude or barrier.

This study shows that various FA sources are suitable as materials for the passive treatment of a variety of AMD flows. Thus significant potential exists to reduce the AMD pollution arising in spoil heaps and underground by application of ash walls to prevent AMD generation, or as passive AMD treatment systems or as barriers to direct AMD flows. Use of FA or solid residues for backfilling thus may play a role in mitigating the environmental concerns around current AMD flows and the future production of AMD.

Table 4.8: XRF for trace metals for Duvha ash columns.

Mass concentration (ppm)	Ba	Co	Cr	Cu	Mn	Mo	Nb	Ni	Pb	Rb	Sc	Sr	Th	U	V	Y	Zn	Zr
0.5 A Top	952	23.5	281	6374	502	3.7	27	99.1	38.5	25.1	30	618	32.5	12.3	104	132	1781	328
0.5 B Top	957	31.1	184	2317	475	8.95	28.3	92.7	51.3	26.1	28.3	629	30.6	10.4	98.6	83.7	894	341
0.5 A Middle	847	37.1	208	44.3	1435	3.38	27.8	74.5	36.9	23.7	23.2	635	33.4	8.62	92.1	52.8	192	331
0.5 B Middle	968	47.4	166	458	755	4.2	30.4	106	39.4	25.4	24.9	705	32.3	7.46	98	88.3	744	353
0.5 A Bottom	874	23.1	142	66.7	1454	3.3	29.2	67.7	40.7	26.4	27	677	35.8	10.6	96	57	86.2	351
0.5 B Bottom	966	20.3	160	45.4	868	3.57	31	70.5	41.9	27.2	26.2	693	34.3	11.3	95.9	58.7	48.5	359
1.0 A Top	941	18.4	143	1942	349	4.98	28	72.6	38.2	24.4	28	590	36.3	7.71	87.2	59.1	393	332
1.0 B Top	947	22.3	151	2894	459	2.8	27.2	78.6	42.5	25.4	29	587	32.4	9.35	95.6	60.6	494	326
1.0 A Middle	982	51.2	259	97.2	1017	4.16	29.8	123	39.8	25.5	23.9	680	33.2	9.8	95.3	58.6	2323	360
1.0 B Middle	836	42	173	103	1203	2.88	28.5	92.9	38.1	25.3	23.1	621	33.3	10.4	93.5	78.8	630	335
1.0 A Bottom	953	19.2	151	50	462	69.6	31.8	71.4	42.1	27.5	26.9	717	35.9	11	101	60.2	53.6	377
1.0 B Bottom	855	38.5	177	44.5	1432	3.09	29.2	75.6	38.7	24.9	25	636	32.2	10.3	92.2	53.1	44.9	343
1.5 A Top	953	9.8	113	5209	255	3.38	28.1	92.9	48.5	25.4	30.2	619	34.6	13.2	143	110	1067	337
1.5 B Top	949	18.4	126	1054	318	2.96	28.7	69.9	57.6	26	22.3	505	29.7	8.65	90.9	49.3	241	343
1.5 A Middle	868	47.6	317	61.9	1028	3.3	27.7	107	36.7	23.4	23.5	623	30.4	9.19	90.6	58.4	698	336
1.5 B Middle	887	40.8	315	965	1727	3.38	28.2	89.8	37.1	23.8	23.5	648	30.7	10.5	95.3	72.8	458	338
1.5 A Bottom	877	34	137	45.9	1536	4.03	29.6	73.7	36.2	23.9	24.5	640	31	9.43	91.4	54.7	44.9	349
1.5 B Bottom	941	18.7	154	48.7	416	13.7	32	71.3	44.8	29.4	27.1	719	38.8	11	98.3	61.6	52.9	379

5. BACKFILL STABILITY ASSESSMENT

An assessment of backfill/ash wall stability was performed for different materials (also see section 2.3.5 and section 4). The aims of these studies were to:

- Investigate the different potential backfill and ash wall materials (e.g. ash, neutralisation residues, neutralisation residues with additives, mine spoil (crushed or otherwise), etc.). Investigate leaching, pressure leaching (to simulate hydrostatic head)
- Assess how the different backfill materials behave when pumped and placed in simulated mine environments.
- Determine desirable mixtures of backfill material, appropriate slurry densities.
- Assess backfill/ash wall stability for different materials.
- Determine effects of loading, sheer strength assessment, etc.
- Assess long-term chemical changes within backfill.
- Investigate the influence of acid or alkaline waters on the chemical stability of backfill (e.g. influence of AMD entering from another part of the mine).
- Assess the physical durability of the backfill materials.
- Assess weathering by flowing fluids, and strength changes with time

Several of the studies that were performed to address some of the aims listed herewith have been covered in sections 2.3.5 and 4.

The investigation presented in this section looks particularly at the application of FA or solid residues as suitable backfill materials for prevention of mine subsidence and underground fires, as well as to provide support to pillars and walls and to reduce the volume of open space underground. Moreover, application of suitable backfill would allow the greater extraction of coal. This would allow the extension of the life of coalmines whilst improving their safety by minimizing the deformation of the surrounding rock mass into the remaining space preventing subsidence and associated air blasts. In this section an overview of the literature on backfilling is firstly presented where after investigations into the appropriate admixtures for physical durability, loading and compressive strength assessment is further detailed.

5.1 INTRODUCTION

Mine backfill refers to waste materials such as waste rock, tailings and alluvial or aeolian sand placed into voids caused by underground mining (Benzaazoua *et al.*, 2002). Backfill is often regarded simply as a filler or waste product. While this may be true in many operations, where backfill is used for waste disposal or to fill stopes; other operations require backfill as part of an overall mining strategy (regional support, cut and fill, primary stope pillars, etc.).

Backfill has been used to prevent subsidence as far back as 1864 but it was not until after World War II that slurry fill, using mill tailings became a central part of mining operations (Archibald *et al.*, 1998).

Ordinary Portland cement, introduced as consolidation agent for mine backfilling in 1950's, became an industry standard by the 1970's and wall support was considered the primary role of backfill and secondly as a means of disposing of tailings. The high price of Portland cement meant an increase of more than 50% in the overall cost of mining

operations making it extremely uneconomical (Nieminen and Seppänan, 1983). This over-expenditure led to the development of alternative binders to replace Portland cement and environmental pressure has influenced backfill technology in terms of type of backfill material, backfill mechanical strength and reduced use of cement and water.

Backfill is becoming increasingly important because as environmental pressures increase more abandoned mines, which are producing acid mine drainage, must be remediated.

5.1.1 Basis for backfilling

There is a need for backfilling of mines to avoid subsidence, to provide support to pillars and walls and to reduce the volume of open space underground (Barret *et al.*, 1978). The placement of fill into open spaces prevents or minimizes the deformation of the surrounding rock mass into the remaining space, effectively increasing the strength and loading bearing capacity of the surrounding rock (Donovan, 1999). Greater mine stability prevents falls and associated air blasts, which greatly improves mine safety (Coates, 1981). Backfilling of mines does not completely eliminate the chance of subsidence but it has been observed that it reduces it by 33% as compared to the non-backfilled mines (National Academy of Sciences, 1975).

The prevention of subsidence is by far the most common purpose of backfilling but there are other, economical reasons such as the further recovery of minerals left as pillars in order to support the roof thereby increasing coal extraction and extending the life of the mine (Ilgner, 2002). Backfilling plays a role in mitigating the environmental concerns of underground fires and the future production of AMD as well as neutralizing existing AMD (USEPA, 1999).

The greatest economic gain for backfilling comes from the recovery of ore. The consequence of extending the life of a mine and fulfilling coal demands, translates into delaying large capital outlays required for opening new mines. Feasibility studies show that with backfilling almost 20% more extraction and 7 years longer life is possible for mines at large depths (>150m). Backfilling mines at shallower depths of 60m result in 10% greater coal extraction but only an extension of approximately 2 years in the life of the mine (Ilgner, 2002).

The important features of backfilling include material transportation and preparation, placement, maintenance, bulkheads and stope preparation. The properties of backfill material that require greatest consideration are compressive strength and permeability.

The compressive strength required, depends on the application. Cut and fill mining requires a 28 day compressive strength of 1MPa, while backfilling in order to facilitate pillar recovery requires a compressive strength of 5 – 7 MPa (Archibald *et al.*, 1998). The stability of the fill is related to the mechanical properties of the rock and the size of the stope. The purpose of backfill is not to transmit rock stress but to reduce the relaxation of the rock mass and insure it retains its carrying capacity (Grice, 1998).

5.1.2 Fill material

The choice of backfill is dependant on the physical, hydrological, chemical and mineralogical characteristics of the material. Long-term stability is especially important

in order to prevent subsidence. Impermeability is also important so that infiltration and conductance of groundwater does not occur to weaken the material and allow the leaching of contaminants (Jude, 1995).

Waste rock, mill tailings, quarried rock, sand and gravel are the commonly used fill material. Of these common types of fill, waste rock and mill tailings are easily accessible and economically viable for backfilling (Danovan, 1999). Twenty-five % of this material is generated from crushed stone, while mineral processing contributes the largest percentage (Arioglu and Biron, 1983).

Fill material is classified into three groups:

- The inert material is the largest part of the fill material. The inert fraction may consist of mill plant tailings, sand, gravel, waste rock.
- The binding agents are added to improve the mechanical properties of the fill material and can consist of Portland cement, ground slag or fly ash.
- Chemical additives refer to any flocculants, accelerants or retardants that are used to improve the flowability of the slurry and the consolidation of the fill.

Soil backfill material may result in non-uniform side support from structure and volume changes in the soil due to varying moisture levels, soil compaction, non-uniform soil density and surface settlement (Cho and Vipulanandan, 2002).

Ordinary Portland cement is the most common type of binder used in backfilling. About 6% by weight is added to hydraulic fill to generate cohesion between particles, while paste backfill requires 4.5 – 5% and cemented rock fill requires 2% cement as a source of fine material. These masses of cement addition ensure cohesion of between 250 to 500 kPa and compressive strengths of between 0.75 and 4 MPa (Grice, 1998).

Farzam *et al.* (1998) advocate the use of admixtures for mine backfill. An admixture is defined by ASTM (1997) as “a material other than water, aggregates, hydraulic cement, and fibre reinforcement, used as an ingredient of concrete or mortar, and added to the batch immediately before or during its mixing.” Admixtures are used to improve the qualities of strength, durability, transportability, pumpability and placeability. By using 3% less cement binder and a water-reducing admixture, Barker and Harter (1997) found that the compressive strength of a cemented rock fill doubled after 29 days, when compared to a mixture with 10% cement and no admixture. Accelerating admixtures can shorten set times while dispersing admixtures may reduce the amount of water needed for flow and may even reduce the amount of binder required and as a result, reduce the cost. Cho and Vipulanandan (2002) used a 5% cement binder and reported that using the superplasticizer Sulfonated Naphthalene-Formaldehyde (a combination of two common dispersants) in a backfill mixture of foundry sand and clay decreased the water demand and increased flowability and compressive strength. A dispersing agent adsorbs to particles, making them negatively charged and causing mutual repulsion. These dispersed particles hydrate more efficiently and tend to be stronger and more durable (Farzam *et al.*, 1998).

In some cases it is desirable to delay cement hydration and stiffening of the paste mixture. In a paste fill case study in Canada, Farzam *et al.* (1998) added a hydration control admixture to the paste material to facilitate the filling of a large cavern in a slow and self-levelling manner, from a single access point.

5.1.3 Backfill classification

There are 3 types of backfilling techniques currently used. They are: 1) slurry or hydraulic fill, 2) paste fill and 3) rock fill. Source of energy plays a key role in selecting a method of placement to put the backfill material underground (Arioglu and Biron, 1983). Apart from this, the choice of the system is site specific and often depends on the cost and necessary constituents at a particular site. In some cases environmental conditions may limit the range of options (Dorricott and Grice, 2002).

5.1.3.1 Slurry backfill

Slurry backfill, or hydraulically placed fill, usually consists of sand and/or deslimed tailings, which is formed into a slurry and transported through boreholes to underground cavities (Farzam *et al.*, 1998). The greatest advantage in using flowable fills as opposed to soil or rock fills is that there is no further need for compaction once the fill is in place (Cho and Vipulanandan, 2002). The composition of the slurry fill, about 75% mass is solid material (Grice, 1998), usually depends on what is cheapest and most readily available.

Hydraulic fill is usually gravity transported and emplaced underground through boreholes where after excess water drains away. Slurry backfill requires large amounts of water in order to facilitate transport and fines are not desirable as they reduce permeability and contribute to clogging (Archibald *et al.*, 1998b). It is estimated that most hydraulic fill can withstand traffic after 24 hours. The advantages to slurry backfill are its ease of transport and emplacement and the relatively low costs it incurs. The disadvantage of hydraulic backfill is the necessity for porous retaining walls to retain the slurry and allow for water drainage. Excess water must then be pumped out of the mine or erosion of the barricades may occur (Grice, 1998).

5.1.3.2 Paste fill

Paste backfill can be defined as a pumpable, non-Newtonian, high density material consisting of mine tailings, water and cement and will retain 100% of the water once placed. The non-Newtonian motion indicates that paste backfills must be pumped (Grice, 1998; Farzam *et al.*, 1998). Sand and gravel are added to paste fills to aid pumpability and to increase fill strength and stiffness (Yaschyshyn and Amaratunga, 1997).

For a material to be defined as a paste, it must contain greater than 15%, by weight, of particles finer than 20 µm. Higher percentages of fine material increase density and reduce permeability. Settling does not occur in paste fills. As a result of compaction, the fine particles act as lubrication for the core of coarser particles and reduce resistance in the pipeline (Archibald *et al.*, 1998b).

Paste backfill has gained popularity as a backfill material due to the low operating costs incurred with placement and high strength (Yilmaz *et al.*, 2003). Apart from this, the paste backfill has other advantages such as reduced pumping requirements and homogeneous mix consistency (Chugh and Dutta, 1998). Cemented paste fill as an underground backfill is a popular and widely used technique (Landriault, 1995; Hassani and Archibald, 1998; Kesimai *et al.*, 2002, Belem and Benzaazoua, 2003 and Benzaazoua, *et al*., 2004). The more dense paste backfills require less cement binder than

hydraulic fill. There is negligible water drainage, so pumping and permeable retaining walls are not required (Grice, 1998). Some studies believe paste backfill to be more economical in disposing of a greater amount of solid waste and more environmentally friendly by using less water; added to this are factors such as greater strength, durability and permeability (Farzam *et al.*, 1998; Archibald *et al.*, 1998b).

According to Yilmaz *et al.* (2003) paste fills may display long-term structural problems and affecting factors such as binder, solids, water and mixing rates in the filling mass must be carefully evaluated. The strength of paste fills can, however, be greatly enhanced with greater addition of fine tailings. An agglomerated tailing paste fill was developed by Yaschyshyn and Amaratunga (1997), which had superior compressive strength, stiffness and a modulus of elasticity triple that of total tailings paste fills of the same binder content and consistency. Benzaazoua *et al.* (2004) indicated that the strength development of the paste fill depends on the physical, chemical and mineralogical properties of the tailings, water chemistry, amount of water, binder type and proportion.

One of the main disadvantages of paste backfills is the higher cost incurred with cement addition, installation of dewatering systems and pipeline supervision to make sure that line plugging does not occur (Grice, 1998). The CaO content of fly ash results in it being a self-hardening and pozzolanic material. These properties may decrease the amount of cement needed, and thereby the cost, if fly ash were to be used as backfill.

5.1.3.3 Rock fill

Waste rock fill consists of unconsolidated material supporting the stope of a typical particle size of around 40 mm (Grice, 1998). Cement is sometimes added to this waste rock and dumped into stopes with sealed accesses (Farzam *et al.*, 1998). Rock fill requires less cement, has a high rate of filling and increases the strength of the stope. Generally this type of fill is prone to segregation because of poor size grading and high voids ratio (Dorricott and Grice, 2002).

5.1.4 Fly ash as backfill

5.1.4.1 Soil Stabilisation

Fly ash may substitute for cement as a binder for soils, aggregates or waste materials. Some fly ashes, which contain large quantities of lime may be defined as self-cementing and may be used as the sole binder in order to stabilise weak soil or gravel. The standards for fly ash bound materials (FABM) in Europe define the quantities of cement, lime and gypsum with fly ash to stabilise soils, sand, and different granular materials.

Fly ash mixed with cement provides sulphate resistance and allows the strength, setting time, flow characteristics, density viscosity and thixotropy to be varied according to the amount of cement added. In Pori, Finland 720 m of the northern highway was built with 5kt of fly ash stabilised with cement. Using fly ash instead of a natural aggregate more than doubled the bearing strength of the road (Smith, 2005).

5.1.4.2 Mine Backfill

Because cement addition as a binder in backfill material to improve cohesion can contribute up to half of the costs of mine backfilling there has been research into using other materials. Palarski (1993) studied the use of fly ash as backfill for coal mines. Fly ash has pozzolanic properties and has been investigated to determine its suitability as a cement replacement (Grice, 1998). Jorgenson and Crooke (2001) found that the permeability of fly ash paste backfill is lower than that of soils or mine spoils and unlikely to leach harmful elements in any great quantity. This study resulted in fly ash being reclassified from special waste to inert waste. Siriwardane *et al*. (2003) reported that backfilling by fly ash reduces subsidence and production of acid main drainage.

There was a substantial recovery of additional coal reserves due to under ground ash filling in South Africa. However, these recoveries came to a halt because of operational constraints, complete extraction of reserves, huge quantities of drainage water and closure of nearby power stations. The benefits of underground ash filling have been re-evaluated due to increasing occurrence of surface subsidence and the limited remaining life of some coal mines (Ilgner, 2000).

In South Africa, Koornfontein is the first colliery where underground placement of ash was attempted to stabilize pillars remaining after mining. But this attempt was in vain as the area that was ash filled collapsed in late 1961. Hydraulic ash filling started in 1963. An average of 66 % of the mining height was filled and no further collapses were observed (Ilgner, 2000). The mine closed its operations in 1970. There was another underground, Lng-term disposal of fly ash attempted in 1973 at Springfield colliery. About 3000 tons of ash were hydraulically placed per day, eventually resulting in the extraction of an additional 5 million tons of coal reserve.

Ilgner (2000) tested the different qualities of coal as pillars confined by cemented and un-cemented fly ash and concluded that backfilling by fly ash can provide sufficient lateral confinement to coal pillars. He noticed a substantial residual strength, which was as a result of the strain hardening of the ash fill after pillar collapse. He also reported reduced surface subsidence, prevention of spontaneous combustion and the neutralisation of acid mine drainage water.

Ilgner (2002) reported that the beneficial uses of ash filling may vary from site to site. For instance, for deeper levels ash fill can be used to extend the life of the mine by increasing the amount of coal extracted. In shallower cases, the benefits of prevention of surface subsidence and remediation of AMD are significant when compared to extension of mine life.

Backfilling by fly ash can provide a safe and eco-friendly alternative to power stations to dispose of ash. Since ash disposal by power stations on the surface has been strongly criticized and with increasing pressure on them to protect the environment in terms of reducing ground water pollution, dust problems and land occupation, backfilling of mines with fly ash could provide an agreeable alternative solution.

5.1.5 Slurry pumping

Hydraulic backfill slurries are transported by gravity through boreholes and pipelines while paste fills are delivered via pipelines with either low pressure (<1MPa), turbulent flow systems or high pressure (>5MPa), laminar flow systems for deslimed slurries (Grice, 1998).

Slurry density is an important property, which influences the transport of a slurry. The slurry density, which is a function of particle specific gravity and is controlled by $\%_{Cv}$ (solids by volume), is calculated to balance ease of transport and lack of plugging against excessive water (Grice, 1998).

Cooke and Lazarms (1993) worked on hydraulic transport systems for the backfilling of deep mines and concluded that the operation of backfill systems at relatively higher densities improves the performance of backfill distribution systems. Ilgner (2003) stated that especially in hydraulic fills the slurry relative density must be optimised in order to reduce the water losses through the geotextile and to avoid excessive pipeline pressure losses. He observed a decrease in the amount of drainage water with increasing slurry relative density and an increase in pipeline pressure losses with increasing fill density.

As a result of the higher viscosity of paste fill the outer portions of the material shear along the sidewall of the pipe while the centre travels as a plug. The pressure needed to pump this material exceeds 5MPa (Grice, 1998). As a result of the high cost of high-pressure pump and pipeline systems and the large distances between power stations and mines it is more feasible to transport fly ash to the mine and create the paste prior to backfilling (Ilgner, 2002). Future studies hope to prove the feasibility of using acid mine water to create the paste, thus neutralising the water and disposing of the residues and neutralised water in the process.

5.1.6 Environmental impacts

Doricott and Grice (2002) found that backfilling results in the reduction of surface disturbance and increased subsequent rehabilitation. This, together with the resultant reduction in acid water generation underground, reduces the overall, negative, environmental impact of the operation.

Data from leaching tests (TCLP method – DWAF, 1998) conducted by the USEPA (1999) indicate that most backfill materials leach high quantities of many metals at health advisory levels. A mine where backfilling is occurring may already contain water that exceeds health advisory limits of heavy metals and thus backfilling aims to improve water quality by limiting the oxygen ingress and neutralising AMD. Some studies show an increase in the concentration of specific elements in mine water while other elements show a decrease. The possibility that mine backfill will leach harmful metals in high quantities is completely dependant on the mineralogy, hydrogeology, backfill characteristics and practices onsite (USEPA, 1999).

Siriwardane *et al*. (2003) demonstrated the successful use of waste by-products in solving potential subsidence and acid mine drainage problems caused by abandoned coal mines. Levens *et al.* (1996) base the efficacy of backfill (i.e. its ability to hamper oxidation of sulphide minerals and prevent the formation of secondary Fe^{3+}) on its permeability.

Water flow through dry backfill will occur through shrinkage cracks and gaps between fill and rock surface. Residual saturation is defined as the water contained in pores smaller than the majority of pores. This water does not contribute to flow and the more pores that remain saturated; the fewer surfaces exist to contribute to mineral oxidation.

Cemented backfill contributes positively to reducing acid mine drainage by:

- Reducing mineral dissolution as a consequence of enhanced buffering capacity.
- Reducing sulphide oxidation due to greater water retention.
- Reducing the movement of metals as a result of low hydraulic conductivity (Levens *et al.*, 1996).

Smith and Rauch (1987) found that using AMD lime treatment sludge as backfill could decrease Fe and Mn concentrations if mine water had a high pH. Sludge backfill into acid mine drainage resulted in dissolution of the sludge and higher concentrations of Fe. Trace metal concentrations did not appear to change but SO_4^{2-} increased. When sludge is mixed with fly ash, acid water will be neutralised and metal concentrations will decrease.

5.2 METHOD

In this investigation, laboratory tests were undertaken to determine how the different backfill materials may behave when pumped and placed in mine environments. Tests were aimed at determining desirable mixtures of backfill material, and appropriate slurry densities. As a result of difficulty obtaining laboratory use and consultants time, only slurry flow and compression density parameters were evaluated during this study. Further aspects of this study should be carried forward to the continuation project scheduled to start in April 2005.

5.2.1 Preparation of the solid residues from the neutralisation of AMD with FA

The solid residues from the neutralisation of AMD with FA were prepared by reacting Navigation AMD and Matla fly ash in a 1:3 ratio (FA:AMD) using an overhead stirrer at a speed of 450 rpm. The solid residues for batch one were prepared by using Matla FA from unit 5 and those for batch two and three by using Matla FA from unit 3. On attaining a pH of 9.0 (for batches one and two) and 11.0 (for batch three) the reaction mixture was filtered and the wet solid residues were pressed at 150 kPa. The pressure was increased gradually to drive out most of the water until bubbling was observed. A sample was preserved for moisture content determination. The remaining solid residues were kept in a tightly locked plastic container.

5.2.2 Moisture content determination

The moisture content was determined, to obtain the dry weight of the solid residues, by drying the wet solids at 105^0 C for 12 hours. The moisture content was in turn used for the calculation of the amount of the binder (ordinary Portland cement) needed for each blending rate. The moisture content of the pressed cake of the solid residues varied from 27.3 % for batch one to 30.8% for batch two.

5.2.3 Marsh cone test

To estimate the amount of water that will be needed to make the slurry suitable for pumping, a marsh cone test was performed upon the solid residues. This was done by adding tap water to a neutralisation slurry containing 3% binder (ordinary Portland cement) until the time for 1 L to run out had dropped to less than 10 seconds. The resulting value was taken as the required water content for make-up of pumpable slurry. Solid residues from batch one and two were submitted to marsh cone test.

5.2.4 Particle size determination

Particle size analysis was done by FRITSCA analysette sieves for particle sizes greater than 38 μm. For particles smaller than 10 μm, a laser particle sizer FRITSCH ANALYSETTE 22 was used.

5.2.5 Preparation of the cylinders and curing

The wet solid residues were blended with a pozzolanic binder (Castle cement) at rates of 1%, 3% and 6% dry weight basis. Several batches of cylinders were prepared, by using ordinary tap water for batch one and by using the process water obtained from the treatment of acid mine drainage with fly ash at a ratio of 1:3 (FA:AMD) for batches two and three. The wet solids were slurried with the required amount of water as determined from the marsh cone test. Then the slurries were poured into the cylindrical tubes and placed in plastic bags, a bottle of water being placed next to them to maintain the required level of humidity for the curing process (Figure 5.1). All samples were duplicated.

Figure 5.1: Solid residues with binder cured in plastic cylinders for strength development testing at Miningtek laboratory.

5.3 RESULTS

5.3.1 Slurry pumping tests

Flow tests were performed using the marsh cone test. The material from the reaction between Matla fly ash and Navigation AMD had a solids fraction of about 0.7: It was necessary to add water in order to achieve reasonable flow rates in separated solid residues. Ordinary tap water was used for batch one and the process water obtained from the treatment of acid mine drainage with fly ash at a ratio of 1:3 (FA:AMD) was used for batches two and three.

Table 5.1 gives parameters of the flow test using the marsh cone for batch one solid residues. For batch one, the addition of 600 g of tap water allowed the slurry to flow through the cone in 9.8 s.

Table 5.1: Physical parameters of slurry flow out for batch one solid residues.

Water mass (g)	Total water mass (g)	Solids (g)	Relative density	Run out time (s)	Flow rate (Tot g/s)	Water to solid ratio	Flowed water (L)	Flowed solid volume (L)
382.2	382.2	733	1.658	-	-	0.521	0.443	0.557
136.6	518.8	669	1.568	-	-	0.776	0.519	0.481
38.7	557.5	653	1.547	20.0	60.53	0.854	0.537	0.463
18.8	576.3	645	1.537	13.5	90.47	0.894	0.545	0.455
28.9	605.2	634	1.523	9.84	125.93	0.954	0.557	0.443

Table 5.2 gives parameters of the flow test for batch two solid residues. For batch two, a run out time of 10.0 sec was obtained after adding an amount of process water (1300 g) twice as much as that required for batch one. The amount of water required thus differed substantially from batch to batch. This is possibly due to a particle size difference in the FA samples used.

Table 5.2: Physical parameters of slurry flow out for batch two solid residues.

Water mass (g)	Total water mass (g)	Solids (g)	Relative density	Run out time (s)	Flow rate (Tot g/s)	Water to solid ratio	Flowed water (L)	Flowed solid volume (L)
801	801.0	698	1.608	-	-	1.15	0.485	0.515
269	1070.0	634	1.523	-	-	1.69	0.557	0.443
169	1239.4	599	1.481	14.3	128.56	2.07	0.593	0.407
21.1	1260.5	595	1.476	11.7	158.59	2.12	0.597	0.403
21.3	1281.8	591	1.471	10.5	178.36	2.17	0.601	0.399
16.2	1298.0	588	1.467	10.0	188.60	2.21	0.604	0.396

By using fly ash from unit 3 of Matla power station (batch two) instead of fly ash from unit 5 (batch one), the flowability of the solid residues is negatively affected. It is not presently known which field these samples were derived from. The particle size of FA from different units and different fields is different and the effect of particle size should be further investigated. This difference may also have been caused by the use of process water in batch two and three. No test was performed using solid residues made with Matla ash from unit 5 and process water. Hence this variable could have contributed to the differences observed.

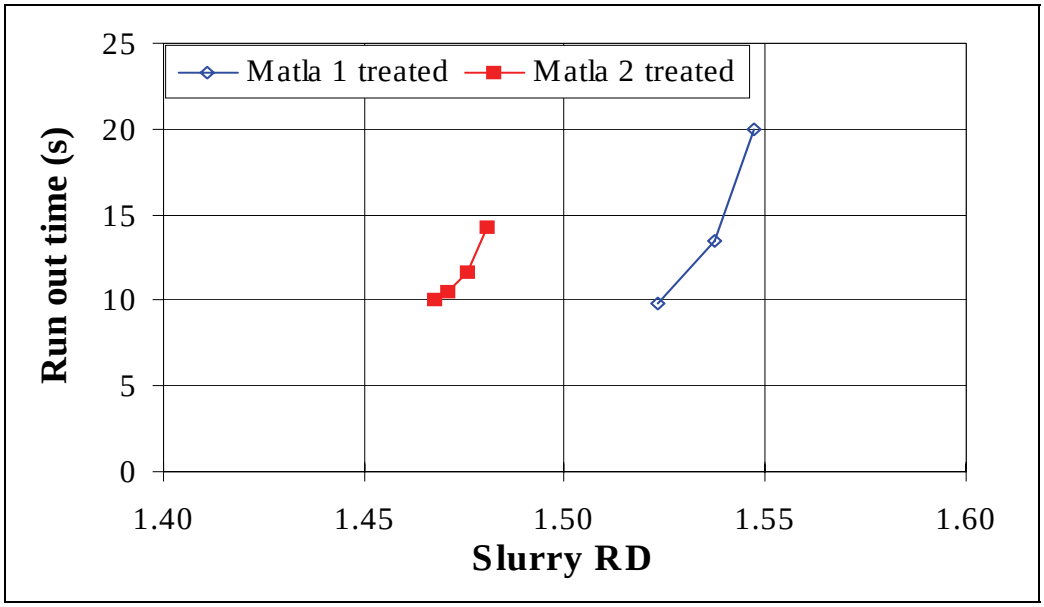

Figure 5.2: Marsh cone run out times as a function of slurry density for batch one and batch two solid residues (RD =relative density).

The run out time of slurries was found to be increasing with an increase in relative density (RD) (Figure 5.2). Accordingly, an increase in RD was responsible for a decrease in flow rate of the slurry (Figure 5.3). This is a consequence of the successive additions of water during the marsh cone test process.

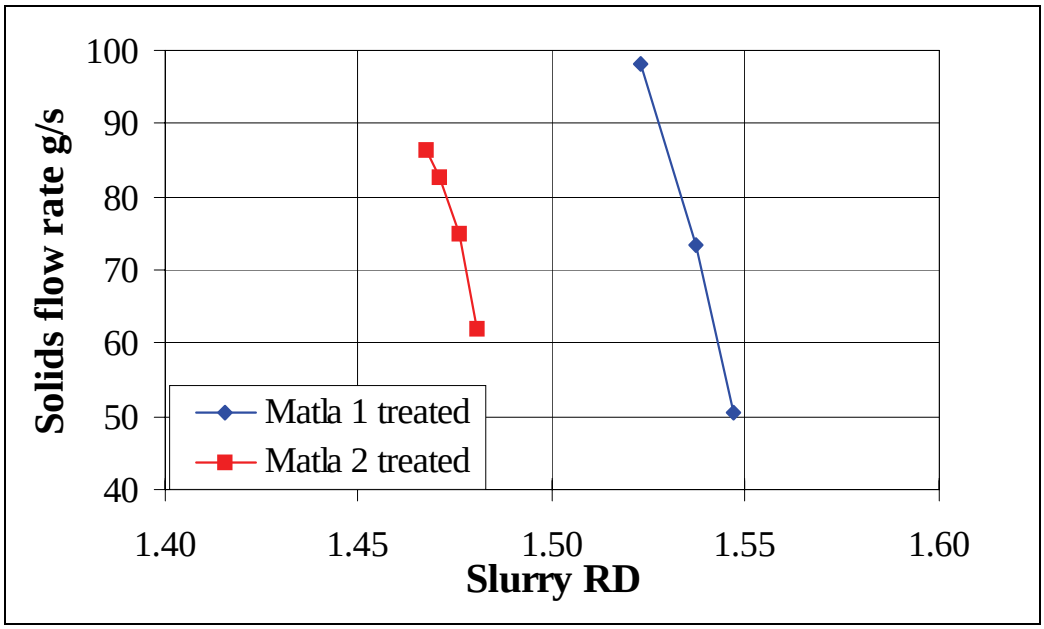

Figure 5.3: Marsh cone solids flow rates as a function of slurry density for batch one and batch two solid residues. (RD =relative density)

These results show the possible influence of the fly ash properties such as particle size on the flowability of the solid residues. Moreover, the need to add water for ensuring correct relative density for run out and solids flow rate in the Marsh cone tests indicates that solid residues need not be completely dewatered prior to their work-up into slurries for use as backfill materials, which will reduce operational costs of backfilling. The process water was also found to be a suitable replacement for ordinary tap water, indicating the

possibility to utilize the process water recovered after the neutralisation process to make up slurries for pumping to backfill. When implementing the neutralisation process at large scale, it will be necessary to adjust the operating parameters of the future treatment plant according to the origin and corresponding properties of the fly ash used.

5.3.2 Comparison of different backfill materials

5.3.2.1 Strength development testing

The water/solid ratios of the solid residue slurries and cured samples from the three different batches are presented in Table 5.3.

Table 5.3: Water/solid ratios of residual slurries and cured samples for batch one.

Batch number	Binder ratio (%)	Water/solid ratio in slurry	Water/solid ratio in cured sample
	1	0.589	0.533
1	3	0.577	0.510
	6	0.559	0.499
	1	0.714	0.538
2	3	0.700	0.612
	6	0.678	0.533
	1	0.860	0.600
3	3	0.850	0.555
	6	0.823	0.625

The initial water/solid fractions in the solid residue material were 0.727, 0.692 and 0.700 for batch one, two and three respectively.

Strength development testing was reported as unconfined compressive strength (UCS) and elastic modulus (EM). Detailed results of the strength testing for the three different batches are given in Tables 5.4, 5.5 and 5.6.

Table 5.4: Strength development results for batch one.

Binder ratio (%)	Curing time (days)	UCS (MPa)	EM (MPa)	Mean UCS (MPa)	Mean EM (MPa)
1	29	0.169	64.8	0.1715	66.15
		0.174	67.5		
	91	0.316	97.8	0.3065	85.25
		0.297	72.7		
	187	0.344	54.6	0.3425	73.80
		0.341	93.0		
3	29	0.49	236.4	0.495	229.5
		0.5	222.5		
	91	0.912	294.0	0.851	292.5
		0.79	290.9		
	187	1.087	436.3	1.104	417.2
		1.121	398.1		
6	29	1.297	428.1	1.258	471.9
	29	1.219	515.7		
	91	1.579	497.6	1.642	513.9
	91	1.705	530.1		
	187	2.161	709.1	2.068	748.5
	187	1.975	787.9		

Table 5.5: Strength development results for batch two.

Binder ratio (%)	Curing time (days)	UCS (MPa)	EM (MPa)	Mean UCS (MPa)	Mean EM (MPa)
1	7	0.008 0.011	- 2.754	0.010	2.754
	28	0.459 0.474	171.9 257.8	0.467	214.9
	89	0.918 0.945	315.1 360.2	0.932	337.7
	185	1.013 1.165	252.1 417.1	1.089	334.6
	349	1.216 1.3 1.182	423.3 556 497.5	1.233	492.3
3	7	0.018 0.011	6.444 4.364	0.0145	5.404
	28	0.777 0.655	302.5 283.6	0.716	293.1
	89	1.317 1.216	337.7 337.7	1.267	337.7
	185	1.367 1.351	423.3 493.3	1.359	458.3
	349	1.486 1.519 1.367	603.5 515.6 556	1.457	558.4
6	7	0.061 0.034	27.01 9.454	0.0475	18.23
	28	1.654 1.553	457.5 489	1.604	473.3
	89	1.975 2.431	511 645	2.203	578.0
	185	2.465 2.414	520.4 597.1	2.440	558.8
	349	3.208 3.005 2.87	859.6 1233.2 1492.8	3.028	1195.2

Table 5.6: Strength development results for batch three.

Binder ratio (%)	Curing time (days)	UCS (MPa)	EM (MPa)	Mean UCS (MPa)	Mean EM (MPa)
1.82	21	0.108	42.65	0.111	40.1
		0.113	37.57		
	28	0.166	70.00	0.158	80.0
		0.149	90.00		
	88	0.392	113.5	0.384	127.7
		0.377	141.8		
	179	0.473	214.1	0.490	230.4
		0.506	246.6		
	342	0.574	180.7	0.603	221.8
		0.635	242.4		
		0.601	242.4		
3	21	0.275	122.0	0.274	118.9
		0.272	115.8		
	28	0.358	186.0	0.351	156.8
		0.343	127.5		
	88	0.797	328.8	0.763	290.5
		0.729	252.1		
	179	0.959	378.2	0.929	416.0
		0.898	453.8		
	342	1.114	497.6	1.097	436.9
		1.114	429.7		
		1.064	383.3		
6	21	0.782	297.3	0.763	290.2
		0.743	283.1		
	28	0.963	383.6	0.949	396.9
		0.934	410.1		
	88	1.681	530.9	1.730	515.3
		1.778	499.7		
	179	1.876	577.3	1.850	615.4
		1.823	653.4		
	342	2.212	849.4	2.123	835.4
		1.964	782.3		
		2.194	874.4		

Strength development in the three different batches was found to be proportional to the proportion of binder used (Figures 5.4, 5.5 and 5.6). A more rapid strength development is observed in the first 28 days of curing for the solid residues formulated with process waters (batch two) than the solid residues formulated with tap water (batch one). This early accelerated strength development could be due to the formation of gypsum on hydration of the cement binder, with the process waters acting as a source of sulphates. Overall the solid residues formulated using the process waters had greater unconfined compressive strength at all levels than the solid residues formulated using tap water.

These results once more emphasize the opportunity to use the process water slurry containing solid residues that have not been dewatered after the neutralisation process. By dewatering only until the correct relative density is achieved it would thus be possible

to pump these materials to the backfill site directly, without costly settling and dewatering.

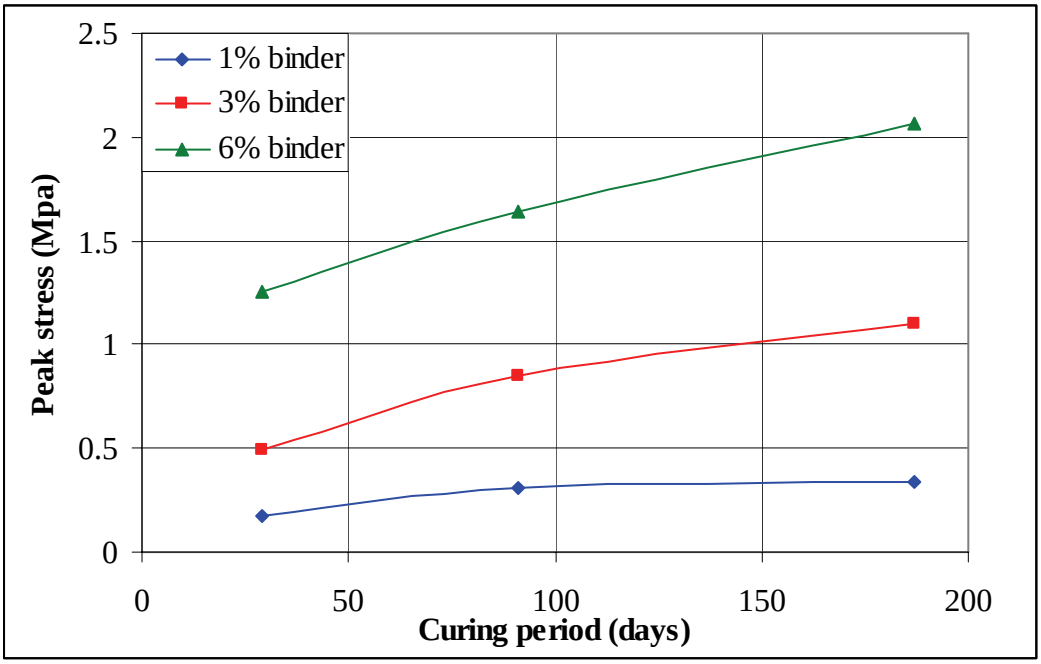

Figure 5.4: Unconfined compressive strength of batch one solid residues.

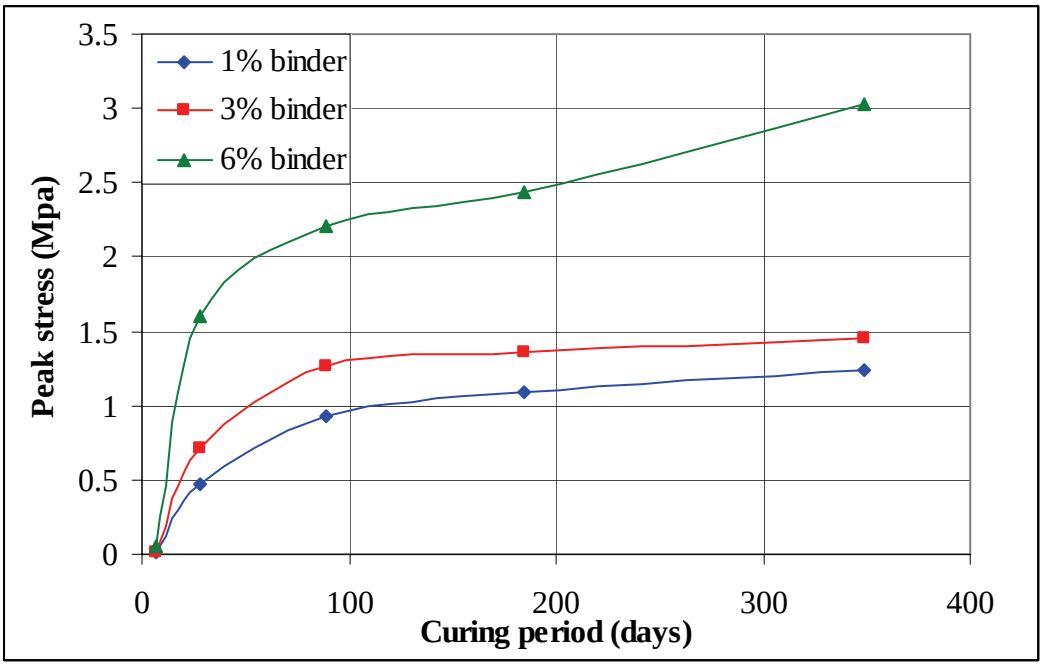

Figure 5.5: Unconfined compressive strength of batch two solid residues.

Moreover similar trends were observed in these studies compared to values obtained from the literature (Grice, 1998) that indicated addition of a binder increased compressive strength, to between 0.75-4 MPa, and values obtained in this study were within this range.

The unconfined compressive strength (UCS) and elastic modulus (EM) are essential for the rock mechanics to model the force interaction and lateral load bearing of cemented

strength. Both compressive strength and elastic modulus were still increasing after one year under the experimental conditions of storage. The best result was achieved by batch two, as the UCS reached 1.23 MPa (with 1% binder mix) to 3.03 MPa (with 6 % binder) after one year. These results tend to further validate the possibility of using solid residues for backfilling.

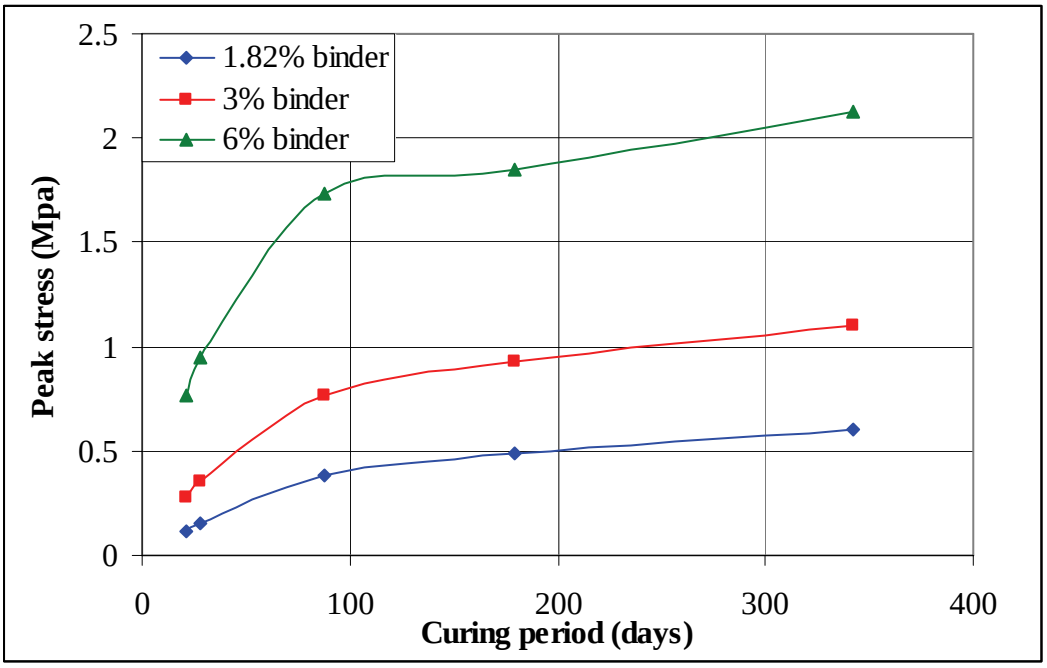

Figure 5.6: Unconfined compressive strength of batch three solid residues.

5.3.2.2 Particle size analysis

Figure 5.7 shows the particle size distribution for unreacted Matla fly ash and AMD reacted fly ash (i.e. solid residues made from the reaction between Matla fly ash and Navigation AMD). After reaction with AMD, there was a slight increase in the percentage of particle size in the range of 1 to 20 µm. This is probably a consequence of the precipitates being formed upon the ash particles during the neutralisation reaction. The other size fractions (< 1 µm and > 20 µm) were not modified by the reaction with AMD. The overall pattern of size distribution is not affected when fly ash is reacted with AMD. Matla fly ash appears to be very fine, all its particles are smaller than 40 µm in size. The particle size analysis did not differentiate between the unit 3 and unit 5 Matla ash.

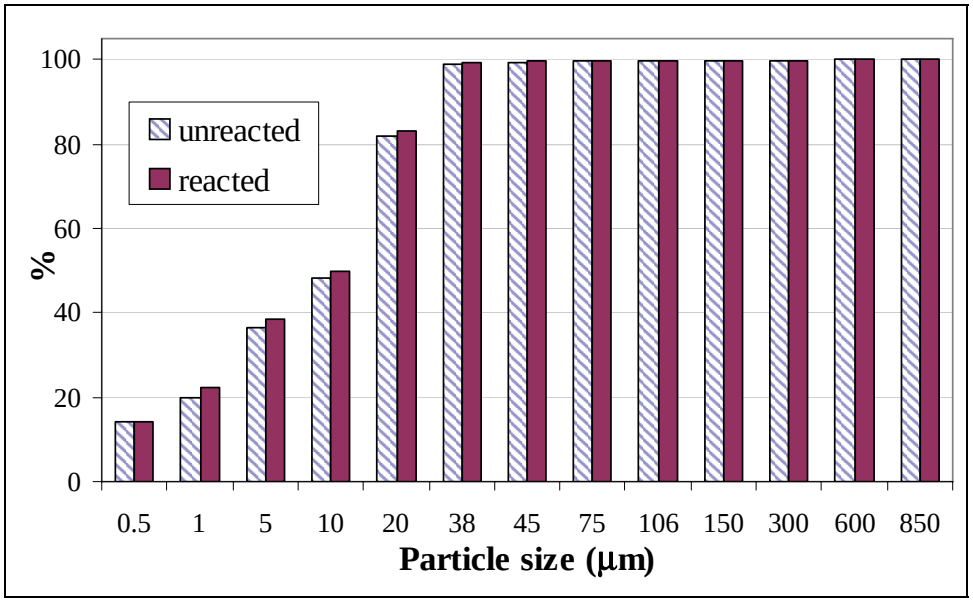

Figure 5.7: Particle size distribution for unreacted and AMD reacted Matla fly ash

5.4 CONCLUSIONS

In conclusion, with the addition of cement as a binder, the strength of the solid residues material is relatively high and it appears suitable for the purpose of confinement of mined-out areas. The stability of the solid residues is demonstrated through its capacity to develop strength over time. Similar results were obtained in a previous study made on unreacted fly ash (Ilgner, 2000).

These results tend to confirm that even after being submitted to the neutralisation reaction with AMD, fly ash remains a suitable material for backfilling. Hence, the proposed use of fly ash to first ameliorate AMD by use as a substitute liming treatment, and then use the recovered solid residues for backfill material is herewith shown to be feasible.

6. ZEOLITE SYNTHESIS: PROCESS PARAMETER ASSESSMENT

This section reports the results of an investigation into zeolite manufacture using the solid residue resulting from the neutralisation of acid mine drainage (AMD) with fly ash (FA) as feedstock. The study incorporated preliminary testing of resultant zeolite phases in simulated wastewater studies for their application as adsorbents in toxic element removal from process waters.

6.1 INTRODUCTION

Zeolites are inorganic compounds with a crystalline oxide framework made of silicon, aluminium and oxygen. The primary building unit of zeolites is a tetrahedron of (TO_4), of four oxygen ions surrounding a central ion of which the central ion (T) ion can either be tertrahedral silica (Si^{4+}) or trivalent alumina (Al^{3+}). Adjacent tetrahedrons are linked at their corners through a common oxygen ion (Figure 2.5), resulting in an inorganic molecule with a structurally distinct three-dimensional framework. This arrangement reduces the oxygen/silicon ratio to 2:1 and in zeolite structures, some of the quadrivalent silica (Si^{4+}) is replaced by trivalent alumina (Al^{3+}), resulting in a deficiency of positive charge in the aluminosilicate framework, which means that a negative surplus charge resides at each tetrahedron in the framework, having aluminum in its center and this is illustrated in Figure 8.1.

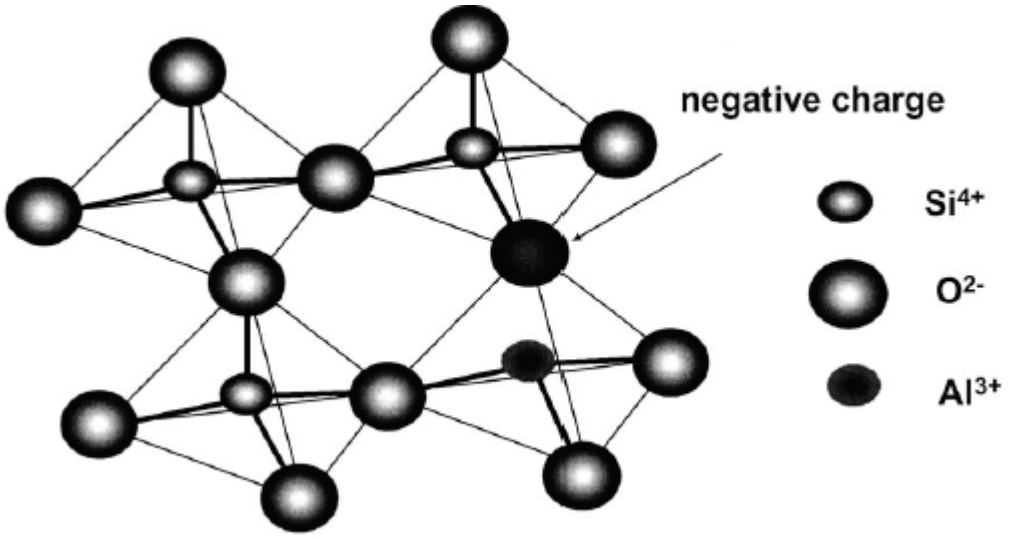

Figure 6.1: Structure of an ideal zeolite framework of tetrahedral $[SiO_4]^{4-}$ with a Si/Al substitution ($[AlO_4]^{5-}$) yielding a negative surplus charge (Alvarez-Ayuso *et al.*, 2003).

The excess of negative charge necessitates the inclusion of charge compensating cations to stabilize the structure. These charge-compensating cations are not covalently bound to the zeolite structure and do not form part of the lattice framework, but have considerable freedom of movement and can readily be substituted with other cations.

The framework structure may contain linked cages, cavities or channels, which are of the right size to allow small molecules to enter. The limiting pore sizes are generally between 3 and 10 Å in diameter. Due to their porosity nearly 50% of the material consists of void volume. As a result of their porous properties and cation exchange capacity zeolites have

important industrial applications in catalysis, as replacements for phosphates in detergents and for the removal of ions and molecules from wastewaters, radioactive wastes and gases (Singh and Kolay, 2002). As cation exchangers they can trap heavy metals.

The production of zeolites from fly ash was explored when the need arose for inexpensive synthetic zeolites with good adsorption properties. Fly ash is a low cost and readily available Si rich raw material for such products. Holler and Wirsching initiated experimenting with the synthesis of zeolites from fly ash in 1985. Testing the potential of zeolite crystallization from fly ash was prompted by the similar chemical composition of fly ash and some volcanic rocks, precursor of natural zeolites, (interaction of volcanic ash with hydrothermal solutions or groundwater transforms it into natural zeolites (Querol *et al.*, 2001; 2002).

Due to the high content of reactive phases such as aluminosilicate glass, and to the high specific surface area of fly ash, these combustion wastes are suitable starting materials for the synthesis of zeolites (Querol *et al.*, 2002). The major components of fly ash are silicon dioxide (SiO_2) and aluminium trioxide (Al_2O_3), which are the essential reagents in the synthesis of zeolites.

All the methods developed for the synthesis of zeolites from fly ash are based on the dissolution of Al-Si-bearing fly ash phases with alkaline solutions (predominantly NaOH or KOH solutions) and the subsequent precipitation of zeolitic material (Querol *et al.*, 2002; Moreno *et al.*, 2001). Zeolite formation proceeds in various stages, during which the Al- and Si- bearing phases of the fly ash are sequentially dissolved. The aluminosilicate glass phase is activated first, followed by the quartz phase and lastly digestion of the mullite phase. Two fly ashes therefore, with similar SiO_2/AlO_3 bulk ratios, but different quartz-mullite/glass, proportions, under the same activation conditions, will consequently produce different zeolites. The SiO_2/Al_2O_3 ratio of the glass matrix exerts a major influence on the type of zeolite produced.

In the previous WRC report 1242 (Petrik *et al*, 2003), some methods were investigated to synthesise a low cost adsorbent using the fly ash from Arnot. The fly ash provides a source of silicate and aluminium needed for the synthesis of zeolites. High and middle temperature syntheses were tested and some variables were explored.

6.1.1 Description of mild temperature treatments investigated

Several lower temperature methods were also tested. The first one is the reflux method, which was adapted from Unine (1998). Solid residues were obtained from the reaction between Arnot FA and Navigation AMD. A mass of 40 g of solid residues, collected at circumneutral pH was mixed with 500 mL of 2M NaOH solution in a 1 litre reaction vessel. The mixture was heated under reflux at 90°C for 4 days. The slurry was filtered and washed 5 times with de-ionised water and dried for 24 hours at 60°C.

After characterisation by XRD of the synthesised product, Zeolite P was identified with quartz overlapping. The presence of quartz after the treatment was the result of incomplete hydrothermal treatment.

In the second hydrothermal treatment method at 100°C, 24.02 g of NaOH pellets were reacted with 19.98 g of solid residues. The reactants were ground together and the mixture was then heated at 100°C for 24 hours. After heating the mixture was mixed with 264 mL of water and left at room temperature for 12 hours to age. Thereafter the mixture was again heated at 100°C for a further 24 hours. The product was recovered by filtration and washed with de-ionised water until the pH of the filtrate was between 10 and 11. The product was dried overnight. The zeolite phase obtained by this treatment was sodalite.

The third method termed the one-step method was adapted from Hollman (1997) in which fly ash was used. 50g of solid residues (Arnot Fly ash and Navigation AMD) was reacted with 200 mL of 2M NaOH solution and was put in a sealed bottle and heated in an oven at 100°C for 96 hours. The product was then filtered and dried at 100°C for 24 hours. The same results as for the reflux method were obtained: formation of zeolite P with quartz remaining.

In this section the zeolite material that will be described was synthesised according to the high temperature treatment where fusion is performed at 600°C. This material was used to treat simulated waste water. The investigation also included the efficiency of such zeolites obtained through hydrothermal synthesis to adsorb residual toxic elements remaining in the secondary process waters recovered after neutralisation of AMD with FA. The efficiency of contaminant removal was compared to a commercial adsorbent, commercial faujasite CBV 400 and to commercial resin, Lewatit TP 207.

6.2 METHOD

This method of synthesis was adapted from the one described by Rayalu *et al.* (2000) in which fly ash is treated with a powder of NaOH and brought to fusion at 600ºC.

The solid residues were fused with NaOH in a ratio 1:1.2 at 600 ºC for 1 – 2 hours. The fused product was then mixed thoroughly with various amounts of distilled water and the slurry was subjected to ageing for 8 hours. After ageing the slurry was subjected to crystallisation at 100 ºC for 24 hours. The solid product was recovered by filtration and washed thoroughly with deionised water until the filtrate reached a pH between 10 and 11. The product was then dried at a temperature of 70 ºC. Different zeolite phases were synthesised according to the variation of some parameters (different starting materials, different amounts of water.). The zeolite phases obtained were sodalite and faujasite of varying purity.

6.3 RESULTS

6.3.1 Characterisation of solids

The solid residues used for synthesis was recovered from the neutralisation reaction between Arnot fly ash and Navigation acid mine drainage. The ratio of the neutralisation reaction was 1:3.5 FA:AMD and the reaction time was five hours. The residual solids were collected at circumneutral pH. XRF analysis was performed to evaluate the ratio between Si and Al present in the solid. The optimum Si:Al ratio to synthesise faujasite zeolite is around 2.

From the XRF results (Table 6.1) of the solid residues the ratio of Si:Al of 1.8 is acceptable to synthesise faujasite.

Table 6.1: Percentage of the major oxides present in the solid residues used as starting material.

Oxide	Mass % of residual solid	Oxide	Mass % of residual solid
SiO_2	48.7	K_2O	0.47
TiO_2	0.62	P_2O_5	0.32
Al_2O_3	23.3	SO_3	3.22
Fe_2O_3	7.53	Cr_2O_3	0.02
MnO	0.11	NiO	0.01
MgO	1.77	H_2O-	1.41
CaO	5.49	LOI	6.50
Na_2O	0.24	Total	99.7

The fusion method at 600°C was used to synthesize the adsorbent using the solid residues as feedstock. The synthesized product recovered was then characterised with x-ray diffraction (XRD). Figure 8.2 shows the XRD spectrum of the synthesised product called ArNavZ3 compared to commercial zeolite CBV400. The pattern of the synthesized adsorbent is similar to the commercial faujasite CBV 400 and to simulated faujasite spectra using X'pert graphics and Identity data collection software. These results indicate that the solid residue feedstock was successfully transformed into relatively pure and crystalline zeolite faujasite under the hydrothermal synthesis conditions applied, with a small percentage of the feedstock mineral phases (quartz and mullite) still remaining in the product..

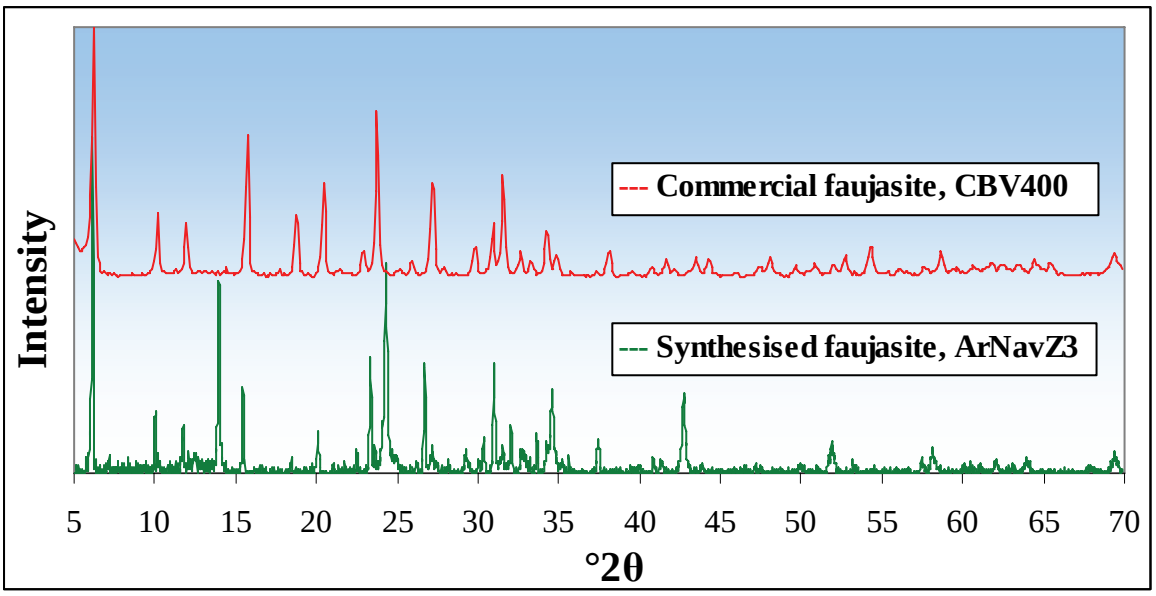

Figure 6.2: XRD pattern of synthesised faujasite, ArNavZ3 with commercial faujasite CBV400 for comparison

6.3.2 Removal performance of zeolite compared to other ion exchange material with simulated waste water

The efficiency of metal removal was tested on simulated waste water containing Mn, Co and Pb. The adsorption capacity over time of the synthetic faujasite, ArNavZ3, a commercial faujasite, CBV400, and a commercial ion exchange resin, Lewatit TP207 were compared. CBV 400 is a commercial faujasite zeolite with a Si:Al ratio of 5, a unit cell size of 24.5 Å and a surface area of adsorbent 780 m²/g. Lewatit TP 207 is an acidic organic ion exchange resin. This resin is specifically used to remove the ions of toxic, heavy metals in waste water (as was recommended by ESKOM). The experiments were set up as follows: 100 mL of simulated water containing the specified toxic element was reacted with 5g of adsorbent. Samples of water were collected at different time intervals between 60 and 1440 min., filtered and analysed by ICP-MS. The results are presented in Figures 6.3 – 6.5.

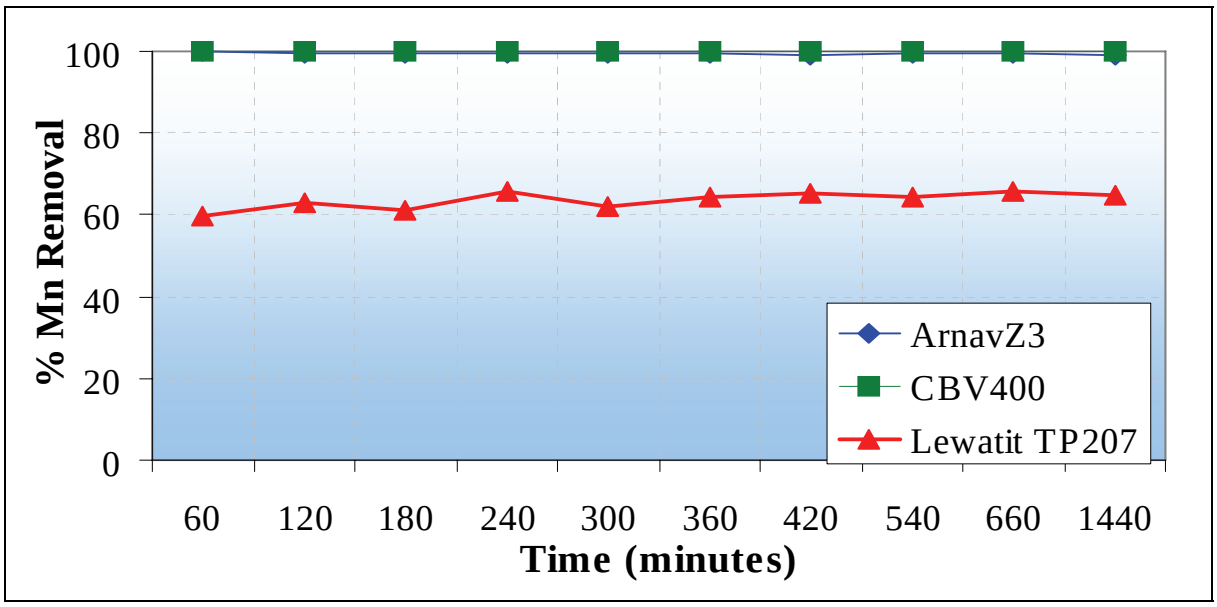

Figure 6.3: Percent of Mn removal for synthesised faujasite, ArNavZ3, commercial faujasite, CBV400 and commercial ion exchange resin, Lewatit TP.

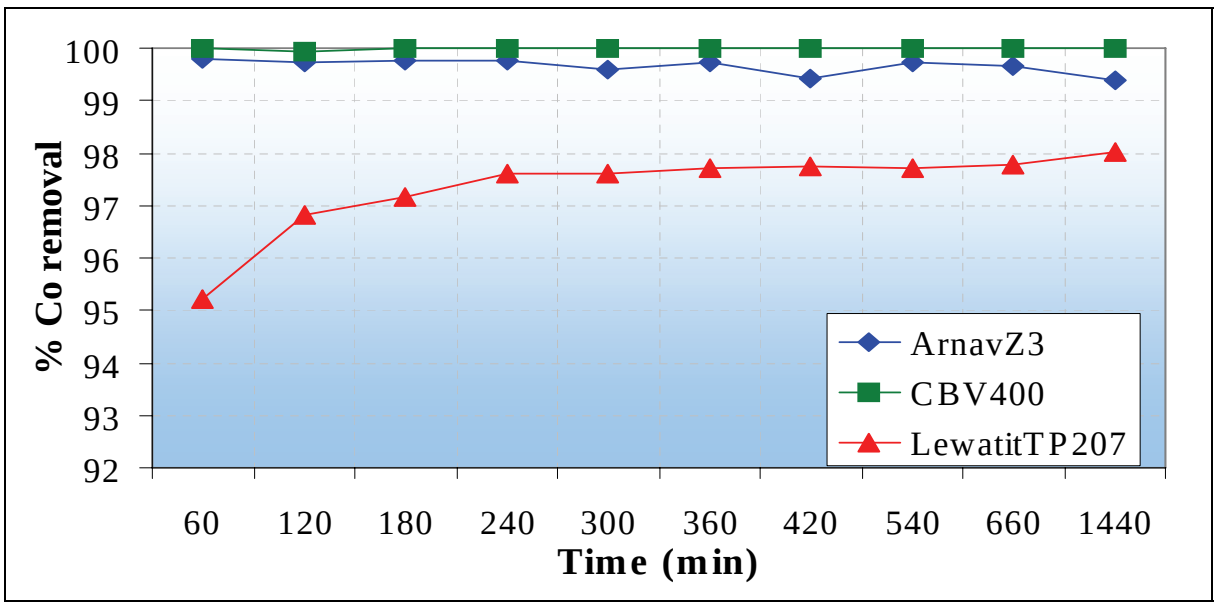

Figure 6.4: Percent of Co removal for synthesised faujasite, ArNavZ3, commercial faujasite, CBV400 and commercial ion exchange resin, Lewatit TP.

Within the first hour of contact, the synthesised adsorbent ArNavZ3 removes the maximum quantity of metal in solution. The commercial resin CBV400 follows the same trend and results in 100% metal removal for each of the three metals. The synthesised faujasite ArNavZ3 removes 100% of Mn in solution and 99.8% of both Co and Pb. The commercial ion exchange resin, Lewatit TP207 does not remove metals very efficiently. Manganese removal is 63%, Co removal is 98% and Pb removal is 96%. Unlike the two faujasites the resin appears to remove slightly more metals from solution with a greater contact time.

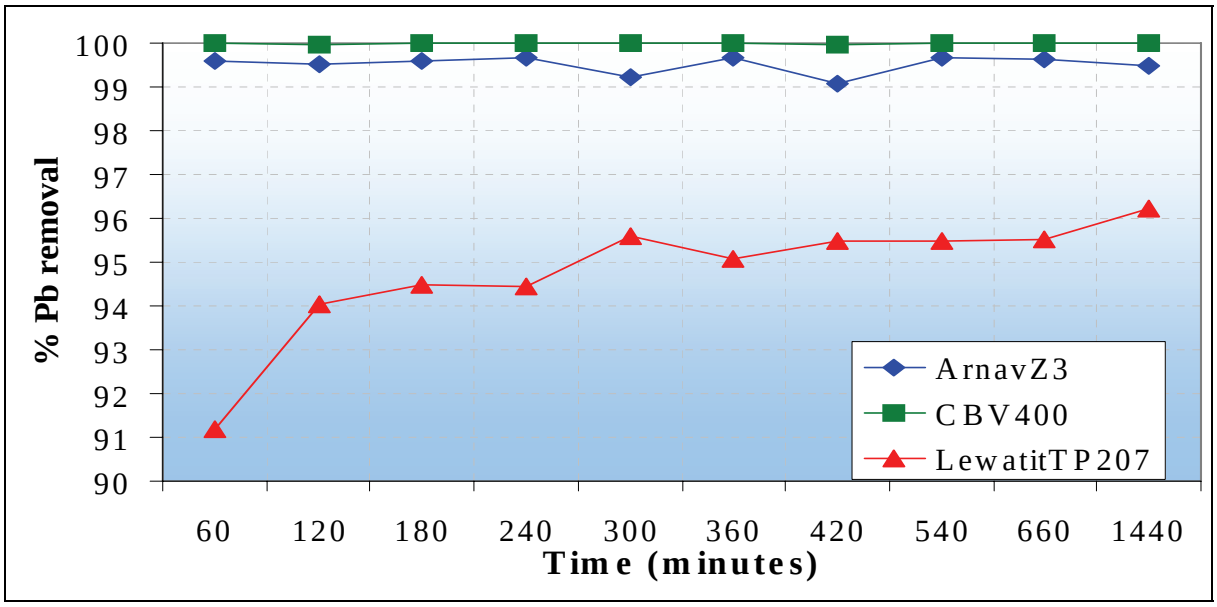

Figure 6.5: Percent of lead removal for synthesised faujasite, ArNavZ3, commercial faujasite, CBV400 and commercial ion exchange resin, Lewatit TP 207.

6.4 DISCUSSION

Both ArnavZ$_3$ faujasite and its commercial counterpart showed considerably high Mn^{2+} removal; with a steep concentration decrease within the first 60 minutes of contact, after which both plots reaches plateau values with correspondingly low residual concentrations for the rest of the time intervals. However, in the case of Lewatit, removal for Mn^{2+} was not as efficient; a steep decrease was observed within the first 60 minutes, only reaching a residual concentration of approximately 1.9 mg/L. From this point on slight fluctuations was observed for the rest of the time intervals; however, residual concentration was maintained at ± 2 mg/L.

All exchangers; both commercial and fly ash-related, showed a similar trend with respect to Co^{2+} removal. A very steep concentration decrease was observed within the first 60 minutes of contact for all exchangers, after which smooth, continuous plateau values were reached observed, with a concomitant low residual solution concentration maintained until the 1440 time interval. Both ArnavZ$_3$ faujasite and its commercial counterpart showed almost complete removal while Co^{2+} concentrations remaining in solution with respect to Lewatit were slightly higher (only 98% removal over time).

Based on the results obtained for the experiments conducted to compare the metal retention ability of ArNavZ3 with its commercial counterpart, as well as with the commercially obtained chelating resin, one can draw the following conclusions:

The selectivity and metal retention capacity of the fly ash-related faujasite-type zeolite was comparable to that of the commercially obtained faujasite. These results indicate that the synthesized zeolite does in fact contain a high fraction of faujasite within the zeolitic structure. One of the objectives, the synthesis and application of a faujasite-type fly ash-related zeolite for the purification of metal-bearing wastewaters (i.e. secondary waters recovered after the neutralisation of AMD with FA), was thus successfully resolved. The low metal uptake shown by the chelating ion exchanger (Lewatit) may be due to the competition between hydronium ions and metal ion for exchange sites since the pH remained below pH 4 for the duration of the experiments.

6.5 CONCLUSION

A zeolitic material can be synthesised using the solid residues from the reaction between fly ash and AMD. The hydrothermal conversion of solid waste residues obtained from the neutralisation reaction between FA from Arnot power station and AMD collected from Navigation plant at Landau colliery was achieved and resulted in the formation of a relatively pure faujasite zeolite with high cation exchange capacity. The feedstock for the preparation of the zeolite adsorbent was a solid waste residue recovered after reacting FA with AMD at a FA: AMD ratio of 1:3.5.

The adsorption capacity of the zeolite faujasite synthesised from waste was compared to the capacity of the commercial synthetic chelating ion exchange resin LewatitTP207 and to a commercial faujasite. The zeolite prepared from solid waste residues with the fusion method was more efficient at toxic element removal than the commercial resin (LewatitTP207) and had a similar capacity of metal removal compared to a commercial faujasite. The faujasite adsorbent prepared from solid residues efficiently removed Mn, Co and Pb (between 99-100% removal) within 1 hour of contact time at the dosage applied.

The zeolite adsorbent faujasite prepared from solid waste residues could thus potentially be applied in treatment of secondary process waters which would complement the primary AMD treatment.

7. GIS MAPPING OF AMD AFFECTED AREA

7.1 INTRODUCTION

The advent of Geographical Information Systems (GIS) has vastly improved both the quality and quantity of data and analysis that can be used to support environmental decision making. Many environmental issues such as impact assessment; analysis of soil and vegetation types, contaminated land etc. can be effectively addressed using GIS. The reason is all most all the environmental issues have a common link and that is geographical location.

Over the years geographic information system (GIS) in South Africa has evolved and become part of many scientific disciplines. Environmental geochemistry is one of those disciplines where application of GIS plays a major role in decision making. This involves integration of different kinds of data and to generate good quality informative maps using GIS. This assists meaningful and object oriented decisions that can be implemented with ease.

The aim of this project was to collate existing water quality data from Coaltech and other sources to compile graphs showing the seasonal variability of water from different mines. The coal mining activity, location of mines and power stations and their proximity towards one another was plotted on GIS maps of the area.

The amount and quality of the data presented in this report make it clear that further studies need to be conducted with more rigorous and accurate data collection. This data is sourced courtesy of Chief Directorate: Surveys and Mapping, Mowbray, Council of Geosciences, Mark Hill of Eskom and Brent Usher from the University of the Orange Free State. Seven 1:50000 digital topographic sheets-shape files (Figures 9.9 to 9.15) of Mpumalanga province were obtained courtesy of The Chief Directorate: Surveys and Mapping, Mowbray, w3sli.wcape.gov.za.

7.2 METHOD

All the GIS maps in this section are produced using Arcview 3.2a and ArcGIS 9.0. Figures 7.1 to 7.8 were produced using the data obtained from the University of the Orange State and Council of Geosciences. A shape file showing coal mining activity in South Africa was cut into different district councils and was overlaid on the respective base maps obtained from University of the Orange State. Since the original digital topographic sheets did not contain information about mines/collieries, seven normal topographic sheets of Mpumalanga province (2529CC, 2529CD, 2529DD, 2927CC, 2629CD, 2629AC and 2628BB) were obtained and digitally photographed. These photographs were georeferenced using ArcGIS 9.0 software and were digitised for mining activities and possible AMD source points. After digitising, these layers were overlaid on the digital topographic sheets to produce Figures 7.9 to 7.15. The water quality data was collected from Coaltech and other sources to compile graphs showing the seasonal variability of water from different mines (Figures 7.16 to 7.24).

7.3 RESULTS

The severity of the problem arising from the need for ash disposal can be seen from Table 7.1. Around 17 million m^3 per annum of FA are produced from 7 power stations that are currently being disposed of in ash dumps. The CaO content indicates that the ash is suitable for AMD neutralisation.

Table 7.1: Tonnages and lime mass percent for several power stations.

Power station	m^3/year	CaO %
Arnot	1 215 000	7.80
Duvha	4 070 000	
Kendal	4 500 000	4.12
Kriel	2 000 000	9.54
Majuba	500 000	
Matla	3 500 000	8.09
Thuthuka	1 300 000	5.56

Table 7.2 shows the water quality of a selection of coal mine drainages in Mpumalanga. These waters are currently generally circumneutral and do not have high EC's or SO_4^{2-} concentrations, relative to their acidic counterparts. It is clear from the pH that Fe concentrations will be low. The neutral pH also suggests that other ions may be prevalent in solution, perhaps Ca^{2+} or Mg^{2+} if the gangue rock being mined is dolomitic.

Table 7.2: pH, EC and SO_4^{2-} concentration of a selection of coal mine drainages.

Collieries	pH	EC mS/m	SO_4^{2-} mg/l
Goedhoop	6.20	160.8	1 234
Kleinkopje	5.76	136.8	799.6
Kriel	6.66	59.90	218.8
New Clydesdale	6.99	38.27	115.3
Sasol Secunda	8.09	544.7	1 094
Tavistock			631.7
TNC	7.79	135.3	558.2
Tweefontein	7.41	162.9	673.0
Arnot	8.10	0.87	221.0
Douglas	6.05	146.7	853.7
Greenside	6.44	156.4	763.6
Koornfontein	7.32	102.1	369.0
Middelburg South	6.67	161.6	1 234
Middelburg	6.62	147.9	825.4
Minaar	6.47	68.46	312.0
Rietspruit	7.70	142.5	907.9
South Witbank	3.75	126.5	733.6

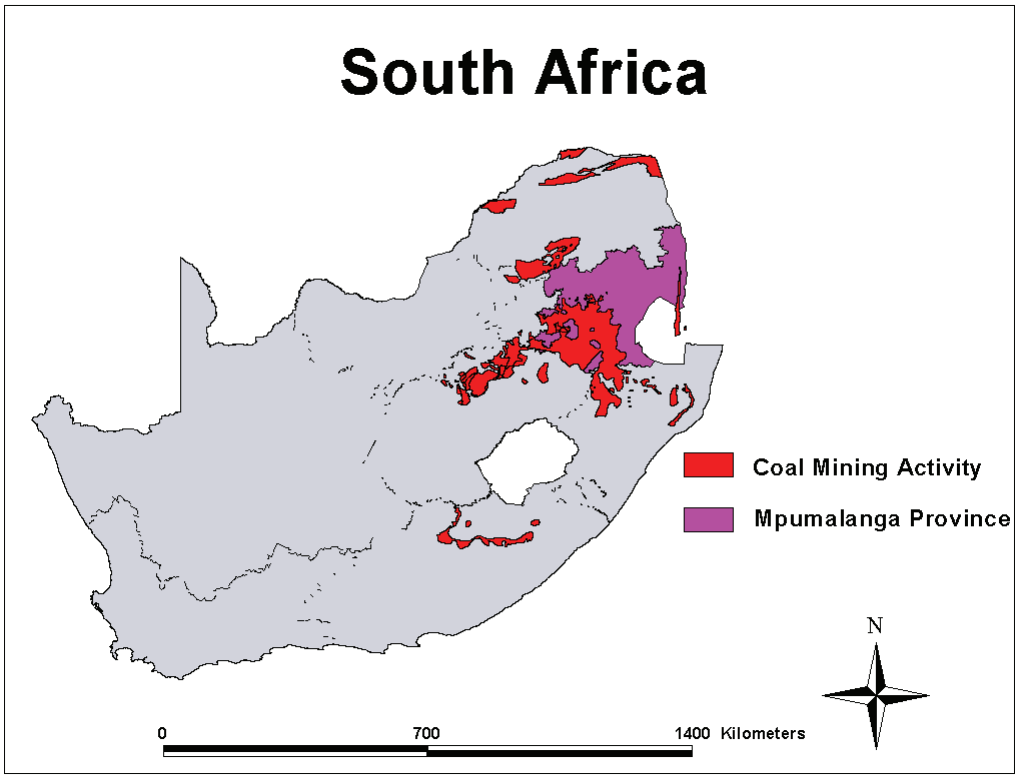

Figure 7.1: Coal mining activity in the Mpumalanga province highlighted.

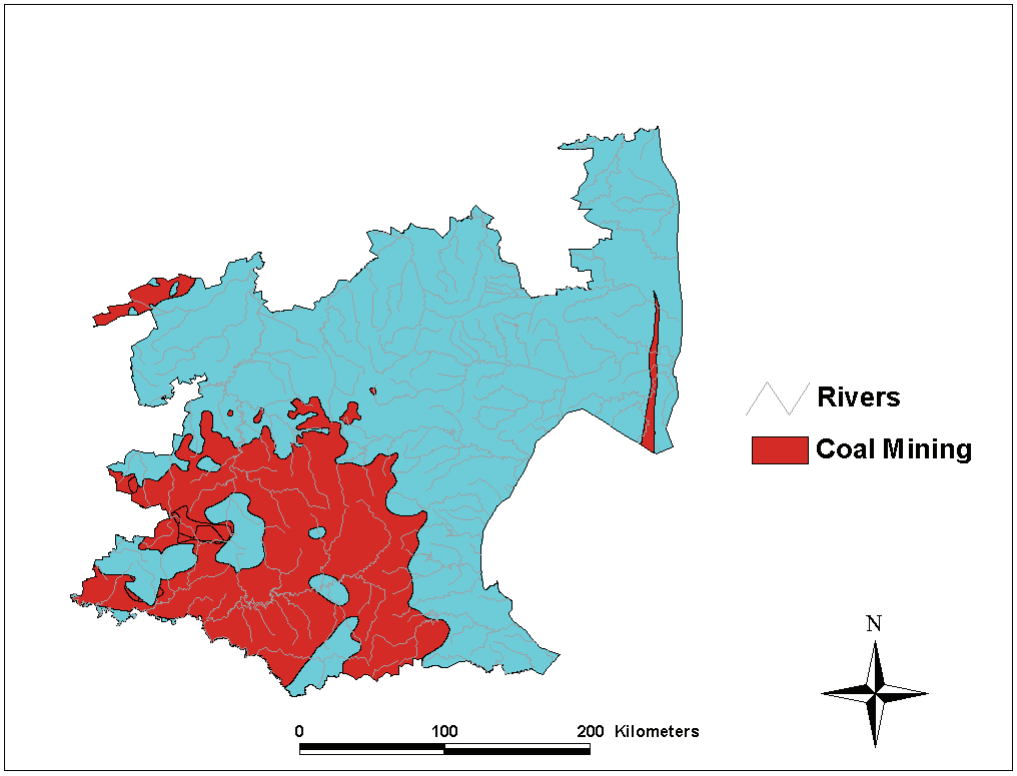

Figure 7.2: Coal mining activity and rivers in the Mpumalanga province.

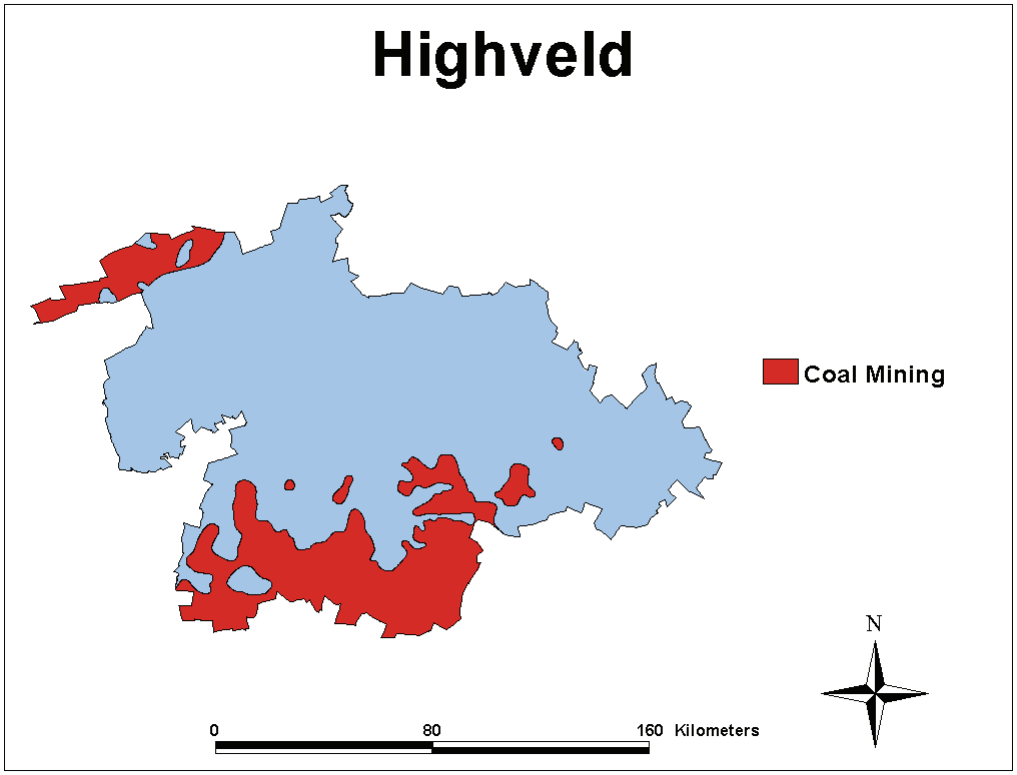

Figure 7.3: Coal mining activity in Highveld District Council.

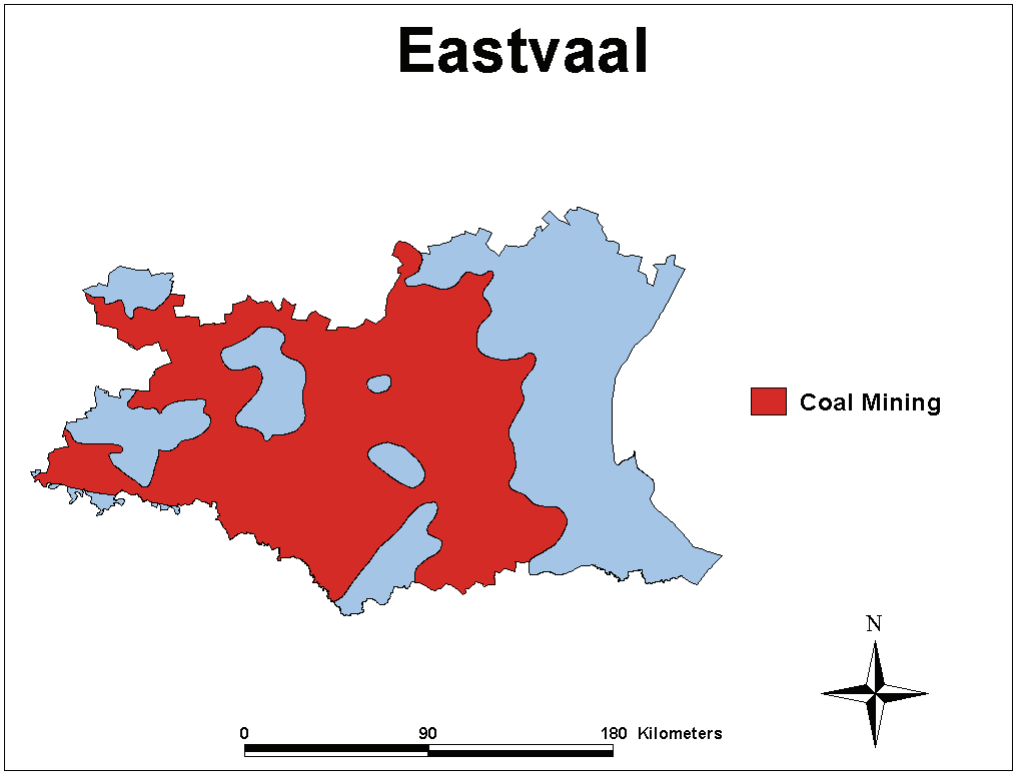

Figure 7.4: Coal mining activity in Eastvaal District Council.

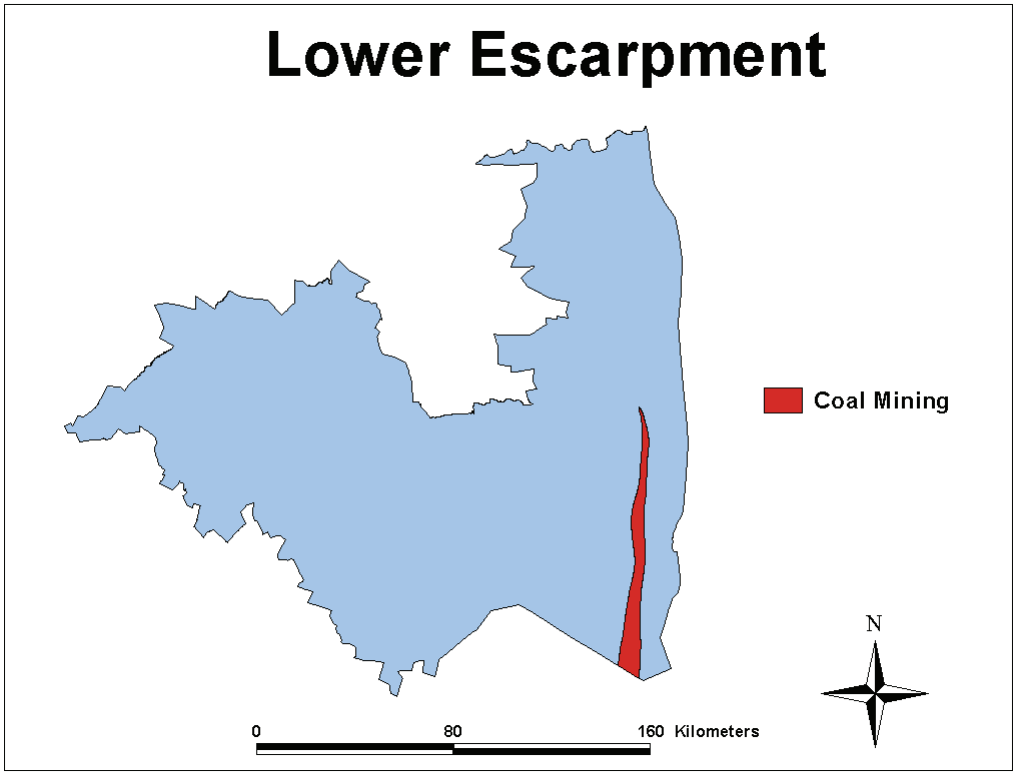

Figure 7.5: Coal mining activity in Lower Escarpment District Council.

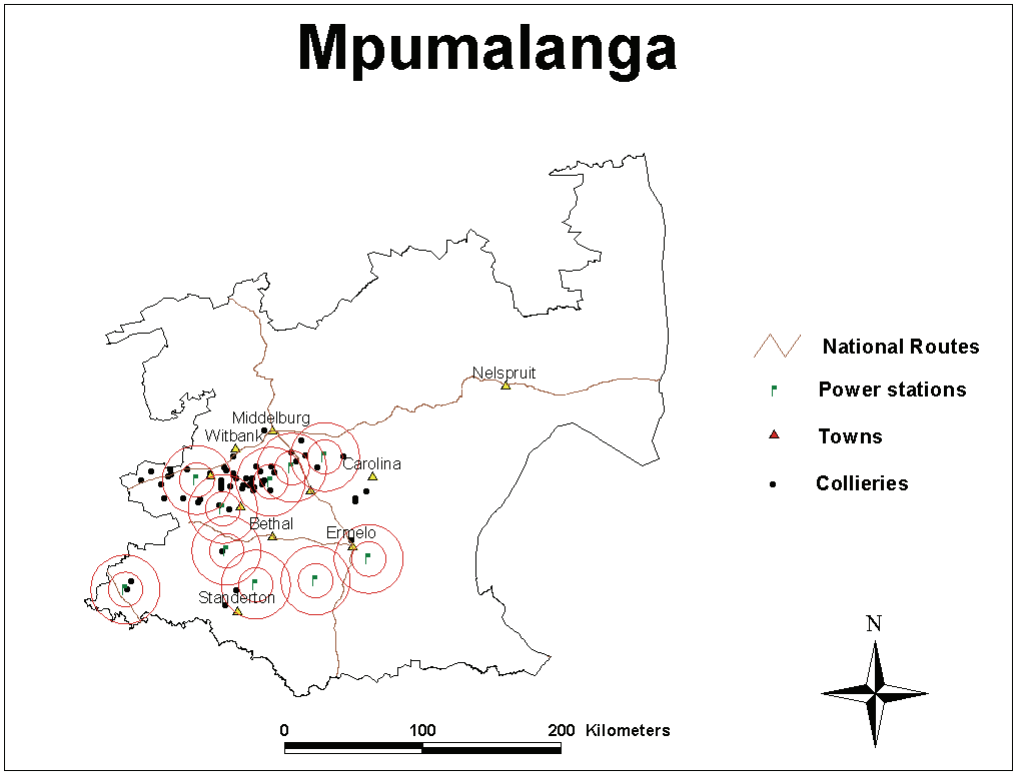

Figure 7.6: Mpumalanga showing power stations, collieries, towns and national highways. The inner red circle denotes 12.5 km radius from power stations and the outer circle denotes 25 km from the power stations.

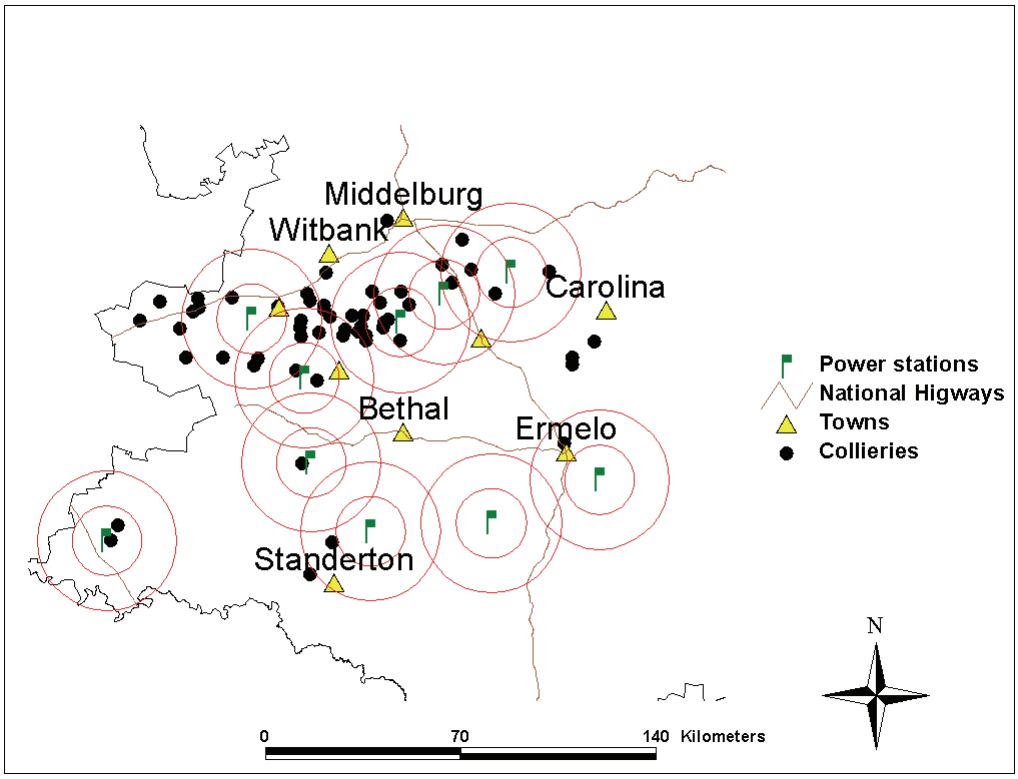

Figure 7.7: Enlarged map of proximity zones around power stations.

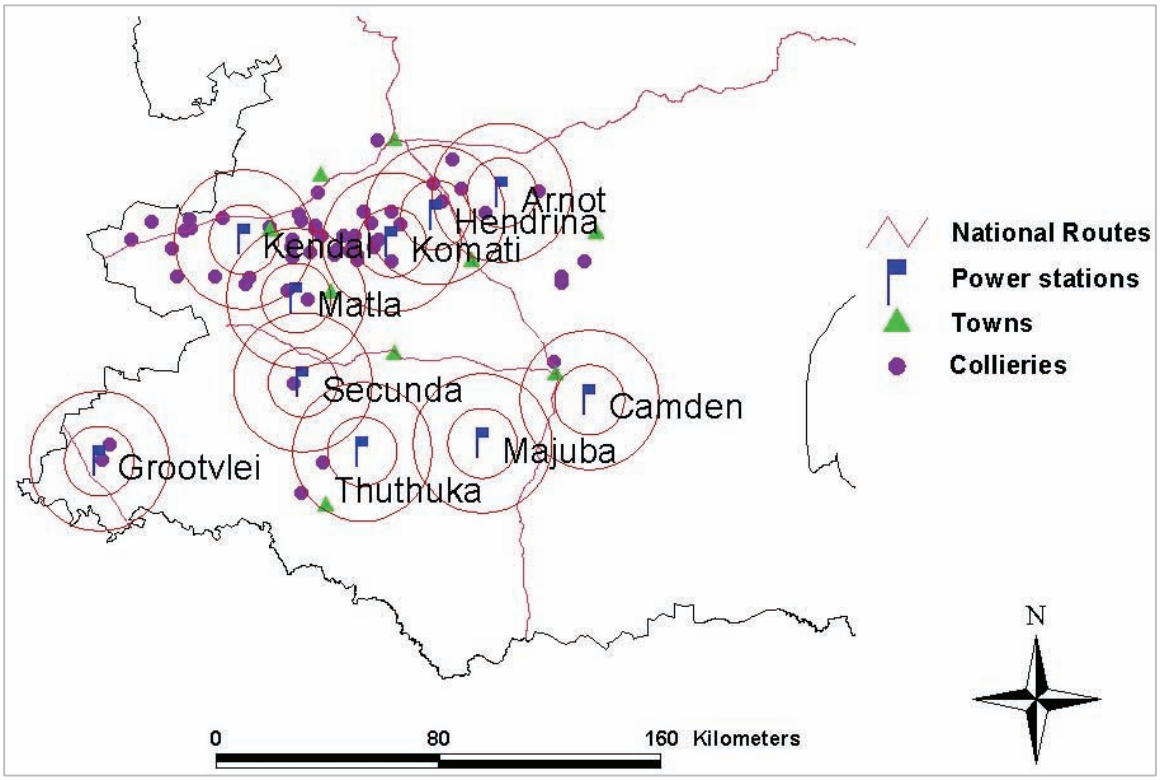

Figure 7.8: Enlarged map of Mpumalanga showing towns.

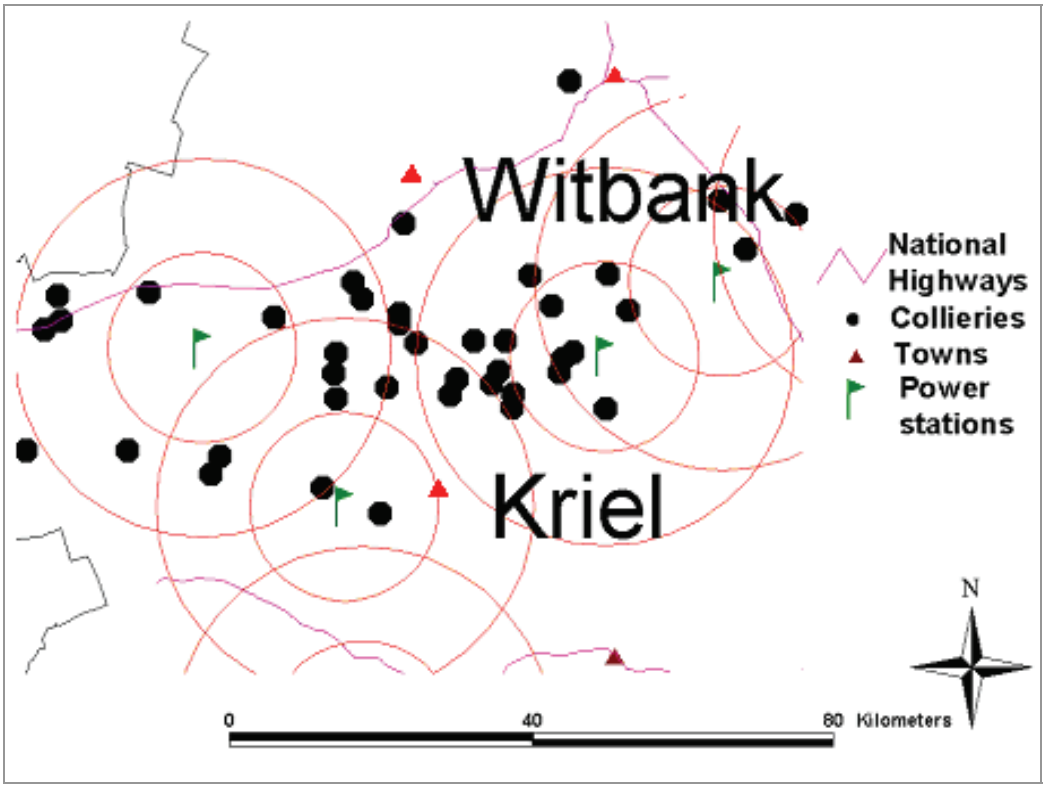

Figure 7.9: Map showing extent of collieries near Witbank.

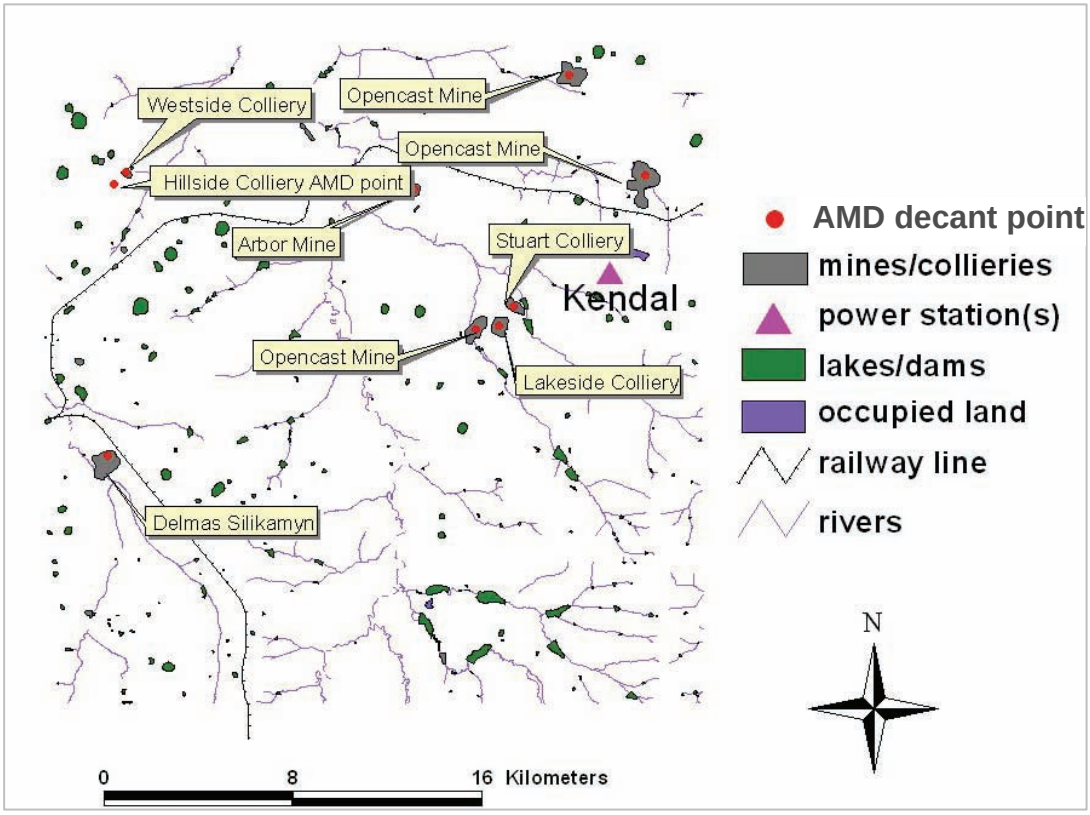

Figure 7.10: Kendal power station, collieries and mines with possible AMD source points.

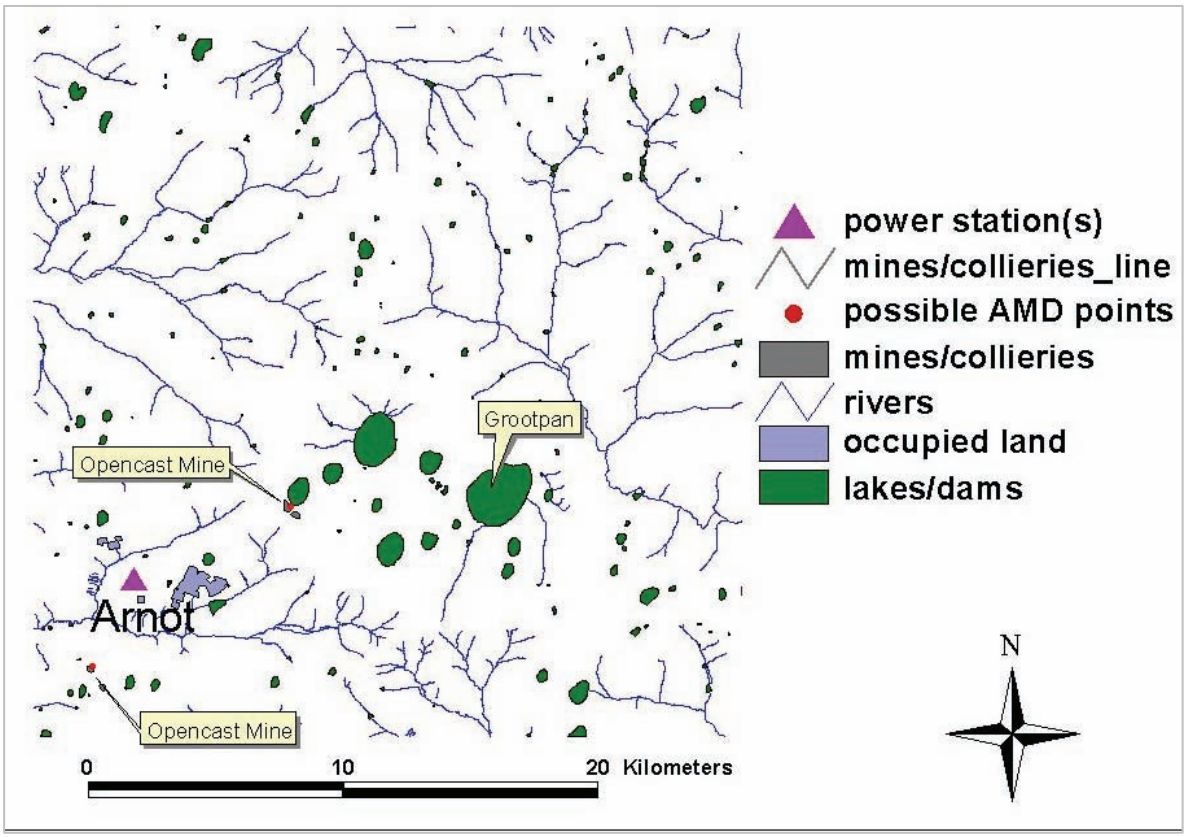

Figure 7.11: Arnot power station, collieries and mines with possible AMD source points.

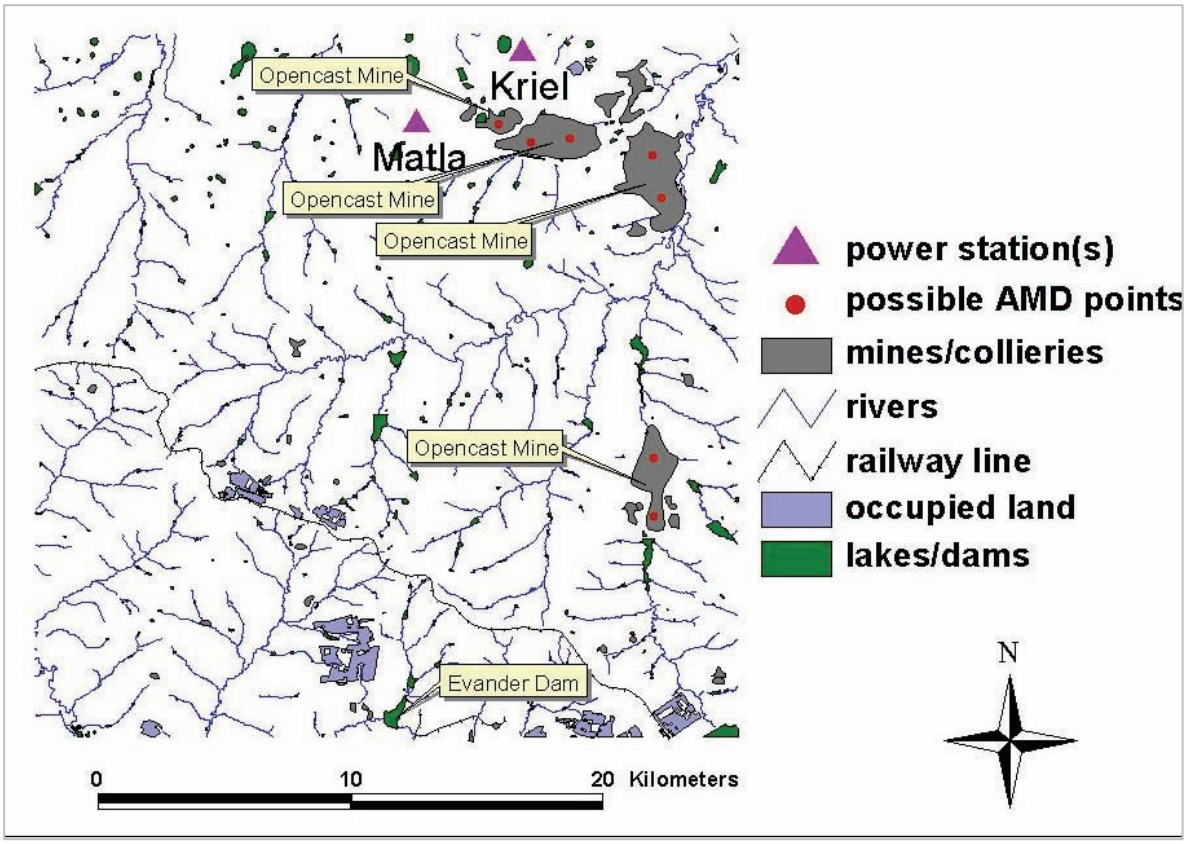

Figure 7.12: Kriel and Matla power stations, collieries and mines with possible AMD source points.

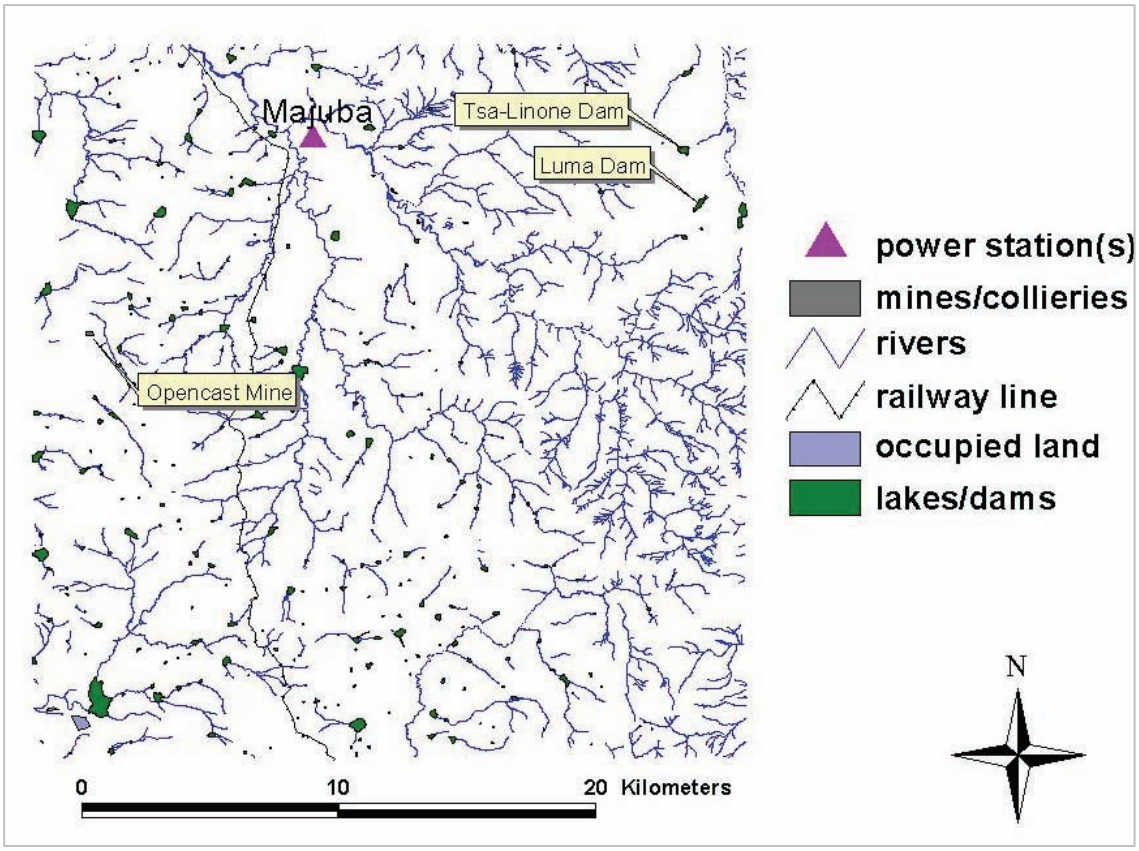

Figure 7.13: Majuba power station, collieries and mines.

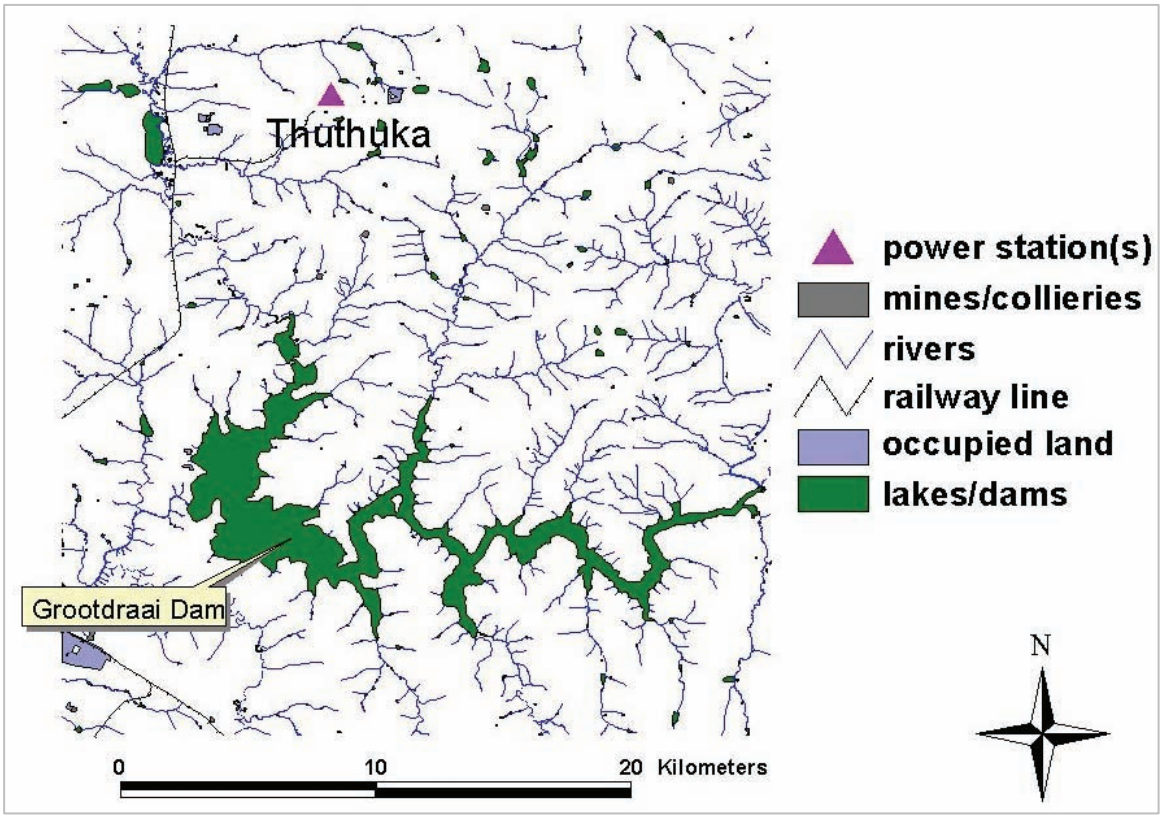

Figure 7.14: Thuthuka power station, collieries and mines.

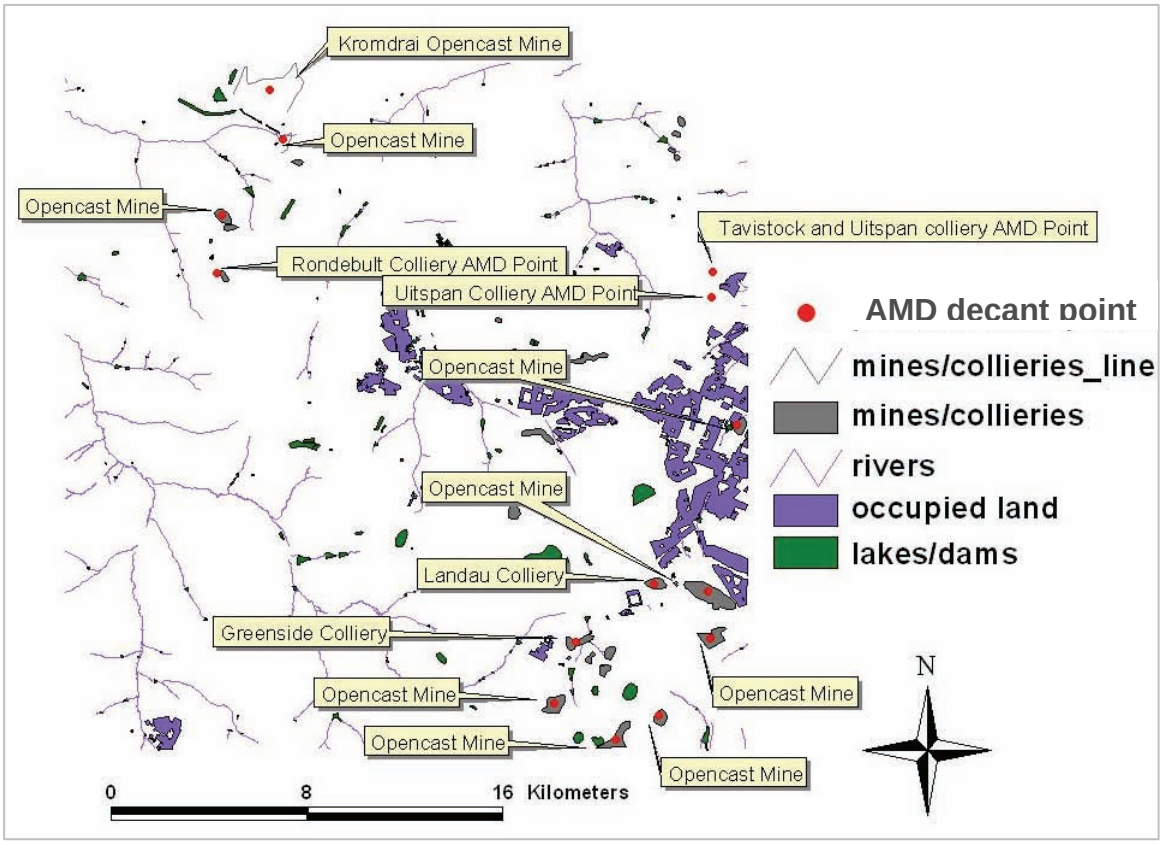

Figure 7.15: Collieries and mines with possible AMD source points near Witbank.

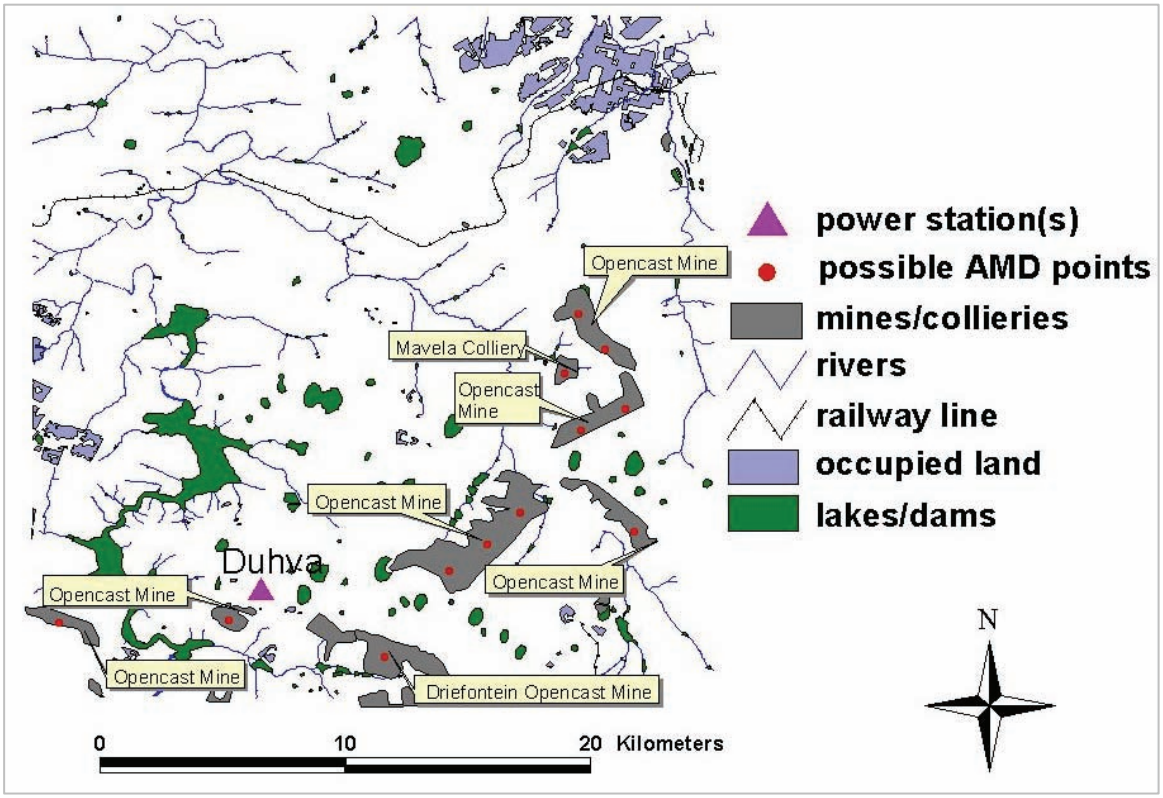

Figure 7.16: Duvha power station, collieries and mines with possible AMD source points.

7.4 DISCUSSION

Figure 7.1 shows most of the coal mining activity in South Africa and in Mpumalanga Province. Figure 7.2 shows the potential capacity for contamination of natural waters by mine waters in Mpumalanga Province. Figures 7.3, 7.4 and 7.5 indicate coal mining activity in Highveld, Eastvaal and Lower Escarpment district councils. It can be noticed from these maps that most of the coal mining activity is limited to Highveld and Eastvaal councils with Eastvaal having the maximum. Lower Escarpment has the lowest mining activity.

Figures 7.6 and 7.7 indicate the close proximity of power stations and collieries. If FA were to be transported to collieries to neutralise AMD the distance to be travelled in most cases is less than 25 km between Witbank and Bethal. There is also a significant number of collieries with in the range of 12.5 km from the power stations between Witbank and Bethal but fewer collieries near to the remaining power stations. There are many collieries within 25 km radius of all the power stations. Figure 9.8 demonstrates the extent of collieries near Witbank.

Figures 7.9, 7.10, 7.11 and 7.15 shows the location of some power stations, collieries and mines with some possible AMD source points. This gives an indication of how close power stations are to the possible source of AMD and also gives an idea of where AMD sources may be located in the colliery or mine. These maps highlight the opportunity to use FA because of its proximity to mines.

7.5 VARIATIONS OF AMD PROPERTIES IN SOUTH WITBANK, KLEINKOPJE AND TNC

AMD analysis at Kleinkopje started in 1990 and was carried out till 2001. Over this decade, most pH values were close to neutral or slightly acidic (Figure 9.16). Only a few data showed values below pH 5. The EC ranged from 20 to 300 mS/m, except on three occasions between 1998 and 2001. These low EC values are in agreement with circumneutral waters. There was no correlation between pH and EC variations. Both parameters were not affected by seasonal variation either.

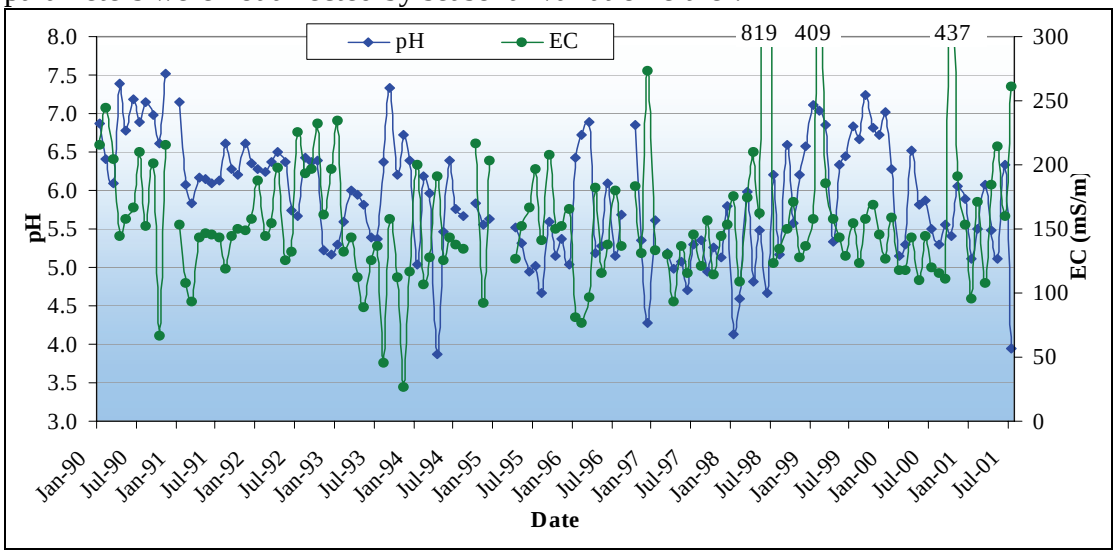

Figure 7.17: Monthly pH and EC values for Kleinkopje colliery drainage water over 11 years (Courtesy Brent Usher, UFS).

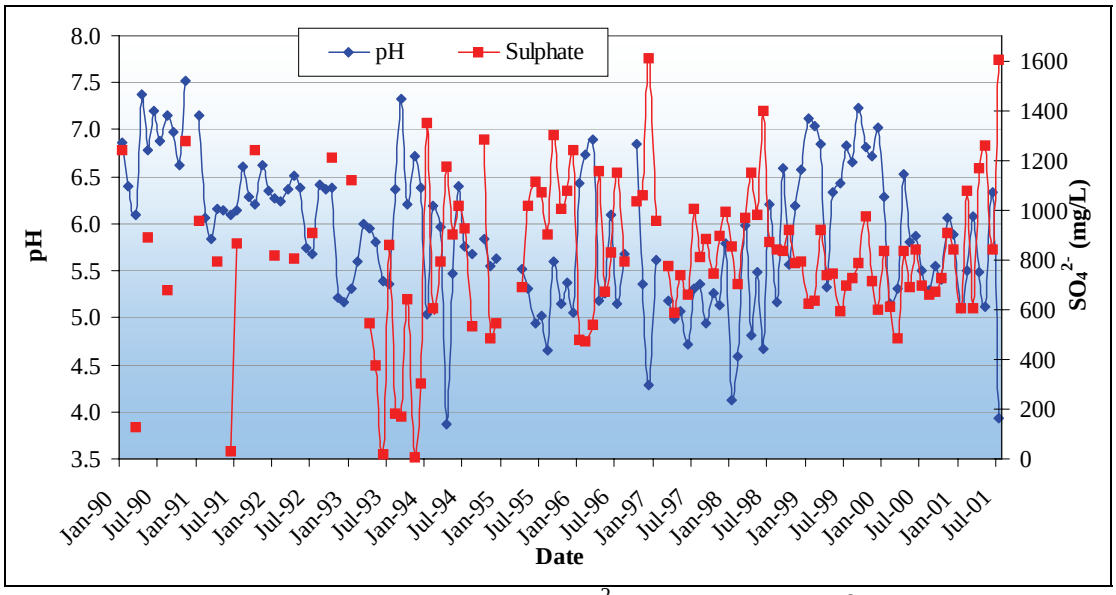

Figure 7.18: Monthly pH values and SO_4^{2-} concentrations for Kleinkopje colliery drainage water over 11 years(Courtesy Brent Usher, UFS).

Sulphate concentrations were low and hardly ever rose above 1500 mg/L (Figure 7.17). Sulphate has average values of approximately 1000 mg/L that are reflected in the neutral or slightly acidic pH values. It has been observed that with high pH values corresponding sulphate concentrations were relatively low which is understandable in terms of neutral pH. Despite this variation, pH did not correlate with sulphate variations.

Between 1993 and 2001, it appeared that the EC followed the same trend as sulphate concentrations (Figure 7.18), but this correlation was not as good as the correlation between EC and SO_4^{2-} in Witbank AMD.

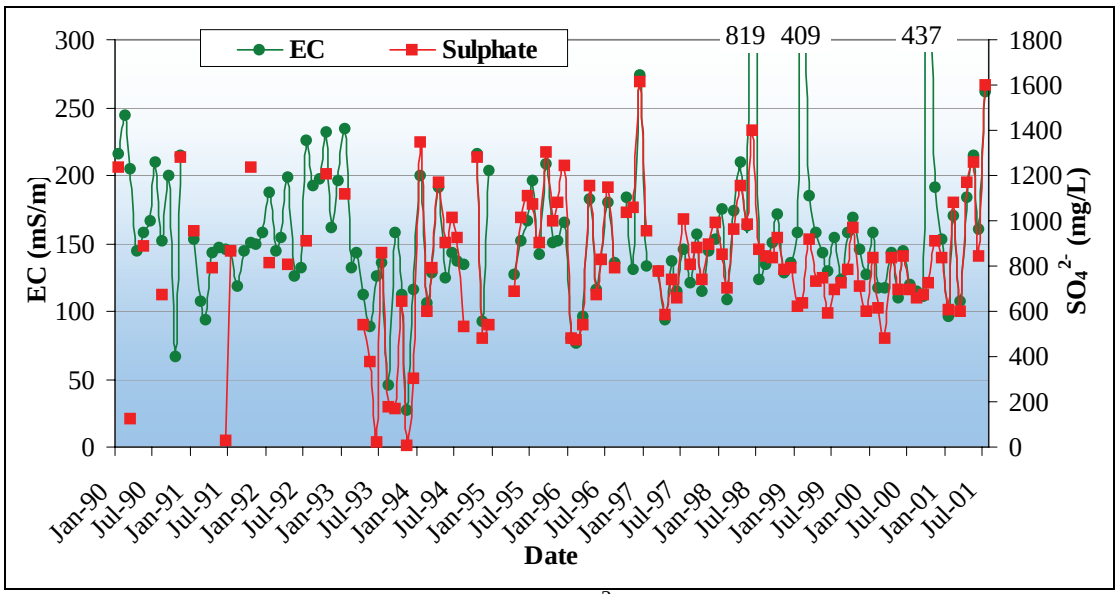

Figure 7.19: Monthly EC values and SO_4^{2-} concentrations for Kleinkopje colliery drainage water over 11 years(Courtesy Brent Usher, UFS).

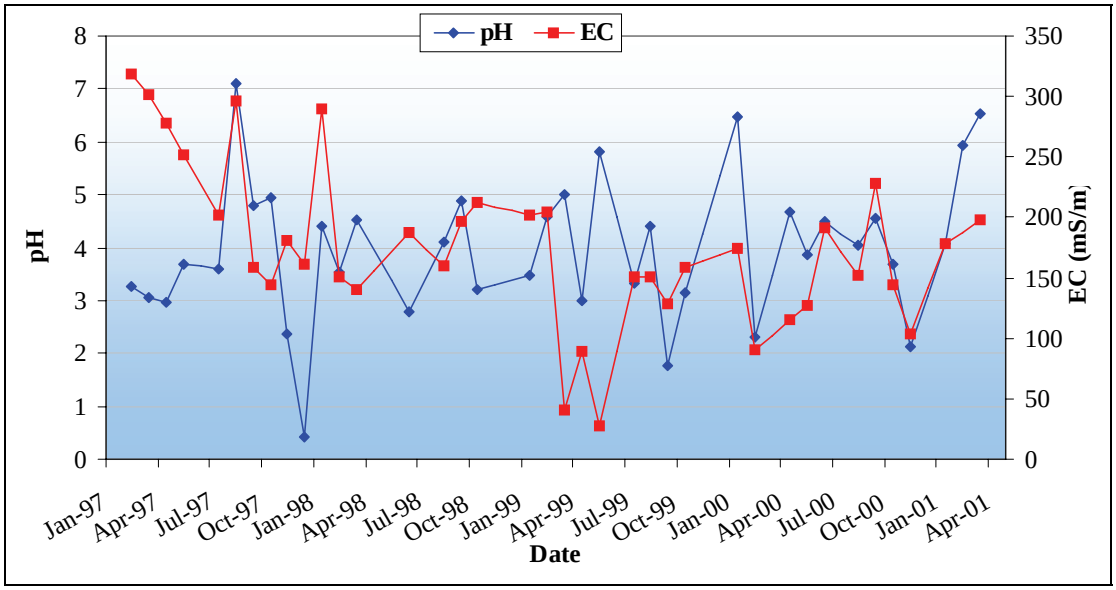

Figure 7.20: Monthly pH and EC values for South Witbank colliery drainage water over 4 years(Courtesy Brent Usher, UFS).

AMD was analysed in South Witbank between 1997 and 2001. The pH values were relatively low, as shown in Figure 7.19. Most pH values were between 3 and 5. EC varied between 50 and 300 mS/m, which seemed quite low for such waters. Especially when pH values are above 6, EC concentrations were very low. EC and pH variations did not seem to correlate, nor did they show any seasonal influence.

Figure 7.20 shows that sulphate concentrations remained below 2000 mg/L over the whole study period, despite acidic or strongly acidic pH. These sulphate concentrations were lower than those that could be expected from AMD, but they correlated well with EC values.

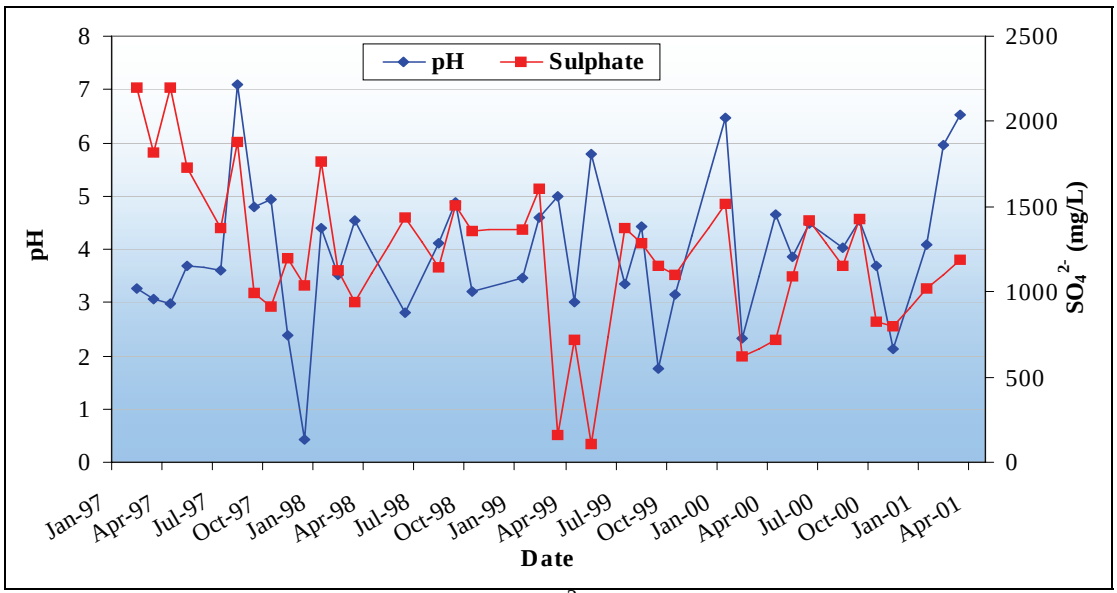

Figure 7.21: Monthly pH values and SO_4^{2-} concentrations for South Witbank colliery drainage water over 4 years(Courtesy Brent Usher, UFS).

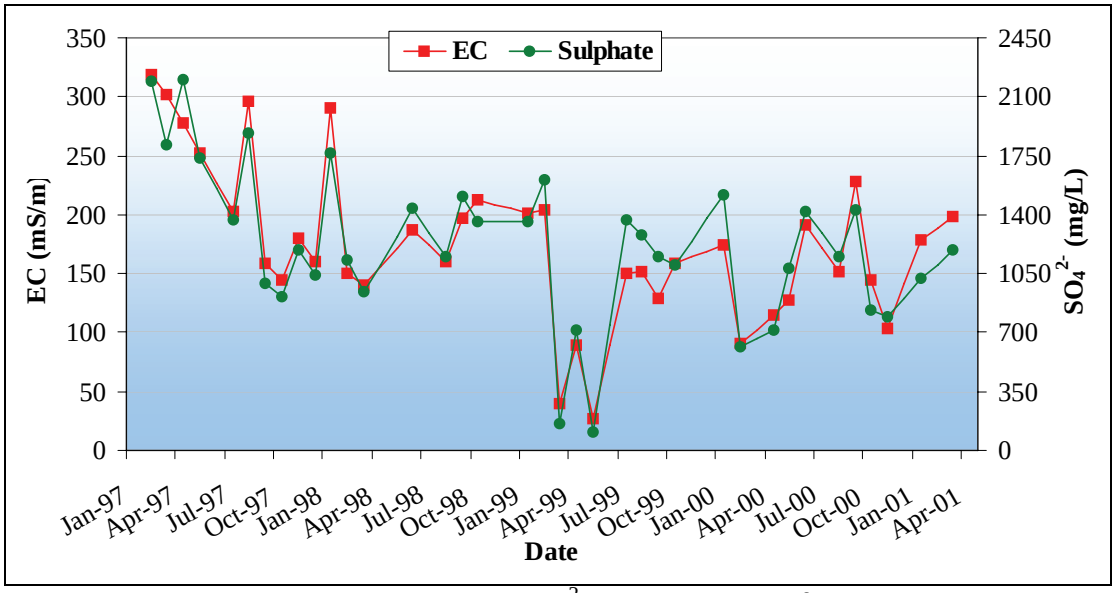

Figure 7.22: Monthly EC values and SO_4^{2-} concentrations for South Witbank colliery drainage water over 4 years(Courtesy Brent Usher, UFS).

Figure 7.21 shows that most of the EC values are in between 100 mS/m to 250 mS/m and in this data set a strong correlation between EC and SO_4^{2-} concentrations exists. This demonstrates that sulphate is a major ion of this AMD. No seasonal variation was identified for sulphate either.

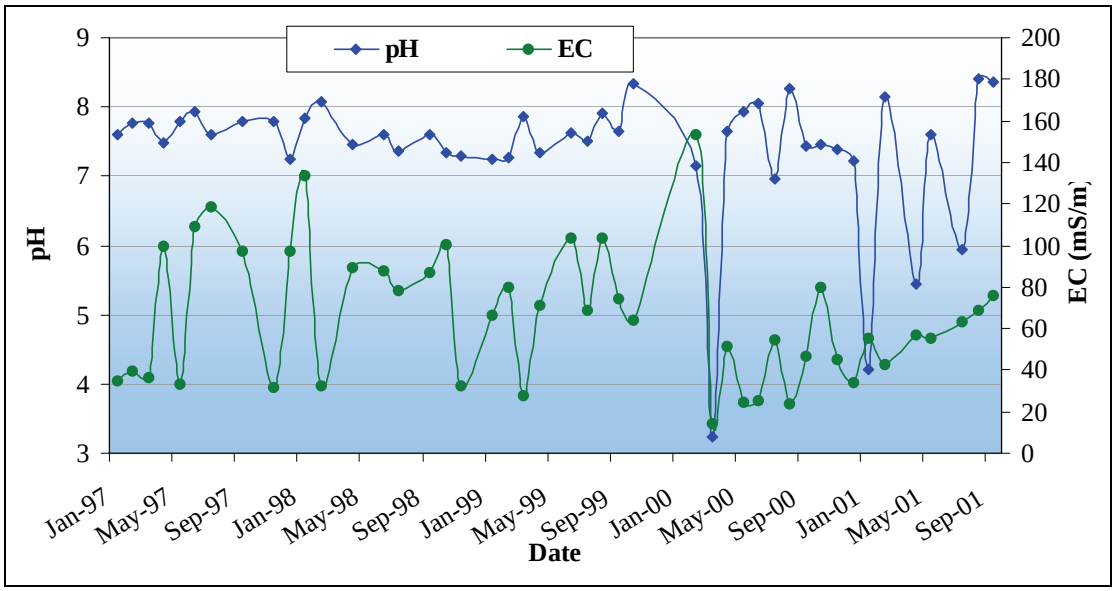

Figure 7.23: Monthly pH and EC values for TNC colliery drainage water over 4 years(Courtesy Brent Usher, UFS).

AMD analysis took place between 1997 and 2001 at TNC. These waters were close to neutral with most pH values ranging between 7 and 8 (Figure 7.22). Only a few points showed values of pH<6 and they are after Jan '00. EC was usually between 20 and 100 mS/m. While pH remained quite stable over the whole study period, EC varied significantly. As a consequence, no correlation could be established between these two parameters. Sulphate concentrations were only <500 mg/L, in agreement with neutral pH. Nevertheless variations in pH and sulphate could not be correlated. Sulphate varied by a

large amount. When focusing on the 1999-2001 period there is a strong correlation between SO_4^{2-} and EC (Figure 7.23). As sulphate is a major ion in these waters, it greatly influenced the EC. EC variations were also compared with other ionic species (Figure 7.24). It appeared that other ions, such as Ca^{2+}, Na^{+} and Mg^{2+}, had the same variations as EC. As these waters do not have high sulphate concentrations, other dissolved species played a major role in the solution properties and due regard must be given them. There is an observable trend in TNC colliery waters as all the parameters remained very low despite pH remained fairly stable (except in 3 or 4 occasions) between May '00 to Sep '01.

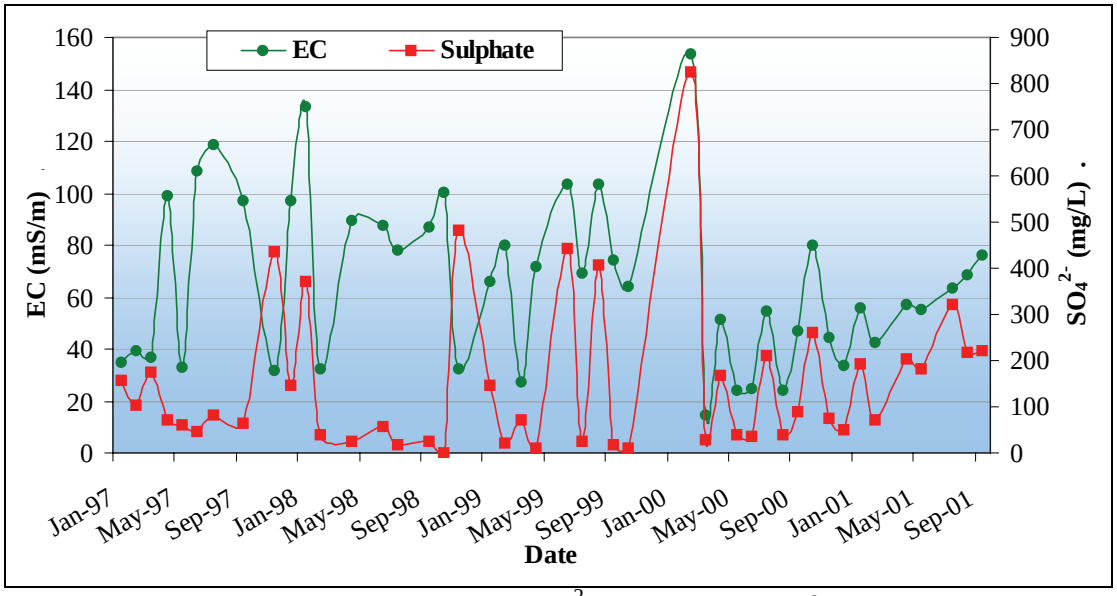

Figure 7.24: Monthly EC values and SO_4^{2-} concentrations for TNC colliery drainage water over 4 years(Courtesy Brent Usher, UFS).

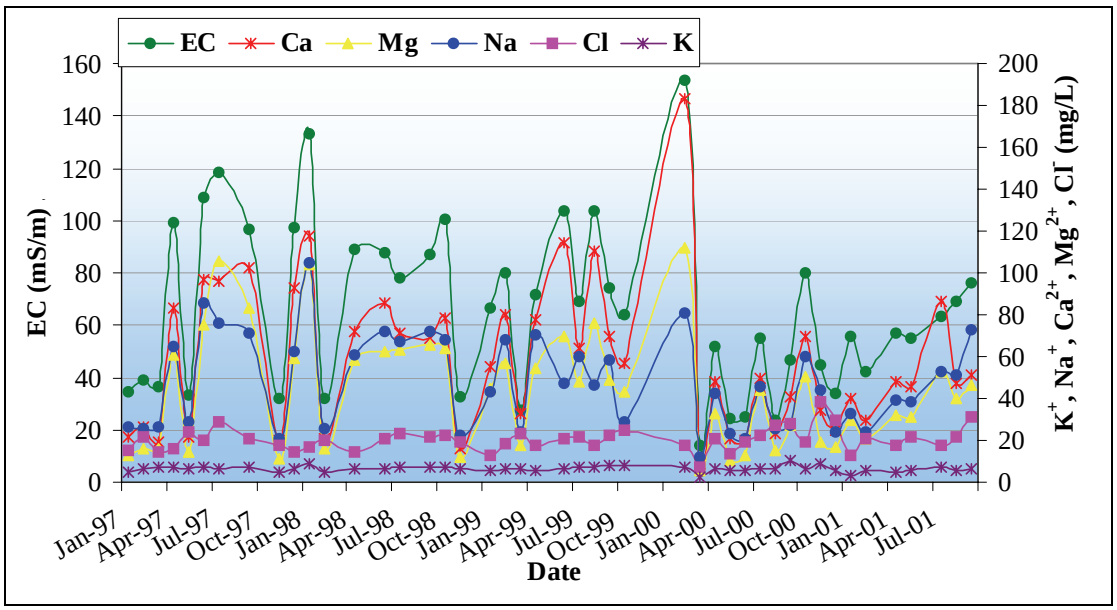

Figure 7.25: Monthly EC values and some ion concentrations for TNC colliery drainage water over 4 years(Courtesy Brent Usher, UFS).

7.6 CONCLUSIONS

In conclusion observable seasonal variations of water quality could not be seen in any of the three AMD's studied. Variations occurred, though, but were not repeated from one year to another. These results show that the pH and concentrations of dissolved species in AMD are under the combined influence of many uneven factors, such as rainfall, amount of pyrite in the coal, composition of gangue rock, rate of coal extraction and etc. It is recommended that the monitoring of AMD properties must be set up on a daily or weekly basis, for a period of several months or years. This could bring a detailed knowledge of AMD characteristics and variations. It would be highly useful in the evaluation of the remediation capacity of FA.

8. GENERAL DISCUSSION – AN INTEGRATED SCHEME

In this section the potential to employ an integrated waste management scheme based upon neutralisation of fly ash and AMD, use of backfill in real coal mines, recovery and reuse of water and application of fly ash for ash walling or lining is discussed based upon the results obtained thus far. Site visits and presentations to market the idea to mines has been successful and proposals that have been accepted or are under consideration at present are appended (see Appendix B). All costs and volumes quoted are estimates based upon the Anglocoal Navigation treatment plant.

8.1 BACKGROUND

The treatment of acid mine drainage with limestone, which, for example, occurs at Anglocoal Navigation mine, is a complicated procedure. An estimated average of 32.5Ml/day of acid mine drainage is treated at Navigation. The water processing takes place across three plants, namely, the primary liming plant (PLP) which treats an acid mine drainage flow of 4.8 Ml/day, the secondary liming treatment plant which treats 27Ml/day and the toe seep plant (TSP) which treats an acid mine drainage flow of 0.7 Ml/day. The annual overall tonnage of limestone used is 15 776 tons. Moreover, recovered water is used in the coal processing plant (CPP) in which coal is washed.

At the first water treatment stage, treating acid mine drainage with limestone in the PLP, only the pH of the water is adjusted. Thereafter, a complex settling, recycling and retreatment of water recovered from this first liming stage occurs, in which steps such as flocculation, biological sulphate reduction, retreatment of coal washing waters etc. occurs.

The current liming treatment has several drawbacks. For instance, only neutralisation of AMD occurs in the PLP which treats underground mine water with a sulphate content of 2 650 mg/l and only a moderate reduction in sulphate content is achieved (typically to levels of about 2 350 mg/l sulphate). In the PLP there is no reduction in toxic elements in the AMD after the 4 – 8 hrs residence time applied. The separated solid sludge (“yellow boy”) that precipitates after the first liming treatment is pumped after dewatering to a lined hazardous waste storage area, which storage is costly (R2 724 400 per annum). The recovered water is then treated, at considerable expenditure, with a polyamide based flocculent in a settling tank to enhance separation of the limestone sludge (cost of flocculent R539 136 per annum). Thereafter, the clarified water is pumped to the sulphate reduction plant (SRP) where the sulphate concentration is reduced to 250 mg/l via microbes in a biological process, which requires heat exchange and a carbon based feed (ethanol). This process is very sensitive to temperature and pH fluctuations and also may result in significant and highly toxic H_2S releases (estimated cost of monitoring is R27 700 per annum). Moreover, if the redox reactions are not carefully controlled the sulphide formed by sulphate reducing bacteria can be converted back to sulphate instead of to sulphur. The overall microbial sulphate reduction process is estimated to cost R5 757 500 per annum.

From the SRP the concentrated waste residual water, which is highly polluted, is recycled back to the PLP. The recovered bulk of low sulphate water is pumped to the CPP to wash coal in the density medium separation plant (DMSP). In this process, which closely mimics the oxidation and hydration of pyritic material that occurs in mines, the newly

remediated water again acquires Fe and SO_4, which, again, reduces the pH. This water is then retreated in the secondary liming plant (SLP) and pumped to a slimes dam which is lined with pyrite containing mine spoil, resulting in a highly acidic toe seepage with a sulphate concentration of 16 000 mg/l due to percolation of the stored water through the pyrite containing slimes dam wall. It is strongly recommended that this particular practice be stopped and an alternative dam wall material (possibly FA, but definitely not pyrite containing tailings) be investigated and utilized to prevent this secondary generation of AMD.

A further treatment step is added in which the toe seep water from the slimes dam is neutralised with limestone in the toe seep plant. Finally, it is planned that the remediated mine water will be sent for final polishing in electrodialysis reverse (EDR) or reverse osmosis (RO) systems, currently being designed and commissioned.

It is unknown at present how the replacement of limestone with fly ash would affect this treatment cycle or its current cost and which steps in the process could be omitted or retained. This information is necessary before a full cost comparison can be made.

An assessment of cost savings can be made from the following comparison and considering the advantages of ash utilisation as further detailed below.

The total estimated alkali cost per annum for the water treatment system at Navigation is: Lime = R7 935 529 pa or $CaCO_3$ = R3 462 210 pa. Moreover the lime has a purity of 85% and the limestone replacement used has a purity of only 69% with a moisture content of 25%. The lime utilisation efficiency is calculated to be 70% and the $CaCO_3$ has an utilisation efficiency of 80%. At Navigation an average of 2 – 2.5 tons of limestone replacement is currently used per day in the PLP and 12 tons in the SLP instead of lime and $CaCO_3$. The 25 m^3/hr limestone treatment capacity at Navigation in the PLP relates to slurry flow at 1.07 SG or some 8 - 10% solids concentration with limestone. The ratio of limestone to AMD is 1:105 (in cases where the limestone slurry uses already treated water, otherwise the ratio is 1:120). Higher ratios are required for limestone replacement with ash and this would depend on the most feasible liquid to solid ratio.

Currently lime costs R750 per ton and $CaCO_3$ costs R170 per ton. Limestone is delivered on site at a cost of R165 per ton including material and transport costs. Fly ash can be delivered on site at R55 per ton and this is only a transport cost, as there is no cost for the material.

The energy input for impeller mixing in the conditioning tank is 37 152 kWh per annum and in the aeration tank 164 160 kWh per annum and this figure is not expected to change if fly ash replaces limestone, unless the slurry take-up method is changed.

Currently at Navigation slurries are pumped using peristaltic pumps for low flows and centrifugal pumps for high flows with monitoring of density, which is a general reflection on flowability, and for various process reasons, for example, to maintain a certain amount of solids in clarifiers as seeding material. In the High density process the discharge density is also monitored to maintain high alkalinity in the conditioning tank.

The advantages of using fly ash instead of limestone for the treatment of acid mine drainage would include its lower cost, and the fact that it is readily available in large quantities in close proximity to the coal mine where the acidic waters are found.

Furthermore, limestone needs to be mined and powdered as well as transported for long distances (resulting in wear on infrastructure such as roads, as well as pollution and environmental degradation of mined-out source areas) whereas ash does not require further mining or crushing and is available in close proximity. Limestone may also be supplied by the paper and pulp industry where it is a waste product. The use of this waste limestone is beneficial to the environment and may be incorporated in the treatment using ash in future.

The utilisation of fly ash for AMD treatment will also reduce the cost of environmental rehabilitation associated with the storage of fly ash. The cost of long-term ash storage will be reduced or avoided and environmental remediation costs resulting from fly ash leaching while in lagoon storage will also be minimized. Its reuse will, however, reduce the potential use of ash dumps as a salt sink, which may be a dubious practice.

The quality of the recovered water is significantly improved even after the first 10 minute contact with specified amounts of fly ash as studies at UWC have shown, and thus there may be significant processing advantages in replacement of limestone with fly ash, and several stages of the described process may be eliminated or their cost reduced, since the burden of pollutants in the recovered water would be lower. It is also possible that the current flocculation stage can be eliminated, representing a large potential cost savings, since the solid residues settle out of suspension very readily when compared with the limestone based sludge.

Depending upon the process conditions chosen in the neutralisation process, different qualities of water may be recovered after treatment with fly ash. Should the pH of AMD be brought to approximately pH 7.00 with fly ash, further treatment of water may be necessary in the SRP to remove the remaining sulphate. It would be more appropriate to raise the pH to between 9 and 10 and remove the major, minor and trace elements to the maximum and thereafter adjust the pH to more circumneutral values. Decreasing the pH of the water to required levels will be easily accomplished since the buffering capacity of elements such as Fe, Al and other toxic metals is reduced as a result of their precipitation as metal hydroxides and subsequent removal in the solid fraction. The quality of the remediated water should make it suitable for reuse and possibly release and would minimize its impact on RO or EDR water treatment systems.

The possible reuse of solid residues as a backfill option could provide an answer to the problem of acid mine drainage production as has been shown in this report. The possibility exists for the production of a durable, stable and environmentally benign fill material in backfilling of mines, by use of the solid residues already available in bulk on site after the neutralisation process requiring no further purchasing and importation of other suitable fill material. Long-term and costly hazardous waste storage of the current “yellow boy” sludge remaining after limestone treatment, would thus also be avoided. In the long-term it can be expected that the amount of AMD to be treated at the mine will be significantly minimized by preventing air ingress by backfilling the voids left underground after coal extraction. Backfilling will also add to the economic lifetime of mines and allow a greater degree of extraction of coal.

The waste solid residues can furthermore be transformed into zeolite adsorbents as has been shown by studies at UWC. By selling such value added zeolite materials, manufactured from the solid residues would represent a source of income. These adsorbents are also excellent at removing toxic elements from water representing another cost saving opportunity by reducing the cost of maintenance and replacement of Reverse Osmosis or Reverse Electro Dialysis systems, by reducing the load of dissolved species in waters currently submitted to these systems for final polishing.

In order to integrate all these various aspects of the use of fly ash in mine water remediation a protocol called the "Petrik's Process" has been developed during the past years of this study at UWC, and is detailed below. The Schematic of the "Petrik's Process" is presented in Figure 10.1.

8.2 NEUTRALISATION OF ACID MINE DRAINAGE WITH FLY ASH: REPLACEMENT OF LIMING TREATMENT

Neutralisation of acid mine drainage with fly ash and replacement of liming treatment according to the protocols developed at UWC will require the following steps to be undertaken:

1. Identification of the point source of acid mine drainage flows in reasonable proximity to coal burning energy generation sites where fly ash is available.
2. Collection and storage of acid mine drainage in a bulk facility from where it is pumped to a treatment plant.
3. Transport to, and bulk storage of, fly ash at the treatment plant in a hopper or silo.
4. Slurry preparation facility – fly ash is fed by a screw type feeder and mixed with water or acid mine drainage. The slurry is blended to a specified density and specific gravity and fed to an agitated holding tank, from where it is pumped to the treatment tank
5. Continuous neutralisation takes place in an aerated tank with strong turbulence, where flow and residence time, as well as pH and EC are monitored.
6. The slurry overflow is pumped to a settling tank for separation of solid residues from water and recovery of water to a storage facility.
7. The solid residues are tapped off into a dewatering and sludge handling facility or directly dewatered or applied as slurry for zeolite production or backfill application respectively.
8. Recovered water is reused on the mine or sold, depending upon its quality.

Step 4 may be replaced with a direct feed of dry fly ash from the hopper or silo into a well stirred premix chamber, in which case the AMD is pumped into the premix tank where the slurry is developed to the correct density and specific gravity and then fed to the main tank and held for the correct contact time, prior to release to the settling tank. This may be the preferred route if it is feasible.

8.3 RECOVERY AND APPLICATION OF SOLID RESIDUES

8.3.1 Synthesis of solid residues into Zeolites

A proportion of solid residues recovered in step 7 above is dried and analysed for its Si and Al content. If the ratio of Si to Al is suitable, the material is subjected to aging at 40°C in a solution of sodium hydroxide (or possibly highly alkaline fly ash leachate derived from lagoon storage) at atmospheric pressure in a stirred tank. This step is followed by hydrothermal treatment at 100°C for 12 – 36 hrs in a stirred reactor tank under controlled pressure in order to transform the solid waste residue into high capacity zeolite adsorbents according to methods developed at UWC. The solid zeolite product is washed free of alkali with water recovered from the AMD neutralisation process and dried. Highly alkaline supernatant liquors or wash waters (essentially NaOH solutions) recovered from the hydrothermal synthesis are reused in the zeolite synthesis procedures until spent, or alternatively used as additional alkali source in the neutralisation of AMD, thus generating no waste stream.

Zeolites prepared from ash or solid residues are then further used for:

(i) Process brine stabilization;
(ii) Removal of toxic elements from various waste water streams such as retentates from RO and EDR systems; and
(iii) Solid acid catalysts for application in processing of hydrocarbon feed stocks at for example Sasol.

8.3.2 Application of solid residues as backfill material

The bulk of neutral, solid residues recovered in step (6) of section 8.2 above is either amended with a suitable % of cement or raw fly ash as binder (typically 3 – 5 % as developed at UWC and CSIR) or used as is, and placed underground as backfill material to allow enhanced extraction of coal, prevent surface subsidence, prevent spalding of pillars, prevent ingress of oxygen and thus prevent the formation of acid mine drainage and to divert underground acid mine drainage flows to suitable collection points and allow greater extraction of coal.

8.3.3 Application of solid residues as fill or soil amendment

The bulk of neutral, solid residues recovered in step (6) of section 8.2 above can be applied as fill material in areas of opencast mining where it is premixed with overburden used as fill, in appropriate ratios to enhance soil texture and particle size. This may be used to enhance the clay fraction of sandy soils, and reduce the cost of rehabilitation of mines since not as much additional fill material needs to be imported to make up for the % void replacement after coal extraction.

8.3.4 Recovery and reuse of water

After neutralisation of AMD with fly ash and depending on the process conditions, recovered water from step (8) of section 8.2 can be reused in coal processing, which may not be cost effective, or depending upon its quality it may be released, either for irrigation or into rivers. If necessary, water can be polished via EDR or RO and could be sold as potable water.

8.4 UTILISATION OF ASH AS LINER OR ASHWALL

Fly ash from step (3) in section 10.2 can be applied as follows:

(i) As a liner under or in spoil heaps to prevent AMD generation or release.
(ii) As liner or bulk material for slimes dams to prevent contact between stored water and the mine spoil currently used as dam wall and thus, reduce and mitigate toe seep or prevent formation of acid mine drainage by preventing percolation of stored water through the pyrite containing dam wall.
(iii) Fly ash can be applied in bulk as a continuous ash wall in growing spoils heaps to direct AMD flows or to prevent generation of AMD.
(iv) Fly ash can be added to solid residues in appropriate ratios to enhance binding capacity and strength development of backfill materials.

Figure 8.1: Schematic representation of the potential use of coal mining and power production waste.

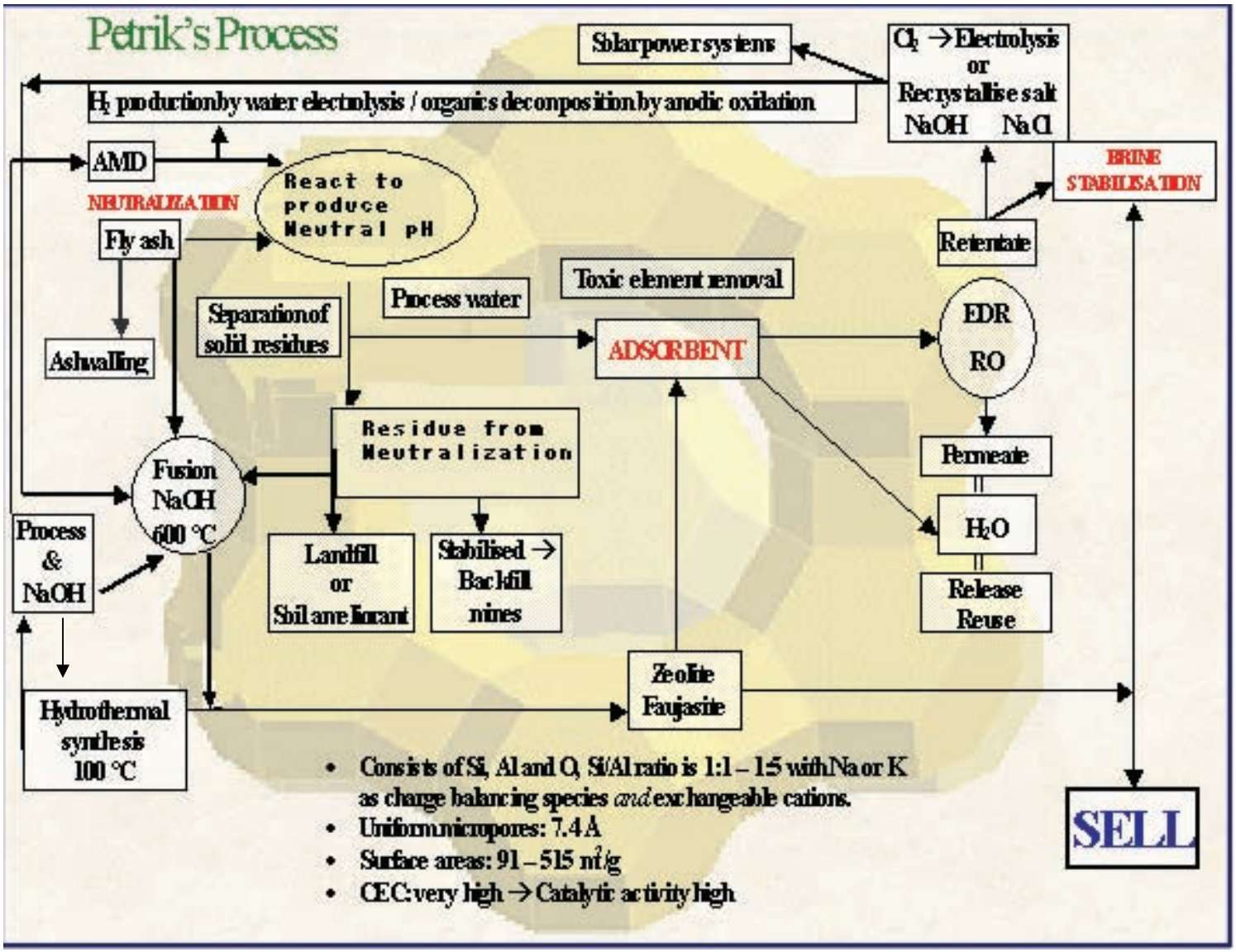

8.5 HYDROGEN PRODUCTION FROM AMD

AMD can be considered a potential electrolyte, and thus may present a suitable matrix to be used in hydrogen production by water electrolysis. It may be feasible to do low efficiency hydrogen production by feeding acidic AMD as catholyte via the cathodic compartment and feed alkaline fly ash leachate via the anodic compartment as anolyte in an electrolyser cell. These electrolytes may have an advantage in terms of reduction of the oxygen evolution potential. Since significant fouling of the electrodes is expected, low cost, discardable carbon based composite electrodes (as developed at UWC) should be applied. The hydrogen produced may be used as feedstock for the microbiological sulphate reduction process.

8.6 SALT RECRYSTALLIZATION

Application of zeolites has the potential to first remove toxic elements from process waters before concentration into brines. Process brines such as the NaCl-containing retentate from RO or EDR systems can also be cleaned of toxic elements by use of zeolite adsorbents as studies at UWC have shown. Moreover the zeolites show significant potential to stabilize process brines, to a much greater extent than ash by itself.

It is also possible to apply these zeolite adsorbents to remove selected elements from brine solutions, thus components in the concentrated but purified saline brine may potentially be recovered. Much purified NaCl may thus be recovered by recrystallisation using solar energy. The production of Cl_2 gas from the concentrated NaCl brine is possible using electrochemical means.

8.7 COST COMPARISONS

The following information is being compiled and some figures were included above with assistance from Anglocoal and CSIR, for a cost comparison to be made in the Navigation on site study in 2005/2006:

- Costs of overall limestone treatment process
- Costs of flocculants for settling of sludge and separation of water and solids
- Costs of biological treatment process
- Costs of H_2S monitoring, and excursion treatment and prevention
- Costs of H_2S scrubbing and conversion to gypsum/sulphur
- Costs of ethanol and any other inputs as biological feedstock
- Costs of energy required to keep biological system functioning
- Costs of energy required for sufficient agitation for all the mixing tanks
- Current handling, treatment and storage costs of sludge (“yellow boy”)

9. GENERAL CONCLUSIONS

The initial study funded by both the WRC and Coaltech2020 during 2001-2003 (WRC Final report K5/1242) provided proof of concept that mixing of coal mine derived AMD and South African fly ash is a suitable method for the low-cost treatment of coal derived acid mine drainage, and allows high recovery of water as well as the preparation of high quality zeolite adsorbents by post process synthesis of solid waste residues. This research received support from industrial partner ESKOM, and is of interest to Sasol and Anglocoal.

The outcomes of the larger scale study funded by the WRC and Coaltech2020 and co-funded by ESKOM during 2004-2005 have been presented in this report. This study determined larger scale neutralisation process parameters. The neutralisation capacity of many different combinations of fly ash and acid mine drainage has been evaluated. Fly ash was sourced from Matla, Arnot, Duvha, Hendrina and Kendal power stations. Acid mine drainage was sourced from Bank, Kromdraai, Brugspruit, Middelburg, Navigation and Landau collieries. The quality of recovered water was determined and a very significant improvement in water quality was observed in almost all cases where fly ash was used to treat acid mine drainage.

The long-term stability, and the extent of potential leaching of toxic heavy metals from ash or solid residues recovered from the neutralisation process was investigated. In particular, the focus was on comparing the stability and performance of backfill materials that were prepared from fly ash residues or ash with various additives as useful materials for passive barriers or underground placement to prevent acid mine drainage generation, subsidence, and air ingress. The physical and chemical properties that were ascertained included characteristics such as hardness, strength as well as the chemistry, and long-term phase transition kinetics of solid fill materials that may in future be in contact with acid mine drainage or waters of seepage.

9.1 NEUTRALISATION OF AMD

The study of the neutralisation of AMD requires the analysis of waters prior to neutralisation and after neutralisation has taken place. This characterisation of waters is necessary to quantify the amount of various elements that is no longer soluble.

The concentration of SO_4^{2-} in the raw AMD can vary by a large margin and even by magnitudes between different samples and between samples of AMD from the same source, drawn at different times. The pH values of AMD waters are between 2 and 3, some concentration events can cause a pH lower than 2, as with Kromdraai AMD. EC and pH are proportional to each other with a lower pH resulting in a higher EC and dissolved solids. Some AMD's had a low buffering capacity and are quickly neutralised. This is a result of low metal concentrations in the AMD.

In recovered, neutralised waters it was found that Fe is reduced to below 0.5 mg/L when the neutralisation reaction is sufficiently aerated or the reaction proceeds for a sufficient length of time to facilitate oxidation (Ash walling study). SO_4^{2-} concentration decreases by a greater amount with higher fly ash to AMD ratios. This indicates that the precipitation of SO_4^{2-} is dependant on alkalinity and more specifically the amount of Ca^{2+} in solution. In general, the concentration of SO_4^{2-} in the water is reduced to around 2000

mg/L or lower. The concentration of Al^{3+} is also alkalinity dependant with the greatest Al^{3+} removal occurring at high fly ash to AMD ratios. Lower ratios do, however, show significant Al^{3+} removal to levels below 6 mg/L. Levels of other minor and trace toxic elements are very significantly reduced.

The amount of alkalinity available or the FA to AMD ratio and the amount time over which the reaction is allowed to proceed determines the final pH of the solution following the neutralisation of AMD. The dissolution and hydrolysis of CaO and MgO from fly ash contribute to an increase in the pH of AMD. This increase in pH causes the precipitation of acid-contributing metals such as Fe^{3+} and Al^{3+} that consume alkalinity and buffer the reaction.

The importance of precipitation was established by calculating the saturation indices of the elements in solution during the neutralisation of AMD. An increased removal of elements such as B, Mg, Mn, Al, Si, total Fe, and Zn was observed at higher FA to AMD ratios. Calculated saturation indices and mineralogical analysis indicated that SO_4, Fe and Al were controlled by mineral solubility. Al concentrations were controlled by secondary phases such as boehmite, basaluminite and gibbsite; Fe by amorphous $Fe(OH)_3$ and goethite and Ca and SO_4^{2-} concentrations were controlled by gypsum solubility. The elements Na, Ca, Ba, Mg, Sr, B, Mo, Se, Si, Mn, and Zn showed development of solubility controls at certain reaction times after the initial dissolution. It is probable that these elements were present as soluble salts and, on dissolution, interacted with components in AMD to form new stable mineral phases that controlled their concentrations.

Mn, Mg, Zn and Cu were removed from solution at a lower pH (5.5 – 7.0) than predicted by thermodynamic calculations, indicating that physical processes such as adsorption and co-precipitation also influence metal removal. The strong association of these elements with the amorphous iron oxide fraction reinforces this hypothesis.

Fe^{2+} is removed through oxidation and subsequent hydrolysis at pH 5.5. A corresponding decrease in SO_4^{2-} concentration is observed, indicating the relevance of the iron-oxyhydroxides in SO_4^{2-} removal.

The extraction process is indicative of the potential fate of the insoluble components of the solid residues recovered after the neutralisation reaction. The extraction established that a very significant percentage of trace elements (except B) is associated with amorphous (cryptocrystalline) Fe-oxides. Fe-oxides are an important sink for trace metals in this process. A significant proportion of Al and Si is associated with the amorphous Fe-oxide phase. Reduction in sulphate concentration was observed when the reaction mixture attained pH 5.5 suggesting either adsorption or incorporation into the iron (III) oxyhydroxides being formed.

A significant finding is that the pollutant species precipitated out of solution upon the FA particulates during the neutralisation reaction are mainly poorly soluble or insoluble. Only Ca, B and Sr remained soluble in water in low percentages.

Active treatment systems:
In order to maximise the benefits of actively neutralising AMD with FA, the optimum process conditions for pilot scale neutralisation of acid mine drainage with fly ash used as

ameliorant or as liming substitute were investigated. Various volumes and sources of AMD were typically contacted with different quantities of FA from various sources in stirred reaction vessels of several different sizes in order to simulate the lime treatment systems currently used for treatment of AMD. Active neutralisation experiments in a pilot scale mixing vessel were conducted for periods longer than those previously used during laboratory scale experiments to ascertain longer term EC and pH trends over the time required for neutralisation.

Numerous experiments were performed to determine the neutralisation potential of various combinations of different fly ashes and AMD's. These experiments were mostly small scale reactions performed in the laboratory. A large scale mixer with a capacity of 250 L was also applied. The motorised, overhead agitation ensures sufficient aeration for rapid Fe^{2+} oxidation. These small and large scale neutralisation experiments were performed with different fly ashes and acid mine drainages at different ratios to determine the optimum conditions for reaction. Fly ash was sourced from Matla, Arnot, Duvha, Hendrina and Kendal power stations. Acid mine drainage was sourced from Bank, Kromdraai, Brugspruit, Middelburg, Navigation and Landau collieries. The pH and EC was recorded over time during the neutralisation reaction and the waters were analysed. The buffer regions associated with neutralisation of natural AMD are observed at pH 2.0-5.0, 5.5-6.0 and 8.5-9.0, as previously reported.

From the reactions between different fly ashes and AMD sources it can be concluded that different ratios and reaction times will apply to different combinations. The various fly ashes and AMD's are all very different from each other, and AMD can vary on a day-to-day basis. The various reactions at different ratios give an idea of which waters require a greater amount of alkaline material or a longer process time.

Fly ash from various sources has the capacity to neutralise AMD at low FA to AMD ratios of 1:6. It is clear that Bank and Landau waters require higher amounts of alkaline material to reach high pH values and be decontaminated because of the high degree of contamination. Kromdraai and Brugspruit waters were not as highly contaminated and required less fly ash. Matla and Duvha ash have a smaller neutralising capacity than Arnot, which appears to contain the greatest amount of alkalinity. Kendal ash does not provide sufficient alkalinity for adequate neutralisation under the conditions tested. The other important factors that control the neutralising capacity of fly ash are particle size and unburnt carbon content which is an indicator of a change in mineralogy of FA due to conditions in the combustion chamber. The smaller the particle size, the more efficient the ash becomes at neutralising AMD. The unburnt carbon in ash may indicate a different mineralogy of the ash due to conditions in the economizer that may reduce the alkalinity available in the fly ash. The variability of the properties of fly ash remains to be investigated.

In a pilot scale neutralisation plant the pH must be constantly monitored and the fly ash feed must be adjusted according to the pH of the reaction to account for variations in AMD and fly ash, or alternatively the contact time should be adjusted.

The active neutralisation of Landau AMD at pilot scale with Arnot fly ash proved feasible at the larger scale, replicating results found in small scale experiments. It was found that lower FA to AMD ratios may be used to achieve a similar, post neutralisation water quality as that for higher FA to AMD ratios, if the neutralisation reaction can

proceed for a greater period of time. Pilot scale studies exhibit some variations in the reaction when compared to the bench scale studies; this is due to greater aeration.

Passive treatment systems:
In order to determine the feasibility of using fly ash as passive barrier or mine backfill, it was necessary to monitor the quality of AMD water in contact with or percolating through ash, in passive systems. This was assessed in passive column studies over a long-term period. The treatment of Middelburg AMD was tested over 280 days using Kendal FA. For treatment of Landau and Navigation AMD, Matla and Duvha FA columns were tested respectively over 45 and 160 days.

The permeate water (also termed leachates) recovered after passive percolation of AMD through columns of fly ash of various lengths was analysed for chemical composition to understand the changes to water quality over time and to model systems in which long-term contact between ash and raw AMD may occur.

It was observed that the shorter the column, the less the pH was buffered and the sooner the pH of the permeate effluent started to decrease, as expected, which indicates the necessity to adjust the dimensions of the ash wall or passive barrier based upon the AMD flows expected and the time of contact. It was found that fly ash can be utilised to treat AMD in-situ in passive systems and that suitable methods of incorporating fly ash into acid generating pyrite containing mine spoil should be devised to control AMD generation. It was also shown that the AMD water quality significantly improves during permeation through fly ash and that the mineralogy of the fly ash changes as a result of contact with the AMD. In all cases the AMD is significantly purified, with the significant reduction in major, minor and trace elements, with the exception of B, Ba and in some cases Cu. Thus, passively neutralising Middelburg AMD with coarse Kendal fly ash has the potential to significantly ameliorate the AMD. Sulphate was not so effectively treated in the shorter columns applied in the case of Kendal FA to treat Middelburg AMD. Better results were obtained for Landau and Matla FA and Navigation AMD and Duvha FA combinations respectively. Column leaching shows excellent improvement in terms of toxic element removal within the first few days and over the longer term.

The fact that columns blocked also indicates the potential to use ash as a passive barrier to direct AMD flows. Long-term column leaching studies suggest that passive barriers constructed with FA or alternatively ash walling with FA in pyrite containing spoil heaps with fly ash has a great potential benefit for AMD remediation.

Thus significant potential exists to reduce the AMD pollution arising in spoil heaps and underground by application of ash walls to prevent AMD generation, or as passive AMD treatment systems or as barriers to direct AMD flows.

Hence, whether fly ash is used as a liming agent in active systems or as a passive treatment option for AMD, a significant improvement in the quality of the recovered water is observed. Around 17 million m^3 /annum of FA are produced from 7 power stations. This FA could find alternative application but is currently being disposed of in ash dumps. The CaO content of FA indicates that the ash is suitable for AMD neutralisation. This research proves that FA is suitable as ameliorant for AMD treatment in either active or passive systems.

9.2 INVESTIGATION OF SOLIDS

Solids refer to fly ash or the solid residues composed of fly ash and insoluble solid precipitates recovered after the neutralisation process. FA ash contains significant quantities of total alkalinity in the form of CaO, MgO, K_2O and Na_2O, thereby increasing the neutralisation potential of FA. Calcium oxide (CaO) is formed upon FA by the oxidation of calcium during coal combustion in the burner of a coal-fired power station.

It is necessary to characterise the mineralogy and elemental composition of solid material in order to gain a complete understanding of the behaviour of elements and ions. There are however difficulties in determining the mineralogy of precipitates from the neutralisation reaction between fly ash and AMD. It is almost impossible to positively identify minerals precipitated during the neutralisation reaction onto the fly ash by XRD because the strong quartz and mullite peaks mask any other less intense peaks.

From the investigation of the various fly ashes used, the following can be concluded:

- There is little significant variation in the mineralogy of different samples of the same ash.
- There is little significant variation in the mineralogy between different fly ash sources and the major component is Mullite and Quartz.
- Alkalinity and particle size show a good, negative correlation (-67%).
- The correlation between alkalinity and surface area is near to perfect (97%).
- The correlation between particle size and surface area is only 54%.
- The presence of significant amounts of carbon in a fly ash sample would indicate mineralogical changes in ash that may severely retard successful neutralisation.
- Elements that form anionic species (As, Se, B, and Mo) at alkaline pH are highly leached from fly ash itself, but were stabilized to lower levels as the pH was increased in the neutralisation reaction between fly ash and AMD.

9.3 PASSIVE BARRIERS AND ASHWALLING

The mineralogical changes in columns of ash after long-term (280 days) exposure to raw AMD flows were examined to assess the physical durability of the ash under simulated weathering conditions.

XRF results give a clear picture of the movement and mobility of elements in the column. Si and Al appear to be highly mobile. In general there are higher amounts of Si and Al towards the bottom of each column. This suggests that as long as the pH of the solution is high enough for Si and Al to be mobile, these elements may be leached out of the column. The initial pH must be greater than 12 for Si and Al to be mobile and a slight decrease of pH will ensure precipitation. Fe and S and hence, SO_4, are concentrated towards the top and middle of columns indicating rapid precipitation, particularly in the case of the Matla FA Landau AMD combination, since the Landau AMD had excessive sulphate levels. The concentration of Fe in the solids recovered from column studies with Kendal ash, show no increase in Fe precipitation as a result of there being very little Fe in the Middelburg AMD to start with. In the Matla and Duvha combinations the concentration of Fe increases after Fe-rich AMD permeation but proportionally there is either not enough of the mineral to be distinguished in XRD, as mullite and quartz peaks tend to mask minerals in lower concentrations, or the Fe precipitates as a mineral with low crystallinity. The concentrations of Mg and Ca, as well as Na, to a lesser degree,

increase towards the bottom of the columns. The most likely reason for this is the matrix effect of the solution.

XRD of the solids recovered from the columns show that Quartz and Mullite originating from the parent FA remained and new mineral phases, namely Gypsum, Calcite and in some cases Hematite or Boehmite were formed after passage of AMD through the FA columns. Although no other clear mineralogical changes could be discerned by XRD, the fact that the columns eventually blocked indicated agglomeration or coalescence of ash particles by insoluble precipitates formed upon contact of AMD with the fly ash.

The AMD has a high EC and as a consequence, a large amount of dissolved constituents, which, combined with dissolved alkalinity from the FA, create a saturated solution. The precipitation of minerals allows other salts to be dissolved, to saturate the solution and precipitate further down the column, thus trapping most pollutants in the ash matrix. Thus, again it is confirmed that ash is suitable for passive treatment of AMD.

9.4 BACKFILLING

A review of the backfilling literature found that several materials had successfully been used as backfill but that fly ash has not been widely considered for that purpose. In terms of backfilling, fly ash has been tested as an additive only to reduce the amount of cement needed. Some studies looked at desirable mixtures of backfill material and assessed backfill stability for different materials, determined effects of loading, sheer strength assessment, etc. Few studies assessed long-term chemical changes within backfill or investigated the influence of acid or alkaline waters on the chemical stability of backfill, or weathering by flowing fluids (e.g. influence of AMD entering from another part of the mine). Some studies assessed the physical durability of the backfill materials and strength changes with time. The literature clearly indicates the beneficial potential of using fly ash as mine backfill. There is apparently no literature concerning the use of solid residues as a backfill material or of utilizing fly ash for ash walling.

The application of suitable backfill would allow the greater extraction of coal. This would allow the extension of the life of coalmines whilst improving their safety by providing support to pillars and walls and minimizing the deformation of the surrounding rock mass into the remaining space preventing subsidence and associated air blasts. Backfilling may mitigate or prevent underground fires and the future production of AMD as well as neutralizing existing AMD.

The choice of backfill is dependant on the physical, hydrological, chemical and mineralogical characteristics of the material. The properties of backfill material that require greatest consideration are compressive strength and permeability. The use of cement addition as a binder in backfill material to improve cohesion can contribute up to half of the costs of mine backfilling. Therefore, investigating the use of other binder materials is of importance.

Investigations were performed into the appropriate admixtures for physical durability, loading and compressive strength assessment to determine how the different backfill materials would behave when pumped and placed in simulated mine environments. Tests were aimed at determining desirable mixtures of backfill material and appropriate slurry densities. The strength development of the solid residues recovered from the

neutralisation of acid mine drainage with fly ash, by itself or blended with ordinary Portland cement or fly ash as binder, was investigated. The moisture content and particle size was determined and a Marsh cone test conducted, prior to curing. Difficulty in obtaining laboratory use and consultants time at CSIR resulted in only the strength development, slurry flow and density parameters being evaluated during this study.

The solid residues recovered from the reaction between Matla fly ash and Navigation AMD were used as test case for the backfill study and had a solids fraction of about 0.7. Flow tests were performed using the Marsh cone test. It was necessary to add water in order to achieve reasonable flow rates in separated solid residues. The amount of water required differed substantially possibly due to a particle size difference in the various FA samples used to prepare solid residues. The results show the influence of the fly ash properties such as particle size on the flowability of the solid residues from the neutralisation of AMD with fly ash.

Moreover, the need to add water for ensuring correct relative density for run out and solids flow rate in the Marsh cone tests indicates that solid residues need not be completely dewatered prior to their work-up into slurries for use as backfill materials, which will reduce operational costs of preparing slurries for backfilling. The process water was also found to be a suitable replacement for ordinary tap water, indicating the possibility to utilize the process water recovered after the neutralisation process to make up slurries for pumping to backfill. When implementing the neutralisation process at large scale, it will be necessary to adjust the operating parameters of the future treatment plant according to the origin and corresponding properties of the fly ash used.

Strength development tests over time were performed. The solid residues were tested by themselves or were blended with a pozzolanic binder (Castle cement) at rates of 1%, 3% and 6% dry weight basis. Strength development in the three different batches was found to be proportional to the proportion of binder used. A more rapid strength development is observed in the first 28 days of curing for the solid residues formulated with process waters than that formulated with tap water. This early accelerated strength development could be due to the formation of gypsum on hydration of the cement binder, with the process waters acting as a rich source of sulphates. Overall, the solid residues formulated using the process waters, had greater unconfined compressive strength at all levels than the solid residues formulated using tap water. These results once more emphasize the opportunity to use the process water slurry containing solid residues that have not been dewatered after the neutralisation process. By dewatering only until the correct relative density is achieved, it would thus be possible to pump these materials to the backfill site directly, without costly settling and dewatering.

With the addition of a binder, the strength of the solid residue material is relatively high and it appears suitable for the purpose of confinement of mined-out areas. The stability of the solid residues is demonstrated through its capacity to develop strength over time. Similar results were obtained in a previous study made on unreacted fly ash (Ilgner, 2000). Moreover, similar trends were observed in these studies compared to values obtained from the literature (Grice, 1998) for fly ash that indicated addition of a binder increased compressive strength, to between 0.75-4MPa, and values obtained in this study were within this range (1.23-3.03MPa - dependent upon binder content (1-6%) and time). Both compressive strength and elastic modulus were still increasing after one year under the experimental conditions of storage.

With the addition of cement as a binder, the strength of the solid residue material is relatively high and it appears suitable for the purpose of confinement of mined-out areas. These experiments tend to confirm that even after being submitted to the neutralisation reaction with AMD, solid residues of fly ash remain suitable as material for backfilling. The stability of the solid residues is demonstrated through its capacity to develop strength over time. Hence, the proposed use of fly ash to first ameliorate AMD by use as a substitute liming treatment, and then use the recovered solid residues for backfill material has been shown to be feasible.

The long-term chemical changes within backfill and the influence of acid waters on the chemical stability of backfill (e.g. influence of AMD entering from another part of the mine) was investigated. Simulated AMD was percolated through fly ash and solid residues resulting from the neutralisation of Navigation AMD with Arnot FA in column leaching studies in order to model the chemical and mineralogical changes that could be expected over time when solid residues are placed underground as fill or backfill material in possible contact with AMD flows. Simulated AMD was used in this study because of logistical constraints and to exclude variability. The solid residues from the neutralisation reaction were compared to blends with unreacted fly ash to give mixtures of varying ratio (5, 25 and 40% unreacted fly ash) and one column was prepared with solid residues blended with 6% cement on a dry weight basis and a further column with fly ash only.

Buffering was observed for all columns but the number of buffering regions and the pH at which the buffering occurred differed. The permeate recovered from the column packed with unreacted fly ash shows a gradual decrease in pH with time from pH 12 – pH 4 after 124 days. The initial pH of the permeate recovered after passage through solid residues was alkaline (pH 8.5). Thereafter pH decreased to 4 for these columns after 124 days. The initial permeates of the 5% fly ash blended solid residues remained neutral for the first 81 days thereafter decreasing to pH 3.5. The initial permeates of the 25% fly ash blended solid residues remained neutral for the first 110 days thereafter decreasing to pH 4. The pH of the 40% fly ash blended solid residues followed the same trend as the column with 25% fly ash. The pH of the permeate of columns containing solid residues blended with 6% ordinary Portland cement dropped to 4 for these columns after only 24 days indicating a reduction in neutralisation capacity when using cement as binder.

The solid residues by themselves performed somewhat similarly to the residual solid/fly ash combinations and considerably better than the Portland cement amended blend, once again highlighting their greater suitability as backfill material, than standard ash/cement binder combinations. It is interesting that the solid residues appear to have a greater buffering capacity for a longer time than the ash by itself. It is also noteworthy that ash as binder replaces cement successfully, and further strength development testing should be performed with these combinations.

The solid residues appeared to have a significant buffering capacity, maintaining alkaline pH for an extended period of time (97 days in the short 0.5m columns used). If placed in a mining area generating AMD, these solids could provide a passive method of treatment of polluted water. The alkaline properties of the original FA or of the solid residues would thus give a possibility to passively treat AMD, with a neutralisation reaction taking place in-situ over an extended period of time. The use of Portland cement as binder reduces this neutralisation capacity to 22 days. Results obtained in the case of addition of

the cement binder may indicate possible excessive aggregation of particles with the Portland cement amendment that may have reduced the permeability by changing the active surface area of particles available for neutralisation. This indicates that caution is necessary in the choice of binder.

It would thus be useful to first apply the FA to actively neutralise the AMD and thereafter apply the recovered residual solids as passive treatment system or as backfill material, so that the full benefit of the FA alkalinity is exploited.

9.5 ZEOLITE SYNTHESIS

Zeolite synthesis from solid residues resulting from the neutralisation of AMD with FA and preliminary testing in simulated wastewater studies was explored. A faujasite rich zeolitic material can be synthesised. The feedstock for the preparation of the zeolite adsorbent was the solid waste residue recovered after reacting FA with AMD at a FA: AMD ratio of 1:3.5. The zeolite adsorbent synthesised with the fusion method has a similar capacity of metal removal compared to a commercial faujasite and better than the commercial ion exchange resin, Lewatit TP207.

The synthesised faujasite removed 100% of Mn in solution and 99.8% of both Co and Pb. In comparison, the commercial ion exchange resin, Lewatit TP207 does not remove metals very efficiently. Manganese removal is only 63%, and over time (24hr) Co removal is 98% and Pb removal is 96%, whereas the zeolite prepared from solid residues removed the maximum amount of all tested contaminant metals after less than an hour of contact with the effluent.

The zeolite adsorbents prepared from solid waste residues could thus be applied in a secondary treatment of process waters which would complement the primary AMD treatment.

9.6 GIS MAPPING OF AFFECTED AREA

GIS mapping to compile maps of the affected area was performed by use of data available from Coaltech2020 partners and/or other sources. It was envisaged that information on volumes of AMD, quality of AMD, neutralising material available, neutralising potential, coal mine locations suitable for backfill, etc. could be mapped, to give some idea of the practicality of neutralisation followed by backfill and the economic potential for this. However, only some of these objectives could be met due to lack of information sharing by mines, government and industry when approached for information. The amount and quality of the data presented in this report make it clear that further studies need to be conducted with more rigorous and accurate data collection, which will require significantly better collaboration between interested parties.

Historic data collected shows that mining water at many Mpumalanga collieries is not yet acidic, including Goedhoop, Kleinkopje, Kriel, New Clydesdale, Sasol Secunda, Tavistock, TNC, Tweefontein, Arnot, Douglas, Greenside, Koornfontein, Middelburg South, Middelburg, Minaar, Rietspruit, whereas South Witbank mining water has a low pH. It is well known, however, that over time mine water tends to become acidic, dependent upon the occurrence of sulphidic minerals in association with the mine.

Most of the coalmining activity is limited to the Highveld and Eastvaal councils with Eastvaal having the maximum activity. There are many collieries within 25 km radius of all the power stations. Duvha is situated 15km east of Witbank, Kriel lies between Ogies and the town Kriel, Matla is 30 km from Secunda, Arnot is 50km east of Middelburg, Kendal is 40km southwest of Witbank and Hendrina is 40km south of Middelburg. The close proximity of these power stations and collieries is important. If FA were to be transported to collieries to neutralise AMD, the distance to be travelled in most cases is less than 25 km between Witbank and Bethal. There are also a significant number of collieries within the range of 12.5 km from the power stations between Witbank and Bethal but fewer collieries near to the remaining power stations.

Observable seasonal variations of water quality for Kleinkopje, South Witbank and TNC could not be seen in analysis of historical data that had been collected over a period of 4-11 years. Variations occurred, though, but were not repeated from one year to another. These results show that the pH and concentrations of dissolved species in AMD are under the combined influence of many uncontrolled factors, such as amount of rainfall, amount of pyrite in the coal, composition of gangue rock, rate of coal extraction, etc.

In future work the monitoring of AMD properties must be set up on a daily or weekly basis for an extended period of several months or years. This could bring a detailed knowledge of AMD characteristics and variations. It would be highly useful in the evaluation of the remediation capacity of FA.

9.7 INTEGRATED AMD/FLY ASH MINE BACKFILL SCHEME

Current AMD treatment plants based on limestone are inefficient and costly and need to be redesigned. A plant using fly ash as the alkaline material is a realistic alternative to more expensive alkaline material. The potential to employ an integrated waste management scheme, “the Petrik Process” based upon the use of fly ash, is presented:

1. Neutralisation of fly ash and AMD from various sources;
2. Use of solid residues as backfill in real coal mines;
3. Recovery of almost all water;
4. Application of solid residues to prepare zeolites;
5. Use of zeolites for brine stabilization
6. Use of zeolites for toxic element removal from dilute process streams
7. Use of fly ash for ash walling or lining;
8. Application of solid residues as soil amendment
9. Hydrogen production from AMD
10. Salt recrystallisation from process brines
11. Chlorine production from process brines
12. Use of recovered water for irrigation

The results obtained thus far at UWC show that items 1-7 are very feasible, and plans are being formulated to investigate the feasibility of items 8-12. Site visits and presentations to market the idea to mines has been successful and proposals for implementation have either been accepted or are under consideration at present. Cost estimates are being prepared for large scale testing of item 1 on site at Navigation. All costs and volumes quoted are estimates based upon the Anglocoal Navigation treatment plant.

10. RECOMMENDATIONS

Use of fly ash to first ameliorate AMD by use as a substitute liming treatment, and then use the recovered solid residues for backfill material is herewith shown to be feasible. It is thus recommended that the full benefit of FA application is exploited by first utilizing FA for neutralisation in active systems and then applying the solid residues as void filler, or backfill with or without suitable binder (e.g. unreacted ash).

Implementation of aspects of the "Petrik's Process" on a larger scale should be now be investigated, in particular: neutralisation of fly ash and AMD from various sources; use of FA derived solid residues as backfill in real coal mines; and use of fly ash for ash walling or lining. The necessary cost evaluation and environmental impact assessment should now be initiated.

Neutralisation using FA to treat AMD requires site specific optimisation.

Long-term studies of causes and trends of variability in AMD should be initiated.

Historic data showing AMD quality trends, sources and volumes should be made available by Coaltech2020-partners for a clear understanding of the neutralisation opportunities available by use of this process.

Variation in AMD and FA quality should be monitored and the process adjusted either by changing the contact time or by adjustment of the FA applied.

The effect of variation of FA mineralogy upon the neutralisation reaction should be further investigated and the effect of differences due to combustion conditions should be established.

It is necessary to investigate the availability of FA from the various power stations in the Witbank area as indications are that not all FA sources are readily exploitable for the neutralisation process, due their alternative application as salt sinks.

Fresh FA collected directly from ash hoppers was utilized in this study. It is not clear whether stored FA would have the same neutralisation capacity and further studies would be required if stored FA from dumps were to be utilized, as the free alkalinity may have been exhausted. Moreover, the composition of some sources of ash may have changed over time because of the practice of using ash dumps as salt sinks or to dispose of other wastes.

Particle size and surface area of FA are important criteria impacting upon available alkalinity versus residual alkalinity. The coarser FA was not as effective as the finer ash in the neutralisation process over the same time period indicating the need for some care in choosing the FA, even from the same source. This also indicates the need for further studies to look at the possibility of using bottom or clinker ash or ash from different combustion processes.

Issues that should be addressed in the continuation study on site at Navigation in 2005/2006 are:

Currently the AMD to Limestone slurry is mixed at a ratio of 250m^3/h to 25m^3/h for the underground mine waters and a significantly higher ratio is used for the "toe seep" AMD waters. This may not be a suitable ratio for the AMD to fly ash option and the process will require optimisation and adjustment in order to be implemented on the existing plant. This will require investigation of the optimum density and specific gravity of fly ash to AMD mixture, the optimum flowability and viscosity of fly ash to AMD mixture as well as optimum flow rates and residence times.

The suitability of feeding the ash directly into the AMD treatment plant must be investigated because the neutralisation process is rapid when a high solid-to-liquid ratio is used and immediately results in a high pH. If AMD is used as makeup water for slurry feed of ash, precipitation of solids will occur, clogging pipes and some alkalinity will be used up, making it difficult to control pH. The most suitable make up water should be investigated if the slurry route is favoured. Slurries may be pumped directly from the ash hoppers instead of first being transported to a dam.

Furthermore, it is necessary to understand the volumes of AMD being treated per year in order to assess the availability of suitable quantities of fly ash. Separate figures should be calculated for treatment of toe seep and underground mine waters. Moreover, the fluctuations in quality of both waters should be well understood.

The relative contribution of immediately soluble and slowly soluble components needs to be established both for neutralisation and for development of pozzolanic characteristics in backfill material.

Application of zeolites to clean various process waters and brine effluent streams should be further investigated at larger scale. In particular, aspects of the "Petrik's Process", relating to: application of solid residues to prepare zeolites; use of zeolites for brine stabilization; use of zeolites for toxic element removal from dilute process streams; should be scaled up and cost estimates and feasibility studies performed.

The possibility to further decontaminate various streams of water prior to being treated by EDR or RO by use of zeolites made from FA or solid residues should be further investigated.

Determination of the degree of recovery of water and the cost necessary to obtain various qualities thereof should be initiated.

Pyrite containing mine spoil should never be used as material for containment of water in dams.

Ingress of water into pyrite containing mine spoil should be avoided.

11. REFERENCES

ABANDA, A.P., Petrik, L. and Fey, M.V. **1999:** Pilot study, Environmental Geochemistry Group, Dept Geological Sciences, University of Cape Town.

ADRIANO, D.C., Page, A.L., Elseewi, A.A., Chang, A.C. and Straughan, A., **1980:** Utilisation and disposal of fly ash and other coal residues in terrestrial ecosystems: A review. *Journal of Environmental Quality*, 9, 333 – 334.

ALVAREZ-AYUSO, E., Garcia-Sanchez, A. and Querol, X. **2003**: Purification of metal electroplating waste waters using zeolites. *Journal of Water Research*, 37, 4855 – 4862.

AMERICAN SOCIETY FOR TESTING AND MATERIALS. **1988**: Standard specification for fly ash and raw or calcined natural pozzolan for use as a mineral admixture in Portland cement concrete. C618 – 88, USA.

AMERICAN SOCIETY FOR TESTING AND MATERIALS, C. 125 – 96 **1997:** Standard Terminology Relating to Concrete Aggregates. Annual Book of ASTM Standards. Vol. 04.02: Concrete and Aggregates, American Society for Testing and Materials, Philadelphia, 61 – 63.

ARCHIBALD, J.F., Hassani, F., Nantel, J. and DeGagné D.O. **1998 a**: Mine Backfill, An Operator's Guide. An interactive CD-ROM for mine operators and engineers. Chapter 1: Introduction. Queens University, Canada.

ARCHIBALD, J.F., Hassani, F., Nantel, J. and DeGagné D.O. **1998 b**: Mine Backfill, An Operator's Guide. An interactive CD-ROM for mine operators and engineers. Chapter 5: Paste backfill. Queens University, Canada.

ARIOGLU, E. and Biron, C. **1983:** Design of Supports in Mines. Wiley and Sons, New York, 248 p.

BARKER, R.M. and Harter, T.R., **1997:** Underground Development at Getchell and Turquoise Ridge. *Mining Engineering*, August, 33 – 41.

BARRET, J.R., Coulthard, M.A. and Dight, P.M. **1978:** Determination of Fill Stability. Mining with Backfill- 12th Canadian Rock Mechanics Symposium, Canadian Institute of Mining and Metallurgy, Quebec, Special vol. 19, 85 – 91

BELEM, T. and Benzaazoua, M. **2003:** Utilisation du remblai en pâte comme support de terrain. Partie I: de sa fabrication a sa mise en place sous terre, In: Symp. Int. Apres-mines, GISOS, Gisos ed., Nancy, France, 5-7 February.

BENZAAZOUA, M., Tokou, B. and Bussiere, B. **2002:** Chemical factors that influence the performance of mine sulphidic paste backfill. *Cement and Concrete Research,* 32, 1133 – 1144.

BENZAAZOUA, M., Fall, M. and Belem, T. **2004:** A contribution to understanding the hardening process of cemented paste fill. *Minerals Engineering,* 17, 141 – 152.

BRITTON, H.T.S. **1956**: Hydrogen ions, fourth edition. Chapman and Hall, London.

BURGERS, C.L., **2003**: Synthesis and characterization of sesquioxidic precipitates formed by the reaction of acid mine drainage with fly ash leachate. *MSc Thesis,* Department of Soil Science, University of Stellenbosch, South Africa.

CAMPBELL, A.E. **1999**: Chemical, physical and mineralogical properties associated with the hardening of some South African fly ashes. University of Cape Town, S.A.

CARLSON, C.L. and Adriano, D.C. **1993:** Environmental impacts of coal combustion residues, *Journal of Environmental Quality*, 22, 227 – 247.

CHAPELLE, F.H., Bradley, P.M. and McMahon, P.B. **1993:** Subsurface microbiology. Chapter 8, In: Alley, W.M. (ed.) Regional Groundwater Quality, Van Nostrand Reinhold, New York.

CHERMAK, J.A. and Runnells, D.D. **1997**: Development of chemical caps in acid rock drainage environments. *Mining Engineering*, June, 93 – 97.

CHUGH, Y.P. and Dutta, D. **1998:** Underground placement of coal processing waste and coal combustion by-products based paste backfill for enhanced mining economics. Mid-Year technical report submitted to Illinois Clean Coal Institute, ICCI project number 97US-1.

CHO, S. and Vipulanandan C. **2002:** Evaluating the Properties of Flowable Fills. Center for Innovative Grouting Materials (CIGMAT) Conference and Exhibition Proceedings: Poster Abstracts, University of Houston, Texas, USA.

COATES, D.F., **1981**: Rock Mechanics Principles. CANMET, Energy Mines and Resources Canada, Monograph No. 874.

COLMER, A.R. and Hinkle, M.E., **1947:** The role of micro-organisms in acid mine drainage. *Science*, 106, 253 – 256.

COOKE, R. and Lazarus, J .H. **1993:** Hydraulic sport systems for the backfilling of deep mines. *Journal of the South African Institute of Mining and Metallurgy,* 93, 2, 25 – 30.

CRAVOTTA III, C.A. and Trahan, M.K. **1999**: Limestone drains to increase pH and remove dissolved metals from acidic mine drainage. *Applied Geochemistry,* vol. 14, 581 – 606.

CROUSE, H.L. and Rose, A.W. 1976: Natural beneficiation of acid mine drainage by interaction with stream water and stream sediment. In: 6th Symposium on Coal Mine Drainage Research, National Coal Association/Bituminous Coal Research, 237 – 269.

DOLD, B. **2003:** Dissolution kinetics of schwertmannite and ferrihydrite in oxidized mine samples and their detection by differential x-ray diffraction (DXRD*). Applied Geochemistry*, 18, 1531 – 1540.

DONOVAN, J.G. **1999:** The effects of backfilling on ground control and recovery in thin seam coal mining. Unpublished Masters Thesis, Mining and Minerals Engineering, Virginia Polytechnic Institute and State University.

DORRICOTT, M.G. and Grice, A.G **2002:** Backfill- The environmentally friendly tailings disposal system. In: Proceedings of Green Processing, The Australasian Institute of Mining and Metallurgy, Melbourne, 265 – 270.

DOYE, I. and Duchesne, J. **2003**: Neutralisation of acid mine drainage with alkaline industrial residues: Laboratory investigation using batch-leaching tests. *Applied Geochemistry*, vol. 18, 1197 – 1213.

DWAF (Department of Water Affairs and Forestry) **1998**: Waste Management Series: minimum requirements for the handling, classification and disposal of hazardous waste. 2nd Edition, Appendix 8.5, Pretoria, South Africa.

EARY, L.E., Dhanpat R., Mattigod, S.V. and Ainsworth, C.C. 1990: Geochemical Factors controlling the mobilization of inorganic constituents from fossil fuel combustion residues: II. Review of the minor elements. *Journal of Environmental Quality*, vol. 19, 202 – 214.

ESKOM Environmental Report, **2001**.

FARZAM, H., Rispin, M. and Karlson, R. **1998:** The use of unique admixture technologies in mine backfill: Technology Description And Case Histories *Minefill*, Ohio, USA.

FISHER, G.L. and Natusch, F.S. **1979:** Size dependence of the physical and chemical properties of coal fly ash. In: Karr, C. Jnr. (ed) Analytical methods for coal and coal products, Vol. III Academic Press, New York. 489 – 541.

GITARI, W.M., Petrik, L., Key, D. and Okujeni, C. **2004**: Neutralisation of acid mine drainage with fly ash: a laboratory investigation of metal and SO_4^{2-} removal in the process water. The *37th National Convention of the South African Chemical Institute*, CSIR International Convention Centre, Pretoria, July 2004.

GRICE, A.G. **1998:** Underground mining with backfill. The 2nd Annual Summit – Mine Tailings Disposal Systems, Brisbane, November.

HASSANI, F., Archibald, J. **1998:** Mine backfill. CD-ROM, Canadian Institute of Mine, Metallurgy and Petroleum.

HOLLMAN, G.G., Steenbruggen, G. and Janssen-Jarkovic, M. **1999:** Two-step synthesis of Zeolites from coal Fly ash. *Fuel*, 78, 1225 – 1230.

HULLET, L.D. and WEINBEGER, A.J. **1980**: Some etching studies of the microstructure and composition of large aluminosilicate particles in fly ash from coal-burning power plants. *Environmental Science and Technology*, vol. 14, 965 – 970.

ILGNER, H.J. **2000:** The benefits of ashfilling in South African Coal Mines, Coal-The Future, 12th International Conference on Coal Research, ICCR, SAIMM.

ILGNER, H.J. **2002:** Cost-effective utilisation of fine and coarse ash to maximise underground coal extraction and to protect the environment. Coaltech 2020 Report, Secunda, Coal Indaba Conference, October, pp 19.

ILGNER, H.J. **2003:** Hydraulic fill or paste? How to make the right decision. 4th one-day seminar on hydraulic transport in the mining industry, 7 April 2003, Indaba Conference Centre.

IWASHITA, A., Sakaguchi, Y., Nakajima, T., Tokanashi, H., Oliki, A. and Kambara, S. **2005:** Leaching characteristics of boron and selenium for various coal fly ashes. *Fuel*, 84, 479 – 485.

JACKSON, M.L., Lim, C.H. and Zelazny, L.W. **1986:** Oxides, hydroxides and aluminosilicates. In: *Methods of Soil Analysis, Part 1, Physical and Mineralogical Methods*, Ed: Klute, A., 2nd Edition, Chapter 6, pp. 101-150. Agronomy Monograph no. 9, American Society of Agronomy, Soil Science Society of America, Madison, USA.

JENKE, D.R. and Pagenkopf, G.K. **1983:** Chemical changes in concentrated, acidic, metal-bearing wastewaters when treated with lime. *Journal of Science and Technology*, 17, 217-223.

JORGENSON, R.R. and Crooke, D.R., **2001:** Fly ash paste utilisation for placement as mine and landfill backfill at Great River Energy's Coal Creek Station, Minefill, Seattle, 187 – 94.

JUDE, C.V. and T.L. Vandergrift. **1995:** Backfilling Materials and Methods for Stress Transfer Modification in Deep Longwall Mines. Washington, DC: U.S. Bureau of Mines.

KESIMAI, A., Yilmaz, E., Ercikdi, B., Alp, I., Yumulu, M. and Ozdemir, B. **2002:** Laboratory testing of cemented paste backfill. *Madencilik*, 11 – 20.

KITANO, Y., Okumura, M. and Idogaki, M. **1978:** Co-precipitation of borate-boron with calcium carbonate. *Geochemical Journal*, 12, 183 – 189.

KOMNITSAS, K., Bartzas, G. and Paspaliaris, I. **2004:** Efficiency of limestone and red mud barriers: Laboratory column studies. *Minerals Engineering*, 17, 2, February, 183 – 194.

KOONER, Z.S. **1993**: Comparative study of adsorption behavior of copper, lead, and zinc onto goethite in aqueous systems. *Environmental Geology*, 21, 242 – 250.

LANDRIAULT, D.A. **1995:** Paste backfill mix design for Canadian underground hard rock mining. In: Proceedings of the 97th Annual General Meeting of the CIM Rock Mechanics and Strata Control Session, Nova Scotia.

LEVENS, R.L., Marcy, A.D. and Boldt, C.M.K. **1996**: Environmental Impacts of Cemented Mine Waste Backfill. Report of Investigations 9599, United States Department of the Interior, United States Bureau of Mines, ISSN 1066-5552, pp 29.

LOEWENTHAL, R.E., Morgan, B.E and Lahav, O. **2004**: Fundamental study of a one-step ambient temperature ferrite process for treatment of acid mine drainage waters. *Rapid communication* Department of Civil Engineering, University of Cape Town, South Africa.

MAREE, J.P., Van Tonder, G.J. and Millard, P. **1996:** Underground neutralisation of mine water with limestone. Water Research Commission Report No. 609/1/96, Pretoria, South Africa.

MATTIGOD, S.V, Dhanpat R., L.E. Eary, and Ainsworth, C.C. **1990:** Geochemical factors controlling the mobilization of inorganic constituents from fossil fuel combustion residues: I. Review of the major elements. *Journal of Environmental Quality,* 19, 188 – 201.

MILLER, S. and Murray, G. **1998:** Prediction of time dependant factors in acid mine drainage. Third International Mine Water Congress, Melbourne, Australia. 165–172.

MITCHELL, P. **2000:** Prediction, prevention, control and treatment of acid rock drainage. Chapter 7, In: Warhurst, A. and Noronha, L. (eds.) Environmental policy in mining: corporate strategy and planning for closure. CRC Press.

MORENO, N., Querol, X. and Ayora, C. **2001:** Utilisation of zeolites synthesized from coal fly ash for the purification of acid mine waters. *Journal of Environmental Science and Technology*, 35, 3526 – 3534.

MULLER, J., Seiler, K.P. **1999:** Relevance of self-sealing processes in pyrite sinters for heavy metal mobility. In: Armanson, A.H. (Ed.), 5th *Symposium in Geochemistry of the Earth's surface* Balkema, Rotterdam, 211 – 214.

NATIONAL ACADEMY OF SCIENCES **1975:** Underground Disposal of Coal Mine Wastes. National Academy of Engineering, Washington, D.C., p 172.

NIEMINEN, P. and Seppänan, P. **1983:** The use of blast furnace slag and other by-products as binding agents in consolidated backfilling at Outokumpu Oy's mines. Proceedings of the International Symposium on Mining with Backfill, Luleâ, June, 49 – 59.

NORDSTROM, D.K. and Southam, G. **1997:** Geomicrobiology of sulphide mineral oxidation. Chapter 11, In: Banfield, J.F. and Nealson, K.H. (eds.) Geomicrobiology: Interaction between microbes and minerals. Rev. Mineral, 35, 361 – 390.

O'BRIEN, R.D. **2000:** The neutralisation of acid mine drainage by fly ash. Unpublished MSc Thesis, University of Cape Town, RSA.

PALARSKI, J. **1993:** The use of Fly Ash, tailings, rock and binding agents as consolidated backfill for coal mines. In: Proceedings of Minefill 93, Ed. Gelen, H.W., The South African Institute of Mining and Metallurgy, 403 – 408.

PANDAY, K.K.; Prasad, G. and Singh, V.N. **1985**: Copper (II) removal from aqueous solutions by fly ash. *Journal of Water Research*, 19, 869 – 873.

PARKHURST, D.L. **1995:** User's guide to PHREEQC: A computer program for speciation, reaction-path, advective-transport, and inverse geochemical calculations. U.S. Geological Survey Water-Resources Investigations Report, 95 – 4227, 143 p.

PETRIK L., White R., Klink M., Somerset V., Key D., Iwuoha E., Burgers C., Fey M.V. **2004a:** Utilisation of fly ash for acid mine drainage remediation. Water Research Commission Final report K5/1242.

PETRIK L., Burgers C., Etchebers, O., Hendricks, N., Maluleke, A. **2004b:** Heavy metal removal from water with electrosorption using zeolite adsorbents made from solid residues. Water Research Commission report K1546.

POLAT, H.; Pankratov, I. and Polat, M. **2004:** A new methodology for the removal of boron from water by coal and fly ash. 163, 173 – 188.

PULLES, W., Heath, R. and Howard, M. **1996**: A manual to assess and manage the impact of gold mining operations on the surface water environment. Water Research Commission Report No. TT 79/96, Pretoria, South Africa.

QUEROL, X., Umana, J.C., Plana, F., Alasuey, A., Lopez-Soler, A., Valreo, M.A., Domingo, M.J. and Garcea-Rojo, E. **2001:** Synthesis of zeolites from fly ash at Pilot plant scale: Examples of potential applications. *Fuel Journal*, 80, 857 – 865.

QUEROL, X., Moreno, N., Umana, J.C., Alastuey, A., Hernadez, E., Lopez-Soler, A. and Plana, A. **2002**: Synthesis of zeolites from coal fly ash: an overview. *International Journal of Coal Geology*, 50, 413 – 423.

RAYALU, S., Meshram, S.U. and Hasan, M.Z. **2000:** Highly crystalline faujasitic xeolites from flyash. *Journal of Hazardous Materials*, B77, 123 – 131.

REARDON, E.J., Czank, C.A., Warren, C.J., Dayal, R. and Johnston, H.M. **1995:** Determining controls on element concentrations in fly ash leachate. *Waste Management and Research*, 13, 435 – 450.

RICOH, P., Lecuyer, I. and Le Cloirec, P. **1999:** Removal of Cu^{2+}, Zn^{2+} and Pb^{2+} by adsorption onto fly ash and fly ash/lime mixture. *Water Science and Technology*, 39, 239 – 247.

ROSE, S and Elliot, W. C. **2000:** The effects of pH regulation upon the release of sulfate from ferric precipitates formed in acid mine waters. *Applied Geochemistry*, 15, 27 – 34.

ROSE, S and Ghazi, M.A. **1997:** Release of sorbed sulfate from iron oxyhydroxides precipitated from acid mine drainage associated with coal mining. *Environmental Science and Technology,* 31, 2136 – 2140.

SAMARIN, A., **1997:** Total Fly Ash Management: From concept to commercial reality. *Australian coal review*. Nov.

SEOANE, S. and Leiros, M.C. **2001:** Acidification-Neutralisation Processes in a Lignite Mine Spoil Amended with Fly Ash or Limestone. *Journal of Environmental Quality*, 30, 1420 – 1431.

SHUMAN L.M. **1982:** Separating soil iron and manganese oxide fractions for micro-element analysis. *Soil Science Society of America Journal*, 46, 1099 – 1102.

SCHULZE, D.G. **1981:** Identification of soil iron oxides minerals by differential x-ray diffraction. *Soil Science Society of America Journal*, 45, 437 – 440.

SCOTT, K.M. **1987:** Solid solution in, and classification of gossan-derived members of the alunite-jarosite family, northwest Queensland, Australia. *American Mineralogy*, 72, 178 – 187.

SCHWERTMANN, U., Schulze, D.G., and Murad, E. **1982:** Identification of ferrihydrite in soils by dissolution kinetics, differential X-ray diffraction, and Mössbauer spectroscopy. *Soil Science Society of America Journal*, 46, 869 – 875.

SINGER, P.C. and Stumm, W. **1970:** Acid mine drainage: The rate determining step. *Science*, 167, 1121 – 1123.

SINGH, D.N. and Kolay, P.K. **2002:** Simulation of ash-water and its influence on ash characteristics. *Progress in Energy and Combustion Sciences*, 28, 267 – 299.

SIRIWARDANE, H.J., Kannan, R.S.S. and Ziemkiewicz, P.F., **2003:** Use of Waste Materials for Control of Acid Mine Drainage and Subsidence, *Journal of Environmental Engineering*, 129, 10, 910 – 914.

SKOUSEN, J., Bhumbla, D.K. and Sencindiver, J. **1997:** Hydraulic conductivity of ash mixtures and their effect on acid mine drainage. Chapter 23, Research in acid mine drainage and mine land reclamation, West Virginia University, West Virginia.

SMITH, D.M. and Rauch, H.W. **1987:** Assessment of Class V Well Injection of Coal Mining Waste into Underground Mines in West Virginia. International Symposium on Class V Injection Well Technology, Washington, DC, 20 – 24 September.

SMITH, I.M. **2005:** Land uses of coal fly ash – benefits and barriers. IEA Clean Coal Centre Report CCC/96, UK, p 30.

STOESSELL, R.K. **1988**: 25^{o}C and 1 atm dissolution experiments of sepiolite and kerolite. *Geochimica et Cosmochimica Acta*, 52, 365 – 374.

STUMM, W. and Lee, G.F. **1961**: Oxygenation of ferrous iron. *Industrial and Engineering Chemistry*, 53, 143 – 146.

STYSZKO-GROCHOWIAK, K., Gołaś, J., Jankowski, H. and Koziński, S. **2004**: Characterization of the coal fly ash for the purpose of improvement of industrial on-line measurement of unburned carbon content. *Fuel: Science and Technology of Fuel and Energy*. 83, 1847 – 1853.

SUMMERS, K.V., Rupp, G.L. and Gherini, S.A. **1993:** Physical-chemical characteristics of utility solid wastes. Research report EPRI EA-3236, Electrical Power Research Institute, Palo Alto, CA, USA.

TAMAURA Y., Katsura, T., Rojarayanont, S., Yoshida, T. and Abe, H., **1991**: Ferrite process; Heavy metal ions treatment system. *Water Science Technology*. 23, 1893 – 1900.

UHLMANN, W, Büttcher, H., Totsche, O. and Steinberg, C.E.W. **2004**: Buffering of acidic mine lakes: the relevance of surface exchange and solid bound sulphate. *Mine Water and the Environment*, 23, 20 – 27.

UNINE, F. **1998:** Surface chemical Characteristics of fly ash derived zeolites. Unpublished B.Sc Hons Thesis, Chemistry Department, University of Cape Town, South Africa.

USEPA (United States Environmental Protection Agency) **1999:** The Class V Underground Injection Control Study: Mining, Sand, or Other Backfill Wells. Office of Ground Water and Drinking Water, Volume 10, pp 74.

VAN DER HOEK, E.E and Comans, R.N.J. **1996**: Modeling arsenic and selenium leaching from acidic fly ash by sorption on iron (hydr)oxide in the fly ash matrix. *Environmental Science and Technology*, vol. 30, 517 – 523.

WARREN, C.J and Dudas M.J. **1984**: Weathering Processes in Relation to Leachate Properties of Alkaline Fly Ash. *Journal of Environmental Quality*, 13, 530 – 538.

WAKSMAN, S.A. and Jaffe, J.S. **1921:** Acid production by a new sulphur-oxidising bacterium. *Science*, 53 – 216.

WEBSTER, J.G., SWEDLUND, P.J. and WEBSTER, K.S. **1998**: Trace metal adsorption onto an acid mine drainage iron (iii) oxyhydroxy sulphate. *Environmental Science and Technology*, vol. 32, 1361 – 1368.

WHITE, R.A. 2000: Behaviour of the rare earth elements in ochreous mine drainage: a laboratory and field study. *Un published PhD*, University oF Wales, Aberystwyth, UK.

YASCHYSHYN, D.N. and Amaratunga, L.M. **1997:** Development of a high modulus paste fill using fine gold mill tailings. *Geotechnical and Geological Engineering*, 15**,** 3, 205 – 219.

YILMAZ, E., Kesümal, A. and Erçikdi, B. **2003:** The factors affecting strength and stability of paste backfill. *Bulletin of Earth Sciences Application and Research*, Centre of Hacettepe University, 28, 155 – 169.

ZIEMKIEWICZ, P.F. and Black, D.C. **2002:** Water Quality Effects of Beneficial CCBs Use at Coal Mines. Proceedings of Coal Combustion By-Products and Western Coal Mines: A Technical Interactive Forum, Eds: Vories, K.C. and Throgmorton, D., April 16-18, Colorado, U.S. Department of Interior, Office of Surface Mining and Coal Research Center, Illinois.

APPENDIX A. CAPACITY DEVELOPMENT AND TECHNOLOGY TRANSFER

WRC K5/1458: Fly ash and AMD neutralisation and Backfill project

The project was carried out at the newly formed South African Institute for Advanced Materials Chemistry (SAIAMC), which now incorporates the formerly known Inorganic Porous Media Group (IPMG) at the University of the Western Cape. In 2004, the IPMG applied for and was granted institutional status by UWC and the SAIAMC is now hosted by the Faculty of Science at UWC.

The submitting organisation, University of the Western Cape (UWC), is a previously disadvantaged institution. The execution of the research project has contributed to a significant improvement in the research capacity of this organisation and, as a result, to higher quality teaching programmes.

A.1 PROJECT PARTICIPANTS

Project leaders: L. Petrik, UWC

A.1.1 Students

This programme in environmental remediation of acid mine drainage, has allowed 9 students to proceed with higher degrees, supported four postdoctoral students, and provided work study to 2 students and research experience to three MSc graduates.

2003: Drs. R. White, R. Jalari (completed in June 2004)
2004/5: Drs O. Etchebers, R. Vadapalli (Post docs)
Students graduated in 2003 on previous associated project WRC K5/1242: C. Burgers (MSc) V. Somerset (MSc); S. Mavundla (Hons)
Graduated in 2004: M. Klink (MSc),
Graduating in 2005-6: N.Hendricks (MSc), T. Sonqishe (MSc pt), M. Gitari (PhD), (UWC); D. Surender (MSc pt); K. Reynolds (PhD pt) (Eskom, UWC)
Workstudy and internships 2004: C. Cakana (Pentech), 2005: M.Ndaba,
Research assistants: C. Burgers (MSc), G. Mongwe (MSc), A. Ellendt (MSc)
This list includes: 14 students of which 8 are women and 10 are historically disadvantaged.

A.2 INDUSTRIAL PARTNERSHIP

Eskom site specific study at Arnot: 2003 2005 Damini Surender;

Eskom leaching and ash walling study; 2003 -2005 Kelly Reynolds

L. Petrik, 2005. COALTECH 2020 (Task 6.1.6). Stability and neutralisation capacity of potential mine backfill material formed by co-disposal of fly ash and acid mine drainage (WRC collaboration K5/1458//3). Continuation study 2005-2007

L. Petrik 2005. Utilisation of Fly Ash to neutralise Acid Mine Drainage at Navigation plant. With Mr. Peter Gunter, Divisional Environmental Co-ordinator, Anglocoal Greenside Colliery - Water and waste management.

L. Petrik, 2005. WRC Project No 1546: Toxic Element Removal From Water With Electrosorption Using Zeolite Adsorbents Made From Co-Disposal Residues.

A.2.1 Summary of interactions with industry

The most important development is the possibility to perform the envisaged large scale study planned for 2005-2006 at Anglocoal, which is currently being negotiated. Meetings were held with Anglocoal P. Günther at Navigation Mine on the 2 June 2004, and again on 8 Feb 2005 and currently the start up of the Second Phase study is underway. Further meetings were held on 8 February, 2005 and 27 May 2005 at Anglocoal Navigation Mine and Environmentek, CSIR Pretoria respectively.

L. Petrik gave a presentation of the progress made on the overall programme at ESKOM Megawatt Park on 1 June 2004.

L. Petrik presented progress on Task 6.1.6 to the Coaltech2020 Steering Committee on the 8 June 2004 and again on 12 April 2005.

A.2.1.1 Consultancy

L. Petrik continued to act as consultant at Eskom TSI Ash Utilisation research management meetings, 2002-2004, Cleveland, Johannesburg, RSA, and currently serves on the Ash Applications Committee. Resources and Strategy Group, C R&D: Water and Applied Chemistry Dept. Eskom

A.3 WORKSHOPS ATTENDED BY THE STUDENTS AND STAFF

2004:
The Coaltech2020 workshop 17-18 June, 2004 in Secunda was attended by L. Petrik, K. Reynolds, and D. Surender.

L. Petrik attended the Renewable Energy and Energy Efficiency Workshop held by InWent and OneWorld in Cape Town on 31 Aug and 1 Sept. 2004

D. Surender attended the WISA Conference in Cape Town on 3-5 May 2004.

D. Surender attended the Fossil Fuel Foundation – Short Course – Coal Ash at Wits University on 8 June 2004.

D. Surender attended the Fossil Fuel Foundation – Coal Indaba in Fourways, Johannesburg on 10-12 November 2004.

K. Reynolds, attended WISA 2004 and presented: The utilisation of an ash wall for the treatment and control of Acid Mine Drainage.

K. Reynolds, attended the Sustainability of Coal Colloquium.2004 and presented: The utilisation of a fly ash wall of the treatment and control of Acid Mine Drainage.

K. Reynolds attended INDABA in Nov 2004 and presented: The use of an ash wall for the treatment of AMD, for Eskom Resources and Strategy.

K. Reynolds attended Biennial Ground water Conference 7-9 March 05 and presented: Ash walling for the treatment and control of AMD, for Eskom Resources and Strategy.

2005:

D. Surender and L. Petrik. Development of a protocol for the neutralisation and amelioration of acid mine drainage with fly ash. Full paper. The World of Coal Ash 2005, incorporating International Ash Utilisation Symposium of the UK CAER and the ACAA's 16th International Symposium, as well as meeting of the U. S. Office of Surface Mining, April 11-15, 2005, Lexington, Kentucky, USA.

M.W. Gitari, V.S. Somerset, L.F. Petrik, D. Key, E.I. Iwuoha and C. Okujeni. Mineralogy and trace element partitioning in coal fly ash/acid mine drainage co-disposed solid residues. Full paper. The World of Coal Ash 2005, incorporating International Ash Utilisation Symposium of the UK CAER and the ACAA's 16th International Symposium, as well as meeting of the U. S. Office of Surface Mining, April 11-15, 2005, Lexington, Kentucky, USA

M.W. Gitari, V.S. Somerset, L.F. Petrik, D. Key, E.I. Iwuoha and C. Okujeni. Treatment of acid mine drainage with fly ash: Removal of major, minor elements, SO_4 and utilisation of the solid residues for wastewater treatment. Full paper. The World of Coal Ash 2005, incorporating International Ash Utilisation Symposium of the UK CAER and the ACAA's 16th International Symposium, as well as meeting of the U. S. Office of Surface Mining, April 11-15, 2005, Lexington, Kentucky, USA

World of Coal Ash Conference 11-15th April, Lexington, Kentucky, Attendance by W. Gitari (PhD), K. Reynolds(PhD), D. Surender (MSc)

A.4 STUDENT DEVELOPMENT (INCLUDING GENDER AND EQUITY)

Students performed different aspects of various tasks of the overall programme as part of their Honours, Masters or Doctoral dissertation or as in service training. N. Hendricks has written up her thesis in 2004, and will be graduating in 2005. T. Sonqishe is a part time student who will continue in 2005 performing aspects of this study. PhD students W. Gitari, K, Reynolds and MSc student D. Surender, continued with their studies in 2004 and hope to complete by the end of 2005 or early 2006.

The student assistants performing research on the associated WRC project for 2004 and that received in service training during 2004 were G. Mongwe (MSc), C. Burgers (MSc).

Students Graduated in 2004 from the associated WRC projects: M. Klink (MSc);
Post-doc completed in June 2004: R. Jalari (supported by the associated WRC project).

2 new Post doctoral fellows started in 2004, namely O. Etchebers and R. Vadapalli, and a new in service trainee, namely A. Ellendt (MSc) commenced her research in Sept 2004.

A.4.1 Post graduate training

Experiential learners (NDT/B. Tech work study): Peninsula Technikon student C. Cakana, successfully did her in service training during 2004 on aspects of the project and will continue to complete her B.tech studies at Pentech in 2005. Interviews were attended by L. Petrik with Pentech supervisors B. Hendry and Mr Farmer on student progress during 2004. A Unisa part time student M. Ndaba has started as in-service trainee during 2005.

Each task of the project has served to prepare students for presentation of their thesis or dissertation. The participation of BSc Hons and NDT or B.Tech in-service trainee students in each task has ensured the continuation of black MSc and PhD students at UWC and also their participation in appropriate areas of science and technology after the completion of their individual projects.

At SAIAMC newly graduated post doctoral students from previously disadvantaged social groups have been given the opportunity for research capacity developed. Team members as well as post doctoral students were allocated to each different task for student guidance.

A.4.2 Staff development

Leslie Petrik
SAIAMC Research Manager, Ms Petrik is currently completing a PhD (part time) focusing on Advanced Nanophase materials for H_2 production.

A.5 PUBLICATIONS IN 2004/5

A.5.1 Theses

Klink, M.J., **2004**: The potential use of South African coal fly ash as a neutralisation treatment option for acid mine drainage. M.Sc (Chemistry). Department of Chemistry University of the Western Cape, South Africa.

Hendricks, N. **2005**. The Application Of High Capacity Ion Exchange Adsorbent Material, Synthesized From Fly Ash And Acid Mine Drainage, For The Removal Of Heavy And Trace Metals From Secondary Co-Disposed Process Waters. MSc (Chemistry), Department of Chemistry, University of the Western Cape, South Africa

A.5.2 Industrial reports

Reynolds, K., **2004**: The use of fly ash for ash walling of acid mine drainage. Report No: RES/RR/02/19247, Project No: 7760T105R, ESKOM Technology Services International.

Petrik, L. and Surender, D. **2004**: The co-disposal and neutralisation of AMD with fly ash: development of a site specific co-disposal protocol for the neutralisation and amelioration of Arnot AMD and fly ash. The co-disposal and neutralisation of AMD with fly ash. Report no: RES/RR/03/21911, Project No: PRJ03-00285900-2010, Eskom Resources & Strategy-Research Development and Demonstration.

L. Petrik, S. Mavundla. **2004**. Characteristics of Classified and Unclassified Ash. Report 1 to Ash Resources (Pty) Ltd, Randburg, Gauteng.

K. Reynolds, L. Petrik. **2004** Acid Precipitation Tests Conducted on Kendal Ash. Task No: 9RE-000049; Project No.: R0089; Generic Contract No.: UWESC001. Report 2

L. Petrik negotiated the following industry studies:
Eskom site specific study at Arnot: 2003 and 2004 - R150 000 Damini Surender
Eskom leaching and ash walling study; 2003 and 2004– R80 000 Kelly Reynolds
Ash Resources, 2004 - R20 000 Sipho Mavundla

A.5.3 Articles in magazines

Petrik L. **2004** Utilisation of fly ash for the neutralisation of acid mine drainage. ESI AFRICA ISSUE 2.

A.5.4 Project reports

L F Petrik, R White, M Klink, V. Somerset, D. Key, E. Iwuoha, C. Burgers and M. V. Fey **2004** Co-disposal of acid mine drainage and fly ash. Research project Water Research Commission (WRC). Final Report No 1242/1/05.

A.5.5 Oral presentations

S. E. Mavundla, V. Somerset, L. Petrik, P. Baker and E.I. Iwuoha. **2004** Fly ash-conducting polymer matrix composites: structural and electrochemical impedance characterisation. ENVIROMIN2004, Environmental and Health Aspects of Mining, Refining and Related Industries, Mowana Safari Lodge, Kasane, Botswana, 28th June to 2nd July 2004.

ESKOM
L. Petrik gave a presentation of the progress made on the overall programme at ESKOM Megawatt Park on 1 June 2004.

Coaltech2020
A full oral presentation overviewing the progress made on associated projects in 2003/2004 was presented to the Coaltech 2020 Surface Environment Steering Committee at CSIR, Johannesburg by L. Petrik on 10 Feb and 8 June 2004, and 12 April 2005.

DWAF
L. Petrik gave a presentation of the progress made on the overall programme at DWAF on 29 March 2005.

A.5.6 Refereed journals

V. Somerset, L. Petrik, O. Etchebers, R. White, D. Key and E. Iwuoha. **2005.** Acid Mine Drainage Transformation of Fly Ash into Zeolitic Crystalline Phases. Fresenius Environmental Bulletin. FEB Vol. 14; No. 10.

V. Somerset, L. Petrik, and E. Iwuoha. **2005** Alkaline Hydrothermal Conversion of Fly Ash Filtrates Into Zeolites 2: Utilisation in Wastewater Treatment. Journal of Environmental Science and Health, 40:1–10, 2005. ISSN: 1093-4529 (Print); 1532-4117 (Online)

V.S. Somerset, E. Iwuoha, L. Petrik, R.A. White, M.J. Klink. **2004.** The use of X-ray fluorescence (XRF) analysis in predicting the alkaline hydrothermal conversion of fly ash precipitates into zeolites. Reference: TAL7145. Journal title: Talanta-Special issue: Southern and Eastern Africa Network for Analytical Chemists - Edited by N. Torto. Vol 64/1 pp 109-114.

VS Somerset, E Iwuoha, L Petrik, RA White, MJ Klink. **2004**. The use of X-ray fluorescence (XRF) analysis in predicting the alkaline hydrothermal conversion of fly ash precipitates into zeolites. Reference: TAL7145. Journal title: Talanta-Special issue: Southern and Eastern Africa Network for Analytical Chemists - Edited by N. Torto. Vol 64/1 pp 109-114

A.5.7 Published Conference Proceedings

L.F. Petrik, M.W. Gitari, O. Etchebers, V.R. Kumar Vadapalli, D. Key, and E.I. Iwuoha. **2005**. Utilisation of fly ash for remediation of coal mines wastewater: reaction on AMD and possible backfilling with residual solids. SAIMM Colloquium: Sustainable Development In The Life Of Coal Mining In South Africa. Carnival City, Boksburg. 13 July. Oral Presentation.

L.F. Petrik, N. Hendricks, V.R. Kumar Vadapalli, O. Etchebers, V.S. Somerset, A. Ellendt, D. Key and E.I. Iwuoha. **2005.** Zeolite Synthesis from solid waste residues: A case study from the treatment of Acid Mine Drainage with Fly Ash. WISA Conference on The Management of Residues Emanating From Water And Wastewater Treatment Sandton Convention Centre. Johannesburg, 9-12 August. Oral Presentation

M.W. Gitari, V.S. Somerset, L.F. Petrik, D. Key, E.I. Iwuoha and C. Okujeni. **2005.** Mineralogy and trace element partitioning in coal fly ash/acid mine drainage co-disposed solid residues. The World of Coal Ash 2005, incorporating International Ash Utilisation Symposium of the UK CAER and the ACAA's 16th International Symposium, as well as meeting of the U. S. Office of Surface Mining, April 11-15, Lexington, Kentucky, USA.

M.W Gitari, V.S. Somerset, L.F. Petrik, D. Key, E.I. Iwuoha and C. Okujeni. **2005.**Treatment of acid mine drainage with fly ash: Removal of major, minor elements, SO_4 and utilisation of the solid residues for wastewater treatment. The World of Coal Ash 2005, incorporating International Ash Utilisation Symposium of the UK CAER and the ACAA's 16th International Symposium, as well as meeting of the U. S. Office of Surface Mining, April 11-15, Lexington, Kentucky, USA.

D. Surender and L. Petrik. **2005**. Development of a co-disposal protocol for the neutralisation and amelioration of acid mine drainage with fly ash. Full paper. The World of Coal Ash 2005, incorporating International Ash Utilisation Symposium of the UK CAER and the ACAA's 16th International Symposium, as well as meeting of the U. S. Office of Surface Mining, April 11-15, 2005, Lexington, Kentucky, USA.

K. Reynolds **2005.** The utilisation of an ash wall for the treatment and control of acid mine drainage. World of Coal Ash 2005, incorporating International Ash Utilisation Symposium of the UK CAER and the ACAA's 16th International Symposium, as well as meeting of the U. S. Office of Surface Mining, April 11-15, Lexington, Kentucky, USA.

M.W. Gitari, L.F. Petrik., D. Key and C. Okujeni. **2004**. Neutralisation of acid mine drainage with fly ash: A laboratory investigation of metal and SO_4^{2-} removal in the process waters. SACI Conference, July 2004

S. E. Mavundla, V. Somerset, L. Petrik, P. Baker and E.I. Iwuoha. **2004**. Fly Ash-Conducting Polymer Matrix Composites: Structural And Electrochemical Impedance Characterisation. ENVIROMIN2004, Environmental and Health Aspects of Mining, Refining and Related Industries, Mowana Safari Lodge, Kasane, Botswana, 28th June to 2nd July 2004

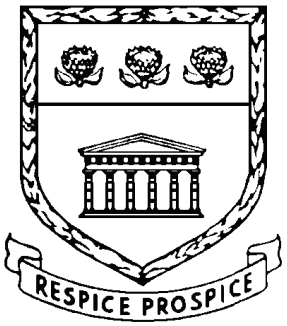

University of the Western Cape
Chemistry Department

APPENDIX B: INTER-LABORATORY LEACHING STUDY WITH USA FLY ASH

Prepared By: C. Burgers

Table of contents **Page**

Inter-laboratory comparison of leaching methods

1. AIM

The participants of the inter-laboratory leaching study were U.S. Department of Energy National Energy Technology Laboratory (NETL), Virginia Tech, University of the Western Cape, West Virginia Water Research Institute, University of North Dakota Energy & Environmental Research Center. The aim of the inter-laboratory leaching study is to characterise the heavy metals released from coal utilisation by-products (CUB). This study is also intended to compare the various leaching protocols in terms of efficacy and precision and to produce comparable data. All participants used one ash derived from the combustion of a bituminous coal from the eastern United States. This ash was observed to be very dark in colour, fine grained and containing Fe.

Three methods were chosen for the ash leaching study performed in the Environmental Research Laboratory in the Chemistry Department at the University of the Western Cape. These methods were the synthetic groundwater leaching and the long-term leaching procedure (SGLP and LTLP), the mine water leaching procedure (MWLP) and the 3-tier leaching protocol (3TLP). The fourth method, serial batch leaching procedure (SBLP) was not tested, as it required the use of an autotitrator, which is not available in the Chemistry Department. Each experiment stage is conducted in triplicate.

To summarise these methods:

- The SGL and LTL procedures are intended to simulate field leaching conditions by shaking an amount of ash with DI water for long periods of 18 hrs and 30 and 60 days.
- The MWL procedure attempts to predict the leachability of metals from CUB's when in contact with acidic water. This is achieved by the sequential addition of low molarity acid to each ash sample until all alkalinity is exhausted and the final filtrate water is similar to the unreacted acid.
- The 3TL protocol consists of several discrete procedures to test the availability of metals at various pH values. First a calibration pre-test is performed to determine the amount of acid required to lower the pH of an ash solution, then an availability test at circumneutral pH is performed, followed by two leachability tests, the first at 11 different pH values and the second with different liquid-to-solid (L/S) ratios.

It was decided that in addition to these three methods, the toxic characteristic leaching procedure would also be performed for comparison, as this is currently the standard method for leaching in South Africa. The TCLP was developed in the USA by the Environmental Protection Agency to measure a waste leachability and the risk it poses to groundwater. The TCLP would be used when a waste is to be landfilled in a site that receives a variety of organic and inorganic wastes and attempts to simulate the dissolving action of the organic acid leachate formed in a landfill. Where a hazardous waste is disposed of in a dedicated landfill, e.g. slags and sludges from mineral extraction and metal manufacturing industries, it is preferable to use the acid rain extraction method. Both methods were tested with the fly ash sample. The complete and detailed methods for all these procedures are given in the methods section (3).

2. MATERIAL

All used the same ash, derived from the combustion of a bituminous coal from the eastern United States. This ash was observed to be very dark in colour and fine grained. X-ray diffraction analysis (XRD) was performed on a PW3830 X-ray generator, PANalytical Philips PW3710 mpd control with CuKα radiation, λ=1.542Å at 40 kV and 25mA. From this analysis (Figure 2.1) quartz, mullite, maghemite and magnetite were identified. It is difficult to differentiate, positively, the magnetite from the maghemite peaks, as there is only a small relative quantity of each mineral in the sample and the mullite and quartz peaks mask their reflections. Figure 2.2 shows the x-ray fluorescence analysis of the ash.

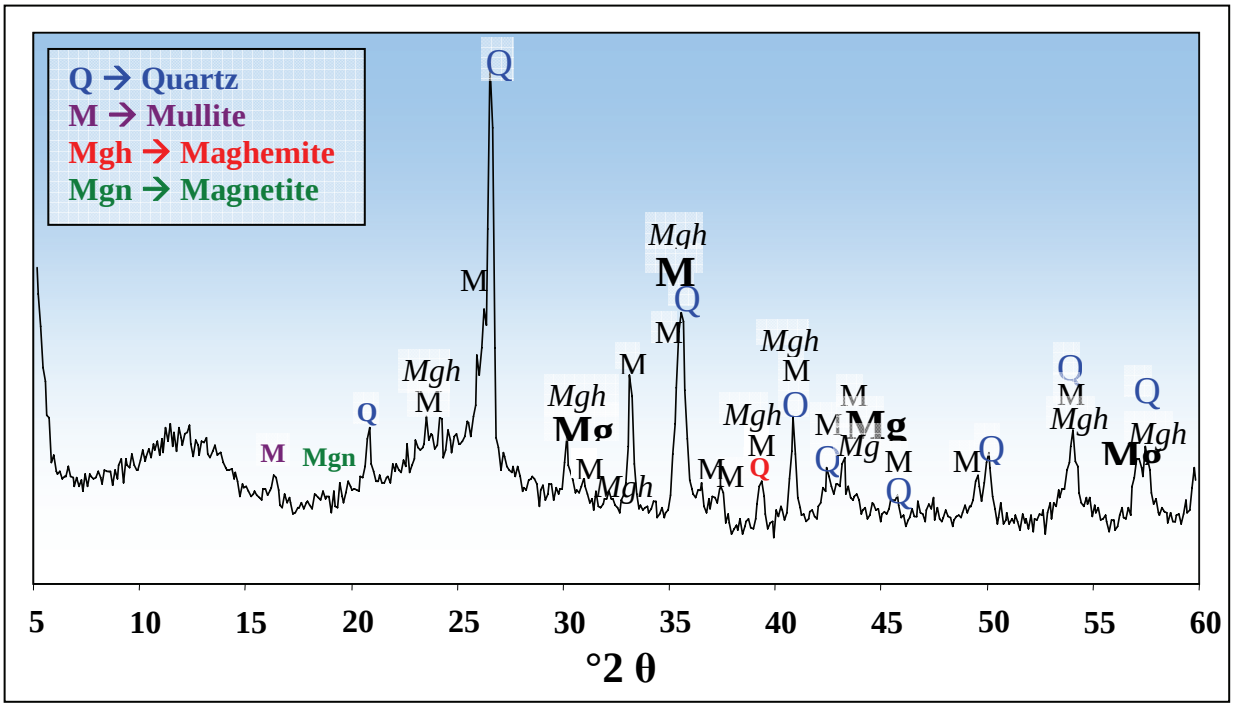

Figure 2.1: XRD pattern for fly ash sample.

Table 2.1: X-ray fluorescence analysis of fly ash.

Major Oxides in wt %				Traces in mg/L					
SiO_2	34.2	K_2O	1.21	S	8461	Rb	64.8	V	187
Al_2O_3	15.5	P_2O_5	0.18	Mo	5.79	Pb	18.0	Ba	445
TiO_2	0.66	SO_3	0.88	Nb	15.2	Zn	56.1	Sc	24.9
Fe_2O_3	15.1	Cr_2O_3	0.02	Zr	174	Cu	78.1		
MnO	0.04	NiO	0.01	Y	39.0	Ni	94.2		
MgO	0.68	H_2O-	0.56	Sr	540	Co	23.5		
CaO	2.30	LOI	28.0	U	1.81	Mn	154		
Na_2O	0.47	Total	99.7	Th	11.6	Cr	122		

3. METHOD

All water samples were analysed by inductively coupled plasma mass spectrometry (ICP MS) on a Perkin Elmer/Sciex Elan 6000. Typical operating conditions were as follows: nebuliser gas flow was ~0.80 L/min, ICP-RF power was 1150 W. The instrument was optimised to minimise oxide and doubly-charged ion formation with Ce/CeO < 0.03 and Ba+/Ba++ < 0.01. Typical instrument sensitivity was ~27 000 cps/ppb for 103Rh.

3.1 DETERMINATION OF MOISTURE CONTENT

Three masses of ash were placed in evaporating dishes and heated in an oven at 100°C. The evaporating dishes were weighed after 6 hours and again after 24 hours. The mass was slightly reduced after 6 hours but had not decreased further after 24 hours (Table 3.1.1). The average moisture content is less than 1% and was thus discounted as having no effect on any experiments.

Table 3.1.1: Moisture content of ash, masses in grams.

Mass of ash	Mass ash + evap. dish	Mass at 6 hrs	Mass at 24 hrs	% Moisture
25.00	181.39	181.23	181.21	0.72
12.00	124.60	124.55	124.55	0.42
17.00	135.82	135.65	135.63	1.12

3.2 SYNTHETIC GROUNDWATER LEACHING PROCEDURE (SGLP) AND LONG-TERM LEACHING (LTL)

Hassett, D.J. **1987**: A Generic Test of Leachability: The Synthetic Groundwater Leaching Procedure. In: Proceedings of the Waste Management for the Energy Industries Conference, University of North Dakota, April 29.

Hassett, D.J. **1997**: The Synthetic Groundwater Leaching Procedure. In: Encyclopaedia of Environmental Analysis and Remediation, Ed: Meyers, R.A., Wiley & Sons: New York, 4797-4803.

3.2.1 SGLP

1. Weigh 100 g sample.
2. Place sample in extractor bottle.
3. Add 2 L DI water (L/S = 20) to extractor bottle.
4. Close the extractor bottle tightly, and place in rotary agitation device.
5. Rotate end over end at 30±2 rpm for 18 hr at room temperature (23 ± 2˚C).
6. Separate leachate by filtering through 0.45 µm filter.
7. Remove aliquot and measure pH.
8. Preserve sample for analysis.

3.2.2 LTLP

9. Repeat above procedure for time periods of 30 and 60 days.

3.3 MINE WATER LEACHING PROCEDURE (MWLP)

Ziemkiewicz, P.F., Simmons, J.S. and Knox, A.S. **2003**: The mine water leaching procedure: Evaluating the environmental risk of backfilling mines with coal ash. . In Chemistry of Trace Elements in Fly Ash, Eds: Sajwan, K. S., Alva, A. K. and Keefer, R. F., Kluwer Academic/Plenum Publishers. 75 – 90.

1. Weigh a 100 gram sample of CCB.
2. Place CUB sample in 2L TCLP bottle.
3. Add 2 litres of mine water or 0.002 N H_2SO_4 (approximate pH = 3) to TCLP bottle.
4. Seal containers with Parafilm® then place lids ensuring a tight seal.
5. Place containers on the rotating platform.
6. Agitate for 18 hours at 30 rpm.
7. At the end of each 18 hr agitation cycle filter contents through 0.7 µm[1] acid rinsed TCLP filter paper using a stainless steel pressure filtration unit at or below 20 psi.
    a. Rinse solids back into corresponding containers using 2 L "fresh" mine water or DI water. Seal containers and place back onto the rotating platform for another 18 hr cycle.
    b. Collect filtrate and measure pH. Divide leachate into 2 aliquots. One is not acidified for pH, alkalinity, acidity and sulphate analysis, and one is acidified with 1 ml of nitric acid for metal analysis[2].
8. Repeat procedure until the pH of the leachate is equal to 3±0.1.

3.4 THREE TIER LEACHING PROTOCOL (3TLP)

Kosson, D.S., van der Sloot, H.A., Sanchez, F. and Garrabrants, A.C. **2002**: An integrated framework for evaluating leaching in waste management and utilisation of secondary materials. *Environmental Engineering Science*, 19, 159 – 204

3.4.1 Titration pre-test (3TLPa)

1. Add sample (8 g dry weight) to 1 L or larger beaker
2. In graduated cylinder measure, 800 mL DI water (L/S = 100) and add to beaker.
    a. Agitate slurry with magnetic stirrer for 5 minutes.
    b. Make 3 pH measurements and record average.
3. If natural pH is above 12, add minimum aliquot of 100 µL 2N HNO_3 and mix at medium speed for 20 minutes.
    a. Allow suspension to settle for 5 minutes, then measure pH
    b. Record volume of acid and pH
    c. Repeat steps adding 100 µL increments of 2N HNO_3 until an approximate pH = 2 is reached.
4. If natural pH of slurry is less than 12, repeat the titration pre-test using 100 µL aliquots of 1N KOH until a pH of approximately 12 is reached.

---

1 If 0.7 µm filter paper is available in your laboratory use it, otherwise use 0.45µm and note it on your log sheets.

2The need for sample preservation is determined by the time between sample collection and analysis. Follow your laboratories normal procedure and note it on the log sheets

5. Record cumulative acid/base volumes, as meq/g, and pH. Plot titration curve (Table 3.4.1 and Figure 3.4.1).

Table 3.4.1: Example of Volume of 2M HNO_3 or 1M KOH added to generate pre-test neutralisation curve.

Added (µL)	Cumulative addition (µL)	Equivalent acid (meq/g)	pH	Added (µL)	Cumulative addition (µL)	Equivalent acid (meq/g)	pH
-1600	-6400	-0.8	12.5	400	400	0.1	5.7
-800	-4800	-0.6	12.1	600	1000	0.25	4.9
-800	-4000	-0.5	11.8	600	1600	0.4	4.3
-800	-3200	-0.4	11.2	400	2000	0.5	3.9
-800	-2400	-0.3	10.3	1000	3000	0.75	3.4
-800	-1600	-0.2	8.8	1000	4000	1	2.8
-800	-800	-0.1	7.9	2000	6000	1.5	2.1
0	0	0	6.8				

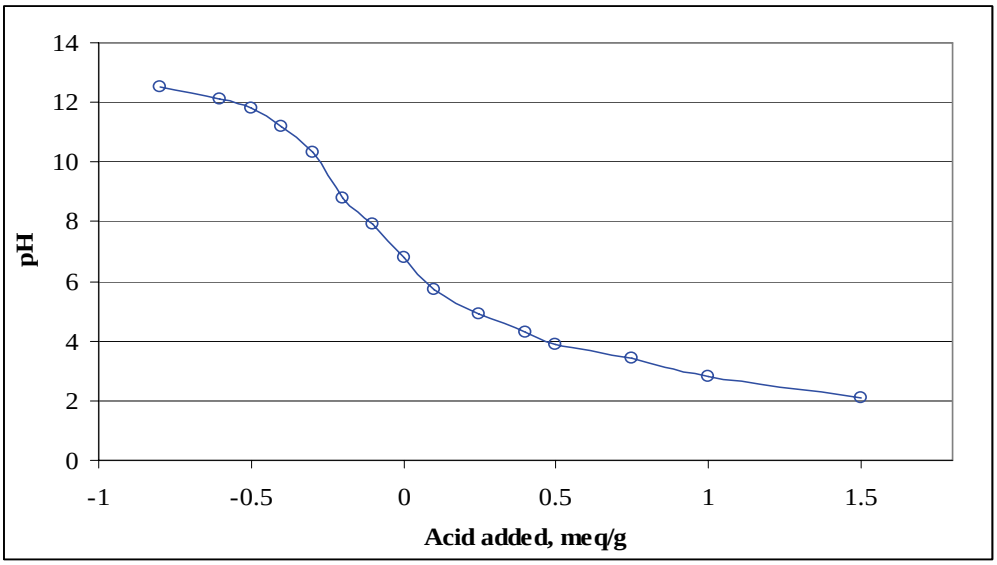

Figure 3.4.1: Example of neutralisation curve for three tier pre-test.

3.4.2 Availability Test (3TLPb)

1. Calculate reagent volumes for 8 g sample at L/S = 100 (Table 3.4.2)
    a. Use the graph generated in the pre-test to estimate the amount of acid needed to obtain pH values of 7.5 (pH target), 7.0, and 8.0 (pH limits).
    b. For a L/S = 100 volume, calculate the amount of 50mM EDTA solution required for each of the three solutions.
2. Place 8 g dry sample in each of 3 high density polyethylene bottles. Label each bottle with target pH value.
    a. Add appropriate volume of 0.05 M EDTA solution to each bottle.
    b. Add appropriate volume of 2N HNO_3 (or 1N KOH) with automatic pipetter to reach target endpoint values.
3. Tighten leak proof seal on each bottle and tumble end-over-end at 28 ± 2 rpm at room temperature for 48 hours.

4. Allow bottles to stand for 15 minutes to clarify leachates. Or centrifuge at 4000 ± 100 rpm for 10 ± 2 minutes.
5. Decant a minimum volume of clear supernatant and measure pH.
    a. Save leachate that is closest to target pH of 7.5
    b. Discard two other leachates.
6. Filter all liquid through a 0.45 µm polypropylene filter membrane with a vacuum filtration apparatus or use non-reactive gas for pressure filtration.
7. Preserve and store leachate for chemical analysis.
8. Calculate availability as

$$AVL_{EDTA} = C_{EDTA} * L / S$$

where AVL_{EDTA} = constituent availability, mg/kg
C_{EDTA} = concentration, mg/L
L/S = liquid-to-solid ratio (100), L/kg.

Table 3.4.2: Example of acid addition and EDTA make-up for availability test.

End-point pH	Acid addition, meq/g	Volume 2N HNO3	Volume 50mM EDTA, mL	Total volume, mL
7	1.05	4.20	795.80	800
7.5	0.93	3.48	796.52	800
8	0.63	2.52	797.48	800

Calculations assume that the sample is dry. If it contains moisture, this must be subtracted from the volume of EDTA added.

3.4.3 Leachability test 1 (3TLPc)

1. Using the curve generated in the pre-test, estimate the amount of 2N HNO_3 or 1N KOH that must be added to reach the 11 target pH values. (See example in Table 3.4.3)
2. Prepare samples
    a. Place 40 g dry sample in each of 11 high density polyethylene bottles.
    b. Label each bottle with extraction number or acid addition
    c. Add volume of DI water as calculated to reach L/S ratio of 10.
    d. Add volume of 2N HNO_3 (or 1N KOH) as calculated to each sample using adjustable pipetter.
3. Tighten leak proof lid and tumble all samples end-over-end at 28 ± rpm at room temperature of 48 hours.
4. At end of extraction period, allow bottles to stand for 15 minutes or centrifuge at 4000 ± 100 rpm for 10 ± 2 minutes.
5. Decant a minimum volume of clear supernatant and measure and record pH.
6. For each leachate, filter all liquid through a 0.45 µm polypropylene filter membrane with a vacuum filtration apparatus or use non-reactive gas for pressure filtration.
7. Preserve and store leachate for chemical analysis.
8. Liquid-solid partitioning curve.
    a. Plot constituent concentration as a function of solution pH
    b. A release based curve can be generated by plotting the measured concentration (mg/L) by the L/S of 10 L/kg versus the pH.

Table 3.4.3: Example of acid (2M HNO_3) or base (1M KOH) addition for leachability test 1 for a 40 g dry sample, L/S = 10.

Extract	Target pH	Equivalent acid or base added[1] (meq/g)	Total acid or base volume (mL)	Volume DI H_2O (mL)
1	12	-1.1	44.0	356.0
2	11	-0.8	30.0	370.0
3	10	-0.6	23.2	376.8
4	9	-0.2	6.0	394.0
5	8	-0.1	3.6	396.4
6	Natural	0.0	0.0	400.0
7	6	0.1	1.6	398.4
8	5	0.1	2.4	397.6
9	4	0.9	18.0	382.0
10	3	1.8	36.0	364.0
11	2	3.1	62.0	338.0

[1]Negative numbers indicate base addition (1M KOH)

3.4.4 Leachability test 2 (3TLPd)

1. Place appropriate dry sample mass (See Table 3.4.4) in each of 5 high density polyethylene bottles.
2. Add appropriate volume of DI water, using graduated cylinder.
3. Tighten leak proof lid and tumble all bottles end-over-end @ 28±rpm at room temperature of 48 hours.
4. Allow bottles to stand for 15 minutes to clarify leachates or centrifuge @ 4000±100 rpm for 10±2 minutes.
5. Decant a minimum volume of clear supernatant and measure and record pH.
6. For each leachate, filter all liquid through a 0.45 µm polypropylene filter membrane with a vacuum filtration apparatus or use non-reactive gas for pressure filtration.
7. Preserve and store leachate for chemical analysis.
8. Analyse extract for common ionic strength contributing cations (Na, K, Ca) and constituents of interest. Determine conductivity and pH
9. Calculate L/S of pore water as:

$$L / S = \frac{n}{\rho}$$

where L/S = liquid-to-solid ratio on a dry basis, mL/g

n = relative porosity, cm^3/cm^3 estimated by measuring the water adsorption capacity of the matrix

ρ = density of dry material, g/cm^3

10. Extrapolate concentration to L/S of pore water
11. Use concentrations of Na, K and pH to estimate pore water ionic strength and activity coefficients.

Table 3.4.4: Sample size and volume for various L/S ratios.

L/S	10	5	2	1	0.5
Sample wt. (g)	40	40	50	100	200
DI H_20 (mL)	400	200	100	100	100

3.5 TOXICITY CHARACTERISTIC AND ACID RAIN LEACHING PROCEDURES (TCLP AND ARLP)

Department of Water Affairs and Forestry **1998**: Waste Management Series: Minimum Requirements for the Handling, Classification and Disposal of Hazardous Waste. 2nd Edition, Appendix 8.5, Pretoria, South Africa.

3.5.1 Samples

1. The sample must be a minimum of 100 g.
2. The sample must be a dry solid.
3. The sample must be able to pass though a 9.5 mm sieve i.e. the particle size of the solid must be smaller than 10 mm.

3.5.2 TCLP extractions

3.5.2.1 TCLP solution No. 1

Add 5.7 mL glacial acetic acid and 64.3 mL of 1M NaOH to 500 mL of reagent quality water (double distilled) and dilute to a volume of 1 L.
When correctly prepared, the pH of this solution will be 4.93 ± 0.05.

3.5.2.2 TCLP solution No. 2

Dilute 5.7 mL Acetic Acid with double distilled water to a volume of 1 L. When correctly prepared, the pH of this solution will be 2.88 ± 0.05

3.5.2.3 Acid rain solution

Prepare 4 L carbonic acid solution (4 L of carbonated double distilled water).
Dilute to 10 L with double distilled water. Acidify to pH 3.6 – 3.8 with atomic absorption quality HNO_3. All chemicals (and water) must be of the highest purity possible. In this regard, atomic absorption quality chemicals are recommended. It should be noted that AA measurements will be in the 10-20 ppb (0,010 - 0,020 ppm) range. Blanks from reagents used will have to be run with all measurements.

3.5.2.4 Preliminary evaluation

This part of the extraction procedure must be performed to determine which TCLP (No. 1 or 2) solution should be used.

1. Weigh out 5.0 g of dry waste into a 500 mL beaker or Erlenmeyer flask. (The particle size should be 1mm or less).
2. Add 96.5 mL of double distilled water, cover with a watchglass and stir vigorously for 5 minutes with a magnetic stirrer.
3. Measure the pH
4. If the pH is less than 5.0 then use TCLP solution No. 1.
5. If the pH is greater than 5.0 then proceed as follows:
6. Add 3.5 mL 1M HCl and stir briefly.
7. Cover with a watch glass, heat to 50°C and hold at 50°C for ten minutes.
8. Let cool to room temperature and record the pH
9. If the pH is less than 5.0, then use TCLP solution No. 1.

10. If the pH is greater than 5.0, then use TCLP solution No. 2.

3.5.2.5 Extraction for analysis of contaminants

1. Weigh out 100 gram of the dry waste that can pass through a 9.5 mm sieve and quantitatively transfer it to the extraction bottle.
2. Add 2 L of the appropriate TCLP solution (No. 1 or 2 as determined by preliminary evaluation) and close bottle tightly.
3. Rotate in agitation apparatus at 30 rpm for 20 hours. Room temperature should be maintained at 23 ± 2°C.
4. Filter through a glass fibre filter and collect filtrate. Record the pH of filtrate.
5. Take aliquot samples from the filtrate for determination of metal concentrations.
6. Immediately acidify each aliquot sample with nitric acid to a pH just smaller than 2.
7. Analyse by AA or the other sensitive and appropriate techniques for different metals.
8. If analysis cannot be performed immediately after extraction, then store the acidified aliquots at 4°C, until analysis (as soon as possible).

3.5.2.6 Acid rain extraction

1. Repeat 1 - 8 of 2.5.2.5: Extraction for analysis of contaminants, as above, except point 2, which must read:
2. Add 2 L of the acid rain solution, as prepared, and close bottle tightly.

3.6 DEVIATIONS FROM STANDARD METHODS

3.6.1 General

All solutions were contained in high density polyethylene (HDPE) bottles of 500 mL, 1 L or 2L in size and were agitated on a platform shaker. Solutions were double filtered through a vacuum pump filtration system, initially using No. 1 Qualitative Whatman paper filters and then with 0.45 µm membrane filters. All samples were divided into 2 sub-samples, the first of these preserved with three drops of concentrated (55%) HNO_3, and stored in hard clear polycarbonate sample bottles.

3.6.2 Synthetic groundwater leaching procedure and long-term leaching

Unfortunately the quantity of ash was severely reduced from having to repeat the pre-test calibration in the three tier leaching protocol. Due to time constraints the long-term leaching procedure could not wait for more ash to arrive, as it would then not be completed before the deadline. Thus only two samples were leached for 30 days and the mass of ash was slightly reduced from 100 g to 98 g in the 60 day and 30 day samples. Consequently, less DI water was added, 1 960 mL, in order to preserve the L/S ratio of 20. Mechanical problems were also experienced. The platform shaker could not cope with 12 litres of water and 600 g of solid for such a long period of leaching. The 60 day experiment was thus terminated at 40 days.

3.6.3 Three tier leaching protocol

The molarity of HNO_3 used in these procedures was 1M HNO_3 rather than 2M as stated in the standard methods. As an alternative to allowing the solution to stand for 15 min to allow for settling or centrifugation, the solution was initially filtered using No. 1 Qualitative Whatman paper filters and was then filtered with 0.45 µm membrane filters.

3.6.3.1 Pre-test calibration

The pre-test calibration was initially performed to the letter of the method. However, when the curve was applied to predict the pH of solids that were leached for 18 hours it failed. The calibration pre-test was then performed again with a longer period of 2 hours between pH readings and further acid addition, as it was determined that the equilibration reaction was much slower than initially predicted. This second calibration curve was then applied in order to predict the amount of acid required to reach a certain pH. This curve also proved inaccurate. The calibration curve was then constructed by leaching two different L/S ratios for 18 hours. A L/S ratio of 10 (400 mL / 40 g) was used to predict pH values greater and smaller than 7, while a L/S ratio of 100 (500 mL / 5 g) was used to estimate the pH between 8 and 7. These ratios were used in accordance with the second and third sections of the three tier leaching procedure, 3.4.2 Availability test and 3.4.3 Leachability test 1.

3.6.3.2 Availability test

Due to time and space constraints only three samples with target pH values of 7.5 were agitated for 48 hours.

3.6.3.3 Leachability test 2

L/S ratios of 1 and 0.5 are under saturated with respect to liquid and as a result were not viscous to enable flow. The wetted ash could not flow and hence could not be agitated or filtered. Thus the only L/S ratios that were tested were 10, 5 and 2.

3.6.4 Toxicity characteristic leaching procedure

3.6.4.1 Acid rain leaching procedure

Commercial soda water was used to simulate carbonic acid. A sample of the soda water was retained for analysis. Concentrated HNO_3 was added to the soda water to acidify to pH 2.70 for sample ARLP1 and to pH 3.64 for sample ARLP3. The carbonic acid solution added to sample ARLP2 was a combination of the waters added to ARLP1 and ARLP 2.

3.7 LIST OF EXPERIMENTS

Tables 3.7.1 – 3.7.6 give a list of samples and their process pH values. The samples were acidified with 3 drops concentrated (55%) HNO_3.

Table 3.7.1: Mine water leaching procedure (L/S = 2L/200g = 20).

Sample name	pH	Sample name	pH	Sample name	pH
MWLP 1 a)	11.39	MWLP 2 a)	11.39	MWLP 3 a)	11.39
MWLP 1 b)	11.27	MWLP 2 b)	11.44	MWLP 3 b)	11.36
MWLP 1 c)	9.54	MWLP 2 c)	9.96	MWLP 3 c)	9.90
MWLP 1 d)	8.08	MWLP 2 d)	8.45	MWLP 3 d)	8.17
MWLP 1 e)	7.47	MWLP 2 e)	7.33	MWLP 3 e)	7.75
MWLP 1 f)	4.95	MWLP 2 f)	4.74	MWLP 3 f)	4.66
MWLP 1 g)	3.95	MWLP 2 g)	3.73	MWLP 3 g)	3.89
MWLP 1 h)	3.82	MWLP 2 h)	3.95	MWLP 3 h)	3.96
MWLP 1 i)	3.60	MWLP 2 i)	3.60	MWLP 3 i)	3.68
MWLP 1 j)	3.77	MWLP 2 j)	3.79	MWLP 3 j)	3.80
MWLP 1 k)	2.59	MWLP 2 k)	2.88	MWLP 3 k)	3.13

Table 3.7.2: Long-term leaching: total samples = 9 (L/S = 2L/200g = 20).

Sample name	pH	Sample name	pH	Sample name	pH
18 LTL 1	12.30	30 LTL 1	11.85	40 LTL 1	11.45
18 LTL 2	12.32	30 LTL 2	11.85	40 LTL 2	11.71
18 LTL 3	12.38	30 LTL 3	11.38	40 LTL 3	11.72

Table 3.7.3: Toxicity characteristic leaching procedure and acid rain leaching procedure (L/S = 20).

Sample name	pH	Sample name	pH
TCLP 1	5.87	ARLP 1	6.33
TCLP 2	5.85	ARLP 2	7.04
TCLP 3	5.82	ARLP 3	7.15

Table 3.7.4: 3-Tier Leaching procedure: Availability test: total samples = 3 (L/S = 100).

Sample name	pH	Sample name	pH	Sample name	pH
3TLP B 1	9.95	3TLP B 2	9.48	3TLP B 3	9.50

Table 3.7.5: 3-Tier Leaching procedure: Leachability Test: total samples = 33 (L/S = 400/40 = 10).

Sample name	pH	Sample name	pH	Sample name	pH
3TLP C 12 a)	11.97	3TLP C 12 b)	12.01	3TLP C 12 c)	12.03
3TLP C 11 a)	11.72	3TLP C 11 b)	11.75	3TLP C 11 c)	11.77
3TLP C 11 d)	11.23	3TLP C 11 e)	11.23	3TLP C 11 f)	11.55
3TLP C 10 a)	10.09	3TLP C 10 b)	10.17	3TLP C 10 c)	9.94
3TLP C 9 a)	9.25	3TLP C 9 b)	8.90	3TLP C 9 c)	8.95
3TLP C 8 a)	7.65	3TLP C 8 b)	7.55	3TLP C 8 c)	7.68
3TLP C 7 a)	6.72	3TLP C 7 b)	6.69	3TLP C 7 c)	6.79
3TLP C 6 a)	5.88	3TLP C 6 b)	5.98	3TLP C 6 c)	5.89
3TLP C 5 a)	4.96	3TLP C 5 b)	4.62	3TLP C 5 c)	4.54
3TLP C 4 a)	4.39	3TLP C 4 b)	4.42	3TLP C 4 c)	4.42
3TLP C 3 a)	3.94	3TLP C 3 b)	3.82	3TLP C 3 c)	3.73

Table 3.7.6: 3-Tier Leaching procedure: Availability test 2: total samples = 9

Sample name L/S = 10	pH	Sample name L/S = 5	pH	Sample name L/S = 2	pH
3TLP D 1 a)	12.45	3TLP D 2 a)	13.11	3TLP D 3 a)	13.35
3TLP D 1 b)	12.73	3TLP D 2 b)	13.01	3TLP D 3 b)	13.08
3TLP D 1 c)	12.91	3TLP D 2 c)	13.08	3TLP D 3 c)	13.13

4. RESULTS

4.1 ACCURACY AND REPRODUCIBILITY OF DATA AND SOURCES OF ERROR

All experiments were performed in triplicate in order to test the reproducibility of results. Values shown in the results sections represent an average of three analyses. All water samples were tested by ICP-MS at the same facility. Standard water samples from the National Institute for Standards Technology (NIST) were analysed for each batch of analyses performed. Another NIST sample sent by NETL was analysed, along with a sample of the de-ionised water used in the chemistry department. A variance (S) around the mean was calculated for the triplicate results to give an indication of reproducibility [1].

$$S^2 = \frac{\sum_{i=1}^{3} (x_i - \bar{x})^2}{3 - 1} \qquad [1]$$

A coefficient of variance (C) was then calculated as a percentage of the mean [2].

$$C = \frac{\sqrt{S^2}}{\bar{x}} \times 100 \qquad [2]$$

The coefficient of variance expresses the difference between individual data points and their mean as a percentage of the mean. A small percentage (small variation) is desired. The coefficient of variance is represented graphically in categories of 10% i.e. 0-10%, 11-20%, etc; with the magnitude of these categories expressed as a percentage of the total number of values. For example if 20 out of the 24 elements have a coefficient of variance (C) between 0 and 10% the first column will have a y-axis value of 83%. Practically this means that a majority of the data has only a small variance and hence the experiment has excellent reproducibility.

The following two sections will discuss the accuracy of the data as compared to NIST samples and the reproducibility as calculated with the coefficient of variance.

4.1.1 Accuracy of experimental data

The accuracy of data as measured by ICP-MS was determined by comparison to a NIST sample, specifically 1640a, during each batch of analyses. Another trace metal standard solution (1643e) was analysed to compare NETL and UWC analytical apparatus.

Table 4.1.1 shows the NIST-1640a sample analyses for all the water samples. Table 4.1.2 lists the sample analyses that accompany each standard reference material analysis. Thus, from Table 4.1.1 it can be seen that the 1st and 2nd reference material analyses were not accurate. The 1st analysis of the reference standard NIST-1640a shows 9 elements that have a greater than 10% difference with the certified values while the 2nd analysis shows 16 elements that have a greater than 10% difference with the certified analysis. The 3rd, 4th and 5th analyses show the same 4 elements with greater than 10% difference with the certified value. The 4th analysis also shows Zn as being analysed inaccurately.

Table 4.1.1: Analyses of standard reference material 1640a, compared to certified value. Values in bold indicate a difference, between the certified value and analysed value, of more than 10%.

Concentration (µg/L)	1640a Certified	1st % Diff Cert	2nd % Diff Cert	3rd % Diff Cert	4th % Diff Cert	5th % Diff Cert
Al	52.00	**10.1**	**24.3**	3.7	0.8	1.2
As	26.67	0.5	**12.1**	0.5	0.2	0.5
B	301.1	2.9	1.4	0.6	1.0	0.2
Ba	148.0	7.5	**18.2**	2.4	6.2	5.5
Be	34.94	0.7	**12.6**	0.5	5.4	0.2
Ca	7 045	**20.7**	0.6	2.2	1.9	5.8
Cd	22.79	2.5	**10.6**	0.9	2.0	2.9
Co	20.28	2.3	**17.9**	1.0	1.9	0.5
Cr	38.60	0.9	**12.1**	0.3	1.2	2.3
Cu	85.20	1.0	**10.7**	0.7	0.5	0.1
Fe	34.30	**38.5**	**47.8**	268	**17.2**	**11.0**
K	994.0	**24.4**	**12.3**	11.6	**10.1**	**12.0**
Mg	5 819	**20.1**	1.0	3.8	2.0	0.6
Mn	121.5	0.3	2.2	0.2	6.7	2.8
Mo	46.75	0.7	7.8	0.0	0.9	3.0
Na	29 350	**23.2**	1.8	4.5	0.0	2.0
Ni	27.40	1.7	**10.4**	1.8	0.6	1.5
Pb	27.89	1.7	**11.2**	0.7	0.2	0.1
Sb	13.79	0.0	9.1	1.2	0.8	1.3
Se	21.96	2.7	1.7	0.3	0.1	1.7
Ti	-	**100**	**100**	100	**100**	**100**
V	12.99	6.8	**20.2**	3.4	6.9	2.7
Zn	53.20	**10.4**	**22.2**	8.0	**10.8**	8.6
Hg	-	**100**	**100**	100	**100**	**100**

From the NIST 1640a analyses it can be clearly seen that the 1st and 2nd experimental analyses were not accurate. These analyses coincide with the majority of samples for the MWL procedure. The accuracy of the data for the other experiments can be said to be good with the exception of data for the elements Fe, K, Hg and Ti. From Table 4.1.1 it can be seen that because of the lack of Ti and Hg in the standard reference solution those elements cannot be analysed for accurately. The ICP-MS method of analysis can suffer from interferences. The argon plasma can contain polyatomic ions that interfere with other elements with the same mass and other elements may also form polyatomic ions that interfere with those elements that have the same mass. Table 4.1.3 gives the polyatomic isotopes that can form and which element they

interfere with. The production of ArO^+ and ArH may be the cause for the inaccurate values of Fe and K, respectively (http://www.wcaslab.com/tech/icpms_drc.htm).

Table 4.1.2: List of samples analysed for each NIST-1640a sample analysis.

1st NIST-1640a	2nd NIST-1640a	3rd NIST-1640a	4th NIST-1640a	5th NIST-1640a
MWLP 1 a)	MWLP 1 i)	MWLP 3 i)	3TLP c12b)	3TLP c3b)
MWLP 1 b)	MWLP 1 j)	MWLP 3 j)	3TLP c11b)	3TLP c2b)
MWLP 1 c)	MWLP 1 k)	MWLP 3 k)	3TLP c11e)	3TLP c6c)
MWLP 1 d)	MWLP 2 a)	18LTL 1	3TLP c10b)	3TLP c5c)
MWLP 1 e)	MWLP 2 b)	18LTL 2	3TLP c9b)	3TLP c4c)
MWLP 1 f)	MWLP 2 c)	18LTL 3	3TLP c8b)	3TLP c3c)
MWLP 1 g)	MWLP 2 d)	30LTL 1	3TLP c7b)	3TLP c2c)
MWLP 1 h)	MWLP 2 e)	30LTL 2	3TLP c12c)	3TLP D1a)
Soda water	MWLP 2 f)	30LTL 3	3TLP c11c)	3TLP D1b)
DI water	MWLP 2 g)	40LTL 1	3TLP c11f)	3TLP D1c)
	MWLP 2 h)	40LTL 2	3TLP c10c)	3TLP D2a)
	MWLP 2 i)	40LTL 3	3TLP c9c)	3TLP D2b)
	MWLP 2 j)	3TLP B1	3TLP c8c)	3TLP D2c)
	MWLP 2 k)	3TLP B2	3TLP c7c)	3TLP D3a)
	MWLP 3 a)	3TLP B3	3TLP c6a)	3TLP D3b)
	MWLP 3 b)	3TLP C12a)	3TLP c5a)	3TLP D3c)
	MWLP 3 c)	3TLP C11a)	3TLP c4a)	TCLP 1.
	MWLP 3 d)	3TLP C11d)	3TLP c3a)	TCLP 2
	MWLP 3 e)	3TLP C10a)	3TLP c2a)	TCLP 3.
	MWLP 3 f)	3TLP C9a)	3TLP c6b)	ARLP 1
	MWLP 3 g)	3TLP C8a)	3TLP c5b)	ARLP 2
	MWLP 3 h)	3TLP C7a)	3TLP c4b)	ARLP 3

Table 4.1.3: List of polyatomic ions that may form and interfere with ICP-MS analyses.

Polyatomic ion	Analyte	Polyatomic ion	Analyte
$^{80}Ar_2^+$	^{80}Se	$^{35}Cl^{16}O$	^{51}V
$^{40}Ar^{16}O^+$	^{56}Fe	$^{40}Ar^{12}C$	^{52}Cr
$^{38}Ar^{1}H$	^{39}K	$^{23}Na^{40}Ar$	^{63}Cu
^{40}Ar	^{40}Ca	$^{40}Ar^{35}Cl$	^{75}As

Table 4.1.4 shows the analyses for the NIST standard reference material 1643e sent by NETL. The high number of elements that have a greater than 10% difference with respect to the certified values may not, in fact, indicate that the ICP mass spectrometer was not functioning satisfactorily. Also in Table 4.1.4 is an analysis of standard reference material 1640a, which is included with every batch of analyses performed. Standard 1640a shows that only two elements (Fe and K) have concentrations that are

more than 10% different from their respective certified values. Thus, the analyses of two NIST standard reference materials appear to give conflicting results of the accuracy of the instrument. The difference in the accuracy of the analyses could be a result of the differences in the standards themselves. The NETL laboratories use ICP-OES for sample analysis, which is not as sensitive as ICP-MS used by UWC. Standard 1643e has higher concentrations of metals than 1640a and thus the inaccuracy of the 1643e analysis may be a result of mass interferences. The two different analytical methods must be taken into account as a source of discrepancy. Another reason why the sample analysis of 1643e may be inaccurate is that samples may have changed en route to UWC from the USA.

Table 4.1.4: Comparison of analysis of NIST standard reference material 1643e with the routine analysis of 1640a included. Values in bold indicate differences of more than 10% between analysed and certified values.

Concentration	1643e	NETL	UWC analysis		% Diff Cert	% Diff Cert	% Diff Cert	1640a	% Diff
µg/L	Cert	analysis	1	2	NETL	UWC 1	UWC 2	Cert	Cert
Al	141.8	272.0	257.9	684.7	**62.9**	**58.1**	**131**	53.01	1.9
As	60.45	60.90	53.72	55.39	0.7	**11.8**	8.7	26.51	0.6
B	157.9	557.0	844.5	839.7	**112**	**137**	**137**	300.2	0.3
Ba	544.2	522.0	543.2	550.0	4.2	0.2	1.1	149.1	0.7
Ca	32 300	30 800	23 728	24 493	4.8	**30.6**	**27.5**	6907	2.0
Cd	6.568	6.300	6.074	5.795	4.2	7.8	**12.5**	22.73	0.2
Co	27.06	27.10	25.03	25.34	0.1	7.8	6.6	20.52	1.2
Cr	20.40	21.30	17.13	20.22	4.3	**17.4**	0.9	37.30	3.4
Cu	22.76	21.40	27.62	24.17	6.2	**19.3**	6.0	84.91	0.3
Fe	98.10	111.0	354.5	202.8	**12.3**	**113**	**69.6**	27.48	**19.9**
K	2 034	2140	16.80	2814	5.1	**197**	**32.2**	810.4	**18.5**
Mg	8 037	8 010	7 633	7 878	0.3	5.2	2.0	5 862	0.7
Mn	38.97	41.90	37.05	37.91	7.2	5.1	2.8	119.9	1.3
Mo	121.4	124.0	107.2	109.5	2.1	**12.4**	**10.3**	46.06	1.5
Na	20 740	21 700	16 762	17 783	4.5	**21.2**	**15.4**	28 576	2.6
Ni	62.41	65.70	55.24	77.78	5.1	**12.2**	**21.9**	27.30	0.4
Pb	19.63	19.10	16.50	16.88	2.7	**17.4**	**15.1**	27.06	3.0
Se	11.97	12.40	14.01	13.28	3.5	**15.7**	**10.4**	21.65	1.4
Sr	323.1	336.0	318.6	322.4	3.9	1.4	0.2	4 159	0.3
V	37.86	35.20	35.26	36.61	7.3	7.1	3.4	124.5	2.8
Zn	78.50	94.40	74.04	111.4	**18.4**	5.8	**34.7**	12.63	1.3

In general the ICP-MS used by UWC, does not produce accurate results for K or Fe. Some of the data reported in following sections, for Fe, is doubtful, as it does not display the expected mobility patterns (high solubility at low pH values).

Table 4.1.5 shows an analysis of one sample of de-ionised water from the DI water source used for all experiments. The concentrations of Na, Ca, K, Cu and Zn are significantly high. Where the concentrations of Na, Ca and K are high in sample

solutions the contribution form the de-ionised water is not significant but concentrations can be low enough in sample solutions for the deionised water to become a factor. The high concentrations of Cu and Zn contribute to the concentration of the solution significantly in all experiments.

Table 4.1.5: Analysis of de-ionised (DI) water used for experiments.

Conc µg/L	DI H_2O	Conc µg/L	DI H_2O	Conc µg/L	DI H_2O
Al	8.10	Cr	1.18	Ni	0.01
As	0.10	Cu	57.9	Pb	0.55
B	BDL	Fe	BDL	Sb	BDL
Ba	0.37	K	169	Se	BDL
Be	0.18	Mg	0.15	Ti	BDL
Ca	445	Mn	BDL	V	0.79
Cd	BDL	Mo	BDL	Zn	32.9
Co	0.04	Na	251	Hg	0.59

4.1.2 Reproducibility of experimental results

The reproducibility of experimental data was determined by calculating the variance and expressing that variance as a percentage of the mean and a coefficient of variance. The following figure (Figure 4.1.1) graphically represents the variance for the experimental data. The reproducibility of the MWLP data is bad; this is most likely as a result of analytical error.

The reproducibility of the data for the 3TLPb and TCLP experiments is excellent, probably as a result of the buffering effect of the solutions used in these methods. The reproducibility for 3TLPc is adequate while the reproducibility for experiments 3TLPd, LTLP and ARLP is not good. The LTLP (which includes the SGLP) was beset with technical problems regarding the equipment and it cannot be guaranteed that equipment was running continuously for the entire period. With regards to the SGLP section of that data, it is possible that equilibrium is not reached after only 18 hours of leaching. The 3TLPd liquid-to-solid ratios were not ideal, and the mixture did not flow well being more of a slurry than a solution. This meant that homogeneity was probably not achieved and the liquid present might well have become saturated, which would result in inconsistent solution concentrations. The ARLP does not display good reproducibility as the acid rain solutions differed in pH slightly. The ARLP, as a method is ill-defined and open to differences in procedure.

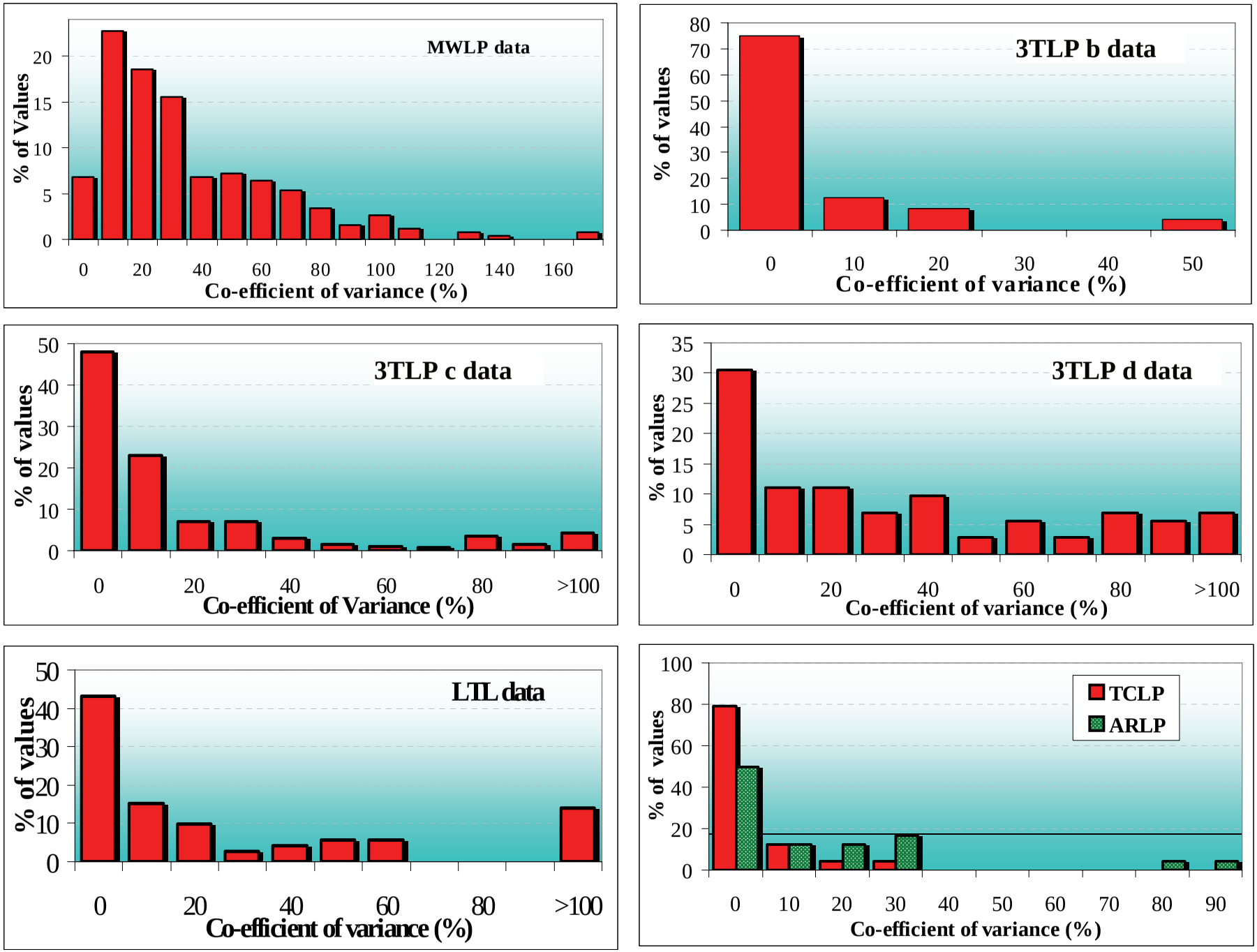

Figure 4.1.1: Co-efficient of variance for MWLP, 3TLP, LTLP and TCLP given as % of total amount of data for each experiment.

4.2 TOXICITY CHARACTERISTIC AND ACID RAIN LEACHING PROCEDURES (TCLP AND ARLP)

4.2.1 Preliminary evaluation

The initial pH on stirring in H_2O was found to be 11.89. After HCl was added and the solution heated to 50°C and then cooled to room temperature the pH of the solution was 3.09. Thus TCLP solution No. 1 (Acetic acid and NaOH) was used.

4.2.2 Results

Figures 4.2.1 – 4.2.3 show the elemental analyses for the TCLP and ARLP experiments. The Tables for these Figures are shown in Appendix A1. The soda water used for the ARLP is shown in Table 4.2.1.

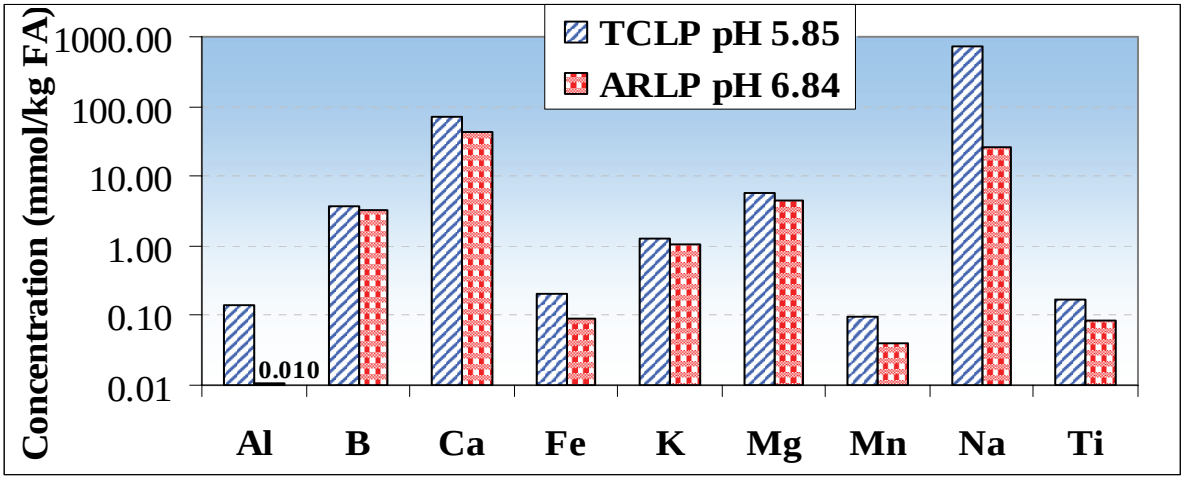

Figure 4.2.1: Major element concentrations for TCLP and ARLP (mmol/kg FA).

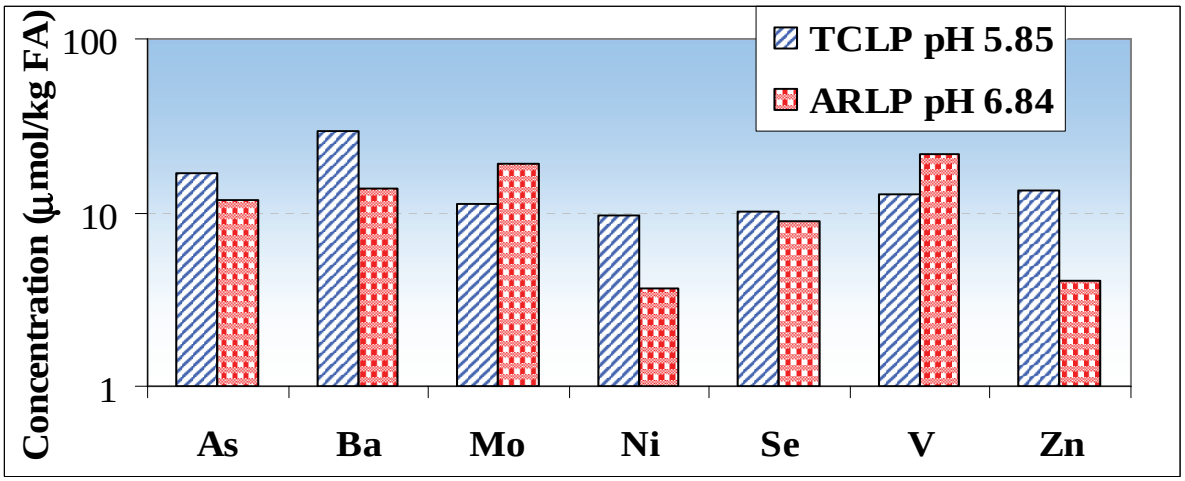

Figure 4.2.2: Minor element concentrations for TCLP and ARLP (µmol/kg FA).

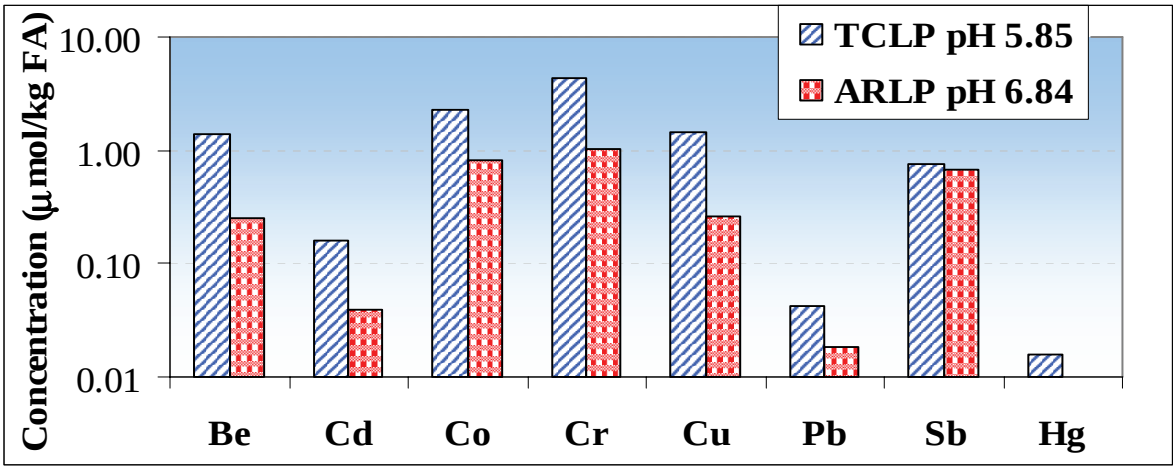

Figure 4.2.3: Trace element concentrations for TCLP and ARLP (µmol/kg FA).

Table 4.2.1: ICPMS analysis of commercial soda water used for ARLP experiment.

Element	Conc. µg/L	Conc. µmol/L	% added	Element	Conc. µg/L	Conc. µmol/L	% added
Al	27.53	1.0210	98.7	**Mg**	783.7	32.244	7.30
As	0.399	0.0053	0.45	**Mn**	BDL	BDL	0.00
B	12.88	0.6850	0.22	**Mo**	0.215	0.0038	0.20
Ba	5.664	0.0360	2.62	**Na**	127 454	5 544.0	>100
Be	1.232	0.1367	>100	**Ni**	1.687	0.0287	7.93
Ca	3 701	92.345	2.19	**Pb**	0.489	0.0024	>100
Cd	0.012	0.0001	2.80	**Sb**	0.176	0.0014	2.13
Co	0.078	0.0013	1.61	**Se**	7.271	0.0921	10.5
Cr	14.48	0.2785	>100	**Ti**	13.44	0.2820	3.32
Cu	1.511	0.0238	89.7	**V**	1.106	0.0217	0.99
Fe	1 767	31.643	>100	**Zn**	2.056	0.0314	7.81
K	249.6	6.3844	6.10	**Hg**	3.078	0.0153	>100

The commercial soda water (Table 4.2.1) contributes a high concentration of metals to the solution. Thus, for the Figures 4.2.1 to 4.2.3 the fly ash contributes only a small percentage of the concentration of the following elements: 19% of Be, 36% of Cr, 29% of Fe, 47% of Na, 76% of Pb and 6% of Hg. As a result of the contribution by the soda water, the concentration of soluble ions is elevated in these cases.

Element concentration in the TCL procedure is consistently higher than for the ARL procedure for all elements except Mo and V. The higher metal concentration in the TCL procedure is likely as a result of lower pH (most metals are more soluble at low pH) and the difference in strength of the acid solutions used for leaching. The acetic acid used for the TCLP is a stronger acid and more highly concentrated than carbonic acid, even when the carbonic acid is further acidified with a small amount of HNO_3. The higher element concentrations found in the TCLP solutions indicate soluble and exchangeable ions. The element concentrations in ARLP probably indicate soluble cations only. The TCL procedure may be compared to other procedures that leach with a weak acid, but the ARL procedure should be compared to procedures that leach with water.

The element concentrations for the TCLP procedure show that Al, Fe, Mn and Ti are in solution in concentrations of a similar magnitude – around 0.1 mmol/kg FA (Figure 4.2.1). Boron, K and Mg concentrations are of a similar magnitude between 1 and 6 mmol/kg FA. Calcium concentrations are around 70 mmol/kg FA while Na concentrations are of an order of magnitude higher at around 720 mmol/kg FA for the TCL procedure.

Minor elements are all of similar magnitudes and fluctuate around 10 µmol/kg FA. Barium is higher with a concentration around 30 µmol/kg FA (Figure 4.2.2). The concentrations of V and Mo are both higher for ARLP than for the TCL procedure, this is because both these metals decrease in concentration with decreasing pH. Thus the lower pH of the TCLP results in a lower concentration of V and Mo when compared to the ARLP.

Trace elements Pb and Hg have concentrations of below 0.05 µmol/kg FA (Figure 4.2.3). The concentration of Cd is just more than 0.1 µmol/kg FA. The concentrations of Be, Cu and Sb are around 1 µmol/kg FA while Co and Cr are between 2 and 4.5 µmol/kg FA.

4.3 SYNTHETIC GROUNDWATER PROCEDURE AND LONG-TERM LEACHING (SGLP AND LTL)

The metal concentrations for the SGLP (18 hrs) and the LTLP (30 and 40 days) are shown in Figures 4.3.1 – 4.3.3. Figure 4.3.1 shows the major elements for these procedures. The concentrations of Al, B, Ca and Fe decrease in solution with time. The concentration of Na increases in solution with time while K concentration increases after 30 days and decreases after a further 10 days.

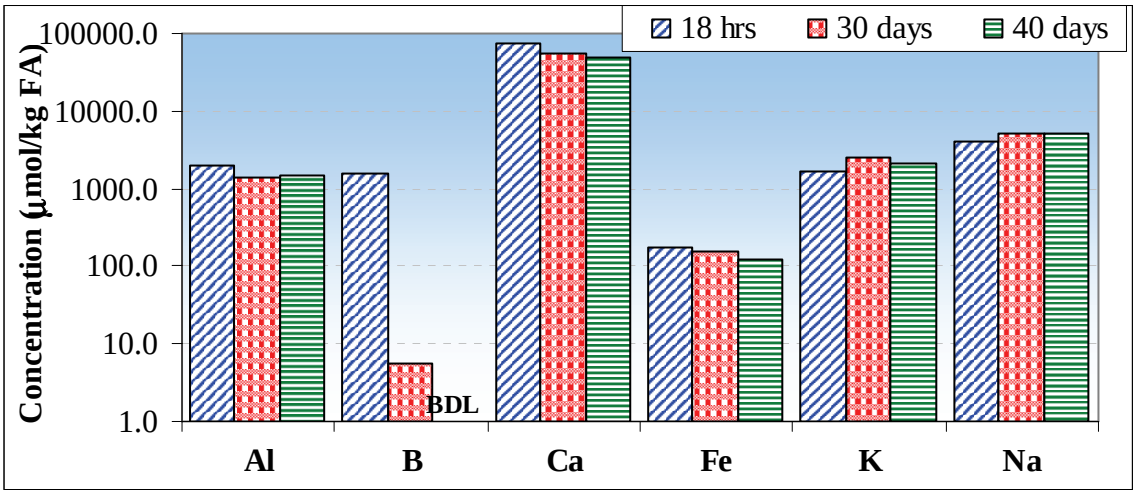

Figure 4.3.1: Major elements for the SGL and LTL procedures (µmol/kg FA).

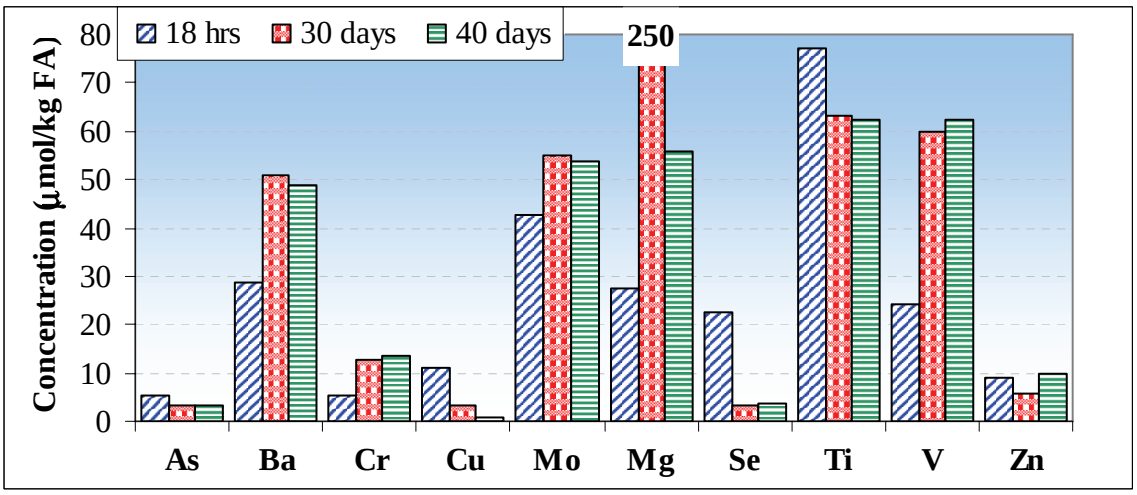

Figure 4.3.2: Minor elements for the SGL and LTL procedures (µmol/kg FA).

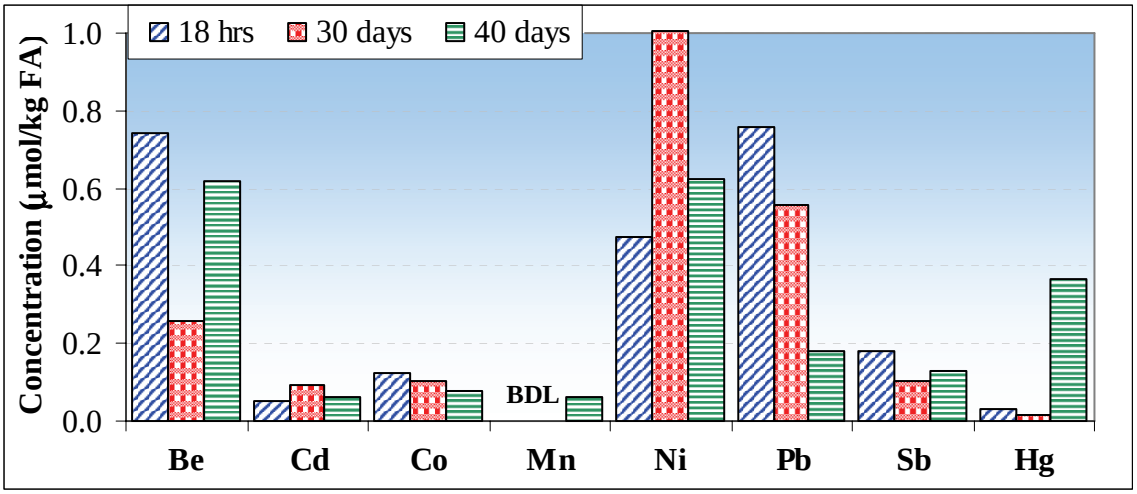

Figure 4.3.3: Trace elements for the SGL and LTL procedures (µmol/kg FA).

The minor elements are shown in Figure 4.3.2. The concentrations of As, Cu and Ti in solution, decrease with time. The concentration of Cr and V in solution increases with time. The concentration of Ba, Mo, Mg, Se, and Zn fluctuates with time; increasing at 30 days and then decreasing after 40 days.

The trace elements are shown in Figure 4.3.3. The concentrations of Co and Pb decrease with time while the concentration of Mn in solution increases with time. The concentrations of Be, Cd, Ni, Hg and Sb vary with time. Beryllium, Hg and Sb concentrations decrease in solution after 30 days of leaching and increase again after 40 days of leaching, while Cd and Ni concentrations increase after 30 days of leaching and decrease after 40 days of leaching.

4.4 MINE WATER LEACHING PROCEDURE (MWLP)

Figures 4.4.1 to 4.4.3 give the elemental data for the MWLP at each incremental acid addition and hence pH. Initially a large amount of Na and Ca is in solution (Figure 4.4.1). With the second leaching this amount decreases significantly. This sudden decrease between the first two leachings is probably a result of the leaching of soluble salts.

Sodium maintains a steady concentration with each successive leaching decreasing slightly for a final concentration of 0.52 mmol/kg FA; this suggests that there is still some Na remaining on the surface of the particles. Calcium decreases from a concentration of around 90 mmol/kg FA (1 mol/kg FA) to around 4 mmol/kg FA. As is common with most fly ashes there are large amounts of available Ca and even after 12 leachings with acid there is still a relatively large amount in solution.

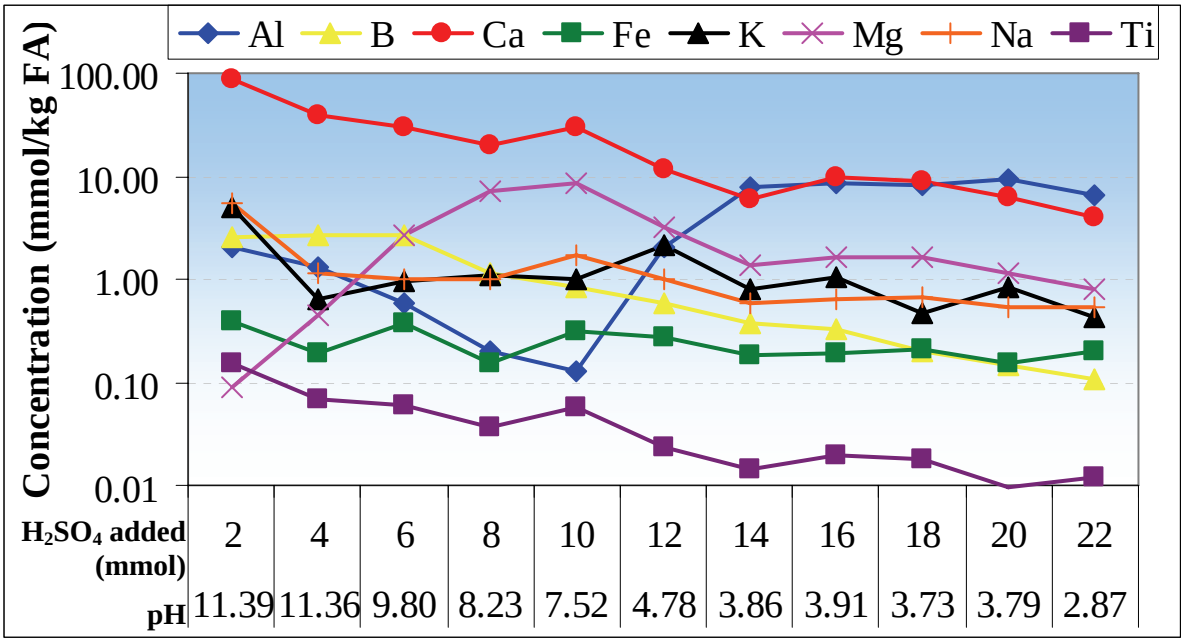

Figure 4.4.1: Major elements for MWL procedure (mmol/kg FA).

There is a steady decrease in all elements with sequential addition of acid, except Mg and Al and K and Fe (Figure 4.4.1). The concentration of Al decreases in solution until 10 mmol of H_2SO_4 have been added or a circumneutral pH has been reached, and then increases with decreasing pH. This is a result of the increased mobility of Al at high and low pH values. The concentration of Mg increases steadily with each acid addition, reaching a maximum around 8 mmol/kg FA with the addition of 10 mmol H_2SO_4. Thereafter the concentration of Mg decreases to around 0.8 mmol/kg FA.

The minor elements Ba and Cu (Figure 4.4.2) show an increase in their concentrations after an addition of 8 mmol H_2SO_4 and around a neutral pH. Mn and Zn concentrations in solution increase after an addition of 4 mmol H_2SO_4 at a pH of 9.8. The concentrations of Zn, Mg and Ba reach a maximum at pH 4.78. Beryllium follows a similar trend as Ba and Cu reaching a maximum at pH 3.86. The concentrations of Se and V in solution follow the same trend, decreasing steadily till pH 4.78 and then maintaining a relatively stable concentration in solution. The concentration of Cr varies around 10 µmol/kg FA.

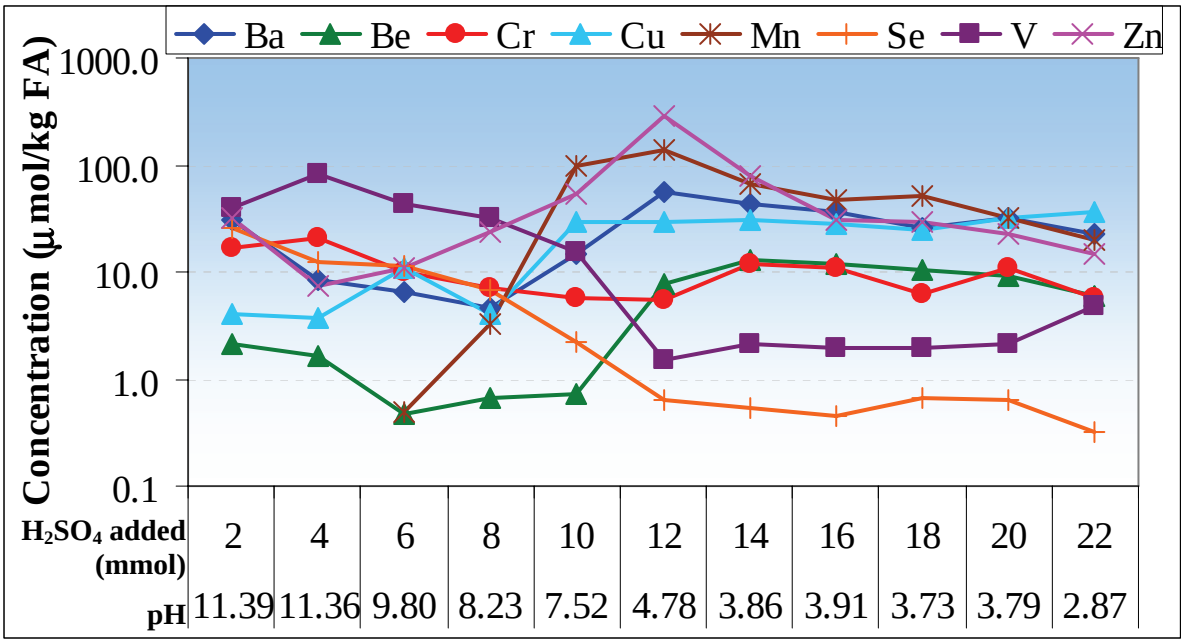

Figure 4.4.2: Minor elements for MWL procedure (mmol/kg FA). Lack of data indicates below detectable limits.

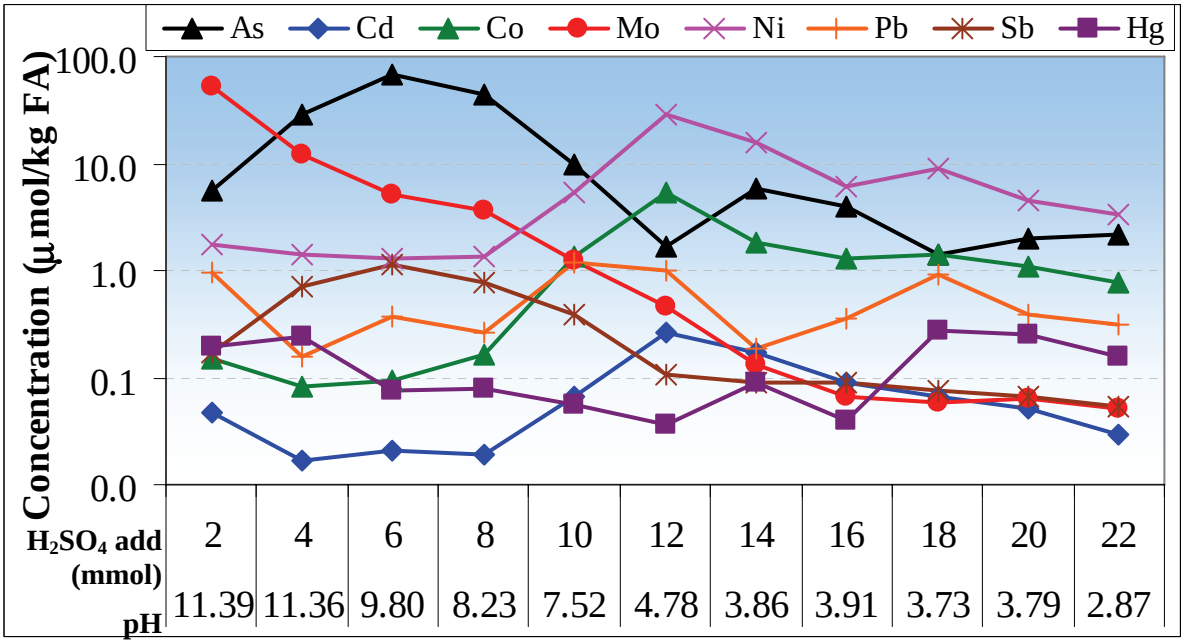

Figure 4.4.3: Trace elements for MWL procedure (mmol/kg FA).

All trace metals concentrations are below 100 µmol/kg FA. The concentrations of As and Sb in solution follow the same pattern of increasing initially and reaching a maximum with the addition of 6 mmol H_2SO_4, then decreasing with further sequential additions of acid until a pH of 5, where concentrations in solution stabilised for Sb, while increasing and then decreasing again for As.

The concentrations of Ni, Co and Cd follow the same trend, maintaining a relatively steady concentration until 8 mmol H_2SO_4 have been added and the solution is at a pH value of around 8. Then the concentrations in solution increase rapidly and reach a maximum concentration at a pH of around 5 (addition of 12 mmol H_2SO_4), thereafter

decreasing. The mobility of Pb and Hg appear not to be affected by the pH of the solution as they show alternately increasing and decreasing concentrations. The concentration of Mo decreases from high initial values of 51.4 µmol/kg FA to 0.05 µmol/kg FA after 16 mmol H_2SO_4 were added.

4.5 THREE TIER LEACHING PROCEDURE (3TLP)

4.5.1 Titration pre-test (3TLPa)

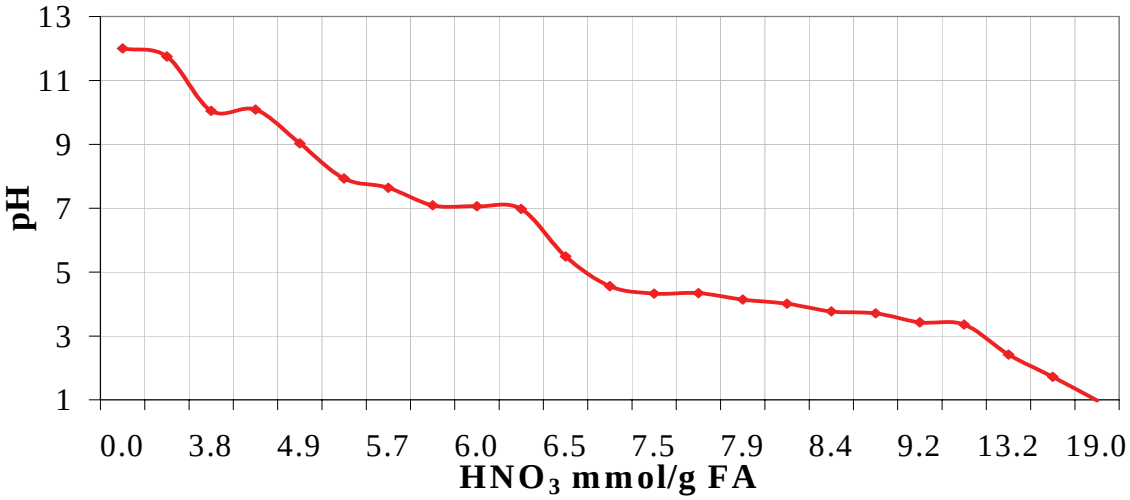

Figure 4.5.1: Calibration curve used to determine acid addition for 3TLP b and c.

The titration curve was generated from batch leaching for 18 hours with varying amounts of HNO_3. Figure 4.5.1 shows the titration curve used. No KOH was used to increase the pH above 12 as the natural pH of the solution was already greater than 12.

4.5.2 Availability test (3TLPb)

The first tier of the 3TLP is the availability test conducted with EDTA as a buffer. This test is similar to the TCL procedure. The leaching is supposed to be conducted at a pH of 7.5 or as close to it as possible. The required amount of HNO_3, according to the calibration curve, was added to each solution to reach a pH of 7.5. After leaching, the pH measured in solution was in fact 2 pH units higher than expected. As a result of the complex nature of the fly ash solution and the reaction that occur when the pH is lowered, it is probable that the EDTA complexed with metals that would have otherwise contributed to the acidity of the solution. For example Al, which is highly soluble at initial pH values, before acid is added, contributes to acidity by associating with OH^-, to form $AlOH_4^-$ at a pH around 8. If Al is scavenged from solution before the pH is decreased more OH^- is available in solution and the pH is higher than expected.

Ethylenediaminetetraacetic acid (EDTA) is an excellent metal chelating agent. For this reason the metal concentrations for this experiment are seen to constitute the maximum metal availability for fly ash in contact with a solution, whether water or acid. As a result of its high buffering capacity, a separate calibration needs to be performed to determine how much acid must be added to ensure a pH of 7.5, as this value is not the same with a fly ash/water solution.

The Na concentrations are not a true reflection of the available Na as a Na-EDTA salt was used to make up the EDTA solution. Figures 4.5.2 – 4.5.4 show the metal concentrations for this test, for the three leachings performed, and give the pH of each.

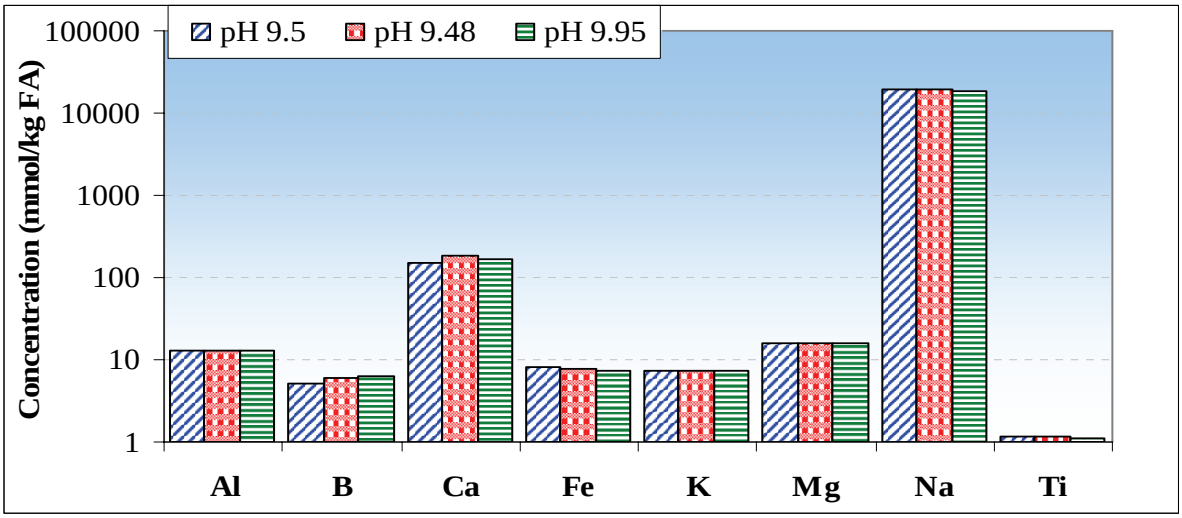

Figure 4.5.2: Major elements for 3TLPb (mmol/kg FA).

The concentrations of B, Fe and K (Figure 4.5.2) are of a similar magnitude being in the region of 6-7 mmol/kg FA. The concentrations of Al and Mg are similar in the range of 12 – 15 mmol/kg FA. The concentration of Ca is high at 184 mmol/kg FA. The pH of these tests is close to that used for determining the hardness of water by Ca determination with titration with EDTA. The extremely high Na concentration of 19 000 mmol/kg FA is due to the Na-EDTA salt used.

The minor element concentrations are shown in Figure 4.5.3. The maximum available amount of As is high at around 0.43 mmol/kg FA. The concentrations of Mn and V are also high at around 0.3 and 0.35 mmol/kg FA respectively. Barium and Cr have similar concentrations of around 0.2 mmol/kg FA and Cu and Zn have similar concentrations of around 1.5 mmol/kg FA.

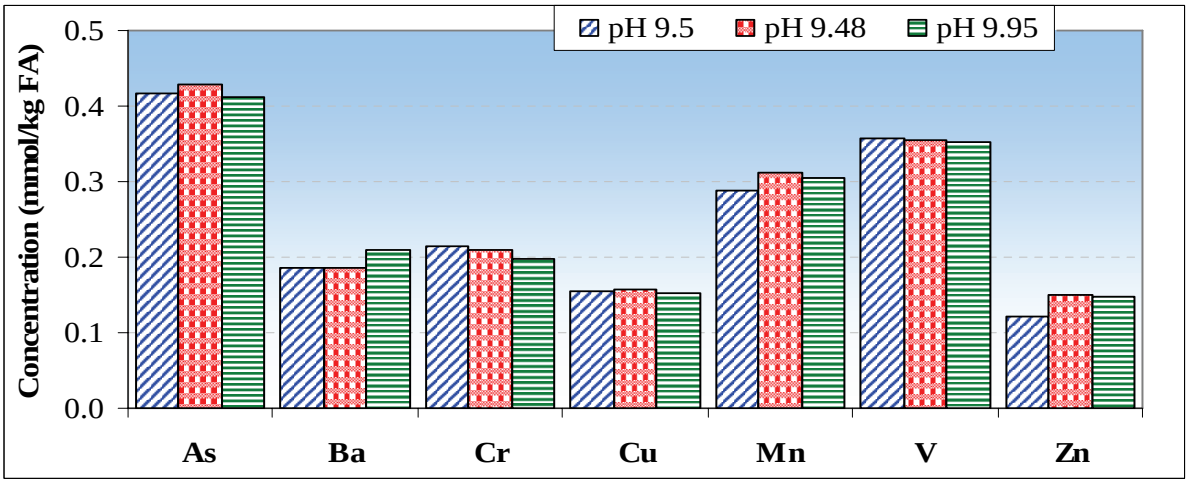

Figure 4.5.3: Minor elements for 3TLPb (mmol/kg FA).

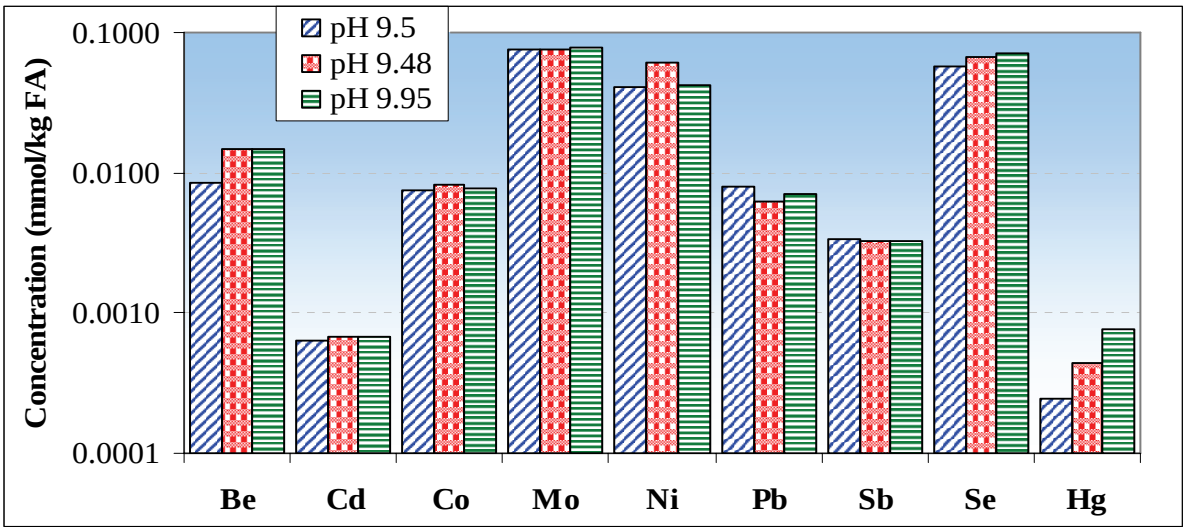

Figure 4.5.4: Trace elements for 3TLPb (mmol/kg FA).

Trace elements concentrations (Figure 4.5.4) are all below 0.1 mmol/kg FA. Molybdenum and Se have similar concentrations of around 0.07 mmol/kg FA. Ni concentrations are as high as 0.6 mmol/kg FA, while Be reaches concentrations of 0.015 mmol/kg FA. The concentrations of Pb and Co reach a maximum of 0.008 mmol/kg FA. The concentration of Sb reaches a maximum of 0.003 while the concentrations of Cd and Hg reach a value of 0.0008 mmol/kg FA.

It can be seen from the graphs that small variations in pH may result in a large difference in element concentrations. Prior to attempting this availability test, the amount of acid needed to reduce the pH of a fly ash EDTA solution to 7.5 needs to be determined separately from the calibration curve. Pre-test samples may be done in triplicate and kept for comparison.

4.5.3 Leachability test 1 (3TLPc)

The second tier of the 3TL procedure involves the batch leaching of the fly ash at different, pre-determined pH values. This test is similar to the MWLP, but where that procedure is continuous and removes elements with each leaching, this experiment is cumulative. So while this test follows the same elemental trends as the MWLP the changes in element concentration are more pronounced as a result of the batch leaching and accumulation of the element at each specific pH value.

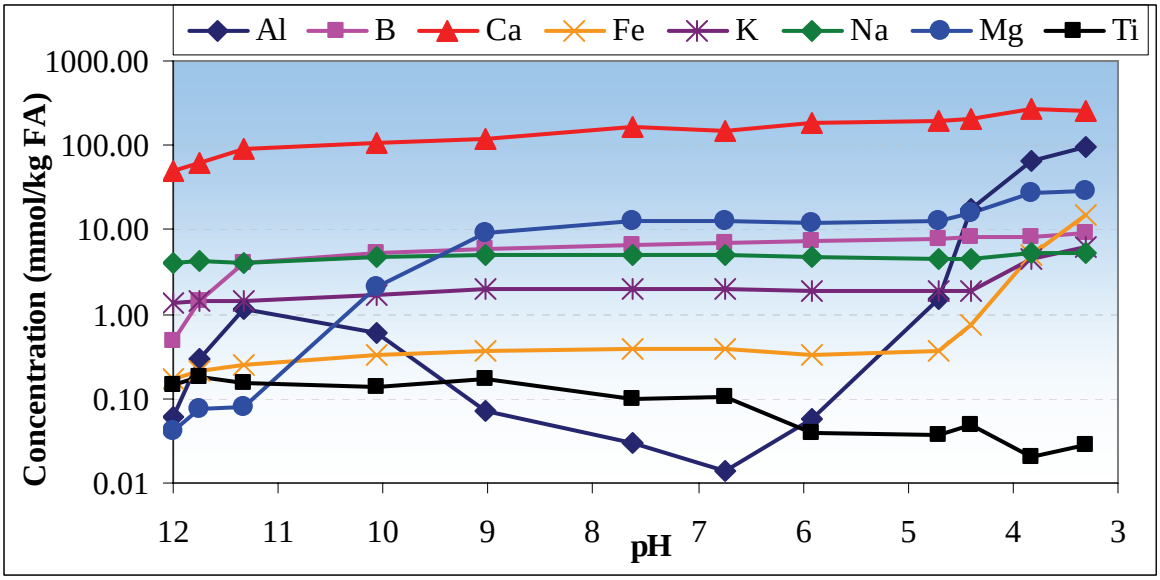

Figure 4.5.5: Major elements for 3TLPc (mmol/kg FA).

The major elements for 3TLPc are shown in Figure 4.5.5. The increase in Ca concentration shows that the solubility of Ca is somewhat pH dependant. Calcium concentration increases in solution with decreasing pH. This is most likely the result of the dissolution of $Ca(OH)_2$ with the addition of a greater amount of acid. Magnesium concentration increases rapidly between pH 12 and 9, thereafter following the same trend as Ca. The increase of Mg with greater amounts of acid, most likely has the same cause as increased Ca concentration: the dissolution of $Mg(OH)_2$. The concentration of K follows the same trend as Ca and Mg, presumably with the same cause. The concentration of Na is not affected by the decrease in pH. The same concentration is soluble despite the pH of the solution. The concentration of Ti decreases with decreasing pH. More B becomes soluble with a small decrease in pH, between pH 12 and 11. Thereafter pH does not have a great influence on the concentration of B in solution, which increases slightly with decreasing pH. The same concentration of Fe is available in solution until pH 4.5. At this pH Fe becomes highly soluble and the concentration in solution increases accordingly. The concentration of Al in solution rises at a rapid rate between pH 12 and 11.5 and pH 5 and 4.5. From pH 11 the concentration of Al in solution decreases rapidly reaching a minimum around pH 7, where after it increases steadily till pH 5.

The rapid increase in the concentration of Al in solution at pH values around 11 and 5 is reflected in the pH of the solution and the very low buffering capacity at those points. It was very difficult to add an amount of acid to get pH values of exactly 11 and 5 because the pH was changing so rapidly. At pH 4.5 a large amount of acidity is being added into the system, or put another way, a large amount of alkalinity in the form of OH^- is being removed from the system by the precipitation of Fe and Al. This consumption of OH^- in solution could result in the increase of Ca, Mg and K at those points.

In general the major cations are not greatly affected by pH with the exception of Al and Mg. Between the pH values of 10 and 5 the concentrations of the major elements do not vary a great deal. The major elements are less pH dependant than the minor and trace elements.

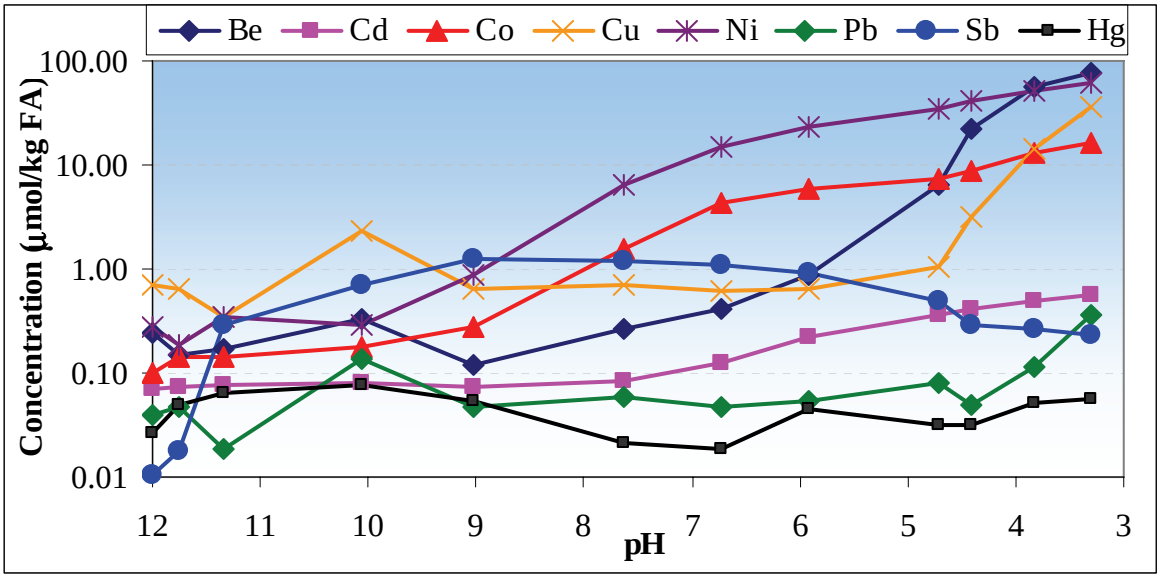

Figure 4.5.6: Major elements for 3TLPc (mmol/kg FA).

Figure 4.5.6 gives the minor elements for 3TLPc. Copper and Pb show similar trends. There is an initial decrease in concentration from pH 12 to 11.3 followed by a rapid increase till pH where after the concentration decreases and remains stable till pH 4.5. At pH 4.5 the concentration of Cu and Pb shows a rapid increase with a maximum at pH 3. The concentration of Be in solution shows a trend similar to those of Cu and Pb except it does not remain stable after the decrease in concentration at pH 9, the concentration increases steadily till a pH of 4.5 where it increases rapidly.

The concentrations of Ni and Co in solution show the same trend. Their concentrations are somewhat stable till pH 9 where after a rapid increase occurs with the highest concentrations at pH of 3. Cadmium shows a similar trend with a much slower increase in concentration.

The concentration of Sb shows a sharp increase till pH 11 then increases more slowly till pH 9 and thereafter the concentrations decreases slowly till pH 3. The concentration of Hg varies with pH, increasing slightly till pH 9 then decreasing to very low values at pH 7 then increasing again slightly.

The trace elements are shown in Figure 4.5.7. The concentration of Mn in solution decreases slightly with the first addition of acid and increases rapidly after pH 10 till a pH of 7.6 where it increases at a slower rate. The concentrations of V and As follow the same trend; increasing between pH 12 and 10 and decreasing rapidly between pH 7.6 and 4.5 whereupon the concentration increases very rapidly again. The concentration of Cr follows a similar trend except it decreases steadily until pH 4.5 whereupon it increases very rapidly.

The concentration of Mo remains relatively constant till pH 7.6 where after it decreases rapidly. The concentrations of Ba and Zn in solution follow similar trends, decreasing slightly till pH 7 then increasing again, slightly. The concentration of Se increases at first but decreases steadily after pH 7.6.

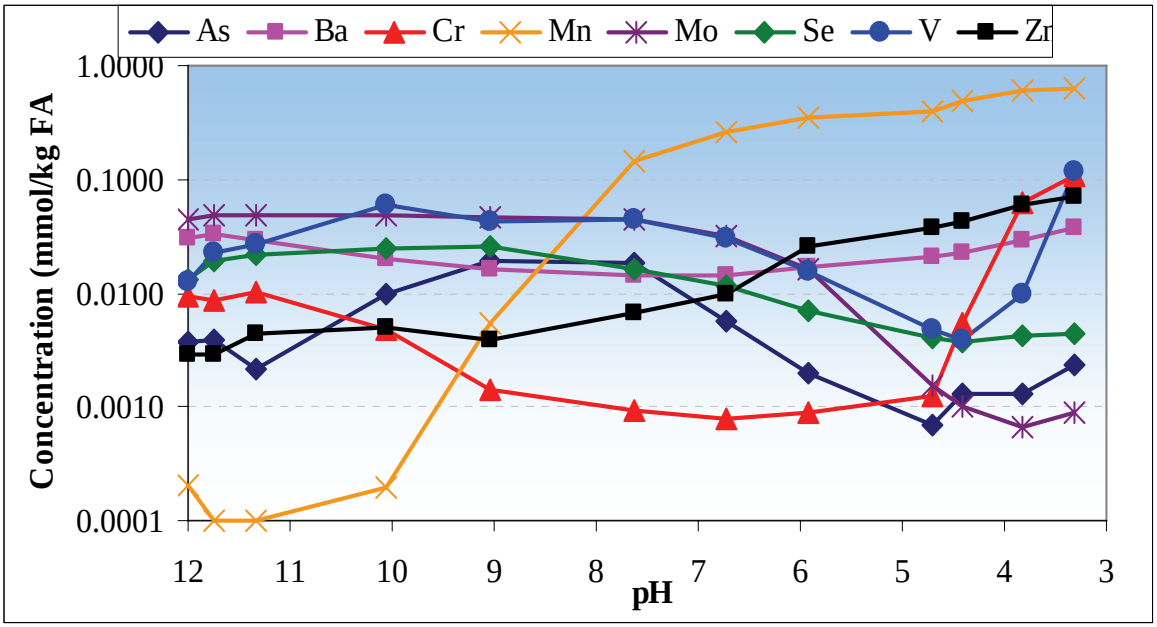

Figure 4.5.7: Major elements for 3TLPc (mmol/kg FA).

4.5.4 Leachability test 2 (3TLPd)

This is the third and last tier of the 3TLP and was designed to estimate initial pore water conditions and initial leachate compositions in a percolation scenario. Figures 4.5.8 to 4.5.10 graphically show the major, minor and trace element concentrations for the three liquid-to-solid (L/S) ratios tested. From Figure 4.5.8 it can be seen that the L/S ratio does not have a great influence on the concentration of the major elements. It is only those major elements that have a low concentration such as Al, B, Mg and Mo that some effect can be seen. In all four cases the higher L/S ratio has a greater concentration of those elements. One explanation for this lack of influence of the L/S ratios on the element concentration is that the solution may reach saturation at low L/S ratios, preventing other soluble elements from entering the solution. When the L/S ratio is slightly higher the solution matrix is less saturated and allows a greater concentration of elements to become soluble.

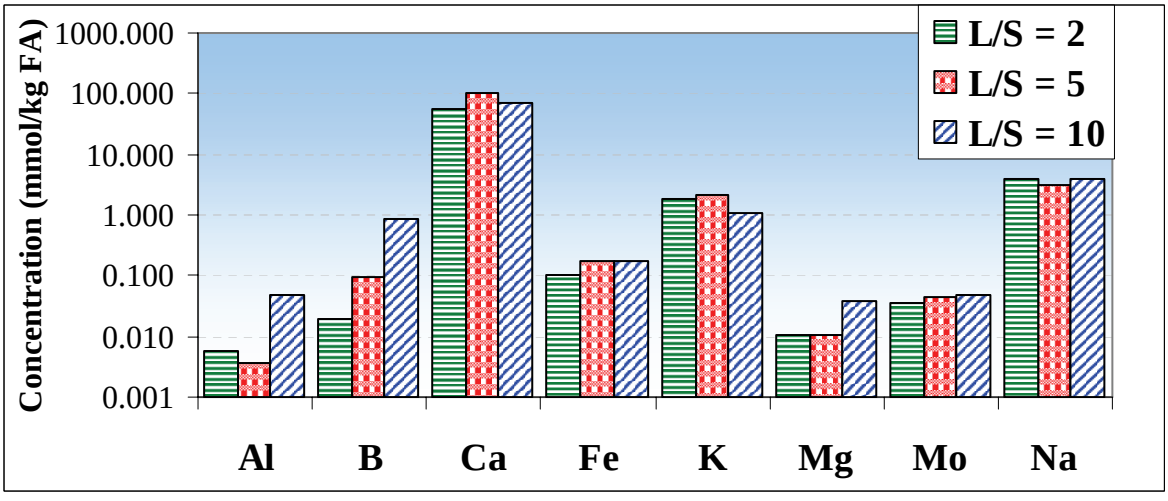

Figure 4.5.8: Major elements for 3TLPd (mmol/kg FA).

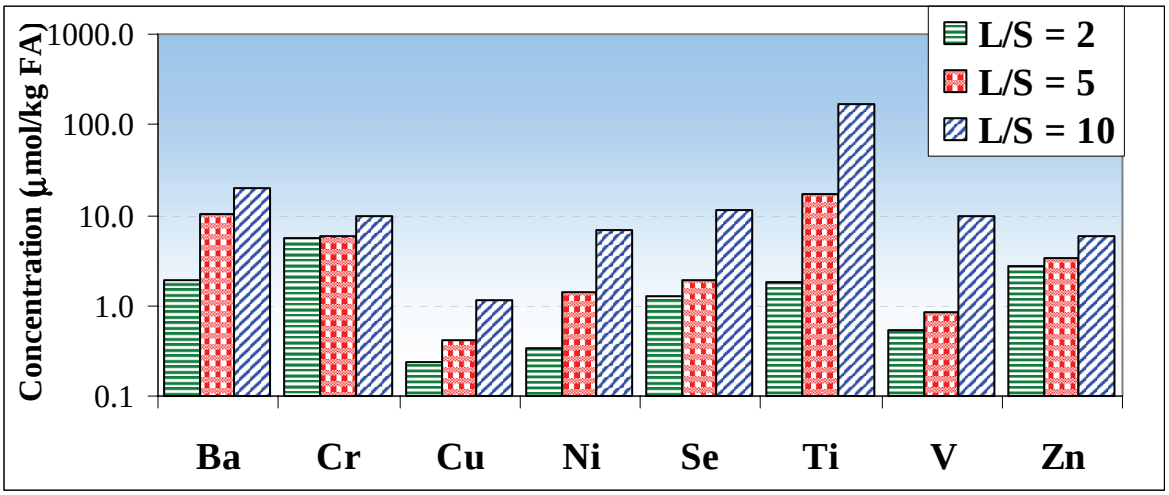

Figure 4.5.9: Minor elements for 3TLPd (mmol/kg FA).

Figure 4.5.9 shows the concentrations in solution of the minor elements. These elements all clearly show greater concentrations in the solutions with higher L/S ratios. The reason for this is possibly that the more soluble elements of Ca, Na and K saturate the solution and prevent the less soluble elements from dissolving.

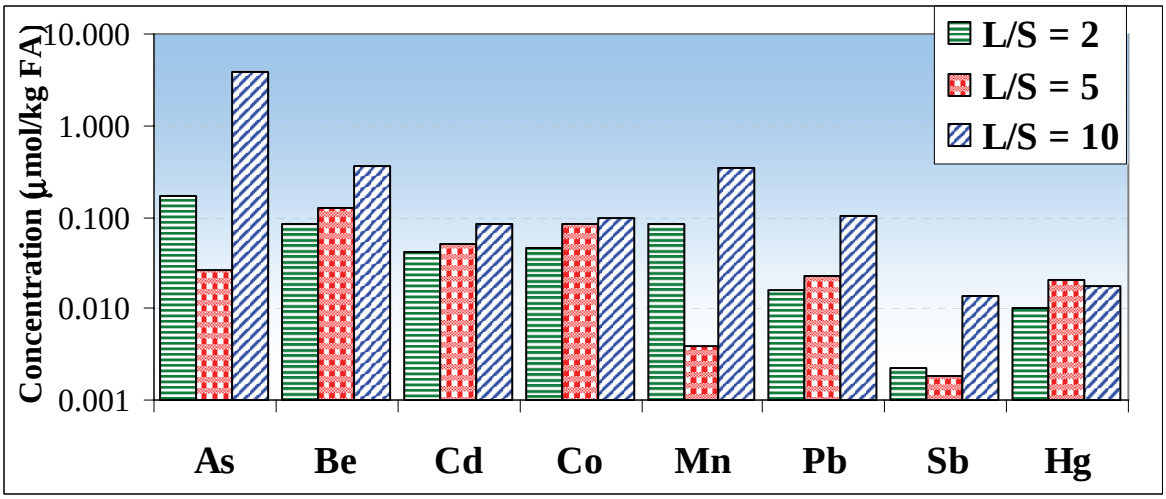

Figure 4.5.10: Trace elements for 3TLPd (mmol/kg FA).

Figure 4.5.10 shows the trace elements concentration for the 3TLPd test. The trace elements also show the same trends with the higher L/S ratio showing a greater concentration of elements than the other two ratios, except for Hg. It is likely that the data for Hg contains errors, and is not accurate.

These results are contrary to what would be expected to happen. The concentration should be higher for lower ratios. The most likely explanation for this anomaly is that the ratios were too low to allow sufficient water movement and the solution quickly became saturated. Testing higher ratios, where the mixture has a consistency closer to that of a solution than a slurry, would allow for freedom of movement of grains and sufficient liquid to prevent saturation.

5. DISCUSSION

5.1 ACCURACY AND REPRODUCIBILITY

The accuracy and reproducibility of data was, in general, not good. In future studies greater care will be taken to ensure analytical accuracy. Samples analysed with NIST standards that do not show sufficient accuracy will be reanalysed. Elements that suffer from interference and polyatomic ion production must be analysed with different methods, especially Fe and K, which this particular ICP-MS has difficulty in analysing accurately. The other analysing techniques that may be used are: anion absorption spectroscopy or ion chromatography, for the major elements and stripping voltametry for elements such as Hg and Ti. More standard reference samples and blanks must be inserted into the sample analyses at random intervals.

To achieve greater reproducibility sources of error must be eliminated. Milli-Q water will be used instead of de-ionised, and each water batch will be analysed.

5.2 GENERAL

Once analysis has been performed for the procedures in which pH is a factor, a liquid-solid partitioning (LSP) curve was generated for each of the elements.

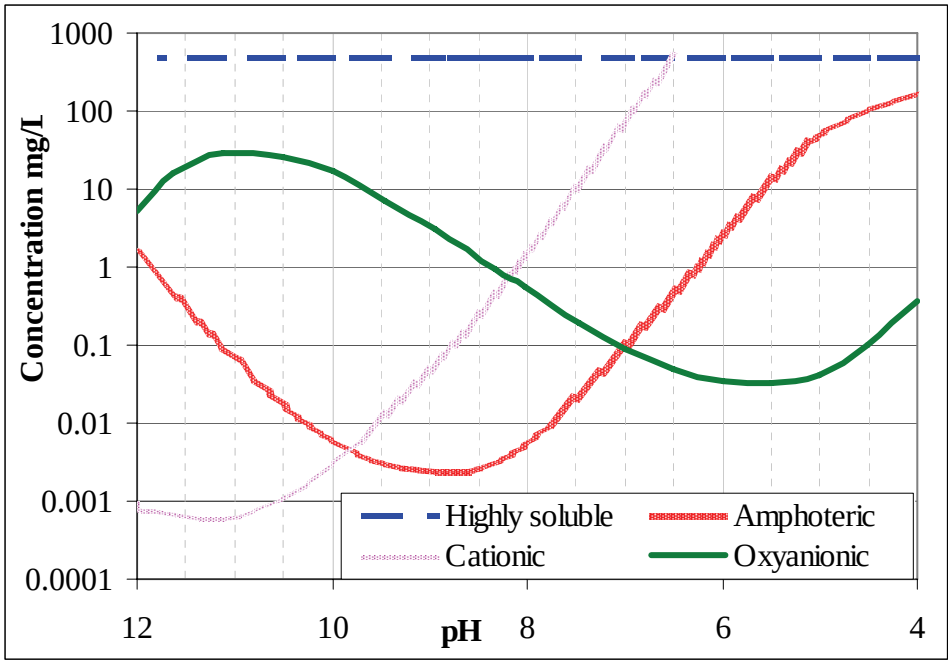

Figure 5.1.1: Liquid-solid partitioning curve (LSP) for cationic, oxyanionic, amphoteric and highly soluble species as a function of pH (Kosson *et al.*, 1996). pH values in reverse order for ease of comparison with other figures.

The curve indicates the equilibrium concentration over the pH range studied. The general shape of the curve is controlled by the equilibrium between the soluble ion in solution (e.g. Ca) and the solid phase species ($Ca(OH)_2$) as a function of pH. The shape and the general location of the minima and maxima of the curve as a function of pH, indicates whether the element in question follows cationic, oxyanionic, or amphoteric behaviour

(Figure 5.1.1). The ionic strength of the solution, the presence of a chelating agent and the presence of other ions that will co-precipitate (e.g. SO_4 or CO_3), have an influence on the LSP curvature and magnitude (Kosson *et al.*, 1996).

Since the fly ash leachate solutions have both high ionic strength (evidenced from high Ca and Na concentrations) and SO_4 (added in MWLP, known to be found in FA) and CO_3 ions (from CO_2 dissolution at high pH), the element LSP curves for the MWLP and the 3TLPc are unlikely to follow the ideal model presented in Figure 5.1.1.

5.3 TOXICITY CHARACTERISTIC AND ACID RAIN LEACHING PROCEDURES

The TCL procedure was designed to determine the mobility of both organic and inorganic analytes present in liquid and solid wastes. The method simulates the dissolving action of an organic acid leachate formed in a landfill with organic and inorganic wastes. The TCL procedure was adopted with the assumption of a worst-case mismanagement scenario. This has resulted in the over-broad application of this test and in many cases an over-estimation of the hazardous material content of certain wastes. In consequence protection methods can be extreme, inefficient and more expensive than necessary.

The ARLP is intended to be more specific to single-waste disposal sites that do not contain any organic material, than the TCL procedure and seeks to mimic the natural acidity of rainwater as a result of dissolved CO_2. The method calls for a saturated solution of carbonic acid, but there are no details on how to achieve this and how to determine whether the solution is saturated or not. This method can, in effect, be best described as leaching with a weak acid and the concentration of elements in solution is proportional to the strength of the acid used.

The TCLP leaches with a relatively weak acid but at a high concentration of 2 M. Since the fly ash is unlikely to come into contact with any organic waste material this leaching could be performed with any acid of a similar strength at high concentrations.

5.4 SYNTHETIC GROUNDWATER AND LONG-TERM LEACHING PROCEDURE

The SGL and LTL procedure attempt to imitate the leaching a fly ash waste dump is subjected to from rain water and groundwater by leaching the fly ash with de-ionised water. When putting this method into practice it proved to be problematic. The large volume of sample, 2L water plus 100g sample, for three replicates and three different samples, and the great length of time required put a great deal of strain on machinery. The platform shaker used in this procedure stopped working after 40 days and may have slowed or stopped unbeknownst at other times. This factor may have contributed to the poor reproducibility of the data.

If the change in concentration of elements over time were as a result of poor solubility then the expected result would be an increase in the concentration over time. If the element was initially soluble but over time precipitated out of solution then the concentration in solution would be expected to decrease.

Except for B, the major cations show very little difference with longer leaching periods. The major elements have a high solubility and their concentrations are not affected by

time. The minor and trace elements are affected by the leaching time. The concentrations of B, Cu, Se, Co, As, and Pb decrease with time and it would appear that these elements precipitate out of solution. The concentrations of Cr and V increase with time and it would appear that these elements have poor solubility and require time to dissolve. However, the behaviour of the other minor and trace elements is not as expected. The concentration after 30 days is either higher or lower than after 18 hrs but after 40 days the concentration does not follow the same trend but is lower or higher, respectively, than the concentration at 30 days. This behaviour is implausible in terms of chemical solubility, as the ionic strength of the solution (indicated by the concentration of the major elements) remains relatively constant with time. The reason for this re-dissolving or re-precipitation over time must be due to the physical agitation involved. The influences of shaking and particle abrasion contribute an unquantifiable influence to the concentration of some elements. This anomalous behaviour is not merely a product of inaccurate data since some elements in the NETL results, which have very good accuracy, displays the same behaviour (See Appendix BB2).

This method does not simulate field conditions adequately as physical agitation does not occur in the field. A column leaching method would better simulate field leaching.

5.5 MINE WATER LEACHING PROCEDURE

This method is a weak acid, sequential leaching procedure similar to that performed in 3TLPc, with the exception that here time is a factor with many leachings of the same material. The difference between the sequential leaching and the batch leaching is one of accuracy. Leaching the same material 11 times with 2 litres of acid and then filtering the 2 L solution 11 times is prone to errors. Sample is easily lost when filtering off solution and the large amount of solid material may not be completely filtered. The other disadvantage of this method is the length of time it takes; large volumes of 3 x 2L, take much time to filter and each leaching takes a day.

With progressive leachings elements are removed so that the species that are highly soluble in solution show a general decrease in concentration, not as a factor of pH, but as a factor of washing.

The major elements in the MWLP study all appear to be highly soluble, except for Al and Mg. The concentration of Al as a function of pH follows the LSP curve (Figure 5.1.1) of an amphoteric species well. The concentration of Mg resembles the cationic LSP curve only slightly. The concentrations of Fe and K in solution do not follow the expected trends of cationic species, but as has been previously stated, the accuracy of the data for the MWLP is very poor, especially for elements such as K and Fe, for which these ICP-MS analyses have poor accuracy.

The minor elements Be, Ba, Cu, Mn and Zn may exhibit some cationic behaviour, but the data is not clear enough to say positively. Chromium appears to be highly soluble in solution and Se and V display oxyanionic behaviour. Of the trace elements As and Sb display oxyanionic behaviour while Ni, Co and Cd display slight cationic behaviour. The other elements do not show any trend, except for Mo. The constant decrease in the concentration of Mo indicates that it is highly soluble and is removed with each successive washing.

5.6 THREE TIER LEACHING PROCEDURE

In general the three tier leaching procedure is an advantageous method. It is simple to follow and is not time consuming. It does lack a determination of the effect of long-term leaching, but that involves separate leaching goals. This method needs to be fine tuned through a process such as this inter-laboratory study to remove the problems.

5.6.1 Calibration pre-test (3TLPa)

Fly ash material varies considerably within power stations, not to mention between different places. The equilibration time after acid addition for each fly ash solution (and for any other material used in this method) should be established first. The amount of alkalinity within a fly ash would influence this equilibration time, the more alkalinity in a fly ash the longer the equilibration time. High concentrations of metals that influence the pH by removing OH^-, such as Al^{3+} and Fe^{3+}, would also influence the equilibration time.

The time to equilibration over the pH scale is not the same, as can be seen by the pre-test calibration curve. Over the buffered areas the equilibration time is slow, while in the non-buffered regions the equilibration time is rapid.

5.6.2 Availability test (3TLPb)

This test is an excellent indicator of the maximum level of constituents available should some form of mismanagement or worst-case scenario befall. The high concentrations of elements removed from the fly ash are unlikely to occur under normal conditions, however but may be viewed as the concentrations for potential long-term release.

Care must be taken to determine the desired pH of the EDTA solution as the addition of EDTA raises the pH above values expected for the amount of acid added.

5.6.3 Leaching test 1 (3TLPc)

The acid batch leaching performed in this method is a good indication of the concentration of each element according to the pH of the solution. This test may be used to determine the concentration of constituents should the fly ash come into contact with acidic waters.

On comparison of the results with the liquid-solid partitioning (LSP) curves shown in Figure 5.1.1 it can be seen that most (B, Ca, K, Na and Ti) of the major elements are highly soluble and do not follow the traditional cationic curve. The elements that follow the cationic curve to some degree (Fe and Mg) have their minima at pH values much lower than that of the minima for the LSP cationic curve. Aluminium follows the amphoteric curve well but with a minimum at lower pH values than those indicated by the LSP curves.

The minor elements show good correlation with the LSP curves in Figure 5.1.1. Vanadium, Mo, As, Se and Cr follow the trend for oxyanionic species. Zinc and Ba do not appreciably follow any trend and as a consequence have good solubility. Manganese is the only minor element to follow the LSP trend for a cationic species.

All the trace elements follow the trend for cationic species, increasing in concentration with decreasing pH, except for Sb, which appears to be oxyanionic.

5.6.4 Leaching test 2 (3TLPd)

This test attempts to determine the leaching that would occur when fly ash comes into contact with low volumes of water. The method is designed to approximate initial pore water conditions and initial leachate compositions in a percolation scenario. This method did not take into account the existence of the many micro and macro pores within fly ash. The liquid-to-solid ratios were too low to allow for a saturated solution of fly ash with respect to water.

A fly ash solution with a liquid-to-solid ratio below that of a saturated paste is unlikely to release much of the absorbed water even under vacuum conditions. The quantity of water needed for a saturated paste should be determined before leaching. The leaching ratios should then be adjusted according to the amount of water required for a saturated paste.

The major, highly soluble elements show little difference in concentration between liquid-to-solid ratios. As a result of this, the solutions with low liquid-to-solid ratios are rapidly saturated with major elements and the concentration of the minor and trace elements is reduced.

5.7 COMPARISON OF METHODS

SGL and LTL procedures use only water to leach fly ash. The concentrations are very low compared to other methods that use acid. When the SGL and LTL procedure is compared to the second leachability test (3TLPd), which also leached with water, the constituent concentrations in the former are at least 2 orders of magnitude higher for all elements. The liquid-to-solid (L/S) ratio in the case of the SGL and LTL procedures was 20. This indicates that the highly soluble elements saturate the solution at low L/S ratios and that a large amount of these elements remain undissolved.

Comparing the TCL procedure to 3TLPb, which uses EDTA to chelate with all available metals shows that the concentrations of elements in the TCLP method are in most cases 2 to 3 orders of magnitude lower. Despite the fact that the TCLP method uses a relatively high concentration of acetic acid it does not represent the maximum concentration of available elements.

The MWLP and the first leachability test (3TLPc) compare well in terms of elemental trends and magnitude, discounting element removal in the MWLP.

6. CONCLUSIONS

- The MWLP is prone to errors as a result of numerous washings and filtering of material.

- The MWLP and 3TLPc have comparable results. Since the 3TLPc is simpler, quicker and has the same results it is preferable.

- The SGLP and LTLP put a great deal of strain on equipment and are inconvenient in terms of the length of time of experimental procedure. This method should be replaced by column leaching.

- At low liquid-to-solid ratios minor and trace element concentrations are reduced as the solution rapidly becomes saturated with the highly soluble major elements.

- Major elements saturate liquid solutions while the concentration of minor and trace elements is proportional to the L/S ratio.

- The ARLP is ill defined and prone to different methodologies.

- The TCLP conducted on wastes containing no organic material is equivalent to leaching with an acid of high concentration.

- The 3TLP combines aspects of the other methods but decreases experimental time. Method needs to be refined, as some aspects do not work in practice.

- The 3TL procedure examines the concentration of elements under acid and water leaching conditions and under extreme leaching conditions with EDTA, thereby addressing all possible scenarios.

- With some adjustment the 3TLP would be a far superior method to the TCL procedure for defining fly ash. This method provides far more information on the behaviour of leached constituents than the concentration when leached with acid.

7. RECOMMENDATIONS

The following are suggestions for additional leaching tests that could be performed on the CUB material in order to provide further information:

- A test to determine the effects of different concentrations of acid on the material seeking to answer the following questions:
- Do the concentrations of the constituents increase with corresponding increase in acid concentration?
- At what concentration of acid are all constituents removed and higher concentrations of acid will not have further effect?

- The 3TLP should perhaps contain a fourth tier to determine the effect of short-term leaching, in hours and days, on the concentration of the constituents as opposed to months.

- Successive leachings of the same material with de-ionised water should be performed to determine the soluble elements in order to compare with the 3TLPb test which indicates soluble and extractable elements.

APPENDIX BA – TABLES

BA1. TCLP AND ARLP TABLES

Table BA1.1: Major elements for the TCL and ARL procedures (mmol/kg).

Element	TCLP (pH 5.85)	ARLP (pH 6.84)
Al	0.138	0.010
B	3.656	3.167
Ca	69.84	42.15
Fe	0.204	0.091
K	1.285	1.047
Mg	5.888	4.420
Mn	0.095	0.040
Na	719.8	26.09
Ti	0.165	0.085

Table BA1.2: Minor elements for the TCL and ARL procedures (µmol/kg).

Element	TCLP (pH 5.85)	ARLP (pH 6.84)
As	16.88	11.90
Ba	29.77	13.76
Mo	11.35	19.03
Ni	9.680	3.624
Se	10.22	8.806
V	12.77	21.91
Zn	13.25	4.027

Table BA1.3: Major elements for the TCL and ARL procedures (µmol/kg).

Element	TCLP (pH 5.85)	ARLP (pH 6.84)
Be	1.37	0.25
Cd	0.16	0.04
Co	2.25	0.83
Cr	4.32	1.01
Cu	1.46	0.27
Pb	0.04	0.02
Sb	0.76	0.68
Hg	0.02	0.01

BA2. SGLP AND LTLP TABLES

Table BA2.1: Major elements for the SGL and LTL procedure (µmol/kg).

Element	18 days	30 days	40 days
Al	2.050	1.369	1.488
B	1.550	0.006	0.000
Ca	74.36	53.96	48.09
Fe	0.178	0.152	0.122
K	1.713	2.452	2.140
Na	4.037	5.096	5.035

Table BA2.2: Minor elements for the SGL and LTL procedure (µmol/kg).

Element	18 hrs	30 days	40 days
As	5.365	3.289	3.367
Ba	28.92	50.95	48.94
Cr	5.329	12.68	13.40
Cu	10.88	3.093	0.728
Mo	42.78	54.85	53.88
Mg	27.45	249.91	55.60
Se	22.40	3.368	3.791
Ti	77.20	63.08	62.35
V	24.35	59.72	62.43
Zn	9.038	5.621	10.04

Table BA2.3: Trace elements for the SGL and LTL procedure (µmol/kg).

Element	18 hrs	30 days	40 days
Be	0.743	0.260	0.616
Cd	0.052	0.094	0.063
Co	0.126	0.101	0.076
Mn	BDL	BDL	0.062
Ni	0.474	1.003	0.622
Pb	0.756	0.557	0.178
Sb	0.182	0.105	0.128
Hg	0.032	0.015	0.368

BA3. MWLP TABLES

Table BA3.1: Major elements for the MWL procedure (mmol/kg).

pH	11.39	11.36	9.80	8.23	7.52	4.78	3.86	3.91	3.73	3.79	2.87
mmol H_2SO_4	2	4	6	8	10	12	14	16	18	20	22
Al	2.060	1.292	0.574	0.204	0.128	2.044	7.879	8.549	8.192	9.418	6.682
B	2.582	2.699	2.616	1.164	0.847	0.591	0.368	0.326	0.203	0.144	0.107
Ca	86.50	38.82	30.54	20.03	29.35	11.64	6.030	9.634	8.873	6.115	3.934
Fe	0.391	0.194	0.375	0.154	0.312	0.274	0.179	0.189	0.210	0.151	0.196
K	4.960	0.644	0.943	1.106	0.980	2.114	0.802	1.028	0.467	0.819	0.432
Mg	0.090	0.442	2.693	7.148	8.476	3.206	1.392	1.602	1.603	1.128	0.807
Na	5.586	1.164	0.997	1.010	1.677	0.985	0.591	0.649	0.670	0.534	0.524
Ti	0.152	0.068	0.061	0.037	0.058	0.024	0.014	0.019	0.018	0.010	0.012

Table BA3.2: Minor elements for the MWL procedure (µmol/kg). BDL indicates below detectable limits.

pH	11.39	11.36	9.80	8.23	7.52	4.78	3.86	3.91	3.73	3.79	2.87
mmol H_2SO_4	2	4	6	8	10	12	14	16	18	20	22
Ba	30.65	8.430	6.549	4.584	14.50	55.39	44.10	36.93	25.54	31.86	22.44
Be	2.109	1.642	0.461	0.658	0.730	7.623	12.74	12.00	10.27	9.207	5.905
Cr	16.76	20.82	9.952	7.067	5.779	5.456	11.70	10.91	6.329	11.12	5.681
Cu	4.020	3.642	11.09	3.990	29.58	29.77	30.74	28.16	25.20	31.35	36.07
Mn	BDL	BDL	0.500	3.217	99.47	138.1	65.41	47.64	51.79	31.96	19.51
Se	26.22	12.51	11.60	6.854	2.252	0.634	0.528	0.453	0.668	0.649	0.314
V	39.29	82.24	42.63	32.29	15.41	1.485	2.149	1.935	1.921	2.144	4.889
Zn	32.12	7.433	11.12	23.51	53.14	291.4	80.58	30.85	28.73	22.61	14.94

Table BA3.2: Trace elements for the MWL procedure (µmol/kg).

pH	11.39	11.36	9.80	8.23	7.52	4.78	3.86	3.91	3.73	3.79	2.87
mmol H_2SO_4	2	4	6	8	10	12	14	16	18	20	22
As	5.679	28.350	67.75	44.73	9.982	1.668	5.771	4.031	1.421	1.987	2.168
Cd	0.047	0.017	0.021	0.019	0.067	0.259	0.172	0.088	0.067	0.051	0.030
Co	0.148	0.083	0.094	0.168	1.332	5.396	1.834	1.322	1.400	1.069	0.785
Mo	51.32	12.21	5.225	3.636	1.214	0.470	0.131	0.066	0.059	0.063	0.051
Ni	1.744	1.424	1.313	1.355	5.259	28.61	15.46	6.084	9.118	4.548	3.405
Pb	0.977	0.154	0.371	0.260	1.212	1.008	0.185	0.350	0.932	0.393	0.314
Sb	0.175	0.703	1.159	0.773	0.381	0.106	0.089	0.091	0.076	0.065	0.054
Hg	0.191	0.239	0.074	0.080	0.055	0.036	0.089	0.040	0.272	0.252	0.160

BA4. 3TLP TABLES

BA4.1 Availability test (3TLPb)

Table BA4.1: Major elements for the 3TLPb procedure (mmol/kg).

Element	pH 9.5	pH 9.48	pH 9.95
Al	12.82	12.85	13.01
B	5.266	5.934	6.304
Ca	151.8	184.3	163.0
Fe	7.993	7.609	7.501
K	7.358	7.528	7.204
Mg	15.46	15.61	15.69
Na	19312	19225	18583
Ti	1.140	1.151	1.108

Table BA4.2: Minor elements for the 3TLPb procedure (mmol/kg).

Element	pH 9.5	pH 9.48	pH 9.95
As	0.417	0.428	0.412
Ba	0.186	0.186	0.209
Cr	0.215	0.210	0.197
Cu	0.154	0.156	0.152
Mn	0.289	0.311	0.304
V	0.358	0.355	0.352
Zn	0.122	0.150	0.149
As	0.417	0.428	0.412

Table BA4.3: Trace elements for the 3TLPb procedure (mmol/kg).

Element	pH 9.5	pH 9.48	pH 9.95
Be	0.0086	0.0148	0.0146
Cd	0.0006	0.0007	0.0007
Co	0.0075	0.0082	0.0076
Mo	0.0756	0.0767	0.0782
Ni	0.0412	0.0607	0.0423
Pb	0.0081	0.0061	0.0071
Sb	0.0034	0.0033	0.0033
Se	0.0573	0.0670	0.0723

BA4.2 Leachability test 1 (3TLPc)

Table BA4.4: Major elements for the 3TLPc procedure (mmol/kg).

pH	12.0	11.7	11.3	10.1	9.03	7.63	6.73	5.92	4.71	4.41	3.83	3.31
Al	0.062	0.301	1.181	0.594	0.071	0.030	0.014	0.059	1.541	17.80	64.94	93.79
B	0.474	1.436	4.065	5.270	5.989	6.736	6.928	7.539	7.962	8.090	8.433	8.985
Ca	51.07	60.83	89.96	106.7	120.4	165.3	144.9	189.2	199.5	206.7	264.9	261.5
Fe	0.174	0.209	0.246	0.322	0.367	0.395	0.387	0.333	0.371	0.763	5.117	15.00
K	1.327	1.444	1.420	1.733	1.972	2.004	1.972	1.889	1.902	1.883	4.473	6.138
Mg	0.042	0.077	0.080	2.114	9.301	12.58	12.44	12.05	12.74	15.63	27.01	28.41
Na	4.133	4.274	4.014	4.730	5.086	5.036	4.925	4.715	4.541	4.444	5.175	5.319
Ti	0.142	0.176	0.156	0.138	0.167	0.099	0.106	0.040	0.037	0.049	0.021	0.028

Table BA4.5: Minor elements for the 3TLPc procedure (mmol/kg).

pH	12.0	11.7	11.3	10.1	9.03	7.63	6.73	5.92	4.71	4.41	3.83	3.31
As	3.676	3.803	2.144	9.851	19.11	18.24	5.760	1.974	0.679	1.326	1.322	2.298
Ba	30.72	32.61	29.29	20.13	16.54	14.38	14.22	16.86	21.09	22.40	29.63	37.06
Cr	9.357	8.677	10.07	4.744	1.393	0.913	0.774	0.884	1.242	5.334	61.67	106.4
Mn	0.205	0.100	0.100	0.197	5.480	144.2	261.6	344.3	397.8	482.5	603.0	642.5
Mo	45.08	47.97	48.52	49.34	47.37	44.51	32.11	16.23	1.519	0.997	0.673	0.874
Se	13.08	19.44	22.00	25.16	25.67	16.53	11.58	6.94	4.047	3.693	4.274	4.375
V	12.45	22.39	26.75	58.80	42.06	44.20	31.02	15.84	4.768	3.932	9.881	116.86
Zn	2.847	2.857	4.332	4.966	3.902	6.698	9.650	25.35	37.84	42.33	58.84	70.23

Table BA4.6: Trace elements for the 3TLPc procedure (µmol/kg).

pH	12.0	11.7	11.3	10.1	9.03	7.63	6.73	5.92	4.71	4.41	3.83	3.31
Be	0.247	0.147	0.169	0.336	0.121	0.265	0.404	0.891	6.357	21.91	57.02	77.23
Cd	0.070	0.072	0.075	0.080	0.073	0.083	0.124	0.221	0.364	0.408	0.500	0.566
Co	0.100	0.144	0.144	0.176	0.271	1.548	4.255	5.914	7.352	8.763	12.96	16.61
Cu	0.706	0.629	0.348	2.331	0.645	0.709	0.618	0.629	1.043	3.175	14.12	35.92
Ni	0.279	0.189	0.346	0.289	0.869	6.331	14.93	23.59	34.34	41.21	50.36	60.30
Pb	0.040	0.047	0.018	0.137	0.047	0.059	0.046	0.055	0.079	0.049	0.115	0.368
Sb	0.010	0.017	0.294	0.714	1.225	1.208	1.104	0.929	0.486	0.296	0.264	0.235
Hg	0.026	0.049	0.064	0.075	0.053	0.021	0.018	0.044	0.032	0.031	0.052	0.056

BA4.3 Leachability test 2 (3TLPd)

Table BA4.7: Major elements for the 3TLPd procedure (mmol/kg). L/S indicates liquid-solid ratio.

Element	L/S = 10	L/S = 5	L/S = 2
Al	0.050	0.004	0.006
B	0.838	0.092	0.020
Ca	69.96	103.7	55.87
Fe	0.171	0.174	0.106
K	1.078	2.144	1.890
Mg	0.038	0.010	0.010
Mo	0.047	0.045	0.036
Na	3.862	3.144	3.869

Table BA4.8: Minor elements for the 3TLPd procedure (µmol/kg). L/S indicates liquid-solid ratio.

Element	L/S = 10	L/S = 5	L/S = 2
Ba	19.53	10.23	1.943
Cr	9.821	5.781	5.486
Cu	1.179	0.422	0.233
Ni	6.933	1.381	0.337
Se	11.23	1.887	1.305
Ti	166.9	16.79	1.836
V	9.671	0.858	0.548
Zn	5.764	3.338	2.687

Table BA4.9: Trace elements for the 3TLPd procedure (µmol/kg). L/S indicates liquid-solid ratio.

Element	L/S = 10	L/S = 5	L/S = 2
As	3.8700	0.0264	0.1708
Be	0.3691	0.1269	0.0830
Cd	0.0846	0.0511	0.0422
Co	0.0971	0.0846	0.0448
Mn	0.3354	0.0038	0.0859
Pb	0.1031	0.0232	0.0161
Sb	0.0139	0.0018	0.0022
Hg	0.0180	0.0202	0.0099

APPENDIX BB – GRAPHS FOR NETL

BB1. NETL GRAPHS FOR MWLP

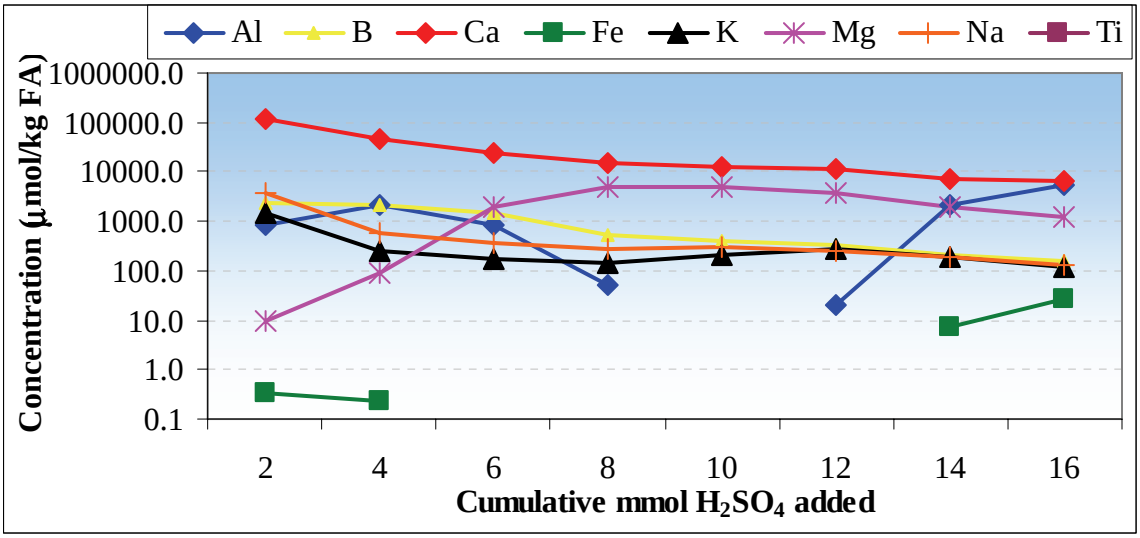

Figure BB1.1: Major elements for MWLP conducted at NETL (µmol/kg FA).

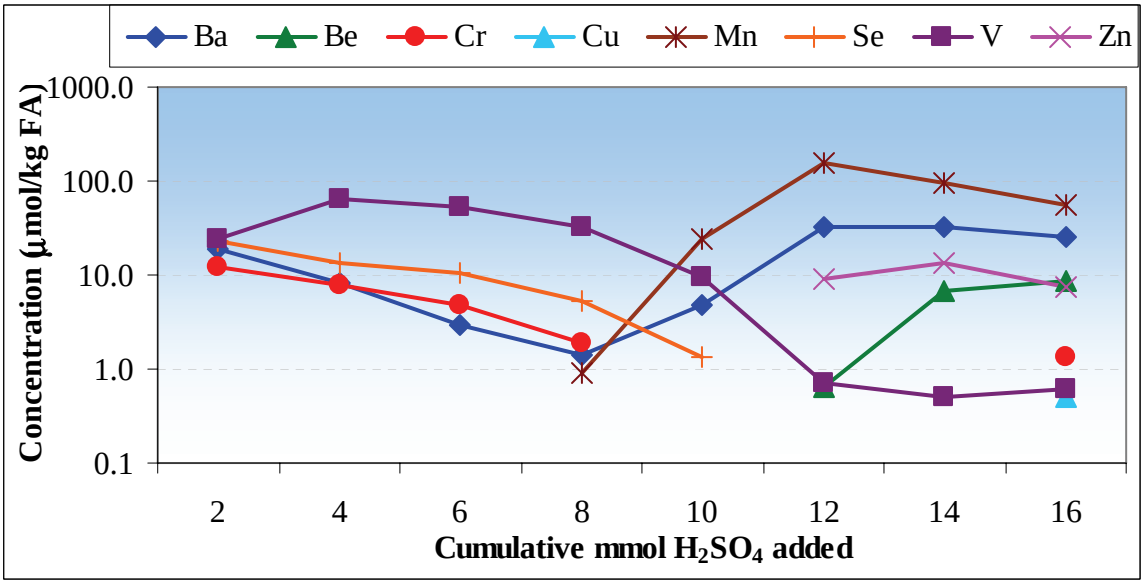

Figure BB1.2: Minor elements for MWLP conducted at NETL (µmol/kg FA).

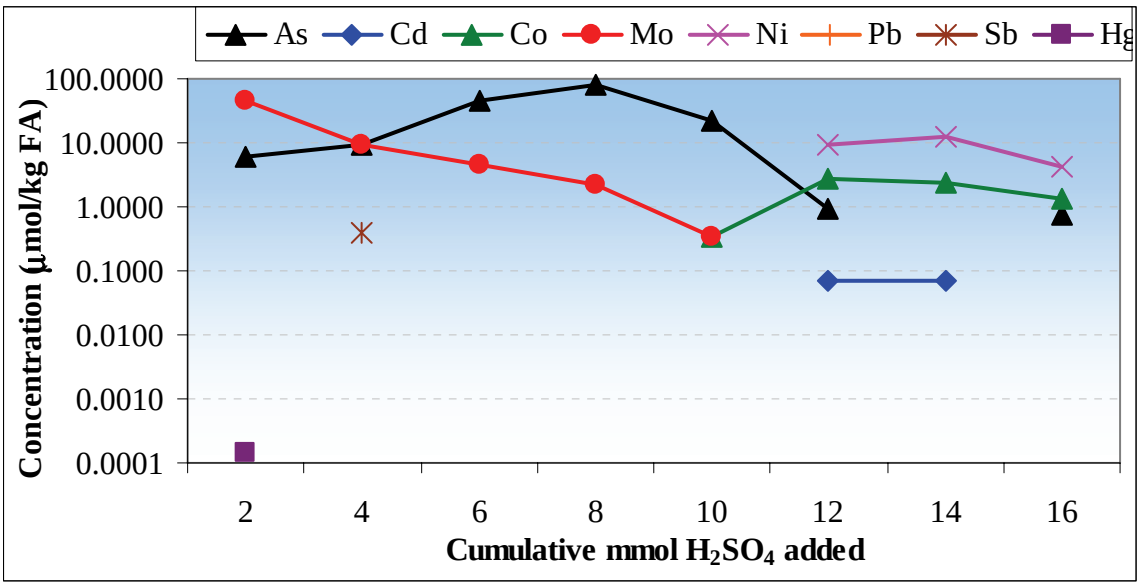

Figure BB1.3: Trace elements for MWLP conducted at NETL (µmol/kg FA).

BB2. NETL GRAPHS FOR SGL AND LTL PROCEDURE

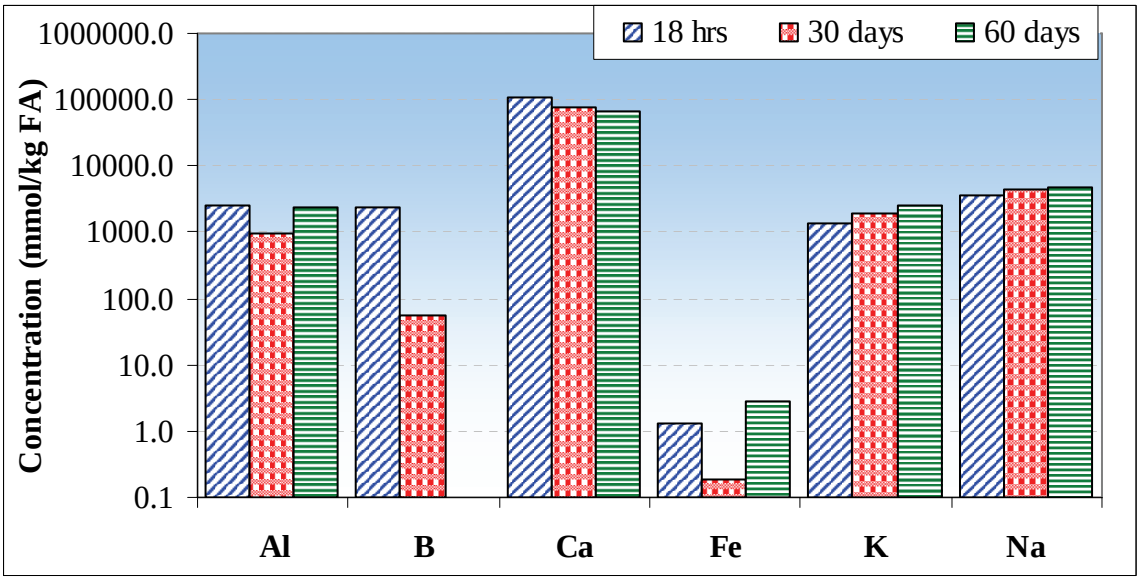

Figure BB2.1: Major elements for SGL and LTL procedure conducted at NETL (mmol/kg FA).

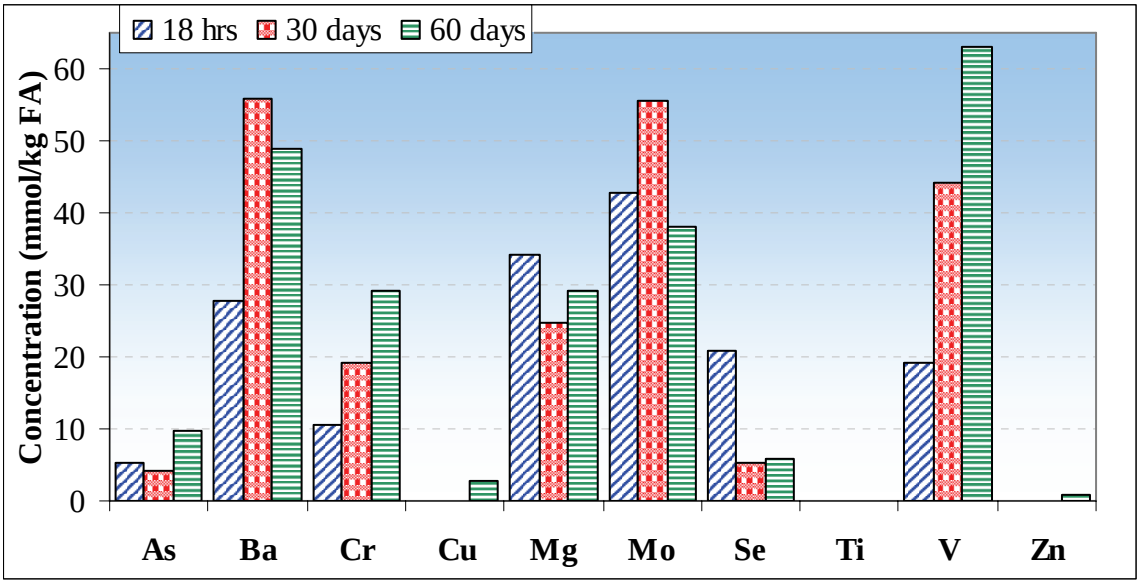

Figure BB2.2: Minor elements for SGL and LTL procedure conducted at NETL (µmol/kg FA).

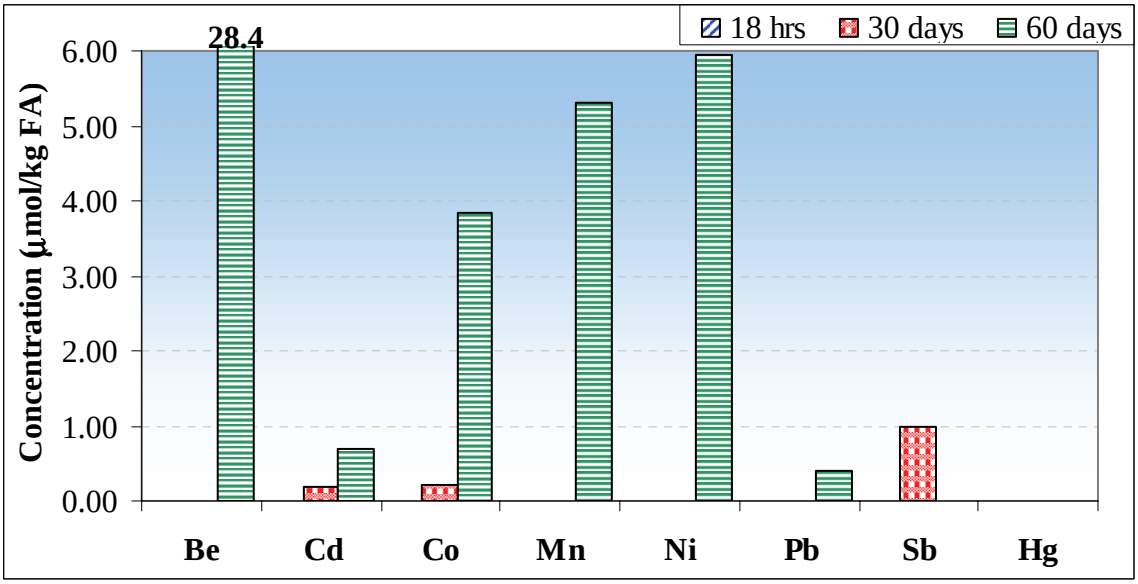

Figure BB2.3: Trace elements for SGL and LTL procedure conducted at NETL (µmol/kg FA).